

# Abstracts of the 2<sup>nd</sup> AMP Europe Congress:

## Clinical Genomics: Beyond the Somatic Mutation

The Association for Molecular Pathology

May 11-13, 2020 (Postponed: September 14-16, 2020)

Milan, Italy

### Selected Oral Abstracts

#### Selected Genetics/Inherited Conditions Abstracts

##### 01-OR01. Benchmarking an Artificial Intelligence Method for Fast Diagnosis of Rare Genetic Disease

F.M. De La Vega<sup>1,2</sup>, B. Moore<sup>3,4</sup>, E. Frise<sup>1</sup>, S. Chowdhury<sup>5</sup>, N. Veeraraghavan<sup>5</sup>, S.F. Kingsmore<sup>5</sup>, M.G. Reese<sup>1</sup>, M. Yandell<sup>3,4</sup>

<sup>1</sup>Fabric Genomics, Oakland, CA, United States, <sup>2</sup>Stanford University School of Medicine, Biomedical Data Science, Stanford, CA, United States, <sup>3</sup>University of Utah, Department of Human Genetics, Salt Lake City, UT, United States, <sup>4</sup>University of Utah, Utah Center for Genetic Discovery, Salt Lake City, UT, United States, <sup>5</sup>Rady Children's Institute for Genomic Medicine, San Diego, CA, United States.

**Introduction:** Evidence is mounting that genome sequencing should be performed as a first-tier test for children in multiple pediatric settings, especially for those in the intensive care unit. As more children are sequenced, the pressures to increase the diagnostic rate and the time to result, while reducing the cost of the process, are amplified. Interpretation of whole-genome or exome variants to diagnose rare genetic diseases continues to be a major bottleneck, as it often consists of time-consuming iterative variant filtering coupled with evidence review for large lists of candidate variants. We showed previously that VAAST and PHEVOR, tools used in tandem to prioritize variants given patient phenotype descriptions in HPO terms, reduced review to 20 variants for 75% of 450 cases with positive findings from the Genomics England 100,000 Genomes Project. **Methods:** Here we benchmark GEM, a novel artificial intelligence-based method, which integrates the outputs of VAAST and PHEVOR with knowledge from OMIM, gnomAD, and ClinVar databases to quickly identify disease-causing variants from genomes. GEM is robust to common sequencing artifacts and cryptic ancestry, predicts consanguinity and inheritance mode, and can take advantage of automated deep phenotyping. GEM outputs a short list of likely disease genes and only returns candidates when a Bayes factor score supports evidence of genetic causality, therefore preventing lengthy and sometimes unnecessary case reviews. **Results:** We are

performing a benchmarking study of GEM by analyzing 200 solved rapid whole genome sequencing cases of seriously ill children from the Rady Children's Hospital NICU. In our preliminary analysis of 56 cases, we show that GEM ranks previously identified disease genes as the top candidates for 82% of cases, and within the top 5 or 10 candidates for 97% and 100% of cases, respectively. The mean number of candidates returned per case is 3.7, with a median and mode of 1. Importantly, automated deep phenotyping by NLP of clinical notes did not degrade the ranking, and in fact improved it despite returning large numbers of HPO terms (e.g., in one case up to 650). Additionally, we analyzed 14 previously unsolved cases where GEM returned new potential findings for 2 cases, without yielding false leads for the others. **Conclusions:** GEM significantly simplifies and improves disease-causing variant prioritization over prior methods, substantially reducing genome interpretation time in the diagnosis of monogenic disease, and could allow cost-effective, automated reanalysis of undiagnosed cases over time.

##### 01-OR02. Characterization of a Rare/Varying Clinical Consequence of CFTR Variants W57G/A234D CFTR Genotype and Theratyping Using Rectal Organoids

C. Sorio<sup>1</sup>, V. Lotti<sup>1</sup>, K. Kleinfelder<sup>1</sup>, A. Farinazzo<sup>1</sup>, S. Preato<sup>1</sup>, F. Quiri<sup>1</sup>, J. Conti<sup>1</sup>, M. Bertini<sup>2</sup>, E. Pintani<sup>2</sup>, G. Tridello<sup>2</sup>, L. Rodella<sup>3</sup>, F. Tomba<sup>3</sup>, M. Cipolli<sup>2</sup>, P. Melotti<sup>2</sup>  
<sup>1</sup>University of Verona, Department of Medicine, Verona, Italy, <sup>2</sup>Azienda Ospedaliera Universitaria Integrata Verona, Cystic Fibrosis Center, Verona, Italy, <sup>3</sup>Azienda Ospedaliera Universitaria Integrata Verona, Endoscopy Unit, Verona, Italy.

**Introduction:** Over 2,000 different variants in the CFTR gene have been described: not all of them cause cystic fibrosis (CF). This study focused on a CF patient carrying the very rare CF-causing CFTR variant W57G (c.169T>G), described in 10 patients in the CFTR2 database and recently found unresponsive to ivacaftor in a human bronchial epithelial cell model, in trans with the A234D (c.701C>A) missense variant that is not described in the above-mentioned database. The complex allele A234D-I1027T has been previously reported by Seia *et al.* ([www.cysticfibrosisjournal.com/article/S1569-](http://www.cysticfibrosisjournal.com/article/S1569-)

1993(06)80002-0/pdf) to be probably a neutral variant in isolation but might significantly impair *CFTR* function when in cis with a *CFTR* mutation. Ivacaftor is a *CFTR* potentiator approved by the US Food and Drug Administration for treating 33 *CFTR* variants in CF patients with no evidence about its effects on the *A234D* variant. *CFTR* modulator therotyping has been proposed to identify rare *CFTR* variants that are responsive to approved or experimental drugs (Clancy *et al.* JCF, 2018). **Methods:** A 36-year-old female CF patient carrying the *CFTR* genotype *W57G/A234D* abnormal sweat Cl (112 mmol/L) is followed at CF Center of Verona since 2014 with pancreatic sufficiency, lung infection (*Pseudomonas aeruginosa*), moderate impairment of lung function (forced expiratory volume in 1 second, FEV1: 65% of predicted value), bilateral bronchiectasis, kidney stones, recurrent sinusitis. Nasal potential difference and intestinal current measurements were both abnormal, supporting CF diagnosis, as was imaged beta-adrenergic sweat rate test (Bergamini *et al.* JCF, 2017). Intestinal organoids were obtained from rectal biopsies after intestinal crypt isolation and evaluated by forskolin (Fsk)-induced swelling (FIS) assay (forskolin stimulation range: 0.02-5  $\mu$ M) and ivacaftor (IVA: 3  $\mu$ M +/- 3  $\mu$ M VX809 or 661 for 24 hrs) alone and in combination. Organoids were acquired by confocal live cell microscopy (Leica, TCS-SP5) from baseline to 60 min and analyzed using ImageJ software. **Results:** *CFTR*-dependent sweating was undetectable in 2 separate tests in this patient, consistent with CF diagnosis. FIS assay showed swelling at the highest doses of Fsk only; ivacaftor alone increased significantly organoid area values with no advantage when pretreated for 24 hrs with *CFTR* correctors VX-809 and VX-661. **Conclusions:** Organoid swelling induced by the *CFTR* potentiator ivacaftor alone suggests that the *A234D* variant might represent a class III mutation and indicate for the first time ivacaftor as a therapeutic candidate for patients carrying this variant. This research was supported by Lega Italiana Fibrosi Cistica (Associazione Veneta-Onlus), Italian CF Research Foundation (FFCgrants#7/2016 and 13/2018), American Cystic Fibrosis Foundation (CFF).

### 01-OR03. The Link between Sleep Duration and Telomere Length: An Exploratory Study in Sicilian Centenarians

A. Aiello<sup>1</sup>, G. Accardi<sup>1</sup>, S. Aprile<sup>1</sup>, C. Caruso<sup>1</sup>, M. Chen<sup>2</sup>, S. Davinelli<sup>2,3</sup>, I. De Vivo<sup>2</sup>, M.E. Ligotti<sup>1</sup>, G. Scapagnini<sup>3</sup>, S. Vasto<sup>1</sup>, G. Candore<sup>1</sup>

<sup>1</sup>University of Palermo, Palermo, Italy, <sup>2</sup>Harvard T. H. Chan School of Public Health, Boston, MA, United States, <sup>3</sup>University of Molise, Campobasso, Italy.

**Introduction:** The aging process is marked by a progressive loss of physiological integrity of many interrelated systems, determining an increased risk of morbidity and mortality. Within the physical changes that occur in getting older, changes to sleep patterns are a part of the normal aging process. In fact, it is

commonplace that sleep needs decline with age. Short sleep duration is associated with different age-related diseases such as cardiovascular disease, raised levels of inflammatory markers, and depressive symptoms. The research of biomarkers of cellular aging, implicated in the onset and progression of age-related diseases, and connected to the duration and the quality of sleep in aged people, is growing. Emerging evidence supports the datum that telomere length can be the molecular link marker between the aging process and duration of sleep. The aim of the current study was to examine the association of sleep duration with telomere length (TL) in a sample of healthy Sicilian subjects, focusing the attention on centenarians. **Methods:** A total of 143 healthy subjects belonging to different age groups were recruited from Palermo and its neighboring municipalities in Sicily (Italy). The study was supported by PRIN-20157ATSLF\_009 (Discovery of molecular and genetic/epigenetic signatures underlying resistance to age-related diseases and co-morbidities). All the recruited subjects gave written and informed consent. A group of trained nutritionists and physicians administered a questionnaire to collect demographic and clinical data, cognitive and health status, eating and sleep habits, and drug use. For the TL analysis, fasting morning blood was collected in EDTA tubes, and DNA was extracted using a commercial kit. Relative TL (RTL) was measured by use of quantitative polymerase chain reaction. **Results:** As expected, the RTL decreases with age in both men and women. RTL has a wider range in men in most age categories. Nevertheless, at older ages, the difference between RTL in men versus in women narrows. Stratifying for age, we saw that nonagenarian women have RTL similar to the typical 70-year-old woman. Moreover, categorizing sleep duration into fewer than 8 hours or 8 hours or more, we found that centenarians who sleep 8 hours or more a day have longer RTL than centenarians who sleep fewer than 8 hours a day. This datum was not statistically significant, likely because of the relatively small sample size of centenarians. **Conclusions:** To the best of our knowledge, this is the first study showing a relationship among centenarians, RTL, and sleep duration. Telomeres are affected by a wide range of factors, including stress hormones such as cortisol, whose levels increase in sleep deprivation.

## Selected Genomics and Renal Diseases Abstracts

### 02-OR04. Molecular Characterization of Nephrosphere-Derived PKH<sup>high</sup>/CD133<sup>+</sup>/CD24<sup>-</sup> Stem-Like Cells Evidenced Possible New Markers for Renal Stem Cells' *in situ* Identification

S. Bombelli<sup>1</sup>, S. Eriani<sup>1</sup>, C. Grasselli<sup>1</sup>, M. Bolognesi<sup>1</sup>, G. Rossetti<sup>2</sup>, V. Ranzani<sup>2</sup>, B. Torsello<sup>1</sup>, S. De Marco<sup>1</sup>, C. Bianchi<sup>1</sup>, G. Cattoretti<sup>1</sup>, R. Perego<sup>1</sup>

<sup>1</sup>University of Milano Bicocca, School of Medicine and Surgery, Monza, Italy, <sup>2</sup>Istituto Nazionale Genetica Molecolare "Romeo ed Enrica Invernizzi", Milan, Italy.

**Introduction:** The mechanism upon which human kidneys undergo regeneration is debated, though different lineage tracing mouse models have tried to explain the cellular types and the mechanisms involved, and different sources of human renal progenitors have been proposed. So the existence and the potential localization of adult renal stem cells are still a matter of debate. We contributed to this debate by isolating a population of adult renal stem cells (RSCs) from human nephrospheres. RSCs are the quiescent (PKH<sup>high</sup>) cells with a CD133<sup>+</sup>/CD24<sup>-</sup> phenotype with self-renewal and multilineage capacity. We now aim to find the molecular signature of RSC subpopulation to better disclose the phenotype hidden behind PKH<sup>high</sup> functional status to prospectively localize them on human healthy and pathological kidneys. **Methods:** We performed transcriptomic analysis of RSCs compared with their PKH<sup>low/neg</sup> progeny, and statistically (t-test; p < 0.05) differentially expressed genes (DEG) with a fold change of >1.5 were evidenced. Bioinformatic gene set enrichment analysis (GSEA) was performed. Potential RSC markers have been validated by real-time polymerase chain reaction (PCR) and immunofluorescence (IF) after cytospin of RSCs sorted from NS. We also performed IF on CD133<sup>+</sup>/CD24<sup>-</sup> fluorescence-activated cell sorting (FACS) from single cell suspension obtained from human kidneys. Preliminary IF experiments were performed on formalin-fixed, paraffin-embedded (FFPE) human healthy kidneys to localize putative markers.

**Results:** The transcriptomic analysis of RSCs compared to their PKH<sup>low/neg</sup> progeny evidenced 137 DEGs identifying our RSC signature. Bioinformatic GSEA suggested a renal early status of differentiation of our RSCs, different from embryonic stem cells. Among the signature genes, we selected *MUC16*, *KRT17*, *FBN2*, and *FHL1* gene products as potential markers. By real-time PCR analysis we validated their overexpression in RSCs with respect to the progeny. We then validated them at the protein level by IF on sorted RSCs. Single cells were obtained from adult human renal tissue for testing the potential stem markers. We identified cells with a CD133<sup>+</sup>/CD24<sup>-</sup>/FBN2<sup>+</sup>/CA125<sup>+</sup>/KRT17<sup>+</sup> phenotype in adult renal tissue by IF after cytospin of CD133<sup>+</sup>/CD24<sup>-</sup> cells. IF preliminary data on healthy renal tissues evidenced a rare population of KRT17<sup>+</sup> cells scattered in the tubules that do not express epithelial tubular markers. Multiplexed sequential immunostaining

is ongoing to better characterize this population.

**Conclusions:** The stem cell signature will allow localization and quantification of adult RSCs in normal and diseased kidney and their direct isolation from tissue by FACS to permit a deep characterization.

## Selected Hematopathology Abstracts

### 03-OR05. ChromoSeq: WGS-based Karyotyping for Hematologic Malignancies

E. Duncavage<sup>1</sup>, M. Schroeder<sup>1</sup>, R. Wilson<sup>2</sup>, S. Kruchowski<sup>2</sup>, A. Bohannon<sup>2</sup>, S. O Laughlin<sup>2</sup>, D. Spencer<sup>3</sup>  
<sup>1</sup>Washington University, Pathology and Immunology, St. Louis, MO, United States, <sup>2</sup>Washington University, McDonnell Genome Institute, St. Louis, MO, United States, <sup>3</sup>Washington University, Division of Oncology, St. Louis, MO, United States

**Introduction:** Cytogenetic testing is an unbiased assay that plays a key role in the diagnosis and prognostic assessment of hematologic malignancies. However, over the last 50 years cytogenetic methods have changed little and still require time consuming cell culture and low resolution evaluation by microscopic visualization of individual chromosomes. In contrast, newer whole genome sequencing (WGS) methods allow for single base resolution of the entire genome without the need for cell culture and provide unbiased detection of the full range of genomic variation. We sought to determine the clinical utility of ChromoSeq, a high-coverage WGS-based assay, compared to routine cytogenetics and fluorescence *in situ* hybridization (FISH) for the genomic evaluation of hematologic malignancies. **Methods:** We performed the WGS-based ChromoSeq assay on a series of 170 retrospective AML/MDS cases to determine the technical performance characteristics of the assay in addition to 22 prospective cases to ascertain clinical performance. The ChromoSeq assay leverages the simplicity of WGS workflows and advanced hardware-accelerated informatics to provide rapid and comprehensive clinical-grade genomic testing. As part of the assay, 500 ng of blood or bone marrow DNA was made into libraries using Illumina Nextera Flex chemistry and then sequenced on an Illumina NovaSeq. Resulting data were analyzed on the cloud using a custom workflow that detects clinically relevant translocations, circulating nucleic acids (CNAs), and gene mutations.

**Results:** Among retrospective cases, the average coverage was 43.4x (range 14.6-69.5x). A total of 26 of 26 (100%) with known recurrent translocations including t(15;17), t(8;21), t(6;9), t(9;22), t(7;21), inv(3), inv(16), and 11q23 were detected by ChromoSeq with no false positives. By cytogenetic testing, 47 cases had complex cytogenetics of which 45 (96%) were called complex by ChromoSeq. CNAs (excluding cases with complex cytogenetics) were identified in 40 cases by cytogenetics/FISH; in 35 cases (85%) the reported CNAs were concordant with ChromoSeq. A total of 12 of 54 (22%) cases with normal cytogenetics had additional clinically relevant findings by ChromoSeq including

losses of chromosomes 5 and 7 and 11q23 rearrangements. We further compared sensitivity to detect gene-level mutations in a subset of 51 cases with high-coverage panel-based sequencing and detected 141 of 179 (79%) of variants. Real-time prospective ChromoSeq testing on 22 cases yielded a median turnaround time of 3 days, compared to 9 days for cytogenetics. **Conclusions:** We demonstrated that the WGS-based ChromoSeq assay has a performance comparable with conventional cytogenetics but with far greater resolution and more rapid turnaround times.

### 03-OR06. Whole Exome Sequencing Data Mining for Germline Genetic Predisposition in Childhood Hematologic Malignancies

H.E. Williams, A.J. Tanaka, D. Ahram, S. Kunnath Velayudhan, S.J. Hsiao, M.M. Mansukhani, C.R. Soderquist  
Columbia University Medical Center, New York, NY, United States.

**Introduction:** Comprehensive genetic studies have elucidated much of the somatic mutational landscape of lymphoid and myeloid neoplasia. However, emerging data indicate that a subset of pediatric and adolescent hematopoietic malignancies are influenced by germline variants in cancer predisposition genes. While the spectrum of predisposing genes, mutation types, and associated syndromes has greatly expanded in recent years, the majority of variants remain uncharacterized and unclassified, and their frequency of occurrence is not well established. In order to further characterize the frequency and nature of predisposing germline variants, we retrospectively analyzed clinical whole exome sequencing (WES) data from a cohort of pediatric and adolescent patients with B-lymphoblastic leukemia/lymphoma (B-ALL), acute myeloid leukemia (AML), myelodysplastic syndrome (MDS), and mixed phenotype acute leukemia (MPAL). **Methods:** WES was performed on tumor and normal control samples from 85 pediatric patients between 2013 and 2018; diagnoses included 36 B-ALL, 40 AML, 4 MDS, and 5 MPAL. The patients' ages ranged from 1 to 23 years (mean = 10.3 years), and 43.8% were females. Constitutional WES data were re-reviewed for the presence of germline variants in 31 lymphoid or 61 myeloid predisposing genes, according to lineage of the neoplasm. The gene list was curated from the 2016 World Health Organization classification as well as recent literature. We filtered for non-synonymous variants with minor allele frequencies <0.01%, in addition to known pathogenic and loss-of-function variants. Biological significance of variants was inferred using primary literature search, ClinVar, HGMD, and OMIM databases, as well as *in silico* pathogenicity predictor algorithms, including (but not limited to) SIFT, PROVEAN, REVEL, CADD, and PeCAN PIE. When indicated by biological mechanism, the concurrent tumor sample was assessed for loss of heterozygosity. **Results:** Re-analysis of the WES data through the application of the ACMG/AMP variant classification

guidelines identified 37 candidate variants in 22 genes. Three germline variants observed in *TP53*, *RUNX1*, and *GATA2* were classified as pathogenic, and 2 additional variants in *TP53* were classified as likely pathogenic. The remaining 32 variants were of uncertain significance (20), likely benign (9), or benign (3) classification.

**Conclusions:** Our re-analysis of germline WES data provides insight into frequency and nature of pediatric hematologic malignancies associated with germline predisposition. Identification of these variants informs both patients and family members, and can aid in early detection, risk stratification, and clinical care.

### 03-OR07. Identification and Management of Myeloid Neoplasm-Associated Germline Variants after Diagnostic Somatic Next-Generation Sequencing

E.M. Azzato<sup>1</sup>, K. Demski<sup>2</sup>, G. D'Aleo<sup>1</sup>, P. Bazeley<sup>3</sup>, R. Noss<sup>4</sup>, D.H. Farkas<sup>1</sup>, J.R. Cook<sup>1</sup>, H. Carraway<sup>2</sup>, D.S. Bosler<sup>1</sup>

<sup>1</sup>Cleveland Clinic, Laboratory Medicine, Cleveland, OH, United States, <sup>2</sup>Cleveland Clinic, Hematology and Oncology, Cleveland, OH, United States, <sup>3</sup>Cleveland Clinic, Quantitative Health Sciences, Cleveland, OH, United States, <sup>4</sup>Cleveland Clinic, Genomic Medicine Institute, Cleveland, OH, United States.

**Introduction:** Identification of myeloid neoplasms with genetic predisposition is difficult, as clinical presentation may be challenging to distinguish from sporadic cases, and germline (GL) variants cannot be confidently defined without skin biopsy. We performed a retrospective review of a hematologic neoplasm somatic next-generation sequencing (NGS) panel to determine if these results could be used to inform best practices for reporting and genetics referral. **Methods:** NGS results from 885 patients, performed as standard of care diagnostic work-up for myeloid neoplasms, were screened for variants in genes associated with World Health Organization (WHO)-defined myeloid malignancies (*CEBPA*, *DDX41*, *ETV6*, *GATA2*, and *RUNX1*). Variant allele fraction (VAF), report interpretations, demographics, genomic tumor board (GTB) review, and physician chart notes were extracted from the medical record. Clinically significant (AMP/ASCO/CAP Tier 1 or 2) variants, or variants of uncertain significance with a second hit in the same gene, were broadly defined as possible high-priority GL variants based on VAF (40%-60%). **Results:** Fifty-six (6%) patients had possible GL variants considered high priority for genetics consultation (GC). Most had no evidence of potential GC follow-up ( $n = 49$ , 87.5%), and only 2 cases (4%) had verified GC. Nineteen cases were reviewed in interdisciplinary GTB (34%); of these, GC was recommended for 3, one of which had a confirmed GC appointment. While the majority of potential GL variants were not identified as such in any portion of the NGS report ( $n = 44$ , 79%), 9 reports highlighted these findings as a prominent component of test interpretation (16%). Discussion in report interpretation was positively associated with physician awareness of the need for GC, as evaluated by presence

of a chart note, either from GTB or elsewhere ( $p = 0.039$ ). Despite this positive correlation, 6 cases with prominent NGS report interpretation lacked discussion of GC in clinician notes. **Conclusions:** Potential GL findings associated with myeloid neoplasm predisposition were observed in a fraction of somatic NGS testing cases (~5%); however, most patients in this broadly defined population had no evidence of additional follow-up. Emphasizing potential GL variants in somatic reporting and GTB review can help facilitate physician awareness of potential genetic predisposition to myeloid neoplasm; however, many cases were not followed up despite these recommendations. While NGS results can provide prompt identification of patients who are at GL risk, report standardization, the formal confirmation of GL risk, and GC referral should be improved. Cooperation and collaboration of the multidisciplinary team (pathology, genetics, medical oncology) are essential to help optimize this unmet need.

### 03-OR08. Myeloma-Induced Glutamine Depletion Inhibits Osteoblast Differentiation by Limiting Asparagine Availability: A Possible Metabolic Mechanism for Bone Lesions

M. Chiu<sup>1</sup>, D. Toscani<sup>1</sup>, R. Andreoli<sup>1</sup>, G. Taurino<sup>1</sup>, V. Marchica<sup>1</sup>, P. Storti<sup>1</sup>, M. Bianchi<sup>1</sup>, N. Giuliani<sup>1,2</sup>, O. Bussolati<sup>3</sup>

<sup>1</sup>University of Parma, Department of Medicine and Surgery, Parma, Italy, <sup>2</sup>Azienda Ospedaliero-Universitaria di Parma, Hematology, Parma, Italy, <sup>3</sup>Università degli Studi di Parma, Medicina e chirurgia, Parma, Italy.

**Introduction:** Glutamine (Gln) is a key nutrient, since it sustains cell metabolism via glutaminase (GLS), and it is the obliged nitrogen donor for the synthesis of asparagine (Asn) through asparagine synthetase (ASNS). Cancer cells that rely on Gln and consume huge amounts of the amino acid are Gln-addicted. We have demonstrated that human multiple myeloma (MM) is a Gln-addicted cancer and that MM patients have a partial Gln depletion in bone marrow (BM) plasma (Bolzoni *et al.* Blood, 2016). Active MM is characterized by bone lesions, caused by a reduced number of osteoblasts (OBs). Recently, it has been shown that Gln metabolism is required to produce bone mass in mice, and that GLS silencing hinders OB differentiation of human mesenchymal stromal cells (MSCs). Therefore, we have hypothesized that the Gln depletion imposed by MM cells may impact OB differentiation in the BM. **Methods:** Human multiple myeloma cell lines (HMCLs) and BM MSCs were grown in Gln- and FBS-supplemented DMEM. MSCs were incubated with osteogenic factors for 14 days, and differentiation was evaluated from the expression of OB markers, as well as from ALPL activity and staining, or by genome-wide transcriptional analysis. Amino acid content was determined with mass spectrometry. Gene expression profiles (GEPs) were performed on primary human BM MSCs and OBs from bone biopsies of both healthy donors ( $n = 7$ ) and MM

patients ( $n = 16$ ). **Results:** HMCLs showed higher Gln uptake than MSCs and depleted medium Gln, inducing the expression of GS in MSCs without affecting MSC viability upon co-culture. The conditioned medium from HMCLs inhibited *COL1A1* and *SPARC* induction by osteogenic factors in MSCs, an effect partially rescued if Gln was restored. Consistently, low Gln levels, comparable to those present in MM BM, hindered OB differentiation of MSCs, which was abolished in Gln-free medium. Asn, but not other non-essential amino acids, restored the expression of osteogenic markers in Gln-depleted MSCs. Moreover, Asn and Gln elicited comparable transcriptional responses in differentiating MSCs. During osteoblastogenesis ASNS and the concentrative Gln transporter SNAT2, encoded by *SLC38A2*, were induced, while ASNS knock-down or transporter inhibition hindered OB differentiation. Differentiation was also associated with the increase of cell Asn, while Gln, glutamate, or aspartate were unchanged. Finally, GEP showed that GLS, ASNS, and *SLC38A2* were more expressed in human primary OBs, while GS expression was higher in undifferentiated primary MSCs. **Conclusions:** These results suggest that Gln-addicted MM cells impose a Gln-restricted BM microenvironment that hinders OB differentiation forcing intracellular Gln synthesis and limiting Asn availability.

### Selected Informatics Abstracts

#### 05-OR09. Dynamic Encryption and Watermarking of Genomic Sequencing Data to Facilitate Privacy-Preserving Ownership-Based Data Governance

X. Gai<sup>1</sup>, A. Ryutov<sup>1</sup>, T. Ryutov<sup>2</sup>, J. Biegel<sup>1</sup>, A. Judkins<sup>1</sup>  
<sup>1</sup>Children's Hospital of Los Angeles, Los Angeles, CA, United States, <sup>2</sup>University of Southern California, Los Angeles, CA, United States.

**Introduction:** Advances in genomic sequencing and its broad implementation in research, clinical diagnosis, and direct-to-consumer testing have led not only to privacy and security concerns but ethical and legal issues as well regarding data ownership, which the current static transactional or consent-based models are poorly suited to address. Data Dignity, the concept that "You should have the moral rights to every bit of data that exists because you exist, now and forever" provides an ethical framework to implement a paradigm shift from static to dynamic consent, and a participant-centric, ownership-based data governance model where the participant ultimately controls access and retains monetary, intellectual, and personal value of the data. **Methods:** To facilitate privacy-preserving ownership-based governance of genomic data, we developed 2 novel algorithms that enable flexible, fine-grained protection and control consistent with the principles of Data Dignity: 1) dynamic privacy-preserving encryption of user-specified genomic regions, and 2) ownership- and utility-preserving watermarking of the sequencing data. These empower individuals to control when, for how long, and for what purpose any portion of their genomic data is

shared, all in an auditable manner. Our dynamic encryption and watermarking algorithms work with the standard and universally accepted Binary Alignment Map (BAM) format and Variant Call Format (VCF) for transparent interoperability with existing pipelines. In addition to encrypting the entire BAM or VCF file and giving access to data from specific genomic regions, our algorithms provide for dynamic encryption by allowing a user to hide certain genes or regions (e.g., *APOE* and *BRCA1/2*), while keeping the rest of the data unencrypted. **Results:** This provides enhanced and multilayered user-defined privacy protection. Our watermarks, on the other hand, are selected from a larger pool of possible watermark elements deterministically by relying upon a secret key. This prevents collusion attacks such that the same BAM file can be shared with multiple entities at multiple times under different policies, yet the unique watermarks will guarantee that it can be reliably determined under which conditions and with what entity the BAM file in question was shared. **Conclusions:** Employing these 2 algorithms, individually or in conjunction with one another, we can address a number of existing technical, legal, and ethical hurdles associated with sharing genomic data effectively, securely, and transparently. Our algorithms will greatly reduce the cost for implementing a dynamic consent platform, support ownership-based genomic data governance, and may become an integral part of a genomic data exchange or a marketplace based on the principles of Data Dignity.

#### 05-OR10. Building Scalable and Robust Informatics Systems for Clinical Genomic Assays in the Precision Medicine Era

A. Sboner<sup>1,2,3</sup>, K. Eng<sup>2,3,4</sup>, P. Zisimopoulos<sup>2,3,4</sup>, A. Sigaras<sup>2,3,4</sup>, M. Simi<sup>2,3,4</sup>, S. Ramazanoglu<sup>2,3,4</sup>, M. Spiewack<sup>2,3,4</sup>, J. Oakley<sup>1,2</sup>, S. Parmar<sup>1,2</sup>, J. Tang<sup>1,2,3</sup>, J. Catalano<sup>1,2</sup>, R. Kim<sup>1,2</sup>, W. Tam<sup>1</sup>, M. Kluk<sup>1</sup>, W. Song<sup>1,2</sup>, O. Elemento<sup>2,3,4</sup>

<sup>1</sup>Weill Cornell Medicine, Pathology and Laboratory Medicine, New York, NY, United States, <sup>2</sup>Englander Institute for Precision Medicine, New York, NY, United States, <sup>3</sup>Institute for Computational Biomedicine, New York, NY, United States, <sup>4</sup>Weill Cornell Medicine, Physiology and Biophysics, New York, NY, United States.

**Introduction:** With the advent of precision medicine, the number of next-generation sequencing (NGS) data generated is ever increasing and more recently has been applied for clinical use to aid in diagnostics and therapeutic decision making. This exponential generation of NGS data has increased the importance to build robust informatics systems that integrate with electronic health records (EHRs) and Laboratory Information Management System (LIMS). These efforts will allow the further development of genomic testing in the clinical space. **Methods:** At the Englander Institute for Precision Medicine (EIPM) at Weill Cornell Medicine/New York Presbyterian (WCM/NYP), we have developed a cutting-

edge informatics architecture that enables the Clinical Genomics Lab of the Department of Pathology and Laboratory Medicine to manage genomics orders, track specimens and lab workflows, automatically run bioinformatics pipelines, facilitate case review and sign-out, and record other relevant data to deliver insights on the genomic data in a timely manner to our molecular pathologists (turnaround time: 11-20 days). Over the years, we have built an infrastructure that leverages containerized solutions (Docker) and continuous integration approaches to rapidly develop orchestration components and a comprehensive API to interface with LIMS and deliver the results of genomics assays to our EHR in discrete format, thus enabling clinicians to query genomics information. Here we propose to further improve our system by extending the architecture with a distributed streaming platform, microservices, container orchestration, and cloud exploitation. **Results:** Based on our experience and increased clinical volume, we have built a prototype informatics system on an infrastructure with advanced informatics services to leverage resource orchestration and pipeline execution and promote loosely coupling interaction. The new system can scale elastically, be more robust and secure, and enable for real-time updates of where each specimen is within our clinical sequencing pipeline, ensuring the turnaround time stays within the nominal time limits assigned. In addition, the new architecture allows users to take advantage of cloud-based solutions, should these be available to the users. The result of this effort is a highly configurable, flexible, and orchestrated system in which new or existing components can be seamlessly integrated and fully benefit from the capabilities it offers. **Conclusions:** We hope by sharing our architecture, best practices, and implementation we will provide the clinical bioinformatics community a resource to enable secure and robust informatics systems that deliver an increasing amount of information to physicians in a rapid manner.

#### Selected Molecular Pathology of Metabolic Diseases Abstracts

##### 07-OR11. Diabetes-Like Environment Affects Epicardial Adipose Tissue-Derived Mesenchymal Stem Cell Fate

S. Cabaro<sup>1,2</sup>, T. Migliaccio<sup>1,2</sup>, E. La Civita<sup>1,2</sup>, V. Parisi<sup>1</sup>, V. D'Esposito<sup>1,2</sup>, L. Petraglia<sup>1</sup>, M. Conte<sup>1</sup>, G. Comentale<sup>3</sup>, I. Cimmino<sup>1,2</sup>, D. Liguoro<sup>1,2</sup>, D. Leosco<sup>1</sup>, F. Beguinot<sup>1,2</sup>, P. Formisano<sup>1,2</sup>

<sup>1</sup>University of Naples "Federico II", Department of Translational Medical Sciences, Naples, Italy, <sup>2</sup>National Council of Research (CNR), URT GDD-IEOS, Naples, Italy, <sup>3</sup>University of Naples "Federico II", Department of Advanced Biochemical Sciences, Naples, Italy.

**Introduction:** Excess of visceral fat is a major culprit in the development of type 2 diabetes (T2D) and related disorders. A growing body of evidence indicates that epicardial adipose tissue (EAT), the visceral fat of the heart, may play an active role in dysregulation of cardiac

function. Indeed, EAT thickness positively correlates with the release of inflammatory molecules and with the severity of heart pathologies, including heart failure, aortic valve stenosis, and coronary artery disease (CAD). Moreover, EAT thickness is inversely associated with insulin sensitivity and positively correlates with metabolic parameters including postprandial glucose, HbA1c level, and HOMA-IR. In patients with diabetes, prolonged hyperglycemia damages several organs, including the heart. Evidence suggests that EAT can act as a transducer to mediate the effects of systemic inflammation to the myocardium. Thus, potent pro-inflammatory activation of EAT suggests a direct involvement of cardiac visceral fat in inflammatory phenomena occurring in patients with cardiovascular diseases. This study aims at investigating whether different glucose concentrations may impact on EAT functions. **Methods:** EAT biopsies were collected from non-diabetic CAD patients enrolled during coronary artery bypass surgery ( $n = 5$ ). EAT-derived mesenchymal stem cells (MSCs) were isolated and cultured in high glucose (HG 25 mmol/l) or normal glucose (NG 5.5 mmol/l) concentration, as control. Cell surface markers were assessed by fluorescence-activated cell sorting (FACS) analysis and gene expression levels by real-time reverse transcription polymerase chain reaction (RT-PCR). Cytokine and chemokine secretions were measured using the Bio-Plex Multiplex assay. **Results:** EAT-MSCs cultured in NG and HG exhibited similar proliferation rate and cell surface marker expression. Interestingly, HG-treated EAT-MSCs displayed a 50% decreased expression of the multipotent markers Oct-4 and Nanog. HG-treated EAT-MSCs maintained their adipogenic and osteogenic potential after the application of appropriate induction media; however, either lipid or calcium accumulation seemed to be lower compared with NG-cultured cells. Moreover, mRNA levels of the senescence markers p21<sup>CIP1/WAF1</sup> and p16<sup>INK4A</sup> were significantly increased in HG-cultured cells, as well as the fibrosis-associated gene *ACTA2*. Consistent with these data, a senescence-associated secretory phenotype (SASP) was observed in HG-treated MSCs. **Conclusions:** Collectively, these data indicate that a diabetic-like environment directly affects the hallmarks of “stemness” of EAT-derived MSCs, driving toward accelerated senescence or fibrosis.

### Selected Solid Tumor Abstracts

#### 09-OR12. Serial Monitoring of Plasma ctDNA in Metastatic Colorectal Cancer Patients Detects Changes in Key Mutations and Disease Progression Using the FOLLOW IT Assay from the Exactis Trial (NCT00984048)

M.K. McConechy<sup>1</sup>, S. McNamara<sup>2</sup>, M. Couetoux du Tertre<sup>2</sup>, K. Gambaro<sup>2</sup>, M. Marques<sup>2</sup>, S. Malikic<sup>1</sup>, K.M. Nip<sup>1</sup>, S. Brahmhatt<sup>1</sup>, A. Kense<sup>1</sup>, K. Tam<sup>1</sup>, J. Khattri<sup>1</sup>, M. Couse<sup>1</sup>, R. Miller<sup>1</sup>, R. Aguirre Hernandez<sup>1</sup>, G. Batist<sup>3,4</sup>

<sup>1</sup>Contextual Genomics, Vancouver, BC, Canada, <sup>2</sup>Exactis Innovation, Montreal, QC, Canada, <sup>3</sup>Segal Cancer

Centre-Jewish General Hospital, Montreal, QC, Canada, <sup>4</sup>McGill University, Montreal, QC, Canada.

**Introduction:** Liquid biopsies are a useful tool in precision medicine for therapy selection, with potential as a disease monitoring tool. Our aim was to determine if longitudinal plasma monitoring in metastatic colorectal cancer (mCRC) patients can aid in predicting clinical progression prior to CT imaging, and identify resistance mechanisms in patients undergoing therapy. **Methods:** From 50 mCRC patients enrolled in the Exactis trial (NCT00984048) undergoing first-line treatment, we assessed for plasma circulating tumor DNA (ctDNA) mutations and correlated with mutations identified in whole exome sequencing (WES) from metastatic tumor biopsies. Approximately 220 plasma samples collected at baseline, on treatment, and at time of clinical resistance were analyzed using the Contextual Genomics FOLLOW IT assay and QUALITY NEXUS bioinformatics analytical pipeline. FOLLOW IT is a clinically actionable hotspot panel that evaluates the ctDNA mutation status of 30 genes, 23 exons, and 146 hotspots. Patient response was based on RECIST v1.0 criteria. **Results:** We detected ctDNA mutations including *KRAS/NRAS* (52%), *PIK3CA* (26%), *BRAF* (6%), and *TP53* (74%) in at least 1 plasma timepoint in 92% of patients, and in 76% of multiple timepoints. In 3 of 4 patients with no ctDNA mutations, tumor WES revealed no mutations in genes covered by FOLLOW IT. The remaining patient harboured both a *KRAS* and *PIK3CA* mutation in the tumor WES; both were present in ctDNA but were below the validated threshold. Plasma baseline sequencing revealed ctDNA mutations in 15 patients that were not identified by tumor WES, of which 13 were *KRAS*. Of 26 responders, 38% harboured *KRAS* ctDNA mutations, 11% *PIK3CA*, and 1 with *KRAS* and *PIK3CA* concurrent mutations. In 24 in the acquired or intrinsic resistance group, 95% harboured ctDNA mutations with 67% as *KRAS* or *NRAS*, 42% *PIK3CA*, and 33% with concurrent *KRAS* and *PIK3CA*. In 17 of 23 (74%) patients, ctDNA mutations were found before progression based on CT scan. For a subset of patients (7) we tested >4 plasma samples within the clinical course to show the dynamics of ctDNA and carcinoembryonic antigen (CEA) levels across treatment. Plasma time points from additional patients will be sequenced to identify earlier detection of ctDNA mutations prior to progressive disease.

**Conclusions:** This study showed that the FOLLOW IT liquid biopsy assay can detect clinically actionable ctDNA mutations within a clinical trial. The use of ctDNA as a longitudinal disease-monitoring tool could allow for re-evaluation and potential change in management of mCRC patients before progression detected by CT imaging. Additionally, detection of concurrent *PIK3CA* and *KRAS* ctDNA mutations within the resistance population warrants further investigation for clinical utility in patient stratification.

### 09-OR13. Toward Internationally Agreed Units for Cancer Genomic Measurement Worldwide: The Role of WHO International Standards

A.P. Sanzone, J. Boyle, R. Hawkins  
National Institute for Biological Standards and Control,  
Advanced Therapies Division, Potters Bar, United  
Kingdom.

**Introduction:** The timely development of well-characterized World Health Organization (WHO) International Standards is a critical aspect in the harmonization of biological measurement worldwide, helping scientists, regulatory authorities, and manufacturers involved in patient care ensure the reliability of *in vitro* diagnostic tests, quality of biological products, consistency of production, and establishment of appropriate clinical dosing. This is especially important in the rapidly expanding field of cancer genomics where testing accuracy is essential and data benchmarks create challenges for the efficient development of the field and appropriate clinical use of results. Toward this, the National Institute for Biological Standards and Control (NIBSC, UK) is developing WHO International Standards for the calibration of secondary standards, assays, and applied research, investigating the relationship between nucleic acids, rare event, and copy number variation (CNV) measurement in both solid tumour and liquid biopsy cancer genomics. **Methods:** Genomic DNAs of the proposed 1st WHO International Reference Panel for *KRAS* codons 12 and 13 mutations and 1st WHO International Standards for Cancer Genomes were evaluated in international collaborative studies to assess their performance in commonly used methods and to derive data for both variant allele percentage and copy number variants (CNVs). The materials were blindly tested at several dilutions by multiple laboratories (n = 35-56) using their routine quantification methods.

**Results:** Consensus variant allele percentages were established from next-generation sequencing (NGS) and digital polymerase chain reaction (dPCR) data for *KRAS*, *PIK3CA*, *TP53*, *NRAS*, *PTEN*, and *MAP2K1/MEK1* variants. Dilution responses of these materials with wild-type genomic DNA (diploid, 2 wild-type gene copies) were used to train a model-fitting algorithm that enabled us to predict the CNV in each of the materials and to predict variant allele percentages resulting from other dilutions; this model fitting was validated for additional lower dilutions for each of the materials with droplet dPCR (ddPCR). **Conclusions:** The strong agreement of the in-house ddPCR data with the collaborative study consensus mutation percentages and the model-derived data provided confirmation of the suitability of model in deriving the CNVs. This approach is now being further validated by NGS and a broader range of samples (CNV materials from commercial providers and patient samples). The 1st WHO International Reference Panel for *KRAS* codons 12 and 13 mutations and 1st WHO International Standards for Cancer Genomes are now endorsed by the WHO and available from NIBSC to aid the global cancer genomics community in standardizing

measurement for both variant allele percentage and cancer gene copy number.

### 09-OR14. SureMASTR SureMASTR HRR Assay Is an Extensive Research Solution for SNV, Indel and CNV/CNA Detection in 17 HRR-Related Target Genes in Blood- and FFPE-Derived DNA

K. Bettens<sup>1</sup>, C. De Vogelaere<sup>1,2</sup>, A. Vanderstichele<sup>3,4</sup>, L. Claes<sup>1</sup>, N. Van Den Broeck<sup>1</sup>, J. Verbist<sup>1</sup>, N. Remmerie<sup>1</sup>, H. Swennen<sup>1</sup>, L. Heyrman<sup>1</sup>, R. De Smet<sup>1</sup>, J. Vermeire<sup>1</sup>, J. De Schrijver<sup>1</sup>, P. Busschaert<sup>3,4</sup>, I. Vergote<sup>3,4</sup>, J. Crappé<sup>1</sup>, A. Rothier<sup>1</sup>, D. Goossens<sup>1</sup>, R. Allen<sup>5</sup>, D. Lambrechts<sup>2,6</sup>, J. Del-Favero<sup>1</sup>

<sup>1</sup>Agilent Technologies, Diagnostics and Genomics Group, Niel, Belgium, <sup>2</sup>Laboratory for Translational Genetics, Department of Oncology, KU Leuven, Leuven, Belgium, <sup>3</sup>Department of Gynaecology and Obstetrics, University Hospitals Leuven, Leuven, Belgium, <sup>4</sup>Leuven Cancer Institute, KU Leuven, Division of Gynaecological Oncology, Leuven, Belgium, <sup>5</sup>Agilent Technologies, Diagnostics and Genomics Group, La Jolla, CA, United States, <sup>6</sup>VIB, Vesalius Research Center, Leuven, Belgium.

**Introduction:** Growing evidence shows that defects in the homologous recombination repair (HRR) pathway underlie hereditary and sporadic tumorigenesis, and that HRR deficiency may underlie sensitivity of tumors to therapies targeting DNA repair, such as platinum-based chemotherapy and PARP inhibitors. The SureMASTR HRR next-generation sequencing (NGS) assay developed by Agilent Technologies contains 17 HRR genes (*ATM*, *BARD1*, *BRCA1*, *BRCA2*, *BRIP1*, *CDK12*, *CHEK1*, *CHEK2*, *FANCA*, *FANCL*, *NBN*, *PALB2*, *RAD51B*, *RAD51C*, *RAD51D*, *RAD54L*, and *TP53*), selected based on mutational analysis of a 52 HRR gene panel in 300 high-grade serous ovarian cancer samples, together with the most recent literature research and input from key opinion leaders. **Methods:** The SureMASTR HRR assay was optimized as a singleplex targeted polymerase chain reaction (PCR)-based assay and comprises 1,119 amplicons, ranging in size from 120 bp to 160 bp. The assay was optimized for cost-efficient use of NGS capacity. The SureMASTR HRR with MASTR Reporter HRR germline and somatic application workflows were verified by Agilent Technologies on 1) Illumina MiSeq and MiniSeq platforms on germline DNA samples, and 2) on NextSeq platform on formalin-fixed, paraffin-embedded (FFPE)-derived DNA samples. **Results:** Verification studies of the SureMASTR HRR assay showed 1) target read mapping (>91.0% for germline, >95.0% for somatic samples), and 2) uniformity of amplification (99.0% for germline, 94.0% for somatic) within 0.2x mean coverage. All germline variants (SNVs, Indels, CNVs in MiniSeq data) were successfully identified by SureMASTR HRR and HRR MASTR Reporter germline application. All somatic variants (SNVs, Indels) were identified by SureMASTR HRR and MASTR Reporter HRR MASTR Reporter somatic application. The average limit of detection of

SureMASTR HRR is 0.36%. **Conclusions:** The SureMASTR HRR assay is a singleplex assay covering 17 most relevant HRR pathway genes, significantly reducing the hands-on time, DNA input and required sequencing capacity. The SureMASTR HRR assay with MASTR Reporter application provides an accurate and precise workflow. The MASTR Reporter HRR somatic application allows visualization of copy number aberrations (CNA) in FFPE-derived DNA. SureMASTR HRR is for Research Use Only. Not for use in diagnostic procedures.

#### 09-OR15. Difficulties in Analyzing Microsatellite Instability in Endometrial Cancer - the Pros and Cons of Four Different PCR-Based Testing Approaches

J. Siemanowski<sup>1</sup>, T. Buhl<sup>1</sup>, B. Schömig-Markiefka<sup>1</sup>, U. Siebolts<sup>2</sup>, A. Haak<sup>2</sup>, W. Dietmaier<sup>3</sup>, N. Arens<sup>4</sup>, R. Büttner<sup>1</sup>, S. Merkelbach-Bruse<sup>1</sup>

<sup>1</sup>University Hospital Cologne, Pathology, Cologne, Germany, <sup>2</sup>University Hospital Halle (Saale), Pathology, Halle (Saale), Germany, <sup>3</sup>University Regensburg, Pathology, Regensburg, Germany, <sup>4</sup>Molecular Pathology Trier, Trier, Germany.

**Introduction:** Microsatellite instability (MSI), a common alteration in endometrial cancers (EMCs), is recently designated as a predictive biomarker for response to immune checkpoint therapy. Using MSI testing methods validated for colorectal cancer (CRC), former studies already described difficulties in analysis due to differences of MSI profiles. These differences enhance the possibility of false negative results. This study compares 4 different polymerase chain reaction (PCR)-based testing approaches for MSI detection initially designed for the detection of MSI in CRC and immunohistochemistry for mismatch repair (MMR) deficiency testing, and visualizes the difficulties of each of them regarding reliability, handling, and cost effectiveness. **Methods:** Twenty-five endometrial tumors immunohistochemically diagnosed as MMR-deficient, MMR-proficient, and with uncertain status were selected. Tumor and paired normal tissue DNA were extracted from formalin-fixed, paraffin-embedded (FFPE) material. MSI testing was performed by fragment length analysis with an in-house Bethesda panel and the MSI Analysis System (Promega) as well as parallel sequencing with a custom GeneRead DNaseq Panels V2 (Qiagen). A total of 10 µm slices of the same FFPE tumor tissues and DNA extracts for re-analysis were taken for the Idylla MSI assay (Biocartis). **Results:** Uncertain MSI status due to inaccurate immunohistochemistry (IHC) was clarified by using the described PCR approaches. Because of differences in MSI profiles for some of the samples, analysis and interpretation of results were more time consuming with the Bethesda panel and Promega analysis. The Idylla MSI assay showed high overall concordance after adjustment of testing parameters. The mean value of deleted bases using the Qiagen approach of endometrial cancer was lower than known for CRC, leading to difficulties in interpretation. **Conclusions:** All

MSI testing methods provided a high overall concordance in their results. Using the Bethesda panel and the MSI Analysis System of Promega, detection of MSI is more time consuming during interpretation to avoid false negative results due to smaller shifts in microsatellite repeat length in endometrial cancer samples. Using parallel sequencing, borderline values for deleted bases showed that additional markers have to be added to the panel, or the average of deleted bases indicating MSI-H status has to be validated in a new context. The Idylla MSI assay with easy result interpretation and short hands-on time is a promising tool to analyze MSI status in endometrial cancer but has to be adjusted regarding the tumor cell content and amount of tumor tissue needed for reliable results. If only 1 MMR marker is lost after IHC, additional testing with a PCR-based method has to be done to avoid false negative results.

#### Selected Other Abstracts

#### 10-OR16. RNA Sequencing Using Non-Cell Block Cytology Slides Demonstrates Specific Advantages over Formalin-Fixed, Paraffin-Embedded Specimens

N. Sidiropoulos<sup>1,2</sup>, D. Francis<sup>1</sup>, J. Armstrong<sup>1</sup>, M. Cameron<sup>1</sup>, K. Hampel<sup>1</sup>

<sup>1</sup>University of Vermont Health Network, Pathology and Laboratory Medicine, Burlington, VT, United States,

<sup>2</sup>Robert Larner College of Medicine at the University of Vermont, Burlington, VT, United States.

**Introduction:** Gene fusions are a significant category of clinically relevant driver mutations in non-small cell lung cancer (NSCLC). Assessment with fluorescence *in situ* hybridization (FISH) and immunohistochemistry (IHC) is common, but direct sequencing of the genes, though challenging, is advantageous. Presented is the experience with RNA next-generation sequencing (NGS) to interrogate 330 NSCLC samples for *ALK*, *RET*, and *ROS1* fusions. Both formalin-fixed, paraffin-embedded (FFPE) and non-cell block (NCB) cytology samples that can be used for RNA NGS are reported with emphasis on the advantages and disadvantages of each.

**Methods:** Amplicon sequencing interrogates select exons in *ALK*, *RET*, and *ROS1*. Amplicon libraries were prepared using ArcherDX FusionPlex reagents, and pooled libraries were sequenced on an Illumina MiSeq. Bioinformatics analysis, results review, and annotation were performed using an ArcherDX Analysis suite hosted in the Clinical Genomicist Workspace (CGW) at PierianDx. **Results:** Overall NCB cytology specimens comprised 60% of RNA sequencing analyses, with the remaining 40% divided among FFPE tissue and cell block preparations. The RNA quantity not sufficient rate was <5% and did not vary with specimen type. RNA extracted from NCB cytology samples is, however, approximately 2-fold higher quality than that extracted from FFPE specimens as quantified by control amplicon unique coverage normalized to the number of sequencing reads. RNA quality failures for the 2

specimen types did not exceed 3% for any specimen source, with the exception of a period of NCB cytology-derived RNA failures. During this time it was determined that Pap-stained RNAs failed quality assessment at a rate of 63% due to a soluble inhibitor originating in the staining reagent mixture. A simple clean-up method is presented that eliminated these failures and restored quality failure rates to <3%. **Conclusions:** RNA NGS for fusion events in NSCLC can be successfully integrated into a clinical NGS workflow where FFPE and NCB cytology samples are routinely used. Validating RNA NGS for gene fusion detection streamlines tissue utilization of small biopsies, easily enables integrated genomic reporting, and adequately interrogates fusion events of *ROS1* intron 31, a site of clinically actionable fusions that is difficult to consistently detect with DNA-based NGS. Removal of substances inhibitory to NGS sequencing library preparation is a significant challenge for clinical laboratories. It will be important to determine if the method we describe here can be of more general utility for the removal of soluble inhibitors in clinical nucleic acid extracts.

### Selected Poster Abstracts

#### Selected Genetics/Inherited Conditions Abstracts

##### 01-P01. Molecular Characterization and Copy Number Analysis of *SMN1* and *SMN2* in Pakistani Patients with Spinal Muscular Atrophy (SMA)

A. Nasir, Z. Ahmed

Aga Khan University, Pathology and Lab Medicine, Karachi, Pakistan.

**Introduction:** Spinal muscular atrophy (SMA) is characterized by muscle weakness and atrophy resulting from progressive degeneration and loss of the anterior horn cells in the spinal cord and the brain stem nuclei. The onset of weakness ranges from birth to adolescence or young adulthood.

**Methods:** Genomic DNA was isolated, and *SMN1* and *SMN2* genes were amplified by multiplex ligation-dependent probe amplification (MLPA), detected by capillary electrophoresis, and analyzed by Coffalyser software. This method is a relatively simple and robust multiplex polymerase chain reaction (PCR) method for detecting chromosomal DNA copy number changes in multiple targets (MRC Holland). **Results:** Out of 142 patients, 67 (47%) were identified as homozygous deletion of *SMN1* gene in exon 7 and 8, whereas 8 (5.6%) patients were identified as heterozygous; among those homozygous, 4 patients have 3 copies of *SMN2* gene, whereas 3 heterozygous patients have 1 copy of *SMN2*. The rest of the patients were reported as 2 copies of *SMN2* gene. **Conclusions:** Multiplex ligation-dependent probe amplification (MLPA) is a

versatile technique for relative quantification of different nucleic acid sequences in a single reaction. Here, we establish a quick MLPA-based assay for the detection of *SMN1* and *SMN2* copy numbers with high specificity and low complexity.

##### 01-P02. Detection of Microdeletion by Fluorescence *in situ* Hybridisation

Z. Ahmed, S. Siddiqui, Z. Khattak, M. Sharif, T. Moatter

Aga Khan University, Pathology and Lab Medicine, Karachi, Pakistan.

**Introduction:** Microdeletions are approximately 1-3 Mb long and cannot be detected by light microscopy; therefore, fluorescence *in situ* hybridization (FISH) provides a powerful tool to identify the deletion on metaphase chromosomes. It has been observed that clinical diagnosis of microdeletion syndrome is difficult due to the large phenotypic variability. It is mostly spontaneous and reported in approximately 5% of patients with unexplained mental retardation with multiple congenital anomalies and developmental delay. We detected microdeletion syndrome in patients clinically suspected of having DiGeorge syndrome, Prader-Willi syndrome, and William syndrome by FISH technique from 2015-2019 at Aga Khan Hospital. **Methods:** FISH testing was performed on the 170 blood specimens of clinically suspected patients from 2015-2019 at Aga Khan Hospital. By using Abbott Molecular FISH probe, 22q11.2 (*TUPLE1*) gene deletion was detected in DiGeorge syndrome, whereas 15q11 (*SNRPN*) gene deletion was detected in Prader-Willi syndrome, and 7q (*ELN*) deletion in William syndrome was observed in metaphases via fluorescence microscope. **Results:** In the current study, we have investigated a total of 170 blood samples of patients referred by pediatricians across Pakistan. These patients were tested for microdeletions at Aga Khan University Hospital over the past 5 years, with ages ranging from 5 months to 18 years. It has been found that 11 (19%) out of 57 samples showed 22q11.2 gene deletion, indicating DiGeorge syndrome; 10 (10%) out of 100 samples showed 15q11 deletion, suggesting Prader Willi syndrome; and 7 (58%) out of 12 samples showed 7q deletion, suggesting William syndrome. **Conclusions:** FISH would help in early detection, so that appropriate clinical management plans could be formulated to manage the other complications arising from microdeletion syndromes. **Keywords:** William syndrome, DiGeorge syndrome, Prader Willi, 7q, 15q, 22q11

### 01-P03. The Frequency of Structural Chromosomal Rearrangements in Susceptible Individuals with Recurrent Abortions and Miscarriages by Karyotyping

Z. Ahmed, K. Sachwani, A. Zehra, S. Sharif, S. Hussain, T. Moatter  
Aga Khan University, Pathology and Lab Medicine, Karachi, Pakistan.

**Introduction:** Recurrent abortions and miscarriages are the most common complications in pregnancy. It can be associated with many factors, including advanced maternal and paternal age, infectious diseases, environmental toxins, congenital and structural uterine anomalies, and genetic abnormalities. The aim of this study is to screen for structural chromosomal abnormalities in couples having recurrent pregnancy loss and the factors most commonly associated with these circumstances. **Methods:** Cytogenetic study was carried out on phytohemagglutinin (PHA)-stimulated peripheral blood specimens collected from January 2017 to September 2019. Culturing, harvesting, and GTG banding protocols were followed per the AGT Cytogenetics Laboratory Manual, and the karyotype designation was done according to the International System for Human Cytogenetic Nomenclature (ISCN 2016). A cytogenetic study was performed on 578 individuals (M:F ratio 1:1) with infertility and/or abortion with age range 18-50 years. **Results:** A total of 578 karyotypes were screened from January 2017 to September 2019 in which normal karyotypes were 548 (95%), and 30 (5%) were positive for structural chromosomal aberrations. Twenty-eight individuals had karyotypes showing balanced translocations; among these, 20 were female and 8 were male carriers. In addition, two females had markers with chromosome and Robertsonian translocation. **Conclusions:** Early genetic counseling and cytogenetic analysis should be offered which could allow the couples to make decisions regarding future pregnancies. This issue can also play a role in the health of pregnant mothers.

### 01-P04. Impaired Prostaglandin E2 Regulation in EAT Is Associated with Maladaptive Cardiac Remodeling in Overweight CVD Population Via EPAC2 and ST2 Expression

E. Vianello<sup>1</sup>, E. Dozio<sup>1</sup>, F. Bandera<sup>1,2</sup>, M. Froidi<sup>3,4</sup>, J. Lamont<sup>5</sup>, L. Tacchini<sup>1</sup>, G. Schmitz<sup>6</sup>, M.M. Corsi Romanelli<sup>1,7</sup>

<sup>1</sup>Università degli Studi di Milano, Department of Biomedical Sciences for Health, Milan, Italy,

<sup>2</sup>Heart Failure Unit, IRCCS Policlinico San Donato, Cardiology University Department, San Donato Milanese, Italy, <sup>3</sup>Università degli Studi di Milano, Department of Clinical Sciences and Community Health, Milan, Italy, <sup>4</sup>IRCCS Policlinico

San Donato, Internal Medicine Unit, San Donato Milanese, Italy, <sup>5</sup>Radox Laboratories LTD, R&D, Crumlin-Antrim, Belfast, United Kingdom, <sup>6</sup>University Hospital Regensburg, Department of Clinical Chemistry and Laboratory Medicine, Regensburg, Germany, <sup>7</sup>IRCCS Policlinico San Donato, U.O.C. SMEL-1 of Clinical Pathology, San Donato Milanese, Italy.

**Introduction:** Recent evidence has demonstrated that the dysfunctional responses of epicardial adipose tissue (EAT) can directly promote cardiac enlargement in the case of obesity. Here we observed a newer molecular pattern associated with heart dysfunction mediated by PGE<sub>2</sub> deregulation in EAT from an overweight cardiovascular disease (CVD) population, associated with the activation of ST2/IL-33 mechanosensitive system via EPAC2 cAMP effectors. **Methods:** A series of 33 overweight CVD males were enrolled, and their EAT thickness and left ventricle (LV) mass and volumes were measured by echocardiography. Blood, plasma, and EAT biopsies were collected for molecular and proteomic assays. **Results:** Our data show that PGE<sub>2</sub> biosynthetic enzyme (PTGES-2) correlates with echocardiographic parameters of LV enlargement: LV diameters, LV end diastolic volume, and LV masses. Moreover, PTGES-2 is directly associated with the EPAC2 gene ( $r = 0.70$ ,  $p < 0.0001$ ), known as a molecular inducer of ST2/IL-33 mediators involved in maladaptive heart remodeling. Furthermore, PGE<sub>2</sub> receptor 3 was downregulated, and its expression was inversely associated with ST2/IL-33 expression. Contrarily, PGE<sub>2</sub> receptor 4 is upregulated in EAT and directly correlates with ST2 molecular expression. **Conclusions:** This indicates that body fat increase can shift EAT transcriptome to a pro-tissue remodeling profile driven by PGE<sub>2</sub> deregulation with consequent promotion of EPAC2 and ST2 signaling.

### 01-P05. Introduction of a New NGS Method to Detect BRCA1/2 Gene Copy Number Variations

Z. Linhua, J. Baolei, G. Huijuan, R. Li, Z. Mike AmoyDx, Xiamen, China.

**Introduction:** Clinical studies have shown that patients with pathogenic mutations in BRCA1 and BRCA2 genes can benefit from PARP inhibitors (PARPi). Large deletions of BRCA1/2 are important mutations, because most of them are (likely) pathogenic. The traditional method for large deletion detection is based on the multiplex ligation-dependent probe amplification (MLPA) method, which is separate from the detection of other mutations (e.g., SNVs and indels) and time consuming. The newly developed next-generation sequencing (NGS) Halo-shape ANnealing and

Defer-Ligation Enrichment (HANDLE) technology enables the copy number variation (CNV) detection together with other mutations from *BRCA1/2* genes. The total turnaround time for library preparation is only 5 hours, with hands-on time of only 1 hour. The objective of this study was to validate the CNV detection performance in samples with known CNV status using the MLPA method. **Methods:** A cohort of 118 blood samples were collected from AmoyDx Medical Institute. Most of the samples were derived from breast cancer patients, one was a pelvic serous carcinoma sample, and 4 samples were from patients with ovarian cancer. All samples underwent blind testing first, and then the results were compared with the MLPA results. A commercial *BRCA1/2* MLPA kit had been used. After DNA extraction, library construction was performed using the ADx *BRCA* NGS kit that was developed based on HANDLE technology. Libraries for all samples were successfully constructed and passed the quality qualification. Sequencing was performed on Illumina NextSeq 500 platform. Data analysis for CNV status of *BRCA1/2* genes was performed using AmoyDx ANDAS Data Analyzer. **Results:** All of the 118 samples were successfully detected, and 19 samples had a CNV in the exon region of the *BRCA1* or *BRCA2* gene. A total of 16 samples were detected with deletion mutations, whereas 3 were detected with gains. The size of CNV varied from ~200 bp to ~78.5 Kbp. By MLPA method, 18 samples were detected with CNV. Using MLPA assay as reference, the positive, negative, and overall concordance rate of CNV mutation status as determined by ADx *BRCA* NGS kit were 100% (118/118), 99% (99/100), and 99.15% (117/118), respectively (Table 1). One sample was detected to gain in exon 2 of the *BRCA1* gene that was negative from the result of the MLPA method. The false positive rate at this region was 0.85% (1/118). **Conclusions:** 1) The data showed a high concordance of *BRCA1/2* CNV status tested by ADx *BRCA* NGS kit compared to MLPA method with a 100% positive and a 99% negative concordance rate. 2) Our data showed that the HANDLE-based NGS technology is a good method for *BRCA1/2* gene CNV testing.

All (N=118) <sup>a</sup>		MLPA <sup>b</sup>		Total <sup>c</sup>
		Positive <sup>d</sup>	Negative <sup>e</sup>	
NGS <sup>f</sup>	Positive <sup>d</sup>	18 <sup>g</sup>	1 <sup>h</sup>	19 <sup>i</sup>
	Negative <sup>e</sup>	0 <sup>j</sup>	99 <sup>k</sup>	99 <sup>l</sup>
Total <sup>c</sup>		18 <sup>g</sup>	100 <sup>m</sup>	118 <sup>n</sup>
Positive predictive value <sup>o</sup>		94.74% (95%CI: 73.97% to 99.37%) <sup>p</sup>		
Negative predictive value <sup>q</sup>		100% (95%CI: 96.34% to 100.00%) <sup>r</sup>		
Positive concordance rate <sup>s</sup>		100% (95%CI: 81.47% to 100.00%) <sup>t</sup>		
Negative concordance rate <sup>u</sup>		99% (95%CI: 94.55% to 99.97%) <sup>v</sup>		
Overall concordance <sup>w</sup>		99.15% <sup>x</sup>		

**[Table 1.** Comparison of CNV between NGS and MLPA methods]

### 01-P07. Exome Sequencing Identifies Genetic Variants Responsible for Down-Sloping Hearing Loss in Korean Deafness Patients

J.H. Rim, J. Jung, M.S. Han<sup>2</sup>, J.Y. Choi, H.Y. Gee  
 Yonsei University College of Medicine, Seoul, Republic of Korea, <sup>2</sup>Seoul National University, Seoul, Republic of Korea.

**Introduction:** Hearing loss is the most common sensory disorder, affecting approximately 1 in every 500 newborns worldwide. As precision medicine in hearing loss patients is applicable in the clinical fields, identification of genetic landscape in certain patients becomes more important. Among various types of adult-onset hearing loss, hearing loss patients with down-sloping audiogram have difficulties in hearing children's voices or high-pitched female voices. Herein, we aim to elucidate genetic factors for down-sloping audiogram hearing loss patients. **Methods:** A total of 14 adult-onset hearing loss patients with ski-slope audiogram defined as normal auditory brainstem response (ABR) thresholds in low frequencies (500 Hz and 1 kHz) but abruptly high ABR thresholds in high frequencies were included in this study. Whole exome sequencing analysis was performed for all the patients, focusing on rare variants with allele frequencies lower than 0.0005. After manual curation of rare variants in multiple patients, candidate genes were prioritized based on evidence including gene features, variant analysis, and clinical characteristics. **Results:** One patient from our cohort was revealed to possess two compound heterozygous missense variants in the *TMPRSS3* gene, which is one of the known deafness genes associated with down-sloping audiogram. Copy number variation using two different algorithms (ExomeDepth, EXCAVATOR) presented no definitive pathogenic mutation responsible for hearing loss. From a total of 4,696 rare variants found in the remaining 13 patients,

we narrowed down to 435 variants in 185 genes, which were found in multiple patients. Finally, a total of 27 candidate genes were selected based on population database frequency, *in silico* results, and inheritance mode in patients. Two missense variants in *DLL1*, one component of Notch signaling, were co-segregated within the families. Functional studies including biotinylation Western blot, immunofluorescence staining, and co-culture assay revealed gain-of-function effects in these variants compared to wild-type. **Conclusions:** We comprehensively studied the mutational spectrum of down-sloping hearing loss patients and presented 27 candidate genes. Our hypothesis for *DLL1* association with down-sloping hearing loss is that missense variants in *DLL1* might not present harmful effects during development but cause activation of Notch signaling by gain of function in only adult cochlea which might have already accumulated acoustic trauma and aging effects with adult-onset phenotypes.

#### 01-P09. Levels and Polymorphisms of Glutathione-S-transferase Omega-1 (GSTO1-1) as Pathogenic Factors and Prognostic Markers in Cystic Fibrosis

A. Corti<sup>1</sup>, S. Piaggi<sup>1</sup>, E. Marchi<sup>1</sup>, V. Carnicelli<sup>2</sup>, R. Zucchi<sup>2</sup>, M. Griese<sup>3</sup>, A. Hector<sup>4</sup>, A. Pompella<sup>1</sup>

<sup>1</sup>University of Pisa, Department of Translational Research NTMS, Pisa, Italy, <sup>2</sup>University of Pisa, Department of Surgical, Medical, Molecular and Critical Pathology, Pisa, Italy, <sup>3</sup>Ludwig-Maximilians-University Munich, Children's Hospital, Munich, Germany, <sup>4</sup>University of Tübingen, Children's Hospital-Section of Pediatric Infectiology and Immunology, Tübingen, Germany.

**Introduction:** The omega class of glutathione S-transferases (GSTO) is the most recently defined class belonging to the cytosolic GST superfamily. Two different GSTO isoforms (GSTO1-1, GSTO2-2) were identified in humans. Recent findings have suggested that the thioltransferase activity of GSTO1-1 might contribute to the redox modulation of different cellular pathways, including the pro-inflammatory LPS/TLR-4-induced activation of NF- $\kappa$ B and the NLRP3 inflammasome activation. Moreover, the association of GSTO1-1 polymorphisms with cancer progression and inflammatory diseases has also been investigated. On the other hand, only a very limited number of studies about chronic obstructive pulmonary disease (COPD) have focused on the possible implication of GSTO1-1 levels and polymorphisms in chronic pulmonary diseases. Our aim was thus to investigate the expression and polymorphisms of GSTO1-1 in samples from cystic fibrosis (CF) patients and their possible correlation with inflammatory markers. **Methods:** We have determined GSTO1-1 levels by immunoblot in

sputum samples included in two large, previously published studies (Griese *et al.* Am J Respir Crit Care Med, 2013; Corti *et al.* J Cyst Fibros, 2017). GSTO1-1 polymorphisms (A140D and E155del) were also evaluated by the restriction fragment length polymorphism (RFLP) technique on blood samples. The biochemical parameters measured in the aforementioned study were re-evaluated for their potential correlations with GSTO1-1 levels and polymorphisms. **Results:** Different levels of GSTO1-1 were detected in CF sputum, and significant correlations between GSTO1-1 and some markers of inflammation (neutrophils count, neutrophilic elastase, IL-8) were found. On the other hand, a negative correlation was found between GSTO1-1 levels and prostaglandin E2 (PGE2), a mediator with bronchodilator and vasoactive effects. A negative correlation was also found between GSTO1-1 and two lung function parameters, namely FEV1% (FEV1/FEV1 predicted) and FEV1/FVC (Tiffeneau-Pinelli index). The latter is a ratio used to discriminate between obstructive and restrictive disease of the lung. Finally, RFLP analysis revealed a negative correlation of GSTO1-1 A140D polymorphism with both PGE2 levels and the Tiffeneau-Pinelli index. **Conclusions:** Our data indicate that GSTO1-1 levels in CF sputum are associated with lung inflammation in CF, even if the source and the mechanism of GSTO1-1 release in the airways need to be elucidated. On the other hand, the presence of the A140D polymorphism could contribute to the development of airway obstruction in CF, suggesting its potential role as a genetic modifier in CF traits. Supported by University of Pisa (PRA\_2015\_0001 funds).

#### 01-P10. VEGF-A Rs3025039 Is a Genetic Susceptibility Factor for Non-Melanocytic Skin Cancer in Aging People

L. Scola<sup>1</sup>, G. Candore<sup>1</sup>, C.R. Balistreri<sup>1</sup>, M. Bova<sup>1</sup>, R.M. Giarratana<sup>1</sup>, G. Pistone<sup>2</sup>, D. Lio<sup>1</sup>, M.R. Bongiorno<sup>2</sup>

<sup>1</sup>University of Palermo, Clinical and General Pathology, Department of Biomedicine, Neuroscience and advanced Diagnostic (Bi.N.D), Palermo, Italy, <sup>2</sup>University of Palermo, Department of Dermatology, Palermo, Italy.

**Introduction:** The incidence of the vast majority of cancers, including melanoma, increases with advancing age. However, the mechanism by which aging influences the risk of developing cancer has not been fully understood, and genetic factors might play a protective or susceptibility role. Increased expression of transforming growth factor- $\beta$  (TGF- $\beta$ ) and vascular endothelial growth factor-A (VEGF-A) characterize the peri-tumoral skin microenvironment in non-melanocytic skin cancers, basal cell carcinoma, and squamous cell

carcinoma (NMSCs), and melanoma. In this view, the role of functionally relevant genetic polymorphisms of the TGF- $\beta$  pathway and VEGF-A in susceptibility to non-melanocytic skin tumor was assessed. **Methods:** A total of 140 patients with skin neoforations (64 affected by clinically and histologically characterized NMSC) and 116 age- and gender-related healthy controls were typed for TGF- $\beta$ 1 (rs1800471), TGF- $\beta$ 2 (rs900), TGF- $\beta$ R1 (rs334348, rs334349), TGF- $\beta$ R2 (rs4522809), and VEGF-A (rs3025039) functionally relevant genetic polymorphisms using on-demand assays developed by KBioscience Ltd. (Middlesex, UK). Tests apply homogeneous fluorescence resonance energy transfer (FRET) detection and allele specific polymerase chain reaction (PCR) (KASPar). **Results:** In spite of the central role of TGF- $\beta$  pathways in skin cancer analyses of genotype, frequencies did not allow us to find significant differences among patients and controls. On the other hand, there was a significant increased frequency of rs3025039 T allele-bearing genotypes in patients older than 65 years old ( $p = 0.0268$ , Odds Ratio = 3.927, 95% Confidence Interval: 1.25 to 12.33 for CT and TT genotypes compared to CC genotype frequency). On the contrary, no significant differences were observed comparing patients <65 years old with age-matched or unmatched controls. An rs3025039 C>T substitution induces the loss of a potential binding site for the transcription factor activator protein-4 that might influence VEGF production. **Conclusions:** The current report seems to suggest an age-related functional pleomorphism of VEGF-A rs3025039 that might impinge on VEGF-A functions differently in young and aging people, behaving as a predisposing factor for NMSC in subjects over 65 years old.

#### 01-P11. Role of *MIF* rs1007888 Polymorphism in Sicilian ESRD Patients and Related Disease

R.M. Giarratana<sup>1</sup>, L. Scola<sup>1</sup>, C.R. Balistreri<sup>1</sup>, M. Guameri<sup>2</sup>, S. Cottone<sup>2</sup>

<sup>1</sup>University of Palermo, Clinical and General Pathology, Department of Biomedicine, Neuroscience and advanced Diagnostic (Bi.N.D), Palermo, Italy, <sup>2</sup>"G.D'Alessandro"- University of Palermo, Unit of Nephrology and Hypertension, Department of Health Promotion, Mother and Child Care, Internal Medicine and Medical Specialties, Palermo, Italy.

**Introduction:** Systemic low-grade inflammation is among the most important causes of frailty, age-related diseases, and deaths. Macrophage migration inhibitory factor (MIF) is a protein that can function as cytokine, hormone, or enzyme, and exhibits a variety of biological roles involved in onset and maintenance of the inflammatory response. Single nucleotide polymorphisms

(SNPs) of the *MIF* gene correlate with increased susceptibility to atherosclerosis, diabetes, obesity, and renal failure. High levels of urinary and serum MIF are found in patients with acute kidney injury and associated with markers of oxidative stress, endothelial dysfunction, and myocardial damage in chronic kidney disease. With this view, we have evaluated the frequency of *MIF* SNPs in patients affected by renal disease at the end stage (end-stage renal disease, ESRD) to understand if their presence might be related to modifications of clinical indicators (hemoglobin, C-reactive protein, blood pressure, weight, albumin, LDL cholesterol) associated with major diseases that complicate ESRD. **Methods:** We selected 2 SNPs of *MIF* genes (rs755622 and rs1007888) located in different positions of genes. Ninety-one end-stage chronic kidney disease (CKD) subjects and 127 healthy controls were recruited. Genotypic analyses were performed using KASPar SNP genotyping method (KBioscience Ltd., Middlesex, UK). Tests apply homogeneous fluorescence resonance energy transfer (FRET) detection and allele-specific PCR. **Results:** The analysis of distribution of *MIF* SNPs underlined that no significant differences were observed between case and control groups. Similar results were obtained by the intra-analysis of CKD patients, stratified according to age. No significant differences were observed by analyzing hemoglobin, C-reactive protein, blood pressure, weight, or albumin according to *MIF* SNP genotypes. On the contrary, *MIF* rs1007888-TC SNP was associated with different levels of serum cholesterol LDL. Actually, patients with CC genotype showed a significantly high serum level of LDL (Mean  $\pm$  SD: 104.69  $\pm$  41.7 patients CC; Mean  $\pm$  SD: 79.78  $\pm$  34.8 Patients T/\*  $p = 0.0171$ ) compared to the carrier of TT or TC genotypes.

**Conclusions:** Our findings strongly suggest that the presence of *MIF* rs1007888 CC genotype might influence lipidic metabolism in ESRD patients. In turn, this can lead to accumulation of plasma LDL in the artery walls, exposing patients to an increased risk of cardiovascular disease, one of the major diseases associated with ESRD.

#### 01-P12. hDNA-Free FLOQSwabs Buccal Swabs, a Screening Tools for the Detection of Inherited Gene Mutations Associated with Cancer

S. Allegrini, S. Landoni, M. Grugni, C. Marcialis, B. Meinardi, E. Repetti  
IMPACTLAB, Busto Arsizio, Italy.

**Introduction:** Genetic testing for inherited gene mutations are recommended in people who have a family history of inherited cancer susceptibility syndromes. Screening of gene mutations is investigated with genetic testing using multiple

gene panels. The sample collection is an important step to perform easy but high-quality genetic tests. Traditionally, genetic testing for inherited gene mutations was performed from blood; dry buccal swabs are a non-invasive sample and easily collected and stored at room temperature. COPAN hDNA-free FLOQSwabs (HDNAFS) with a dry active system were developed for the collection of buccal swabs for genetic screening. The objectives of this study were to evaluate: 1) the stability, quality, and quantity of patients' DNA collected with HDNAFS buccal samples sent dry to the laboratory, and 2) the performance of DNA from buccal samples collected with HDNAFS for gene mutations.

**Methods:** Buccal swabs (N = 100) collected with HDNAFS, delivered dry to the Impact Lab Unit, were used in this study. HDNAFS were processed with a COPAN NAO (nucleic acid optimizer) basket, and nucleic acids were extracted with the MagCore Genomic DNA Tissue Kit on the MagCore H16 Plus instrument. DNA quantity and quality were evaluated with the Qubit dsDNA BR Assay Kit on the Qubit 3 fluorometer. Next-generation sequencing (NGS) analysis of a multigene panel including *ABRAXAS1*, *ATM*, *APC*, *BARD1*, *BRCA1*, *BRCA2*, *BRIP1*, *CDH1*, *CHEK2*, *EPCAM*, *MLH1*, *MRE11*, *MSH2*, *MSH6*, *MUTYH*, *NBN*, *PALB2*, *PIK3CA*, *PMS2*, *PMS2CL(1)*, *PTEN*, *RAD50*, *RAD51C*, *RAD51D*, *STK11*, *TP53*, and *XRCC2* was performed with the Hereditary Cancer Solution kit on the MiSeq (Illumina), and data were analyzed with the SOPHiA DDM software. Hotspot mutations were confirmed with Sanger sequencing analysis, and copy number variations (CNVs) were confirmed with MLPA assay, both performed on SeqStudio Genetic Analyzer (Thermo Fisher). **Results:** In the 100 buccal swabs, delivered at room temperature and analyzed within 3 weeks, good quality and quantity of DNA was obtained from all samples. NGS sequencing detected valid data for hotspot mutations and CNV analysis in 90 of 100 (90%) samples; 10 samples had invalid data for CNV (10%); the probable causes related to the failure of the analysis need further investigation. Genotyping detected 10 of 90 (11%) samples with inherited gene mutations, most of them in *BRCA1* (3/10, 30%) or *BRCA2* (6/10, 60%), whereas 80 of 90 (89%) samples were WT for all the genes tested. **Conclusions:** Data generated in this study demonstrated that DNA extracted from buccal swab samples, collected with hDNA-free FLOQSwabs by the patients and sent dry to the laboratory, were suitable (good quantity, quality, and stability) for genetic screening of inherited gene mutations.

#### 01-P14. Next-Generation Sequencing-Based Approaches for mtDNA Analyses in Patients with Mitochondrial Disease

A. Nasca<sup>1</sup>, A. Legati<sup>1</sup>, N. Zanetti<sup>1</sup>, E. Lamantea<sup>1</sup>, D. Ghezzi<sup>1,2</sup>

<sup>1</sup>Institute of Neurology Besta, Milan, Italy,

<sup>2</sup>Università degli Studi di Milano, DEPT, Milano, Italy.

**Introduction:** Each human cell has thousands of mitochondria, and within each single mitochondrion, multiple copies of mitochondrial DNA (mtDNA) are present. Usually, all of these copies are identical, a status known as homoplasmy, but mutant mtDNA can coexist with wild-type (wt) mtDNA in the same cell (heteroplasmy). This is a dynamic phenomenon, and the proportion of mutated versus wt mtDNA may be different among cells in the same individual. Mitochondrial diseases (MD) are a clinically heterogeneous group of inherited disorders caused by mutations in mtDNA or in nuclear DNA genes coding for proteins that participate in mitochondrial functioning. MD have been associated with a wide range of multisystem phenotypes affecting primarily tissues with high energy demand, such as muscle and brain. Most of the mtDNA-related MD are due to heteroplasmic mutations, with higher mutation load in affected cells. The availability of DNA from affected tissues represents a crucial issue; muscle has been considered the best source for heteroplasmic point mutation analysis, and DNA from other specimens has been considered unreliable, because standard techniques (e.g., Sanger sequencing or restriction fragment length polymorphism) showed low sensitivity, incapable of detecting heteroplasmy below 10%-15%.

**Methods:** Whole mitochondrial DNA was amplified by PCR producing a single amplicon of 16.5 Kb. PCR product was then processed according to Nextera XT DNA library Prep Kit (Illumina) and sequenced on MiSeq benchtop sequencer (Illumina). For DNA extraction we used standard blood sampling and a non-invasive sample collection device (FLOQSwab, COPAN, Italia), suitable for shipping. **Results:** mtDNA sequencing showed a very good depth of coverage (>5,000x), with homogeneous distribution, allowing us to identify haplogroups and detect heteroplasmic point mutations with high accuracy even for mutations with very low percentages of heteroplasmy (about 2%-3%) and for mtDNA macrodeletions. Hence, we tested buccal swab as an easy and non-invasive sample collection method to have DNA for genetic analyses in MD patients. We found that the obtained DNA was suitable for the amplification of small amplicons from mtDNA and nuclear DNA, but also for amplification of whole mitochondrial

genome. In these samples, through next-generation sequencing (NGS) analysis it is thus possible to detect haplogroups, heteroplasmic mutations, and large deletions of the mtDNA.

**Conclusions:** We developed an integrated NGS approach, based on mtDNA sequencing at a very high depth of coverage, able to identify very low percentages of heteroplasmy. The increased sensitivity allows the use of DNA from specimens with low levels of heteroplasmy (e.g., buccal swab) for mtDNA mutation detection.

#### 01-P15. *SMN1* and *SMN2* Copy Number Distribution in 733 Clinical Cases of Carrier Screening for Spinal Muscular Atrophy

D. Toledo, E. Hughes, M. Johnston, G. Tsongalis, J. Lefferts

Dartmouth-Hitchcock Medical Center, Department of Pathology and Laboratory Medicine, Lebanon, NH, United States.

**Introduction:** Spinal muscular atrophy (SMA) is an autosomal recessive neuromuscular disorder characterized by degeneration of alpha motor neurons, leading to muscular weakness and atrophy. SMA is usually caused by a homozygous deletion of the *SMN1* gene, including at least exon 7. In patients with SMA, disease severity correlates with copy number of the *SMN1* paralog, *SMN2*. SMA carrier screening is now recommended to all women considering pregnancy or who are currently pregnant, leading to significant increases in screening volumes in the clinical lab. The pan-ethnic population carrier frequency of SMA is approximately 1 in 50, and as high as 1 in 35 in white/Caucasian ethnic populations. This study reviews the results from the first 733 carrier screening cases and the distribution of *SMN1* and *SMN2* copy numbers across our patient population. **Methods:** Extracted DNA from whole blood was obtained from 733 patients undergoing SMA carrier screening. We validated the droplet digital PCR (ddPCR; Bio-Rad) assay and currently utilize it to clinically assess copy number variation of *SMN1* and *SMN2*. A DNA input of 40 ng is used for the ddPCR protocol, which targets exon 7 of the *SMN1* and *SMN2* genes, as well as a reference gene. Allele, carrier, and presumed silent carrier frequencies for the first 733 cases are reviewed. **Results:** The first 733 clinical carrier screening cases processed in our lab resulted in the copy number distribution seen in Table 1. The SMA carrier frequency identified in our population is approximately 1 in 32 (23/733 have 1 copy of *SMN1* only), which is similar to or slightly higher than the Caucasian population frequency estimate of 1 in 35. The allele frequency of a zero-copy allele of *SMN1* is at least 23/1,466 (~1.57%). In addition, if we assume that individuals with 3 or 4

copies of *SMN1* have 2 copies of *SMN1* in cis, then 61/1,466 alleles in our population have duplicated *SMN1* copies on the same allele. Combining this frequency with the allele frequency of zero copies *SMN1* (23/1,466) gives a 0.065% or a 1 in 1,538 chance of being a silent (2 + 0) carrier in our population. Given our SMA carrier frequency of 1 in 32, these results indicate that approximately 1 in 48 carriers are silent carriers (2.08%), which is similar to the estimated 2% of carriers quoted in the literature. **Conclusions:** Using ddPCR for the first 733 carrier screening cases showed an interesting *SMN1*/*SMN2* copy number distribution, and suggests an expected or slightly higher SMA carrier rate in our rural population of New Hampshire and Vermont. This analysis of our SMA ddPCR assay is useful as a quality assurance metric, demonstrating ongoing high-quality assay performance.

n = 733	Copy Number 0	Copy Number 1	Copy Number 2	Copy Number 3	Copy Number 4	Copy Number >
SMN1	0 (0%)	23 (3.14%)	650 (84.6%)	59 (8.05%)	1 (0.14%)	0 (0%)
SMN2	79 (10.8%)	278 (37.9%)	351 (47.9%)	24 (3.27%)	0 (0%)	1 (0.14%)

**Table 1.** *SMN1* and *SMN2* copy number distribution of the first 733 clinical carrier screening cases]

#### 01-P16. Clinical Whole Genome Sequencing in Inherited Retinal Dystrophies

V. Jobanputra<sup>1,2</sup>, A. Rehman<sup>1</sup>, A. Thomas<sup>1</sup>, S. Guha<sup>1</sup>, H. Poisner<sup>1</sup>, A. Wilson<sup>1</sup>, A. Abhyankar<sup>1</sup>, S. Tsang<sup>2</sup>

<sup>1</sup>New York Genome Center, New York, NY, United States, <sup>2</sup>Columbia University Medical Center, New York, NY, United States.

**Introduction:** Inherited retinal dystrophies (IRDs) are a group of heterogeneous disorders that cause visual impairment in >2 million people worldwide. Determining the molecular basis of these ophthalmic disorders, associated with extreme clinical and genetic heterogeneity, has the ability to effectively diagnose and treat patients in the era of precision medicine. Whole genome sequencing (WGS) is a comprehensive test which provides better overall coverage of coding regions and can detect variants not identified by panels, exomes, or microarrays. We describe our experience of performing clinical WGS in >68 probands suspected to have IRDs. **Methods:** Genomic DNA libraries were prepared using KAPA Hyper Prep kit. Sequencing was performed on an Illumina HiSeq X instrument with 150-bp paired-end reads. Samples were sequenced to 30X mean coverage with a minimum of 85% of bases sequenced at 20X coverage. Sequencing

was mapped to the Genome Reference Consortium Human genome build 37 (GRCh37) sequence, and analysis performed using an in-house proprietary analytical pipeline. Variants were classified according to guidelines of the American College of Medical Genetics and Genomics. WGS detected single nucleotide variants including protein-coding and deep intronic non-coding variants, insertion-deletion (indels), copy number variants, and single and multi-exon deletions in disease genes associated with the individual's primary phenotype. Medically actionable secondary findings were reported for consented patients in the 59 genes recommended by the American College of Medical Genetics (ACMG SF v2.0). **Results:** Of the 60 cases analyzed to date, a positive finding of pathogenic or likely pathogenic variant(s) in genes that potentially explained the phenotype was noted in 21 cases, providing a positive genomic test yield of 35%. There were 5 cases which were only solved by WGS. In 3 cases, WGS revealed the "missing" second alleles, either rare deep intronic variants or multi-exon deletions in genes associated with an autosomal recessive IRD. One case had a homozygous 353-bp insertion of an Alu repeat in exon 9 of the *MAK* gene associated with retinitis pigmentosa 62. One case had a heterozygous deletion of exons 4 through 13 of *PRPF31*, a gene associated with autosomal dominant retinitis pigmentosa 11. The majority of patients opted in to receive secondary findings (49 of 60; 82%). Secondary findings were reported in 2 of 49 cases. **Conclusions:** This study demonstrates the power of WGS and its potential to provide higher diagnostic yield than conventional genetic testing. Performing WGS has a significant impact on the diagnostic accuracy of IRDs, which has direct impact on the patient care. Early detection of syndromic disease has important implications for other family members of the patient.

#### 01-P18. An International Interlaboratory Study of Complex Variant Detection in Clinical Genetic Testing

S. Lincoln<sup>1</sup>, A. Fellowes<sup>2</sup>, S. Chowhurdy<sup>3</sup>, S. Mahamdallie<sup>4</sup>, E. Klee<sup>5</sup>, R. Truty<sup>1</sup>, J. Zook<sup>6</sup>, S. Kingsmore<sup>3</sup>, M. Ferber<sup>5</sup>, M. Salit<sup>7</sup>, R. Nussbaum<sup>1</sup>, B. Shirts<sup>8</sup>

<sup>1</sup>Invitae, San Francisco, CA, United States, <sup>2</sup>Peter MacCallum Cancer Centre, Melbourne, Australia, <sup>3</sup>Rady Children's Hospital, San Diego, CA, United States, <sup>4</sup>Institute of Cancer Research, London, United Kingdom, <sup>5</sup>Mayo Clinic, Rochester, MN, United States, <sup>6</sup>National Institute of Standards and Technology, Gaithersburg, MD, United States, <sup>7</sup>Stanford University, Palo Alto, CA, United States, <sup>8</sup>University of Washington, Seattle, WA, United States.

**Introduction:** Next-generation sequencing (NGS) is a capable technique for detecting small nucleotide variants (SNVs) and small indels in relatively accessible parts of a patient's genome. However, conventional NGS has limitations. An analysis of over 150,000 patients, tested using sensitive methodologies across 1,000 genes, showed that variants of other, technically challenging types comprise up to 20% of the pathogenic findings, depending on indication. Approximately 50% of these variants were of challenging types (e.g., large indels, single exon CNVs), 20% were in challenging regions (homopolymers, duplications), and 15% were poorly covered by standard commercial kits. A further 15% presented multiple challenges. It can be difficult to evaluate the sensitivity of tests for such variants. Recent AMP/CAP NGS guidelines (Roy *et al.* JMD 2018) recommend that at least 59 variants of each type be included in validation studies, a number that is difficult to achieve for challenging variants given the relative scarcity of positive control specimens. **Methods:** We developed a pilot synthetic DNA specimen containing 22 challenging variants of diverse types in 7 commonly tested genes. NGS data for these synthetic variants mimicked that of the endogenous variants and presented similar technical challenges. This specimen was sequenced using 10 different NGS tests by an international group of collaborating laboratories. These tests employed different sequencing platforms, targeting methods, and bioinformatics pipelines. **Results:** All 10 tests detected all of the relatively "easy" SNVs and small indels present (with 1 exception). However, only 10 of the 22 challenging variants were detected by all tests, and just 3 tests detected all 22. Limitations with large indels, homopolymer associated variants, variants in non-unique regions were observed. Many but not all of these limitations appeared to be bioinformatic in nature. Some of these limitations were not previously known to the respective laboratory directors, demonstrating the utility of this approach. **Conclusions:** The data described above are available and can help laboratories optimize their tests for high clinical sensitivity. The control reagent has been commercialized (SeraCare, Gaithersburg, MD, US) and additional synthetic variants can be added to order. Separately, the GET-RM consortium has begun an effort to recruit patients harboring challenging variants into public biobanks, and other collaborators are using CRISPR editing of cell lines for similar purposes. These tools complement our separate interlaboratory work [Lincoln *et al.* JMD 2019] on reducing confirmatory testing while still maintaining high specificity. Collectively, these

resources can help laboratory directors worldwide improve sensitivity and specificity of their clinical NGS-based tests.

**01-P19. Identification of a Novel Mutation in C11orf70 Gene in Multiplex Kuwaiti Family with Severe Chronic Respiratory Symptoms and Randomization of Left/Right Body Asymmetry**

D. Al Mutairi<sup>1</sup>, B. Alsabah<sup>2</sup>, B. Alkhaledi<sup>3</sup>, H. Omran<sup>4</sup>

<sup>1</sup>Kuwait University, Faculty of Medicine, Department of Pathology, Kuwait City, Kuwait, <sup>2</sup>Zain Hospital for Ear, Nose and Throat, Shuwaikh, Kuwait City, Kuwait, <sup>3</sup>Pediatric Pulmonary Unit, Al-Sabah Hospital, Kuwait City, Kuwait, <sup>4</sup>Hospital Muenster, Muenster, Germany.

**Introduction:** Primary ciliary dyskinesia (PCD) is one of the congenital thoracic disorders caused by dysfunction of motile cilia, resulting in insufficient mucociliary clearance of the lungs. Approximately 50% of all PCD patients have Kartagener syndrome, a triad of bronchiectasis, sinusitis and situs inversus totalis. The overall aim of this study is to identify causative mutated genes for PCD and congenital heart disease (CHD) in the Kuwaiti population. **Methods:** A cohort of multiple consanguineous PCD families was ascertained from Kuwaiti patients and genomic DNA from the family members was isolated using standard procedures. The DNA samples from all affected individuals were analyzed using whole exome sequencing (WES) technology and the Sanger sequencing method. Transmission electron microscopy (TEM) and immunofluorescence staining (IF) for patient samples obtained by nasal brushings in Kuwait was performed in order to identify the specific structural abnormalities within ciliated cells. Here we present one multiplex family from our cohort that has a novel mutation in the recently published gene *C11orf70*. **Results:** WES has shown that the patients from this family have a nonsense homozygous loss-of-function mutation (c.175A>T; p.Lys59\*) in exon 2 of the *C11orf70* gene that predicts a premature termination of translation. Sanger sequencing was performed for the patients and the parents, and the results confirmed the patients carry a homozygous mutation, and the parents are both carriers for the mutations. In addition, TEM for the patients show lacking of outer dynein arms (ODAs). IF staining shows the patients carrying the mutation in the *C11orf70* gene are also lacking ciliary DNAH5, DNAI1, DNAI2, and DNAL1 proteins compared with other ciliary proteins tested in this study such as GAS8, DNAH11, and RSPH9. **Conclusions:** Mutations in the *C11orf70* gene can cause severe symptoms of PCD with randomization of left/right body asymmetry. This study helped the PCD families to get confirmed diagnosis of PCD firstly

by determining the defects in the cilia ultrastructure using IF and TEM, and then by mapping the disease mutations. Genetic screening is confirming the type of ciliary defect for each family under study.

**01-P20. Mutational Analysis of the AVP Gene in a Calabrian Family Affected by adFNDI**

M. Mirabelli<sup>1</sup>, V. Tocci<sup>1</sup>, H. Kvistgaard<sup>2</sup>, D.M. Corigliano<sup>1</sup>, B. Arcidiacono<sup>1</sup>, J. Knudsen<sup>2</sup>, E. Chiefari<sup>1</sup>, D.P. Foti<sup>1</sup>, J.H. Christensen<sup>3</sup>, A. Brunetti<sup>1</sup>

<sup>1</sup>University Magna Graecia, Department of Health Sciences, Catanzaro, Italy, <sup>2</sup>Aarhus University Hospital, Department of Pediatrics and Adolescent Medicine, Aarhus, Denmark, <sup>3</sup>Aarhus University, Department of Biomedicine, Aarhus, Denmark.

**Introduction:** The autosomal dominant form of familial neurohypophyseal diabetes insipidus (adFNDI) is a rare disease characterized by childhood onset of polyuria and deficient neurosecretion of the antidiuretic hormone, also known as arginine vasopressin (AVP). Since 1991, adFNDI has been linked to over 70 different mutations of the 2.5 kb *AVP* gene, which consists of 3 exons and 2 introns and encodes a composite precursor susceptible to proteolytic cleavage on the axoplasmic route to neurohypophysis. These mutations tend to cluster in specific regions of the *AVP* gene, such as those coding for the signal peptide, and result in folding incompetent precursors with neurotoxic activity on magnocellular secretory cells that prevent the expression of the normal allele. In the current study, we describe the first Calabrian family with adFNDI in which mutational analysis of the *AVP* gene was performed. **Methods:** Involvement of human subjects was approved by the Ethical Committee of *Regione Calabria Sezione Area Centro*, and informed consent was obtained from all participants. The index patient was a young adult woman who sought medical attention for her polyuric state at our endocrinology outpatient clinic (A.O.U. Mater Domini, Catanzaro). Since 7 to 8 years of age, she had been dealing with a diagnosis of early central diabetes insipidus and receiving replacement therapy with the synthetic AVP analogue desmopressin. The family medical history revealed an early onset and pure form of adFNDI, with 5 affected relatives over 3 generations, including her mother and brother, who were also willing to consider genetic testing. To this end, genomic DNA was isolated from whole blood samples by standard precipitation methods, and the entire coding region of the *AVP* gene was PCR amplified and sequenced. **Results:** Direct DNA sequencing of PCR products revealed a heterozygous G-to-A transition in nucleotide 279 of exon 1 (g.279G>A), in

accordance with an autosomal dominant pattern of inheritance. The finding was confirmed on independent PCR products with the diagnostic BstUI restriction enzyme digestion assay.

**Conclusions:** The g.279G>A variant, resulting in an alanine-to-threonine change in the last amino acid of the signal peptide, is the most common disease-causing mutation described in adFNDI, as it has been identified in several apparently unrelated families in the US, Asia, Denmark, and Southern Europe. The finding of this common variant in Calabria, where lower genetic diversity is negatively impacting on various hereditary neurodegenerative disorders, constitutes an argument against the potential role of a founder effect.

**01-P21. Hereditary Hemochromatosis Type 3: Analysis of M172K Mutation, a Rare Pathogenic Sequence**

C. Fabi<sup>1</sup>, G. Poli<sup>1</sup>, E. Illiano<sup>2</sup>, A. Mariottini<sup>3</sup>, S. Brancorsini<sup>2</sup>

<sup>1</sup>University of Perugia, Terni, Italy, <sup>2</sup>University of Perugia, Perugia, Italy, <sup>3</sup>Hospital of Terni, Terni, Italy.

**Introduction:** Hereditary hemochromatosis (HH) is an autosomal recessive disorder due to a heterogeneous group of mutations. The most common HH haplotype is the homozygous C282Y mutation of *HFE* gene mapped on 6p21.3 chromosome. A new mutational variant has been identified known as HH non-HFE, a recessive hereditary disease linked to *TFR2* gene mutation placed on 7q22 chromosome that causes severe iron overload, hepatomegaly, abdominal pain, and progressive increase in skin pigmentation.

**Methods:** Fifteen polymorphisms of *HFE* (exons 2, 3, and 4); *TFR2* (exons 2, 4, and 6) and *FPN1* (exon 5) genes were evaluated in 257 patients (194 male and 63 female) with hemochromatosis 15 mutations-specific kit. Moreover, laboratory tests were used to reveal abnormal values linked to possible iron disorders such as sideremia, transferrin saturation, and ferritin. **Results:** In 257 enrolled patients, this test revealed a single M172K mutation only in a 33-year-old man; contrariwise, no other mutations for *HFE* and *FPN1* genes were observed in the same case.

**Conclusions:** This report adds more information about hereditary hemochromatosis and associates a rare novel mutation to this pathology. The severe pathogenic mutation M172K increases the list of gene mutations involved in HH, but the diagnosis remains difficult and unclear because of the limited scientific knowledge about this pathology. For this reason, further investigation can contribute to a better understanding of *TFR2* gene function in HFE-hemochromatosis.

**01-P22. The Usefulness of Gene Panel Sequencing for Diagnosis of Genetic Diseases: A Single Center Experience**

S.Y. Kim, J. Kim, M. Koo, H. Kim, Q. Choi, J. Kim, G.C. Kwon, S.H. Koo

Chungnam National University College of Medicine, Department of Laboratory Medicine, Daejeon, Republic of Korea.

**Introduction:** For the diagnosis of rare genetic diseases, gene panel sequencing has been widely used after the introduction of next-generation sequencing (NGS) technology. In South Korea, with approval of gene panel testing in the reimbursement system in 2017, the diagnostic tests using gene panels have been increasingly used and are rapidly replacing conventional testing using Sanger sequencing. Here, we report a single center experience of gene panel testing for the diagnosis of patients who are suspected to have rare genetic diseases. **Methods:** Patients who were suspected of having the following genetic diseases were tested using gene panel sequencing: hereditary hearing loss, hereditary cancer syndrome, hereditary endocrine disorder, hereditary growth disorder, hereditary respiratory system disorder, hereditary heart disease, hereditary epilepsy, hereditary leukodystrophy, malformation of cortical development, hereditary skeletal disorder, hereditary movement disorder, hereditary hematologic disorder, hereditary renal disease, and hereditary neuromuscular disorder. We determined gene panels for each group of patients composed of about 100 to 400 genes. We performed NGS testing using either custom gene panel tests (for hereditary hearing loss and hereditary epilepsy) or Illumina TruSight One (Illumina, San Diego, CA, US). **Results:** From October 2018 to November 2019, a total of 146 patients who were visited and treated in a tertiary hospital were tested for genetic diseases using gene panels testing. Among them, 88 (60.3%) were male patients and 58 patients were female. A total of 102 patients (69.9%) were pediatric patients (age ≤ 18 yr) and 44 patients were adults (median age, 11 yr; range, 0 to 77 yr). The most frequently requested genetic disease group was hereditary skeletal disorder (15.1%), followed by hereditary neuromuscular disorder (13.7%), hereditary epilepsy (12.3%), hereditary endocrine disorder (12.3%), hereditary movement disorder (10.3%), and hereditary hematologic disorder (10.3%). Among total patients, 52 patients (35.6%) presented either pathologic/likely pathologic variants (50/146) or variants of uncertain significance (VUS) which were specific for the disease (2/146). In 73 patients (50.0%), VUS which were uncertain for the relation with the phenotype of the patients were detected. Among diagnosed genetic disorders, very rare diseases

such as Baraitser-Winter syndrome could only be diagnosed after the genetic testing. **Conclusions:** The use of gene panel testing was useful for diagnosis of rare genetic diseases with increased rates of finally confirmed diagnoses and detection of very rare diseases.

**01-P23. Two Cases of Germline *EPCAM* Mutation(s) as a Rare Cause of Hereditary Colorectal Adenocarcinoma (Lynch Syndrome)**

K. Patel<sup>1</sup>, N. Arora<sup>1</sup>, B. Pal<sup>1</sup>, P. Gupta<sup>1</sup>, V.K. Thantam<sup>1</sup>, D. Dey<sup>2</sup>, P. Roy<sup>2</sup>, M. Parihar<sup>3</sup>, M. Mallath<sup>4</sup>, T. Chawla<sup>5</sup>, M. Roy<sup>6</sup>, S. Ganguly<sup>7</sup>, A. Mannan<sup>8</sup>, D.K. Mishra<sup>1</sup>

<sup>1</sup>Tata Medical Centre, Molecular Genetics, Kolkata, India, <sup>2</sup>Tata Medical Centre, Department of Histopathology, Kolkata, India, <sup>3</sup>Tata Medical Centre, Department of Cytogenetics, Kolkata, India, <sup>4</sup>Tata Medical Centre, Department of Digestive Medicine, Kolkata, India, <sup>5</sup>Tata Memorial Centre, Department of Pharmacogenomics, Kolkata, India, <sup>6</sup>Tata Medical Centre, Department of Surgical Oncology, Kolkata, India, <sup>7</sup>Tata Medical Centre, Department of Medical Oncology, Kolkata, India, <sup>8</sup>Strand Life Sciences, Molecular Genetics, Bangalore, India.

**Introduction:** Lynch syndrome (LS) is an autosomal dominant disorder caused by germline mutation in one of several DNA mismatch repair (MMR) genes and, rarely, *EPCAM* gene mutations. Deletions involving the *EPCAM* gene are causative in 1% to 3% of families with Lynch syndrome. Herein we describe 2 rare cases of colorectal adenocarcinoma showing germline *EPCAM* gene deletions.

**Methods:** A 51-year-old female presented with diarrhea, haematochezia, abdominal pain, and loss of appetite. Family history of colon carcinoma in a cousin and unknown cancer in an uncle was noted. Subsequent laparoscopic anterior resection for a recto-sigmoid growth (>5 cm in size) revealed moderately differentiated mucinous adenocarcinoma (pT3N0), with brisk lymphocytic infiltrate. Immunohistochemistry revealed intact nuclear staining for *MLH1* and *PMS2*, complete loss of nuclear staining for *MSH2*, and intraglandular loss of *MSH6*. MSI-PCR (Promega MSI Analysis System, US) showed instability of all microsatellite markers (BAT-25, BAT-26, NR-21, NR-24, and MONO-27), interpreted as MSI-high. Germline mutation analysis using a TruSight cancer panel (Strand Life Sciences, Bangalore, India) for the commonly implicated hereditary genes, as recommended by ACMG, revealed a pathogenic heterozygous deletion of exons 8 and 9 in the *EPCAM* gene. A 34-year-old male presented with passing loose stools admixed with blood. No loss of appetite seen; however, weight loss was noted. There was no history of

recreational drug abuse or any habits/addictions. A hard mass was palpable on per-rectum examination. Family history revealed colorectal carcinoma in a paternal uncle, esophageal carcinoma in 2 paternal aunts, and another aunt with breast and ovarian carcinomas. Colonoscopy revealed a large circumferential ulceroproliferative tumor in recto-sigmoid colon. Subsequent laparoscopic anterior resection revealed moderately differentiated adenocarcinoma with peri-tumoral "Crohn's-like" lymphocytic response. Germline mutation analysis using a TruSight cancer panel revealed a pathogenic heterozygous deletion of exons 5-9 in the *EPCAM* gene.

**Results:** Worldwide, a variety of *EPCAM* gene deletions that differ in size and location have been described. Some studies suggest that the frequency of *EPCAM* deletions as a cause of Lynch syndrome is up to 30% in patients with *MSH2*-negative tumors or approximately 20% of LS patients without a mutation in MMR genes. The risk of colorectal cancer in carriers of *EPCAM* deletions is comparable to that of *MSH2* mutation carriers. **Conclusions:** These cases suggest that *EPCAM* deletions are a recurrent cause of LS, and detection should be implemented in routine LS diagnostics.

**01-P24. Mutational Analysis of *BRCA* Genes in Breast Cancer Patients from Eastern Sicily**

S. Stella<sup>1</sup>, S.R. Vitale<sup>1</sup>, M.S. Pennisi<sup>1</sup>, S. Di Gregorio<sup>1</sup>, A. Puma<sup>1</sup>, S. Bianca<sup>2</sup>, C. Barone<sup>3</sup>, L. Manzella<sup>1</sup>

<sup>1</sup>University of Catania, Department of Clinical and Experimental Medicine, Center of Experimental Oncology and Hematology, A.O.U. Policlinico-Vittorio Emanuele, Catania, Italy, <sup>2</sup>ARNAS Garibaldi - Nesima, Catania, Italy, <sup>3</sup>ASP 8 Siracusa, Siracusa, Italy.

**Introduction:** Although 85%-90% of breast (BC) and ovarian cancers (OC) are sporadic, 5%-15% are defined as hereditary tumors. Of these tumors, 25% are linked to germline mutations in *BRCA* genes, and patients harboring *BRCA* mutations present a higher risk to develop BC and OC. Moreover, the introduction of target *BRCA* therapies in clinical practice has allowed personalized medicine in preselected patient cohorts. The aim of this study was to investigate the incidence of *BRCA* mutations in BC patients from eastern Sicily and to evaluate their associations with BC molecular features.

**Methods:** The mutational status of *BRCA* was investigated in a cohort of 76 BC patients. Genomic DNA was extracted from peripheral blood samples collected in EDTA tubes. The Oncomine *BRCA* Research Assay panel was used to perform next-generation sequencing (NGS). *BRCA* pathogenetic mutations were validated by

Sanger sequencing. **Results:** Twenty-three (30.26%) of 76 patients had a triple negative breast cancer (TNBC), 21 (27.65%) a luminal A-like cancer, 19 (25%) a luminal B-like tumor, 8 (10.52%) a HER2 positive luminal B-like disease, and 5 (6.57%) carried an HER2 positive BC. Of the 23 TNBC patients, 34.78% subjects presented a *BRCA1* mutation, 13.05% individuals displayed a *BRCA2* VUS, and in 4.35% of patients a novel variant on *BRCA2* gene was found. Of the 21 luminal A-like BC patients, 4.76% presented *BRCA2* mutations, 4.76% of subjects had 2 different mutations on the *BRCA2* gene, 9.52% of patients exhibited a VUS on the *BRCA2* gene, and 4.76% of subjects displayed a *BRCA1* novel variant. In luminal B-like BC patients, 10.52% of patients presented mutations in the *BRCA1* gene, and 5.26% of women showed a *BRCA2* mutation. We found a significant association between pathogenic mutations/VUS alterations and TNBC ( $p < 0.001$ ). The luminal A-like tumor subtypes showed more VUS alterations compared to the luminal B-like and HER2 positive luminal B-like types. No variants were found in the HER2 positive tumor subtype. **Conclusions:** Our findings confirm the utility of *BRCA1* and *BRCA2* mutation analysis by NGS to study hereditary breast and ovarian cancer. Moreover, our results are in accordance with previously published data on BC patients from Sicily. In the future, the screening for *BRCA1/2* mutation status in BC, as already performed in OC, could potentially help clinicians to make the appropriate treatment decisions.

### Selected Hematopathology Abstracts

#### 03-P01. Spectrum of Beta Globin Gene Variants in Pakistani Beta Thalassemia Patients: A Retrospective Study

Z. Ahmed, A. Nasir, T. Moatter  
Aga Khan University, Pathology and Lab Medicine, Karachi, Pakistan.

**Introduction:**  $\beta$ -thalassemia is an autosomal recessive disorder which results in the formation of abnormal hemoglobin due to a variety of different mutations found in the *HBB* gene. These mutations render patients incapable of producing the correct form of hemoglobin. The aim of this study was to identify *HBB* gene mutations in  $\beta$ -thalassemic patients not included in the common-mutation panel of ARMS PCR by sequencing *HBB* coding, intronic, and promoter. **Methods:** A total of 10 samples previously tested for *HBB* gene mutations by ARMS PCR common-panel (i.e., IVS 1-1, IVS 1-5, codon 8/9, codon 41/42, and 619 bp deletion) were analyzed by Sanger sequencing. Two healthy subjects were included as negative controls. Genomic DNA was isolated and *HBB* gene was

amplified. Column purified amplified products were utilized for bidirectional cycle sequencing (BigDye Terminator, ABI, US). **Results:** In the current study, a total of 10 samples were analyzed. Four were males and 6 females. The mean of the patients was 3 years. All patients were diagnosed as  $\beta$ -thalassemia major based on their family history, and clinical and laboratory findings. On average, patients were receiving transfusions every second week. Seven rare mutations in the *HBB* gene were detected, including point mutations. The mutations spanned in the promoter region HBB:c.138C>A (-88 C>A), exon 1 HBB:c.17\_18 delCT (codon 5 - CT), HBB:c.47G>A (codon 15 G>A), HBB:c.92G>C (codon 30 G>C), HBB:c.50A>C (CAP+1 A>C), exon 2 HBB:c.118C>T (codon 39), and intron 2 HBB:c.315+1G>A (IVS II-I G>A), a heterozygous change at codon 6 (GAG→GTG), and a heterozygous mutation at codon 121 (GAA→CAA). All control subjects showed normal *HBB* gene sequence. In addition, a polymorphism T>C in codon 3 at position HBB:c.59 was detected in a majority of the patients and controls. **Conclusions:** Although ARMS PCR is a fast and convenient method for detection of common mutations in the *HBB* gene, a small subset of patients may be missed because of rare mutations, which would require other means for diagnosis. Sanger sequencing is an accurate and robust technique to manage such patients. **Keywords:** Thalassemia,  $\beta$ -globin, Sequencing

#### 03-P02. Spectrum of BCR-ABL Rearrangement Variants in Pakistani Patients with Chronic Myeloid Leukemia and Acute Lymphocytic Leukemia

Z. Ahmed, U. Fatima, M. Ahmed, A. Qamber  
Aga Khan University, Pathology and Lab Medicine, Karachi, Pakistan.

**Introduction:** The aim of this study is the occurrence of the most frequent *BCR-ABL* transcript variants (b3/a2, b2/a2, and e1/a2) in chronic myeloid leukemia (CML) and acute lymphocytic leukemia (ALL) diagnosed in patients in the Pakistani population. The site of breakage in chromosome 22 (*BCR* gene) can occur in different regions within a 5.8 kb region known as the major breakpoint cluster region (M-bcr), spanning 5 exons previously known as b1 to b5 but now known as exon 12 to 16. In CML, the breakpoint in the *BCR* gene mostly (95%) falls within the M-bcr with b2a2 at 40% and b3a2 at 55%. **Methods:** The number of reported patients was 686 over a period of 2 years and 10 months (from October 2016 to July 2019). Males comprised 58% of the total, whereas females were 42%. The male-to-female ratio was 1.4:1. **Results:** Out of the tested 686 patients, 303 were reported to have the *BCRABL1* transcript, of which 54.2% were males and 45.9% were females. The

ratio of patients diagnosed with CML to ALL was 9.8:1. A total of 9% of the patients had the mutation e1a2, whereas 32% had b2a2, and 59% were reported with b3a2. The ratio of b2a2 mutation to b3a2 mutation was 1:1.84. **Conclusions:** We conclude that the distribution of *BCR/ABL* transcript types in patients with CML and ALL differs from most but not all other populations studied. Currently, there are no data from studies of CML and ALL in analyzing a comparable number of cases. The underlying mechanism and causes for the sex-dependence distribution of the *BCR/ABL* transcript types remains open to speculation. **Keywords:** Ph Chromosome, BCR/ABL1, CML, ALL

**03-P03. Real-World Experience Using Gene Expression Profiling of Large B-Cell Lymphomas with Formalin-Fixed, Paraffin-Embedded Tissue in a Clinical Molecular Diagnostics Laboratory**

R. Robetorye, C. Ramsower, T. Yip, B. Glinsmann-Gibson, L. Rimsza  
*Mayo Clinic in Arizona, Phoenix, AZ, United States.*

**Introduction:** Diffuse large B-cell lymphoma (DLBCL) is the most common type of non-Hodgkin lymphoma in Western countries and consists of a clinically heterogeneous group that exhibits similarities in morphology and immunophenotype. However, gene expression profiling (GEP) can further classify DLBCLs into distinct molecular subgroups based on cell-of-origin (COO), including germinal center B-cell (GCB), activated B-cell (ABC), or unclassified (UNC). COO assignment of DLBCL has important biological and prognostic significance, as well as potential therapeutic implications, with the ongoing development of selective agents for treatment of specific DLBCL subtypes. Here, we describe the use of a digital GEP assay (Lymph2Cx) to perform COO assignment in the routine work-up of DLBCL using formalin-fixed, paraffin-embedded (FFPE) tissue sections and describe the results of 180 consecutive DLBCL cases analyzed prospectively by a College of American Pathologists/Clinical Laboratory Improvement Amendments (CAP/CLIA)-certified clinical molecular diagnostics laboratory. We also describe the development of a new clinical GEP assay (Lymph3Cx) that can determine COO in DLBCL as well as robustly distinguish between DLBCL and primary mediastinal large B-cell lymphoma (PMBL). **Methods:** Microscopic inspection of H&E-stained slides was performed to determine tumor content prior to analysis. Tumor tissue comprising  $\geq 60\%$  of the surface area was macrodissected from corresponding unstained FFPE tissue sections, and total RNA was extracted and hybridized overnight on a thermal cycler for the 20 gene probes in the Lymph2Cx panel or the 58 gene probes in the Lymph3Cx panel. Probe/RNA

complexes were purified on a NanoString nCounter Prep Station (NanoString Technologies, Inc., Seattle, WA) and analyzed on a NanoString nCounter Digital Analyzer. The Lymph2Cx assay produces a calculated score to classify the COO of each DLBCL sample as GCB, ABC, or UNC type. The Lymph3Cx assay can determine COO as well as distinguish between DLBCL and PMBL.

**Results:** Large B-cell lymphoma cases analyzed so far include approximately 66% excisional biopsies, 33% needle core biopsies, and 1% cell blocks. Testing requires 2-4 unstained 10-micron tissue sections for all case types. Average turnaround time for the assays is 2.3 business days in laboratory. **Conclusions:** This report describes the prospective application of the Lymph2Cx and Lymph3Cx assays as laboratory-developed tests in a clinical diagnostics laboratory and clearly illustrates how these assays can be incorporated into a routine workflow for the work-up of large B-cell lymphoma cases to determine COO as well as robustly distinguish between DLBCL and PMBL.

**03-P04. Detection of Partial Tandem Duplications in Acute Myeloid Leukemia Using Next-Generation Sequencing**

K. Chin<sup>1</sup>, S. Grenier<sup>1</sup>, B. Nwachukwu<sup>1</sup>, T. Stockley<sup>1,2</sup>, J.-M. Capo-Chichi<sup>1,2</sup>

<sup>1</sup>University Health Network, Genome Diagnostics-Department of Clinical Laboratory Genetics, Laboratory Medicine Program, Toronto, ON, Canada, <sup>2</sup>University of Toronto, Department of Laboratory Medicine and Pathobiology, Toronto, ON, Canada.

**Introduction:** Next-generation sequencing (NGS) technologies are revolutionizing current practice in molecular diagnosis of cancer by enabling the detection of genetic mutations in many genes simultaneously. Although these methodologies have the potential of detecting a wide range of genetic alterations in DNA and RNA, the use of NGS data is mostly limited to the analysis of single nucleotide variants (SNVs) and small insertion/deletions (indels). At the Genome Diagnostics Laboratory of the University Health Network (GD-UHN), we have developed a hybrid-capture NGS panel using gene-specific probes customized by Oxford Gene Technologies (OGT) for genomic profiling in acute myeloid leukemia (AML). We explored the use of the GD-UHN AML NGS test for the detection of partial tandem duplications (PTD) in the *KMT2A* gene, which is a key biomarker in the diagnosis and management of patients with AML. **Methods:** We conducted a retrospective analysis of AML patients sequenced over 3 months (N = 120) at GD-UHN using our AML NGS test. We identified 17 individuals suspicious for a *KMT2A*-PTD based on higher average coverage of probes across the *KMT2A* gene. We

investigated the presence of a *KMT2A*-PTD from the NGS data generated from these 17 cases using a bioinformatic algorithm developed by OGT. The performance of this *in silico* NGS tool was compared to alternative non-NGS methods for the detection of copy number variations (MLPA and qPCR). **Results:** Bioinformatics analyses detected the presence of a *KMT2A*-PTD from NGS data in 6/17 patients; these PTDs involved exons 2-10 (N = 2), exons 2-8 (N = 2), exons 4-6 (N = 1), and exon 3 (N = 1). MLPA and qPCR analyses confirmed the presence of these PTDs. For implementation of this algorithm in our routine AML NGS workflow, we will conduct a retrospective analysis of 500 AML patients sequenced over a year using the GD-UHN AML panel. **Conclusions:** A total of 5% (6/120) of the AML patients in our study cohort have a *KMT2A*-PTD that was not identified using standard NGS analyses. The use of NGS data can be expanded to include the detection of *KMT2A*-PTD. From this pilot study, we learned that biological factors such as the karyotype complexity in the cancer specimen tested, its low tumor content, and the small percentage of cells harboring the variants analyzed are limiting factors to consider while analyzing non-SNV/indel variants from NGS data. Bioinformatics tools have the potential to improve the diagnosis and management of AML by enabling the detection of cryptic genetic lesions that are not amenable using traditional approaches in cytogenetics (e.g., *KMT2A*-PTD versus *KMT2A* gene fusions).

### 03-P05. Validation and Implementation of NGS-Based Combined DNA and RNA Sequencing in Myeloid Neoplasms

K. Saha<sup>1</sup>, K. Patel<sup>1</sup>, S. Banerjee<sup>1</sup>, P. Santra<sup>1</sup>, S. Bhav<sup>2</sup>, V. Radhakrishnan<sup>2</sup>, R. Nair<sup>2</sup>, M. Chandy<sup>2</sup>, M. Parihar<sup>2</sup>, D. Mishra<sup>1</sup>, N. Arora<sup>1</sup>

<sup>1</sup>Tata Medical Centre, Molecular Genetics, Kolkata, India, <sup>2</sup>Tata Medical Centre, Kolkata, India.

**Introduction:** The objective of this study was to validate and implement the OncoPrint Myeloid Research Assay (comprising 40 DNA target genes, 29 driver genes, and 687 variants) at our institution for combined DNA and RNA sequencing in myeloid neoplasms. **Methods:** Ion Torrent PGM platform was used to validate the archived DNA samples (n = 18) with known mutations (*FLT3-ITD*, *CALR*, *CEBPA*, *NPM1*, *PTPN11*, *cMPL1*, *IDH1/2*, *TET*, *EZH2*, *U2AF1*, *SETBP1*, *ASXL1*, *TP53*). Fluorescence *in situ* hybridization (FISH)/RT-PCR confirmed fusions (*NUP 214*, *RUNX1*, *PML RARA BCR 1*, *PML RARA BCR 3*, *MLL3*, *B14A3*, *B19A2*) were retrieved as positive controls for the RNA validation (n = 11). These known samples were used to determine the assay sensitivity, specificity, and reproducibility. The LOD for missense variation was estimated using known Horizon control of JAK

Val617Phe mutations (*HD649*). The sequences were analyzed using the Ion reporter plugin, and the OKR (OncoPrint Knowledgebase Reporter) was used to identify clinically relevant variants. After thorough optimization and validation, this panel was used for prospective analysis in patients with myeloid disorders (AML [n = 22], MDS [n = 12], MPN [n = 5], AUL [n = 1]). These clinical samples (n = 40) were cross-evaluated for *FLT3-ITD/NPM1* mutations by a validated gene scan-based assay. **Results:** In the 4 validation runs (318 chip-4 DNA/RNA, 4.53 million average reads and 1893X coverage) comprising 29 known variations, all mutations/rearrangements were concordant except 2 cases (*FLT3-ITD* >200 bp and *SETBP1*, G870S 3.2%). The LOD for our assay was set at 5% with 95% uniformity and 2000X coverage. For the prospective myeloid disorders (39), mutations were observed in 26 genes, with maximum cases having *IDH1* (n = 5) mutations. The second most frequently mutated genes were, *FLT3*, *NRAS*, *RUNX1*, *ASXL1* (n = 4). Twenty-two of the 40 patients had mutations in more than one gene, 11 cases had single gene mutations, and no mutations were detected in 9 patients. In 5 cases fusions were detected, *BCR-ABL*, *MLL*, *PML-RARA (bcr3)*, and *RUNX1T1*, B3A3 (n = 1). The *RUNX1T1* rearranged AML-M2 and had additional mutations in *NRAS*. The *PML-RARA (bcr3)* was FISH negative and had additional mutations in the *SF3B1* gene. The *FLT3-ITD/NPM1* gene scan results were concordant in all the evaluated clinical samples (n = 40). With this Ion PGM platform, the results were deliverable to patients within 7 days from library preparation. **Conclusions:** Thus, this study demonstrates the stringent validation and institutional implementation of an NGS-based assay which provides both fusion and DNA mutations in a single NGS run for routine clinical use in myeloid malignancies.

### 03-P06. Role of Glutamine in the Modulation of the Sensitivity of Stem Cells of Chronic Myeloid Leukaemia Refractory to Standard Therapy

P. Dello Sbarba<sup>1</sup>, M. Poteti<sup>2</sup>, E. Rovida<sup>1</sup>

<sup>1</sup>Università degli Studi di Firenze, Scienze Biomediche Sperimentali e Cliniche, Firenze, Italy, <sup>2</sup>Università degli Studi di Firenze, Firenze, Italy.

**Introduction:** We demonstrated that the stem cell potential of chronic myeloid leukemia (CML) cell populations is maintained at very low oxygen tension (0.2% oxygen), where the oncogenic BCR/Abl protein, but not the relative transcript, is suppressed. Thus, leukaemia stem cells (LSC) that are adapted to oxygen (and then glucose) shortage persist independently of BCR/Abl signalling and, as they lack the molecular target of BCR/Abl-active tyrosine kinase inhibitors (TKI), are completely refractory to current CML therapy. Indeed, *in vivo*,

LSC home stem cell niches are physiologically low-oxygen sites where the BCR/Abl protein is expected to be suppressed. However, as LSC adapted to energy shortage remain genetically leukemic, they are capable of re-expressing BCR/Abl protein once permissive conditions are (re)established, a phenomenon which leads to clonal expansion and relapse of disease in CML patients. On this basis, we hypothesized BCR/Abl protein suppression in low oxygen to be the key factor sustaining minimal residual disease (MRD) of CML, and undertook the deepening of metabolic control of BCR/Abl protein suppression as a premise to design strategies capable of suppressing TKI-resistant MRD. **Methods:** The experimental approach is based on our previous findings indicating that the metabolic compartmentalization of CML cells, LSC in particular, that occurs *in vivo* in function of space can be mimicked *in vitro* via the progressive exhaustion of nutrients in the function of incubation time. This enables us to study separately, at different times of culture, LSC subsets with different BCR/Abl protein expression and metabolic profiles. Cells were incubated in atmosphere at 0.2% oxygen in "hypoxic" workstations, culture conditions were modulated by adding or subtracting metabolites or inhibitors, and the maintenance of stem cell potential at the end of incubation was assessed by *in vitro* assays. Basic biochemical studies were carried out using CML cell lines, and the most relevant results were then confirmed with primary cells explanted from CML patients. **Results:** At 0.2% oxygen, BCR/Abl protein was maintained and expressed in the absence of glutamine, where glucose consumption was reduced, and in the presence of glutamine, when glycolysis was inhibited via treatment with 2-DG, indicating that glutamine controls glucose catabolism, which in turn drives BCR/Abl protein suppression. Glutamine-supplemented cultures exhibited the maintenance of TKI-refractory stem cell potential, whereas in the absence of glutamine or in the presence of glutamine plus 2-DG, stem cell potential was rapidly exploited, a kinetic typical of the clonal expansion of TKI-sensitive LSC where BCR/Abl signaling is maintained. **Conclusions:** Glutamine is a key regulator of the maintenance of LSC of CML in low oxygen.

### 03-P07. Myeloid Neoplasms with Classic and Variant *MECOM* Rearrangements Have Distinct Clinicopathologic Features

M. Sukhanova, X. Lu, L. Jennings, J. Gao  
Northwestern University Feinberg School of  
Medicine, Pathology, Chicago, IL, United States.

**Introduction:** Only classic *MECOM* rearrangements  $inv(3)(q21q26.2)/t(3;3)(q21;q26.2)/RPN1-MECOM$  were recognized as distinct entities in the WHO classification. Variant *MECOM* rearrangements have been noted in myeloid neoplasms (MNs), but clinicopathologic features have not been well studied. **Methods:** We compared clinicopathologic features of 19 MNs with *MECOM* rearrangements detected by fluorescence *in situ* hybridization (FISH) and chromosome analyses: 9 cases with classic  $inv(3)/t(3;3)$  and 10 cases with variant rearrangements. **Results:** The 9 classic  $inv(3)/t(3;3)$  cases included 5 *de novo* AML, 2 therapy-related AML, and 2 MDS/MPN. Interestingly, 67% of classic cases presented with leukocytosis (33.2~342 K/uL) and dysplasia, mostly megakaryocytic and erythroid. The  $inv(3)/t(3;3)$  was the sole abnormality in 89% of cases, except 1 AML with complex karyotype with -7 and structural abnormalities. Molecular studies were available for 6 cases: mutations in spliceosome (*SRSF2*, *SF3B1*, *ZRSR2*) were most frequent (4/6). The 10 cases with variant *MECOM* rearrangements included 6 MDS and 4 AML. In contrast to cases with classic  $inv(3)/t(3;3)$ , none of the cases presented with leukocytosis. Dysplasia was present in 80% of cases, mostly megakaryocytic and erythroid. Only 2 cases had *MECOM* rearrangement as a single genetic abnormality (20%), specifically the  $t(3;12)$ . A majority of cases (8/10) revealed complex karyotype, most commonly with abnormalities of chromosome 7. In 1 case, the  $t(3;21)$  was acquired only in a sub-clone at the time of AML relapse. Molecular studies were performed for 4 cases: mutations in spliceosome (*SRSF2*, *SF3B1*) were noted in 2 MDS cases. **Conclusions:** The classic and variant *MECOM* rearrangements are associated with different clinicopathologic features in MNs. While megakaryocytic and erythroid dysplasia was noted in both cohorts, cases with classic  $inv(3)/t(3;3)$  are associated with leukocytosis. Also, classic cases often show  $inv(3)/t(3;3)$  as a sole abnormality in MNs, confirming the role of *MECOM* in control of proliferation and differentiation of hematopoietic progenitors, whereas variant *MECOM* rearrangements often occur in the context of complex karyotype or as an acquired event during clonal evolution, and may be a contributing factor interacting with other partners. Our study reveals the importance of karyotype analysis and clinicopathological correlation in *MECOM*-rearranged MNs, and suggests that variant

MECOM rearrangements should be classified independently from classic WHO entities.

	Gender	Age at Dx	Diagnosis	WBC (K/ $\mu$ l)	Hemoglobin (g/dl)	Platelets (K/ $\mu$ l)	Chromosome abnormalities	Mutated genes
WHO classic MECOM rearrangement	M	61	AML	20.5	8.5	42	inv(3)	IDH2, KRAS, SRSF2, DNMT3A, ZRSR2
	F	70	t-AML	33.2	7.1	1741	t(3;3)	ASXL1, SRSF2, STAG2
	F	40	AML	1.7	7.1	117	t(3;3)	JAK2, SF3B1, GATA2
	M	57	AML	12	7.5	115	t(3;3)	RUNX1, TET2, FLT3-ITD
	M	73	AML	3.8	7.5	49	inv(3)	IDH2
	F	86	MDS/MPN	175.3	11.6	62	inv(3)	CUX1, SRSF2, ASXL1
	F	66	AML	60.7	8	20	inv(3), -7, inv(4), add(1q), t(2;12), add(7p), del(14q)	Not done
	M	40	t-AML	46.2	9.7	41	inv(3)	Not done
	M	70	MDS/MPN	9.4	12.7	93	t(3;3)	Not done
	Variant MECOM rearrangement	F	72	MDS-EB2	1.4	8.2	34	t(3;21), -7
M		69	MDS-EB1	6	10.8	N/A	t(3;8), r(7)	SRSF2, NRAS, ASXL1, RUNX1
F		68	AML	16.14	9	60	t(3;12)	BCOR, NRAS, WT1
M		72	t-MDS	9.2	10.4	82	inv(3)[p24q26-2], add(1q)	IDH2
M		63	MDS-EB1	3.5	11.4	251	t(2;3), del(12p), del(7q), der(10)t(1;16)	SF3B1, RUNX1, IKZF1, TET2, GATA2, TET2
M		46	AML	1.1	8.9	33	t(3;7), del(1;7), +12, +13, der(13;21)+21	Not done
M		66	MDS-MLD [CL1]	18.8	11.6	86	t(3;15), t(10;15), del(13q)	Not done
M		67	AML	1.7	7.7	16	t(3;2)	Not done
F		31	t-AML	4.4	8.5	186	t(2;3)+X, del(7p), +6, +8, +12, +20, +21	Not done
F		83	MDS-MLD	5.7	8	390	add(3q), add(7p), add(10q)	Not done

[A comparison of MNs with classic and variant MECOM rearrangements]

### 03-P08. A Silica-Based Targeted Delivery System Increases the Efficacy of Bortezomib Towards Multiple Myeloma

C. Morelli<sup>1</sup>, A. Nigro<sup>1</sup>, M. Greco<sup>1</sup>, A. Comandè<sup>1</sup>, M. Pellegrino<sup>1</sup>, E. Ricci<sup>1</sup>, I. Perrotta<sup>2</sup>, D. Sisci<sup>1</sup>, L. Pasqua<sup>3</sup>, A. Leggio<sup>1</sup>

<sup>1</sup>University of Calabria, Department of Pharmacy and Health and Nutritional Sciences, Rende, Italy,

<sup>2</sup>University of Calabria, Department of Biology, Ecology and Earth Sciences, Rende, Italy,

<sup>3</sup>University of Calabria, Department of Environmental and Chemical Engineering, Rende, Italy.

**Introduction:** One of the main challenges in cancer treatment is to develop a therapeutic strategy able to selectively target tumor cells while preserving normal tissues from unwanted side effects.

Localized drug delivery should cope with this aim. A patented mesoporous silica-based nanodevice (EP 3 288 955 B1) bearing the antineoplastic drug bortezomib (BTZ) whose release is triggered by the acidic tumor environment and grafted with the targeting function folic acid (FOL) on the external surface, was developed (FOL-MSN-BTZ) and tested *in vitro* and *in vivo* against multiple myeloma (MM) cells and in xenograft models, respectively.

**Methods:** FOL-MSN-BTZ efficacy studies were conducted by means of growth experiments, TEM, TUNEL assay, and Western blot (WB). *In vivo* studies were performed on mice models bearing RPMI 8226 (RPMI) MM cell-derived tumors.

**Results:** FOL-MSN-BTZ was able to kill folate receptor overexpressing (FR+) cancer cells, but not FR- normal cells, whereas free BTZ was toxic for all

cell lines tested, regardless of FR expression. MSN uptake occurred exclusively in FR+ RPMI cells through FR-mediated endocytosis, whereas no uptake was observed in FR- cells. Both FOL-MSN-BTZ and free BTZ led to comparable apoptotic rates in RPMI cells, but only BTZ, and not the FOL-MSN-BTZ device, also caused death in FR- normal cells. In mice bearing RPMI-derived tumors, the FOL-MSN-BTZ nanosystem resulted in significantly more efficacy than the free drug, as soon as after the first administration. **Conclusions:** These data show the outstanding specificity of FOL-MSN-BTZ toward FR+ tumor cells, and together with the highly promising *in vivo* studies, pave the way for future exploitation of our MSN technology for drug targeting applications, particularly in cancer therapy.

### 03-P09. Mutational Profiles of Persistent versus Relapsed/Recurrent Acute Myeloid Leukemia: A Two-and-a-Half-Year Experience of a Cancer Center

H. Nguyen<sup>1</sup>, J. Mallick<sup>2</sup>, P. Aoun<sup>1</sup>, R. Pillai<sup>1</sup>, M. Telatar<sup>1</sup>, H. Yew<sup>2</sup>, C. Louie<sup>2</sup>, H. Wei<sup>2</sup>, D. Gu<sup>1</sup>, A. Jariwala<sup>1</sup>, I. Aldoss<sup>2</sup>, A. Salhotra<sup>2</sup>, H. Ali<sup>2</sup>, D. Snyder<sup>2</sup>, G. Marcucci<sup>2</sup>, A. Stein<sup>2</sup>, R. Nakamura<sup>2</sup>, M. Afkhami<sup>1</sup>

<sup>1</sup>City of Hope National Medical Center, Pathology, Duarte, CA, United States, <sup>2</sup>City of Hope National Medical Center, Duarte, CA, United States.

**Introduction:** Acute myeloid leukemia (AML) is a heterogeneous group of hematopoietic stem cell disorders. The most recent World Health Organization (WHO) 2016 edition integrated certain molecular markers in the AML classification. With the development of sequencing techniques, more new mutations are being introduced, which gives more insight into disease pathogenesis and treatment options. Many studies have reported the common mutations in *de novo* AML, but relapsed/recurrent (rAML) and persistent AML (pAML) have rarely been studied. The aim of this study was to find the most common molecular and genetic alterations seen in this population at our institution. **Methods:** We identified 75 patients with a diagnosis of persistent or recurrent AML (31 pAML and 44 rAML) between August 2016 and April 2019 at our institution. Persistent AML was defined as having no complete remission after a course of intensive induction. Relapsed/recurrent AML patients were those who had achieved complete remission lasting  $\geq 1$  month and had a subsequent clinical/hematologic relapse. A custom-targeted panel of 73 most frequently mutated genes in acute myeloid leukemia was used. Genomic DNA was extracted from the bone marrow aspirates, and libraries were prepared using the SureSelect Target Enrichment System (Agilent Technologies Inc.), and then sequenced on MiSeq instruments

(Illumina). Variants reported in germline population databases at minor allele frequencies greater than or equal to 1% were excluded from analysis. The data were curated on the basis of in-house molecular pathology and national databases.

**Results:** Of the 25 detected mutated genes, persistent AMLs have an average of 2.85 mutations, and relapsed AMLs have an average of 2.6 mutations per case. *DNMT3A*, *NRAS*, *TET2*, *WT1*, *NPM1* were among the most commonly mutated genes in both. However, *FLT3 ITD*, *FLT3 TKD*, and *TP53* were found commonly in rAMLs (27.2%, 18.2%, and 25.0%, respectively), whereas they were not frequently detected in pAMLs (9.7%, 3.2%, and 9.7%, respectively). The *RUNX1* mutation was found in less than 15% of cases in both groups. *STAG2* was only seen in the pAMLs (12.9%). **Conclusions:** Introduction of a next-generation sequencing panel as a routine test in AML at the beginning of therapy in our institution enables the use of many molecular markers beyond those included in the current classification. Our findings suggest that incorporation of more genes may help enhance risk stratification in persistent and recurrent leukemia.

### 03-P10. Next-Generation Sequencing-Based Mutation Profiling of Acute Myeloid Leukemia and Myelodysplastic Syndrome

E.-H. Yoo, A.-J. Lee, S.-H. Mun, H.S. Suh, C.-H. Jeon, S.-G. Kim  
Daegu Catholic University School of Medicine, Department of Laboratory Medicine, Daegu, Republic of Korea.

**Introduction:** Genetic analysis of acute myeloid leukemia (AML) and myelodysplastic syndrome (MDS) is essential for disease diagnosis, classification, prognostic stratification, and treatment strategy. Next-generation sequencing (NGS) has been proved as a useful tool for comprehensive analysis of genetic variants in patients with hematologic malignancy in a single approach. We investigated the frequency and spectrum of mutations in Korean patients with AML and MDS and their association with clinical parameters. **Methods:** Thirty-two patients diagnosed with AML (N = 21) and MDS (N = 11) from April 2018 to October 2019 at the Daegu Catholic University Medical Center were included. DNA was extracted from diagnostic bone marrow samples. We targeted 40 recurrently mutated genes and 29 RNA fusion transcript driver genes consisting of 526 amplicons (113,517 bp), and performed massive parallel sequencing using the Ion Torrent S5 XL platform (Thermo Fisher Scientific, Waltham, MA, US). **Results:** Thirty-one (96.9%) patients carried at least 1 mutation in the recurrently mutated genes. A total of 91 pathogenic mutations (48 missense, 30 frameshift, 9 nonsense,

and 4 other mutations) were detected in 26 genes. The median number of mutations per patient was 3 (range 1-6) in AML and 1 (range 0-5) in MDS. The frequently mutated genes were *TET2* (15%), *DNMT3A* (11%), *RUNX1* (11%), and *ASXL1* (8%) in all patients. *TET2* (16%) was the most frequently mutated gene in AML, followed by *DNMT3A* (13%), *RUNX1* (9%), *NRAS* (7%), and *FLT3* (7%). *U2AF1* (20%) and *RUNX1* (20%) were the most frequently mutated genes in MDS, followed by *ASXL1* (15%) and *TET2* (15%). *TET2*, *DNMT3A*, and *U2AF1* mutations were found with higher variant allele frequencies than other accompanying mutations, suggesting these mutations occur early in disease pathogenesis. *U2AF1* mutations were found only in MDS patients and related to MDS with multilineage dysplasia (MDS-MLD) in the current study ( $P = 0.0152$ ). **Conclusions:** The frequency and spectrum of mutations were different between AML and MDS. Mutations in epigenetic regulator genes including *TET2* and *DNMT3A* were frequently found in AML patients. *U2AF1* gene mutations were associated with MDS-MLD. The NGS-based approach allows comprehensive mutation profiling in AML and MDS in the clinical laboratory.

### 03-P11. A Custom NGS-Based Panel for Genetic Testing of Lymphoid and Myeloid Malignancies

C. Fritz<sup>1</sup>, K. Zimmermann<sup>2</sup>, M.C. Weller<sup>2</sup>, C. Boudesco<sup>2</sup>, T. Zenz<sup>2</sup>, M. Rechsteiner<sup>1</sup>, E. Haralambieva<sup>1</sup>, S. Balabanov<sup>2</sup>, U. Wagner<sup>1</sup>  
<sup>1</sup>University Hospital Zurich, Department of Pathology and Molecular Pathology, Zurich, Switzerland, <sup>2</sup>University Hospital Zurich, Department of Hematology, Zurich, Switzerland.

**Introduction:** Over 900,000 people worldwide are diagnosed with blood cancer every year (World Cancer Research Fund International). Next-generation sequencing (NGS) is emerging as an important integral part of the diagnostics and follow-up of patients with hematological malignancies.

**Methods:** We designed, tested, and validated a custom NGS panel covering oncogenic hotspots for all exons of 107 genes involved in myeloid and lymphoid malignancies. The panel is based on anchored multiplex PCR chemistry running on the Illumina NextSeq platform. Panel performance was assessed by sequencing 14 DNA samples from blood or bone marrow aspirate with 8 corresponding bone marrow biopsies from patients with myeloid malignancies with previously verified pathogenic mutations. We also sequenced DNA from 13 lymphoma cell lines (some fresh and some from paraffin cell blocks) with previously identified mutations and 2 well-characterized and commercially available control samples: the AcroMetrix Oncology Hotspot Control (AOHC) and the Horizon OncoSpan gDNA (HOG). **Results:** The analysis of the AOHC and HOG variants was

carried out in triplicates. Comparing the detected with the expected variants resulted in very high recall values (>98%) and very good correlation of variant allele frequencies. For the myeloid part of our custom panel, we could show very good correspondence between the variants found in patient samples based on the new platform and the Illumina TruSight Myeloid Sequencing Panel and/or Sanger sequencing. Finally, to characterize the lymphoid-specific genes in our new panel, we conducted variant calling for well-characterized lymphoma cell lines. Although we found considerable discrepancies at first between our results and the variants listed for these cell lines in the literature (COSMIC), we were able to rule out these discrepancies using Sanger sequencing with the exception of 1 mutation. The resulting recall value was >95% for those samples, with sufficient DNA quality. **Conclusions:** We developed, validated, and implemented a custom NGS-based strategy for lymphoid and myeloid cancer diagnostics that extended our previous workflows. The design allows the flexibility to report mutations in all genes in cases where all are needed or in only a subset of genes for either myeloid or lymphoid samples.

### 03-P12. A Novel 1-Step NGS Assay for Accurate Diagnosis and Ultrasensitive Monitoring for Detection of *FLT3*-ITD in AML Patients

P. Bhanshe, R. Salve, C. Kakirde, A.F. Shaikh, S. Rajpal, S. Chaudhary, S. Joshi, P.G. Subramanian, N. Patkar

Tata Memorial Centre, Hematopathology Laboratory, Mumbai, India.

**Introduction:** Next-generation sequencing (NGS) technologies have made their way into molecular pathology laboratories and enabled us to sequence large numbers of genes cost effectively. Internal tandem duplications of the FMS-like tyrosine kinase 3 (*FLT3*-ITD) are critical determinants of outcome as well as therapy in AML. Unfortunately, short read sequencers as well as informatics algorithms are not very accurate in detection of *FLT3*-ITD. Here we describe a novel assay and use a bioinformatics algorithm for detection of *FLT3*-ITD in AML.

**Methods:** A total of 393 cases of AML were accrued over 6 years and 7 months with a median follow-up of 25.9 months. *FLT3*-ITD positivity was detected by capillary electrophoresis-based fragment length analysis (FA). The samples of AML patients who tested positive for *FLT3*-ITD by FA were then subjected to 1-step PCR strategy using adapter as well as patient-specific indices in the same step. These samples were sequenced on our Illumina MiSeq benchtop sequencer using paired-end 500-base pair V2 chemistry. FASTQ files were analysed using ITD software. ROC curves were used to calculate appropriate cut-offs for allelic ratio

(AR) as well as for variant allelic frequency (VAF). A linear regression analysis was used to compare AR as well as size of ITDs when compared to conventional FA. OS and RFS were calculated per standard recommendations. Dilution experiments were also performed to determine the lower limit of detection for the assay. **Results:** Out of the 393 AML patients, 71 patients who tested positive for *FLT3*-ITD were subjected to NGS assay for *FLT3*-ITD. The cut-off value for defining high *FLT3*-ITD AR was 0.38, and high VAF was 26.45 by using ROC curve. Patients with high *FLT3*-ITD AR at the diagnostic time point showed inferior overall survival (median OS: 11.9 months [95% CI: 8-16],  $P = 0.006$ ) and relapse-free survival (RFS) (median RFS: 11 months [95% CI: 9-17.4],  $P = 0.03$ ) compared to patients having low AR or who were *FLT3*-ITD negative. VAF also correlated with inferior overall (median OS: 14.2 months [95% CI: 9-17],  $P = 0.005$ ) and relapse-free survival (median OS: 12.4 months [95% CI: 8-16],  $P = 0.006$ ) in patients with high VAF values compared to patients having low VAF or who were *FLT3*-ITD negative. The limit of detection of this assay is 1 in 500,000.

**Conclusions:** We designed a novel 1-step NGS assay for accurate diagnosis and ultrasensitive monitoring for detection of *FLT3*-ITD in AML patients. The major limitation of this assay is that it cannot detect large ITD.

### 03-P13. A Novel UMI-Based Assay to Identify Chimeric Gene Fusions by Targeted RNA Sequencing (ANUBIS)

S. Chaudhary, S. Rajpal, P. Bhanshe, P. Surve, P. Subramanian, N. Patkar

ACTREC, Tata Memorial Center, Molecular Hematopathology, Navi Mumbai, India.

**Introduction:** In the last decade we have identified key somatic alterations in cancers that have influenced their diagnosis, classification, and treatment. We recognize many leukemias are driven by chromosomal translocations that result in chimeric gene fusions (CGF). Identification of these fusions is cumbersome using conventional techniques such as fluorescence *in situ* hybridization (FISH). We present ANUBIS, a scalable, modular, targeted RNA sequencing tool for detection of CGF in leukemia. It identified 141 CGF including 4 CGFs not described in literature, highlighting the power of ANUBIS. **Methods:** Blood or bone marrow were used. RNA was converted to ss cDNA and subjected to enzymatic fragmentation, end repair, A-tailing, and ligation with strand-specific unique molecular motifs (sp-UMM). spUMMs incorporate an 8-base UMI into each molecule of cDNA, marking it uniquely for downstream applications. This product is amplified using a gene-specific primer pool (i.e., myeloid or lymphoid) and a universal primer. Later

amplifications incorporate 10 bp sample-specific dual indices and Illumina adapters. Primer pool targeted exons of genes depending upon the module (*ABL1*, *ABL2*, *AF4*, *ALK*, *CSF1R*, *CRLF2*, *CREBBP*, *DUX4*, *EPOR*, *ERG*, *ETV6*, *EBF1*, *FGFR1*, *GLIS2*, *IKZF1*, *IKZF3*, *JAK2*, *KAT6A*, *KDM5A*, *KMT2A*, *MLLT3*, *MLLT4*, *MLLT10*, *MEF2D*, *MYC*, *MYH11*, *MKL1*, *MLLT3*, *MYH11*, *NTRK3*, *NUP214*, *NKT3*, *NUP98*, *P2RY8*, *PICALM*, *PML*, *PAX5*, *PDGFRA*, *PDGFRB*, *RUNX1*, *RUNX1T1*, *TCF3*, *TYK2*, *TAL1*, *RUNX1T2*, *ZNF384*). Consensus reads were generated using Minn v1.0. CGFs were detected using FusionCatcher v1.2 and functionally annotated using Oncofuse v1.0.9. To establish assay performance metrics, we serially diluted *KMT2A-MLLT3* in normal cDNA. Further assay sensitivity was demonstrated by known *BCR-ABL1* positive sample with qPCR. New fusions were validated with RT-PCR. **Results:** ANUBIS could detect fusions as low as 1%. In an initial validation phase, It detected known CGFs as documented by FISH. A total of 141 CGFs included newer entities such as fusions associated with Ph-like ALL, and myeloid/lymphoid neoplasms with *FGFR1*, *PDGFRA*, and *PDGFRB* were detected. Rare fusions involving *DUX4*, *ALK*, *ZNF384*, *TCF3-HLF* were detected in ALL. Similarly, cryptic translocations involving *NUP98-NSD1* and novel fusions *DNM2-ETV6*, *KMT2A-MTMR2*, *PAG1-PDGFRB*, and *TCF3-ONECUT3* were also detected. It also helped the diagnosis of a CMML associated with *RANBP2-ALK* fusion and a small cell variant of anaplastic large cell lymphoma (harbouring *NPM1-ALK*) that mimicked ETP-ALL. **Conclusions:** ANUBIS is a scalable, modular, open-source assay that in our opinion represents a significant technical advance due to its ability to detect fusions where the partner is unknown. In addition, it helps us to sensitively monitor disease at different treatment time points.

### 03-P15. Genomic Landscape of Indian Paediatric Acute Myeloid Leukaemia Patients: A Single Centre Experience

S. Joshi<sup>1</sup>, S. Rajpal<sup>1</sup>, D. Yadav<sup>1</sup>, S. Chaudhary<sup>1</sup>, P. Bhanshe<sup>1</sup>, P.G. Subramanian<sup>1</sup>, P. Tembhare<sup>1</sup>, M. Prasad<sup>2</sup>, C. Dhamne<sup>2</sup>, G. Narula<sup>2</sup>, S. Banavali<sup>2</sup>, S. Gujral<sup>1</sup>, N. Patkar<sup>1</sup>

<sup>1</sup>Tata Memorial Centre, Hematopathology, Kharghar, Navi Mumbai, India, <sup>2</sup>Tata Memorial Centre, Kharghar, Navi Mumbai, India.

**Introduction:** Acute myeloid leukaemia (AML) is a rare and genetically heterogeneous disease that constitutes 15% to 20% of childhood leukaemia and has become the leading cause of childhood leukemic mortality. Although extensive genomic studies have not been reported to date in paediatric AML, it is important to identify additional genetic or

molecular abnormalities to predict outcome and serve as novel therapeutic targets. We aimed to study the genomic landscape of paediatric AML patients by comprehensively evaluating the mutational profile using high-throughput next-generation sequencing (NGS). **Methods:** This was a retrospective study in which the cases of paediatric AML registered in Tata Memorial Centre since January 2018 were included in the study. Clinical and cytogenetics data were obtained from the electronic database. DNA was extracted from blood/bone marrow samples using Qiagen Genra Puregene method. For mutational screening we developed a 51-gene (103 kB) low-cost hybrid capture-based targeted sequencing myeloid panel involving single molecule molecular inversion probes implicated in myeloid malignancies. All samples were sequenced at high coverage on an Illumina MiSeq. Sequencing data analysis was done using custom bioinformatics pipeline. Targeted RNA sequencing was also performed using an in-house amplicon-based assay. **Results:** A total of 130 patients were included, out of which 45 were female and 85 were male. Median age at diagnosis was 8 years (Range 0-15 yrs). Among 130 cases, 59 patients (45.30%) harboured mutations in one of the RAS/MAPK pathway genes. The most frequently mutated genes in our cohort were *KIT* (31, 23.8%), *ASXL1* (11, 8.46%), and *FLT3* (18, 13.8%). Interestingly, 53% (69) of children had more than 1 mutation. Six (4.8%) cases showed coexistence of *NRAS* and *FLT3* gene mutations. Less frequently mutated genes that we found were *GATA1*, *GATA2*, *JAK2*, *PTPN11*, *NPM1*, *RUNX1*, *STAG2*, *WT1*, and *U2AF*. No mutations were detected in 19 (14.6%) patients. Median variant allele frequency for all mutations was 23.6%. The most frequent mutation amongst core binding factor leukaemia cases (n = 50, 38.4%) was in the *KIT* gene (n = 15, 39%). *KMT2A* rearrangement was found in 13 (10%) of the patients, and the most frequent fusion partner detected was *MLLT10* (n = 4, 3.07%). *NUP98-NSD1* fusion was detected in 4 (3.07%) patients. **Conclusions:** The mutational spectrum of the paediatric AML cohort is different from the adult AML cohort; hence, we cannot generalize the findings of adult AML patients to paediatric AML patients. Our study shows 85.3% of paediatric leukaemia cases harbour at least 1 mutation/fusion. It is important to study the prognostic significance of these mutations/fusions, and there is a need to develop age-tailored targeted therapies for the treatment of paediatric AML.

### 03-P16. Myeloid Neoplasm with Eosinophilia/Basophilia and *ETV6-ABL1* Rearrangements: Cell of Origin and Response to Tyrosine Kinase Inhibition

J. Yao<sup>1</sup>, L. Xu<sup>2</sup>, U. Aypar<sup>1</sup>, D. Londono<sup>1</sup>, Q. Gao<sup>1</sup>, J. Baik<sup>1</sup>, J. Dietz<sup>1</sup>, R. Benayed<sup>1</sup>, A. Sigler<sup>1</sup>, M. Yabe<sup>1</sup>, A. Dogan<sup>1</sup>, M. Arcila<sup>1</sup>, M. Roshal<sup>1</sup>, Y. Zhang<sup>1</sup>, M.J. Mauro<sup>3</sup>, W. Xiao<sup>1</sup>

<sup>1</sup>Memorial Sloan Kettering Cancer Center, Pathology, New York, NY, United States, <sup>2</sup>Shanxi Medical University 2nd Affiliated Hospital, Hematology, Taiyuan, China, <sup>3</sup>Memorial Sloan Kettering Cancer Center, Hematology, New York, NY, United States.

**Introduction:** *ETV6-ABL1* rearranged myeloproliferative neoplasms (MPNs) show clinical features mimicking chronic myeloid leukemia (CML) and empirically respond to tyrosine kinase inhibitors (TKI). These cases are commonly diagnosed as Philadelphia chromosome negative CML (Ph-CML), CML with atypical *ABL1* fusions, or atypical CML. In contrast to CML, eosinophilia is a hallmark in nearly all cases. A few *de novo* acute myeloid leukemia (AML) and acute lymphoid leukemia (ALL) cases with this fusion also present with eosinophilia, raising the possibility of a progression from an underlying chronic phase of myeloid/lymphoid neoplasm. The classification of these groups of patients has not reached consensus yet. **Methods:** Fluorescence *in situ* hybridization (FISH) analysis using *ETV6* and *ABL1* break-apart probes and Archer FusionPlex, a customized 199-gene RNA sequencing panel, were performed to detect *ETV6-ABL1* fusion. Large panel next-generation sequencing (NGS) was conducted using FoundationOne Heme (Foundation Medicine 406 gene panel) and MSK-IMPACT Heme (400-gene panel). To study the cell of origin of this fusion, various cell populations were sorted based on immunophenotype by flow cytometry, and then FISH was performed on the sorted cells. **Results:** We identified 4 patients with *ETV6-ABL1* rearrangements. Their clinicopathologic features, and cytogenetic and molecular testing results were reviewed. They all presented with myeloproliferation and eosinophilia, diagnosed as CML with atypical *ABL1* fusion (2), atypical CML (1), and essential thrombocythemia (ET; 1). Three patients were treated with TKI and showed complete cytogenetic response 3 months after initiation of treatment. The ET patient failed multiple lines of treatment and progressed 4 years later to AML. Archer FusionPlex demonstrated the *ETV6-ABL1* transcripts involving the same breakpoints with *ETV6* exon 5 and *ABL1* exon 2 in all cases. NGS testing detected *ARID2* truncating mutations in 2 patients, and they each had additional *TP53* point mutations or *CDKN1B* truncating mutations. The remaining 2 cases were

negative. Cell-of-origin study on flow sorted cells demonstrated that *ETV6* rearrangements were observed in CD34+CD38- (enriched for hematopoietic stem cells, HSC), CD34+CD38+ (hematopoietic progenitors/blasts), monocytes, and granulocytes but not in mature lymphocytes, supporting *ETV6-ABL1* fusions originate from the myeloid biased HSCs. **Conclusions:** In summary, our approach combining FISH and Archer FusionPlex can detect *ETV6-ABL1* fusions in myeloproliferative neoplasms accurately and further direct these patients to appropriate TKI treatment. We propose to classify this group of diseases as myeloid neoplasms with eosinophilia and *ETV6-ABL1* rearrangement, for better unifying the clinical management.

### 03-P17. A Next-Generation DNA Sequencing Assay to Detect SNV, Insertion, Deletion and Copy Number Variants in 25 Lymphoma Genes in FFPE Samples with 20 ng DNA

F. Hyland<sup>1</sup>, C. Scafe<sup>1</sup>, Y. Zhu<sup>2</sup>, C. Yang<sup>1</sup>, Y.-T. Tseng<sup>1</sup>, C. Allen<sup>1</sup>, S. Sadis<sup>3</sup>, S. Roman<sup>2</sup>

<sup>1</sup>Thermo Fisher Scientific, South San Francisco, CA, United States, <sup>2</sup>Thermo Fisher Scientific, Carlsbad, CA, United States, <sup>3</sup>Thermo Fisher Scientific, Ann Arbor, MI, United States.

**Introduction:** Lymphomas, including Hodgkin's lymphoma, diffuse large B-cell lymphoma (DLBCL), and other lymphomas, are clinically heterogeneous: certain individuals respond well to therapy, but many succumb to the disease. The literature suggests that much of this variability in response reflects molecular heterogeneity in the tumors. Characterizing somatic variants including SNVs, insertions, deletions, and copy number variations (CNVs) is important in characterizing these samples. Further, it is highly desirable to be able to detect variants using fine needle aspirate (FNA) samples, low abundance DNA, and formalin-fixed, paraffin-embedded (FFPE) samples. **Methods:** We describe a next-generation sequencing (NGS) assay with 25 genes, the OncoPrint Lymphoma Panel, including *ARID1A*, *ATM*, *B2M*, *BCL2*, *BCL6*, *BRAF*, *BTK*, *CARD11*, *CD79B*, *CDKN2A*, *CREBBP*, *EZH2*, *GNA13*, *HIST1H1E*, *KMT2D*, *MTOR*, *MYC*, *MYD88*, *PIM1*, *SF3B1*, *SQCS1*, *TNFAIP3*, *TNFRSF14*, *TP53*, and *XPO1*. This panel comprises 976 amplicons in total. The assays for these genes have been optimized, and performance has been tested on control samples and on representative clinical research samples. Another 10 genes relevant to lymphoma (with optimized and verified performance) are available for addition to this panel. This panel is designed for FFPE samples and can also be used with samples having non-degraded DNA, with 20 ng DNA input. A comprehensive bioinformatics analysis solution was developed to detect SNPs, indels, and CNVs;

to perform filtering for the most relevant variants; to annotate these variants with a wide variety of bioinformatics databases; and to report on the interpretation of the selected variants. **Results:** We tested this panel on various types of input material, including control samples and FFPE samples. Uniformity, coverage, on-target mapping, reproducibility, and sensitivity to detect variants were high in all cases and above established quality criteria (>90% or >95%). Finally, a coordinated analysis solution uses information about the panel and provides an integrated analysis pipeline with a simple and powerful visual interface, including variant calling, CNV detection, functional annotation, population MAF, predicted protein effect, and annotations including ClinVar, COSMIC, etc. Filtering tools utilizing this information facilitate variant prioritization. **Conclusions:** An NGS assay with a comprehensive data analysis approach was developed that is capable of detecting both small mutations and CNVs simultaneously with high sensitivity in FFPE samples, which is an important tool for lymphoma translational research.

**03-P-18. Detection of IGHV Somatic Hypermutation (SHM) in Chronic Lymphocytic Leukemia/Small Lymphocytic Lymphoma (CLL/SLL) Using Next-Generation Sequencing (NGS): A Quaternary Care Medical Center Experience**

Y. Lin<sup>1</sup>, B. Anderson<sup>1</sup>, L. Prewitt<sup>1</sup>, A. Scott<sup>1</sup>, M.B. Datto<sup>2</sup>, C.M. McCall<sup>2</sup>, J.L. Neff<sup>2</sup>, S. Sebastian<sup>2</sup>  
<sup>1</sup>Duke University Medical Center, Clinical Laboratories, Durham, NC, United States, <sup>2</sup>Duke University Medical Center, Pathology, Durham, NC, United States.

**Introduction:** Detection of somatic hypermutation (SHM) of the immunoglobulin heavy chain variable region gene (*IGHV*) in chronic lymphocytic leukemia/small lymphocytic lymphoma (CLL/SLL) stratifies patients into prognostic groups and predicts responses to chemioimmunotherapy and novel therapeutic agents. The gold standard for assessing SHM in CLL/SLL is multiplex PCR using genomic or cDNA as the template. The recent availability of next-generation sequencing (NGS) methods allows for B-cell clonality testing and the assessment of SHM status in a single test with improved sensitivity and specificity. Here, we report the validation of an NGS-based assay to assess SHM status and our initial clinical experience in 100 CLL/SLL cases. **Methods:** We used the NGS-based LymphoTrack IGH Assay and the Ion Torrent PGM platform to determine SHM status using genomic DNA as a template and PCR amplification employing primers targeting the variable (FR1) and joining regions of the *IGH* gene. Results were compared against our previous clinical assay, which involved multiplex PCR of genomic DNA

using BIOMED-2 primer sets, agarose gel electrophoresis, isolation of clonal products, and Sanger sequencing. The IgBLAST database and the ImMunoGeneTics Information System vQuery and Standardization Alignment Tool (IMGT/V-QUEST) were used to determine variable gene usage and percent homology to the corresponding germline sequences. **Results:** During assay validation we compared NGS results with PCR/Sanger results on 49 patients, with 97% agreement on SHM call and 100% agreement on *IGHV* gene identification. Of 8 patients where results were not evaluable by PCR/Sanger, 7 yielded interpretable results by NGS. Only 1 case with clonal PCR/Sanger results did not yield a clone by NGS, due to a mutation in an NGS primer binding site. NGS test data of 100 consecutive clinically tested CLL/SLL cases revealed 41% mutated, 3% borderline mutated, and 42% unmutated cases. A total of 6% of cases had a clone involving the *IGHV3-21* region, which is associated with a worse prognosis irrespective of the mutation status. A total of 6% of cases were assessed as indeterminate due to unproductive rearrangements or mixed mutated and unmutated clones. A total of 8% of cases did not yield a clone by NGS, and of these, a clone was detected by leader sequence primer PCR/Sanger test in 3 cases (3% of total), suggesting mutation in NGS primer binding, and 5 cases (5% of total) failed due to insufficient amount of clonal B-cells. We compared the rates of these NGS results with 235 consecutive PCR/Sanger results and did not find any significant differences. **Conclusions:** NGS-based *IGH* sequencing is an effective method for determining the SHM status of patients with CLL/SLL and can resolve cases that are uninterpretable by PCR/Sanger sequencing.

**03-P19. Muddy Waters: A Report of Granulocyte Infusion Confounding Next-Generation Sequencing Interpretation**

T. Qdaisat, T. Greiner, A. Cushman-Vokoun, J. Cox  
 University of Nebraska Medical Center - Omaha, Pathology and Microbiology - Molecular Genetics Pathology, Omaha, NE, United States.

**Introduction:** Many factors can confound the interpretation of myeloid mutation panels. Ensuring proper patient identification within clinical assays is an essential quality metric. This can be elaborate (e.g., short-tandem repeat analysis) or simpler (e.g., confirming the presence/absence of X/Y-linked gene loci). Regardless, interpretation of these metrics should be incorporated into the standard clinical workflow of the molecular pathologist. Patient factors and clinical therapies can confound the interpretation of these observations and must be considered when encountering unintuitive results. **Methods:** We

present a case of a 57-year-old female with acute myelogenous leukemia (AML-NOS). As part of her initial work-up, a next-generation sequencing (NGS) myeloid panel was conducted. During her treatment she was profoundly neutropenic (100-400 cells/ $\mu$ L). To treat her neutropenia, 7 separate granulocyte infusions were performed. To assess disease status, an additional bone marrow (BM) biopsy was performed 6 months after her initial diagnosis, ~24 hours following her final granulocyte infusion. As part of this follow-up BM biopsy, NGS studies were performed. **Results:** Examination of the initial BM aspirate demonstrated the following mutations: SRSF2 p.P95\_R102del (VAF: 39%) and SETBP1 p.G870S (VAF: 31%). Assessment of the quality metric data was consistent with a female patient. Specifically, coverage of gene loci located on the X chromosome (e.g., *STAG2*, *BCOR*) was consistent with diploid read-depth. Amplification of *AMELX* gene alone was also seen. Together, these findings were indicative of an XX chromosomal status. Conversely, discordant findings were noted upon examination of the quality data sequencing run using the follow-up BM aspirate. In particular, both *AMELX* and *AMELY* genes were amplified. Further, the examination of the read-depth of genes located on the X chromosome was compatible with a haploid karyotype, consistent with an XY chromosomal status. These features were concerning for a potential specimen mix-up. Analysis of the data did demonstrate the presence of low-level mutations in the *SRSF2* and *SETBP1* genes, both at a VAF of ~1%, consistent with the patient's previously documented pathogenic mutations. Short-tandem repeat analysis was conducted to verify the presence of multiple individual profiles within the BM aspirate. Together, these findings were interpreted as low-level residual involvement of the BM by AML, complicated by granulocyte infusion from male donors. **Conclusions:** This case highlights, at least at our institution, an infrequent procedure that may confound the interpretation of these basic quality measures. Moreover, this provides an additional consideration when data do not entirely fit a preliminary view of the clinical picture.

### 03-P20. Mutation Analysis in Korean Patients with T-Cell Acute Lymphoblastic Leukemia

K.-J. Park<sup>1</sup>, I.-S. Kim<sup>2</sup>, E.J. Yang<sup>2</sup>, Y.T. Lim<sup>2</sup>, S.-H. Cho<sup>2</sup>

<sup>1</sup>Myongji Hospital, Goyang, Republic of Korea,

<sup>2</sup>Pusan National University Yangsan Hospital, Pusan National University School of Medicine, Yangsan, Republic of Korea.

**Introduction:** Genomic studies have illuminated the alterations in pathways underlying T-cell acute lymphoblastic leukemia (T-ALL) pathogenesis, but detailed mutation data by next-generation

sequencing have not been reported in Korean patients. We aimed to investigate mutation frequency, spectrum, and pattern in the Korean patients with T-ALL. **Methods:** We designed a multigene panel targeting 101 genes and validated it using 10 reference materials. The mutation analysis was done in a total of 10 patients with T-ALL. Clinical data and laboratory tests including immunophenotyping, cytogenetics, and molecular genetic tests were also investigated. **Results:** All of the 10 patients harbored at least 1 mutation (range, 1 to 6 per patient). A total of 34 clinically significant mutations including 15 novel mutations were identified in 23 genes. The median of variant allelic frequencies (VAFs) and blasts were counted up to 33% (range, 5%-91%) and 79% (range, 38%-90%), respectively. Recurrent mutations were involved in epigenetic regulators (60%), NOTCH1 signaling (40%), PI3K-AKT (40%), JAK-STAT (30%), and transcription factors (30%). We found that both NOTCH signaling and JAK-STAT signaling were positively associated with epigenetic regulators, while showed mutually exclusive patterns with PI3K-AKT pathway. **Conclusions:** This study showed that the frequency of mutations in epigenetic regulators in Korean patients was significantly higher than expected. Distribution of VAF as well as mutation spectrum is considerably heterogeneous in Korean patients with T-ALL. Although from a limited number of patients, this study provides the first detailed mutational portrait of T-ALL of Korean patients, and gives additional insight into the molecular pathogenesis of the disease.

### 03-P21. Targeting Extracellular Vesicles in Multiple Myeloma: A New Role for the Notch Pathway

D. Giannandrea<sup>1</sup>, M. Colombo<sup>1</sup>, N. Platonova<sup>1</sup>, M. Mazzola<sup>2</sup>, F. Baccianti<sup>1</sup>, R. Adami<sup>1</sup>, L. Cantone<sup>3</sup>, E. Milano<sup>1</sup>, C. Velluti<sup>4</sup>, A. Pistocchi<sup>2</sup>, V. Bollati<sup>3</sup>, S. Ancona<sup>1</sup>, E. Lesma<sup>1</sup>, M. Turrini<sup>5</sup>, R. Chiamomonte<sup>1</sup>

<sup>1</sup>University of Milan, Department of Health Sciences, Milan, Italy, <sup>2</sup>University of Milan, Department of Medical Biotechnology and Translational Medicine, Milan, Italy, <sup>3</sup>University of Milan, Department of Clinical Sciences and Community Health, Milan, Italy, <sup>4</sup>University of Pavia, Department of Biology and Biotechnology, Pavia, Italy, <sup>5</sup>Valduce Hospital, Division of Hematology, Como, Italy.

**Introduction:** Multiple myeloma (MM) is the second most common hematological disease, and it is still incurable mainly because of the pathological interaction with the bone marrow (BM) which promotes its progression. Aberrant Notch signaling determined by the deregulated expression of Notch2 and the ligands Jagged1 and 2 in MM cells mediates their pathological communication with BM

niche. Recently, extracellular vesicles (EVs) have been reported as a further way of communication between tumor and stroma besides cell-cell interaction and communication mediated by soluble factors. Thereby, in this work we aim to assess the tumorigenic effect of MM-derived EVs and elucidate the role played by the Notch pathway in EV-mediated communication between MM cells and the BM cells. **Methods:** We confirmed the pro-tumorigenic ability of EV isolated from the BM aspirates of MM patients to induce drug resistance to standard-of-care drugs mediated by bone marrow stromal cells (BMSCs), a key event in MM progression. EVs derived from the MM cell line RPMI8226 (RPMI8226-EVs) or from RPMI8226 silenced for Jagged1/2 (RPMI8226<sup>J1/2KD</sup>-EVs) and Notch2 (RPMI8226<sup>N2KD</sup>-EVs) were isolated and characterized for size, concentration (nanoparticle tracking analysis), and Notch-related cargo (Western blot). Their ability to activate the Notch pathway was assessed in recipient BMSCs (HS5) and by using 2 days post-fertilization Notch-reporter Tg(T2KTp1bglob:hmgf1-mCherry)<sup>h</sup> transgenic zebrafish embryos. Finally, we compared the ability of RPMI8226-EVs to that of RPMI8226<sup>J1/2KD</sup>-EVs and RPMI8226<sup>N2KD</sup>-EVs to boost BMSCs to produce key cytokines involved in MM cell survival and promote the development of pharmacological resistance. **Results:** Patient-derived BM-EVs increase the ability of BMSC to induce MM cells' resistance to bortezomib and melphalan. The amount of Notch2 and Jagged ligands in EVs is determined by the producing cells; indeed, RPMI8226-EVs carry Notch signaling members, which are downregulated in RPMI8226<sup>J1/2KD</sup>-EVs and Notch2 RPMI8226<sup>N2KD</sup>-EVs in accordance to their ability to activate Notch signaling in BMSCs and in the BM of the Notch-reporter zebrafish embryos. RPMI8226-EVs displayed the ability to promote BM stromal cell-induced drug resistance along with the reduction of the level of pro-tumor cytokines released; RPMI8226<sup>J1/2KD</sup>-EVs and RPMI8226<sup>N2KD</sup>-EVs lost this ability. **Conclusions:** MM-EVs mediate the pathological communication of MM cells with the BM niche and affect the progression of this disease by promoting the development of drug resistance. In this context, Notch signaling members play a key role in participating in EV-mediated communications. Targeting the Notch pathway may therefore represent a suitable strategy to hamper drug resistance development in MM.

### 03-P22. A New Conservative and Non-Denaturing Lysis Buffer to Maintain BCR-ABL1 Integrity in CML Leukocytes

C. Boni<sup>1</sup>, M. Vezzalini<sup>1</sup>, L. Scaffidi<sup>2</sup>, D. Paladin<sup>3</sup>, D. Boscarino<sup>3</sup>, M. Krampera<sup>2</sup>, M. Bonifacio<sup>2</sup>, C. Sorio<sup>1</sup>  
<sup>1</sup>University of Verona, Department of Medicine, General Pathology Division, Verona, Italy,  
<sup>2</sup>University of Verona, Department of Medicine, Hematology Division, Verona, Italy, <sup>3</sup>AB Analitica Srl, Padova, Italy.

**Introduction:** Chronic myeloid leukemia (CML) caused by the acquisition of t(9;22) translocation (the Philadelphia chromosome) occurs in a hematopoietic stem cell and transforms it into a leukemic stem cell (LSC). This event results in the constitutive expression of the fusion tyrosine kinase BCR-ABL1 that is able to alter different pathways including self-renewing, proliferation, and differentiation factors that contribute to commence a myeloproliferative disease. It is known from the literature that conventional lysis buffer is not suitable for preserving BCR-ABL1 in chronic phase (CP)-CML cells. Peripheral blood mature leukocytes present a fast degradative activity, which rapidly and permanently destroys BCR-ABL1 and cABL1, precluding accurate quantification. Many groups have tried some strategies to overcome BCR-ABL1 degradation where enzymatic activity was inhibited with lysis buffers in extreme denaturation conditions: boiling lysis buffer (i.e., 95°C) or adding 1 M NaOH. **Methods:** For this purpose, we set up our new approach both on a CML model (CML cell lines added to healthy donor blood with a ratio of 1:5) and then on primary CML samples, to validate it. To preserve the target, we started with a blocking step of the proteases' activity directly on blood before proceeding with cell lysis. This 2-step non-denaturing protocol indeed starts with blood incubation with a proprietary cocktail of different protease inhibitors (Leukoprotect-AB Analitica-PD) and is followed by use of a unique formulation of lysis buffer that abrogates the degradative activity in CP-CML peripheral blood cells as demonstrated by immunoprecipitation and Western blot analysis. **Results:** We demonstrate that this procedure allows detection of BCR-ABL1 in native lysis conditions levels along with additional kinases analyzed, such as JAK2, BTK, and SYK, that were lost using standard lysis buffer despite the use of commercially available protease inhibitor cocktails. **Conclusions:** We describe the ability of Leukoprotect lysis buffer to preserve BCR-ABL1 protein derived from peripheral blood CML cells and maintain it under non-denaturing, neutral pH conditions. This protocol could facilitate proper evaluation of protein-protein interactions by preserving protein complexes for immunoprecipitation and would allow the evaluation

of BCR-ABL1 kinase intrinsic features through functional assays. Moreover, an optimal preservation of numerous additional targets present in primary cells and lost when traditional non-denaturing lysis procedures are applied may allow the study of the kinome and its deregulation in many diseases.

### 03-P23. Selective Targeting of the Notch Pathway in Multiple Myeloma Using New Small-Molecule Compounds

N. Platonova<sup>1</sup>, C. Parravicini<sup>2</sup>, L. Palazzolo<sup>2</sup>, M. Colombo<sup>1</sup>, D. Giannandrea<sup>1</sup>, V. Vallelonga<sup>1</sup>, I. Eberini<sup>2</sup>, R. Chiaramonte<sup>1</sup>

<sup>1</sup>Università degli Studi di Milano, Health Sciences, Milano, Italy, <sup>2</sup>Università degli Studi di Milano, Department of Pharmacological and Biomolecular Sciences, Milano, Italy.

**Introduction:** Multiple myeloma (MM) is the second most common hematological malignancy characterized by accumulation of pathological MM cells in the bone marrow (BM). Despite clinical advances, it is still an incurable disease due to a tight interaction of malignant plasma cells with the BM microenvironment that promotes tumor growth, immunosuppression, drug resistance, neo-angiogenesis, and bone destruction. The oncogenic Notch signaling plays a crucial role in MM. In particular, aberrant Notch2 receptor activation and overexpression of Notch ligands, Jag1 and Jag2 stimulate MM cells to establish pathological interactions with BM that trigger MM progression. Previously, we showed that these effects might be interfered with by knocking down Jag1 and Jag2 expression. Indirect approaches to inhibit Notch signaling are mainly based on inhibition of g-secretase that catalyzes Notch activation resulting from all 4 Notch receptors and catalyzes other several g-secretase substrates. Inhibition of all 4 Notch receptors is associated with a gut toxicity. This evidence prompted us to develop a therapeutic tool to selectively inhibit Notch2 signaling triggered by Jag1 and 2. **Methods:** To identify compounds able to uncouple Notch-Jagged interaction, we have applied *in silico* protein-protein docking and virtual high-throughput screening (HTS) of an Asinex library to select druglike small molecules. The biological activity was validated through a Notch responsive gene reporter and viability assays. **Results:** Based on previous setup of an integrated *in silico* pipeline, we applied a strategy to exclusively uncouple Notch2::Jag1/2, leaving unaltered the interaction with the other family of Notch ligands, Delta-like ligands (Dll). A total of 100 top-scoring compounds directed exclusively to the Notch2::Jag2 surface were selected by HTS. Two of 100 compounds were validated *in vitro* by the Notch responsive reporter assay on HEK293T cells and showed a significant reduction in Notch

transcriptional activity. The co-culture assay of HeLa cells overexpressing Notch2 with NIH3T3 overexpressing Jag1 or Dll4 ligands identified one promising compound that specifically inhibited Notch2::Jag1 and not Notch2::Dll4 interactions. To confer a translational relevance to the study we verified the effect of one of the small molecules identified on MM cell drug resistance. This compound sensitized MM cells co-cultured with BM stromal cells to standard-of-care drugs such as bortezomib, melphalan, and lenalidomide.

**Conclusions:** Overall, our results showed that the identified compound can selectively antagonize Notch activation and contribute to disrupting the pharmacological resistance, thus providing a basis for an effective and safe anti-Notch therapy in MM and other Notch-dependent tumors.

### 03-P24. Culture Independent Aneuploidy Testing for Hematological Neoplasms

T.L. Chan, C.H. Au, D.N.Y. Ho, E.Y.L. Wong, W.W.L. Choi, E.S.K. Ma  
Hong Kong Sanatorium & Hospital, Pathology, Happy Valley, Hong Kong.

**Introduction:** Clinical utilization of low-pass whole genome sequencing (lpWGS) for preimplantation genetic testing (PGT) provides a rapid screen for copy number variations (CNV) across all chromosomes. Karyotype analysis remains a mandatory investigation at diagnosis of many hematological neoplasms. Around 10%-14% of all acute myeloid leukemia (AML) cases show complex karyotypes that are associated with poor prognosis. Since conventional cytogenetics (CG) involves cell culture, the drawbacks are relatively long turnaround time and poor growth. **Methods:** lpWGS was performed by a methodology borrowed from PGT. Either a single or a few blood or bone marrow leukocytes were subjected to whole genome amplification (WGA), or 1 ng of DNA without WGA, for testing by next-generation sequencing (NGS). NGS library preparation was performed according to the manufacturer. The libraries were sequenced by MiSeq. A minimum of 500 k reads per case should be able to map to the reference. The bioinformatic analysis was performed by an in-house validated CNV pipeline. Fluorescence *in situ* hybridization (FISH) analysis was used to validate the lpWGS finding. **Results:** Forty cases were subjected to lpWGS with paired karyotype. Apart from 3 cases with balanced translocation, pericentric inversion, and near triploidy that are known to be undetectable by this approach, 9 cases were positive for chromosomal aberrations, but only 4 were concordant with the corresponding karyotypes. All discrepancies except 1 were associated with suboptimal results. One discordant AML case with a history of -7 at diagnosis showed normal karyotypes (NK) upon a repeat just before induction chemotherapy. The lpWGS detected -7,

which confirmed the genuine loss of chromosome 7 and was used as a treatment response indicator. Another discordant case showed NK in 4 metaphases. IpWGS identified 7p- together with simultaneous 7q+ and +8. These abnormalities were confirmed by FISH. This signature combined with the clinical feature of hepatosplenomegaly and morphologic and flow cytometric findings of abnormal T cells in bone marrow coined a difficult diagnosis of hepatosplenic T-cell lymphoma, where i(7q) and +8 were frequent events. In addition, clonal rearrangements were detected in the T cell receptor beta and gamma chain genes by NGS technique in this patient, further confirming the presence of a T-cell non-Hodgkin lymphoma. Among 7 poor growth cases, 3 showed detectable chromosome aberrations by IpWGS. **Conclusions:** The IpWGS is an effective and complementary approach to classical CG. It accelerates the aneuploidy test and helps in stratifying patients within days. It overcomes the poor growth issue. The new approach can eliminate the culture bias, but the disadvantage is that small sub-clones may not be detected.

### 03-P26. Study of Different *BCR-ABL* Transcript Types in Moroccan CML Patients Analysed by Multiplex PCR (About 100 Cases)

H. Azami Idrissi<sup>1,2</sup>, L. Bouguenouch<sup>1,2</sup>, B. El Makhzen<sup>2</sup>, R. Berrady<sup>3</sup>, Z. Khammar<sup>3</sup>, H. Benchakroun<sup>4</sup>, K. Melliani<sup>1,3</sup>, S. Belmiloud<sup>5</sup>, M. El Azami El Idrissi<sup>1</sup>, K. Ouldin<sup>1,2</sup>

<sup>1</sup>Sidi Mohamed Ben Abdellah University, Biomedical and Translational Research Laboratory, Fez, Morocco, <sup>2</sup>CHU Hassan II Fez, Unit of Medical Genetics and Onco-genetics, Central Laboratory of Medical Analysis, Fez, Morocco, <sup>3</sup>CHU Hassan II Fez, Department of Internal Medicine and Onco-hematology, Fez, Morocco, <sup>4</sup>CHR Fez, Hematology Department, Fez, Morocco, <sup>5</sup>CHU Hassan II Fez, Department of Pediatrics, Fez, Morocco.

**Introduction:** The main product of the translocation t(9, 22)(q34, q11) is the hybrid gene *BCR-ABL*, located in the first chromosomal abnormality associated with a specific malignant disease in humans, the Philadelphia chromosome (Ph), characteristic of chronic myeloid leukemia (CML).

**Methods:** For 15 years, the diagnostic and therapeutic management of CML has been rattled. Molecular understanding of leukemia and the possibility of having targeted therapies that affect the molecular dysfunction of this disease have improved patient outcomes, and despite the fact that the World Health Organization (WHO) estimates leukemia at 250,000 cases a year worldwide, it considers that these cancers have high cure rates if treated correctly. Multiplex PCR is a simple, inexpensive, and rapid technique that allows the specific and simultaneous detection of

different *BCR-ABL* variants. The presence of these transcripts associated with CML can help in the prognosis and treatment of the disease. **Results:** In this context, we conducted a molecular study of this pathology through the analysis of variants of the *BCR-ABL* fusion gene in 100 patients followed in the pediatric and internal medicine departments of the CHU HASSAN II in Fez, and also in the service of hematology, CHR of Fez. This study confirmed the diagnosis of CML, as well as the data of the literature, by showing b3a2 type fusion rate (59%) higher than b2a2 type (41%). This proves the need to make systematic, qualitative research of *BCR-ABL* transcripts by multiplex RT-PCR to have sufficiently informative data for variant transcripts, thus making it possible to choose the specific primers for the subsequent follow-up of the molecular response under treatments.

**Conclusions:** From a practical point of view, this technique has enormous advantages over conventional RT-PCR, especially in terms of time saving. Keywords: Chronic myeloid leukemia, *BCR-ABL* fusion gene, Multiplex RT-PCR.

### 03-P27. Notch and CXCR4 Partners in Acute T-Cell Leukemia Progression

S. Patel<sup>1</sup>, G. Tsaouli<sup>2</sup>, G. Bernardini<sup>2</sup>, G. Peruzzi<sup>3</sup>, M. Del Gaizo<sup>2</sup>, M.P. Felli<sup>4</sup>

<sup>1</sup>Sapienza - University of Rome, Roma, Italy,

<sup>2</sup>Sapienza - University of Rome, Molecular Medicine, Roma, Italy, <sup>3</sup>Istituto Italiano di tecnologia (IIT), Roma, Italy, <sup>4</sup>Sapienza - University of Rome, Experimental Medicine, Roma, Italy.

**Introduction:** Acute T-cell lymphoblastic leukemia (T-ALL) is a result of malignant transformation of normal developing thymocytes. It has been shown that 15% of children and 25% of adults are affected by this. T-ALL is characterized by the infiltration of immature T cells in the bone marrow (BM).

Activating mutations of *NOTCH1* and *NOTCH3* receptor genes have been implicated in T-ALL development. Due to a deregulated Notch signalling pathway, malignant lymphoblasts expressing immature T cell markers escape thymus retention and infiltrate the BM. These cells could possibly represent "pre-leukemic" cells, and the mechanisms underlying their dissemination need to be clarified. To understand this process we performed experiments with a transgenic mouse model, characterized by constitutive activation of the intracellular domain (IC) of Notch3 receptor (N3-IC) in immature thymocytes (N3-ICtg), that recapitulates some of the hallmarks of human T-ALL. Hyperactive Notch3 drives to aberrant pre-T cell development, while during Notch3-induced T-ALL progression the thymus of these mice becomes fibrotic and poorly populated by mature thymocytes. The crosstalk among CXCR4, Notch, and pre-TCR pathways shows the link between the

survival and proliferation of DN thymocytes. Our study was focused to correlate the expression of cell-surface markers with proliferation and survival programs of early intrathymic progenitors, comparatively between N3-ICtg and WT mice. A better understanding of the Notch3/CXCR4 cross-signaling in cancer progression could hopefully provide new avenues for therapeutic intervention in Notch3-dependent T-cell leukemia. **Methods:** Flow-cytometry analysis of N3-ICtg and WT thymocytes correlated CXCR4 and Notch3 cell-surface expression with different DN1-4 T cell stages. Transcriptional and post-transcriptional gene regulating programs (*Cxcr4* gene) were investigated in sorted DN-T cells. *Ex vivo* experiments evaluated the proliferative and survival properties of selected DN thymocytes of N3-ICtg and WT mice. **Results:** In Notch3-induced T-ALL progression, the DN-T cell population expanded and deregulated. CXCR4 cell-surface receptor expression were characterized in N3-ICtg mice. The hyperactive Notch3 downregulates the *Cxcr4* gene expression in DN-T cells. We observed that different CXCR4-dependent survival and proliferation programs are activated in the thymus of N3ICtg mice as compared to WT. **Conclusions:** Our study demonstrates that Notch3 overexpression increases the DN T cell subset and downregulates the *Cxcr4* gene expression, leading to decreased CXCR4 cell-surface expression. CXCR4 down-modulation has been correlated to solid tumor dormancy. Further studies can reveal the role of intrathymic Notch3 and CXCR4 crosstalk in T-ALL progression.

### 03-P28. Molecular Alterations Obtained by High-Throughput Methods in Multiple Myeloma Patients with Recurrent or Refractory to Heavy Treatment Regimens Could Guide Alternative Targeted Therapies

I. Kuzu<sup>1</sup>, G. Cengiz Seval<sup>2</sup>, S. Yuksel<sup>1</sup>, G. Kaygusuz<sup>1</sup>, K. Dalva<sup>2</sup>, M. Ozcan<sup>2</sup>, M. Beksac<sup>2</sup>  
<sup>1</sup>University of Ankara, Pathology, Ankara, Turkey,  
<sup>2</sup>University of Ankara, Hematology, Ankara, Turkey.

**Introduction:** Disease evolution in multiple myeloma presents a spectrum in which several cumulative somatic chromosomal alterations can be demonstrated. The prognostic genetic alterations are well defined. The heavy treatment regimens and age factors increase mutation load. Next-generation sequencing (NGS) methods can give information about cumulative mutation load of the disease and haematopoietic cells. These results could also be used for searching the suitable drug targets. **Methods:** In this small study, we examined the mutational profile of the neoplastic plasma cells and the microenvironment for 16 multiple myeloma patients by NGS. DNA extraction was performed from the bone marrow aspirate smears, formalin-

fixed, paraffin-embedded (FFPE) tissues involved in the disease, or anti-CD138 coated magnetic bead sorted plasma cells. NGS was performed on Illumina MiSeq platform (US) by using QIAseq targeted DNA panel (12). Human myeloid neoplasm panel covers all exons and exon-intron junctions of 141 target genes. For the data analysis, QCI Analyze Universal 1.5.0 was performed. The proliferation status of the plasma cells was examined on CD138 and Ki67 double labeled immunohistochemistry slides. **Results:** Point mutations of RAS/MAPK pathway genes *KRAS*, *NRAS*, and *BRAF* were detected. In addition, myelodysplasia associated mutations were detected in genes *Tet 2*, *FLT3*, *KDM6*, *FAM7A*, *RUNX1*, *ATM*, *EP300*, *PTEN*, *IDH1*, *SH2B3*, and *KDR*. *PTEN* mutation was frequent. Ki67 proliferation indices were high. **Conclusions:** The mutation load in multiple myeloma patients is high related to the progression of the disease and treatment history. Most frequent mutations are in targetable driver genes. These results could bring the application of alternative targeted therapy options for these patients.

### Selected Infectious Diseases Abstracts

#### 04-P01. Human Erythrocyte's O- $\beta$ -N-Acetylglucosaminidase as a Possible Biomarker of Oxidative Stress in Prosthetic-Joint-Associated Infections

L. Massaccesi<sup>1</sup>, M.M. Corsi Romanelli<sup>1,2</sup>, E. Galliera<sup>1,3</sup>

<sup>1</sup>Università degli Studi di Milano, Department of Biomedical Sciences for Health, Milano, Italy,  
<sup>2</sup>IRCCS Policlinico San Donato, U.O.C SMEL-1 Patologia Clinica, San Donato, Italy, <sup>3</sup>IRCCS Orthopedic Institute Galeazzi, Milano, Italy.

**Introduction:** Total joint arthroplasty has been increasing over the past few years. However, it may fail, requiring revision surgery. Postoperative prosthetic joint infection (PJI) is the most serious complication of knee and hip arthroplasty requiring revision surgery, but the diagnostic approach is still limited. Therefore, to optimize the diagnostic process, infection biomarkers with fast response and high sensitivity and specificity for infection are needed. In this scenario a pivotal role in the pathophysiologic "vicious cycle" of inflammation, deeply related to infection, is played by oxidative stress (OS) due to an overproduction of reactive oxygen species (ROS) commonly produced during the inflammatory response. Recently, the degree of the protein O-GlcNAcylation has been showed as able to influence the stress response pathway; cellular levels of O-GlcNAc, regulated by O-GlcNAc transferase (OGT) and O- $\beta$ -N-acetylglucosaminidase (OGA), are considered as OS sensors and are implicated in the aetiology of

various diseases. OGA was also found in human erythrocytes where it has a role in signaling early membrane alterations in pathologies related to strong oxidative stress, such as Down syndrome or erectile dysfunction. For these reasons its use as a new marker of cellular oxidative stress has been suggested. **Methods:** To compare the oxidative status of 11 patients with PJI ( $60.2 \pm 16$  years) and 30 matched uninfected controls ( $66.8 \pm 13$  years), plasma lipid hydroperoxide levels (ROS) (by colorimetric method), and OGA activity (by fluorimetric assay) were evaluated. **Results:** PJI patients showed significantly higher OGA activity ( $P < 0.05$ ) as well as ROS levels ( $P < 0.001$ ) compared to controls. **Conclusions:** OGA evaluation highlights a condition of strong oxidative stress in PJI, and supports the possible use of OGA as an early biomarker of oxidative stress and as a potential new tool to detect PJI infections, and to monitor conditions of PJI patients under therapies in order to manage and/or prevent the prosthesis loosening and septic complications of PJI.

#### 04-P02. Cytomegalovirus (CMV) DNA Quantification in Urine with Newborns

K. Woo

*Dong-A University Hospital, Laboratory Medicine, Busan, Republic of Korea.*

**Introduction:** The incidence of cytomegalovirus (CMV) is 0.2%-2.4% in all newborns, and approximately 5%-10% of CMV-infected newborns have symptomatic CMV infection. In the US the incidence of perinatal sensorineural hearing loss (SNHL) is estimated to be 0.186%, and the prevalence of hearing loss (HL) among 4-year-olds is estimated to be 0.27%. Some cases of perinatal SNHL and HL are estimated to be caused by CMV infection. In this study, DNA was extracted from liquid urine and subjected to qPCR to diagnose for CMV infection. Subsequently, the association between the qPCR results and incidence of hearing loss was examined.

**Methods:** The study included newborns from 1 tertiary hospital in Korea. Urine screening for CMV infection (quantitative real-time PCR) and newborn hearing screening (automated auditory brainstem response [AABR] testing) were conducted.

**Results:** The incidence of CMV infection was 0.18%. AABR testing revealed abnormalities in 4 of the 469 (.0085%) newborns that were given a hearing screening test. Newborns with both CMV and hearing loss had a higher urinary CMV DNA copy number than newborns with CMV without hearing loss. **Conclusions:** Hearing loss was associated with urinary CMV DNA copy number. Quantification of urinary CMV load may effectively predict the incidence of neurodevelopmental disorders.

#### 04-P03. Composition of Gut Microbiota in Non-Toxigenic and Toxigenic *Clostridioides* (*Clostridium*) *Difficile* Colonization and Infection

S.H. Han<sup>1</sup>, J.W. Yi<sup>2</sup>, J.H. Kim<sup>1</sup>, H. Kim<sup>2</sup>, H.W. Moon<sup>2</sup>

<sup>1</sup>BioCore Co., Ltd, Biotechnology, Yongin, Republic of Korea, <sup>2</sup>Konkuk University School of Medicine, Laboratory Medicine, Seoul, Republic of Korea.

**Introduction:** Data concerning the human microbiota composition during *Clostridium difficile* infection (CDI) using next-generation sequencing (NGS) are still limited. To the best of our knowledge, data for the human microbiota composition in *C. difficile* colonizers are very sparse, and there are no data of comparison of toxigenic and non-toxigenic *C. difficile* colonizers or infection. The current study aimed to evaluate the composition of the gut microbiota in *C. difficile* colonizers and compare it with non-colonized controls and CDI. Also, we tried to find the differences between toxigenic and non-toxigenic *C. difficile* colonizers or infection. **Methods:** We included randomly selected 102 glutamate dehydrogenase (GDH)-negative samples (group I, *C. difficile* non-colonizers) with 93 GDH-positive samples (group II, *C. difficile* colonizers). Among 93 GDH-positive samples, 13 samples were *tcdB* gene positive. In addition, we collected 89 GDH positive samples from patients with significant diarrhea ( $\geq 3$  unformed stools in 24 hours which include 20 *tcdB* gene negative and 69 *tcdB* gene positive (group III, diarrhea with *C. difficile*). Bacterial 16S rRNA genes were amplified and sequenced using the Ion S5 XL system with Ion 530 Chip Kit. Operational taxonomic units (OTUs) were clustered based on 97% sequence similarity with at least 10 identical sequences and assigned against the curated Greengenes v13.8 reference database at the Quantitative Insights into Microbial Ecology (QIIME) website. The Chao1 index for alpha diversity was calculated and principal coordinate analysis was performed for beta diversity using the QIIME pipeline. The mean relative abundance in each group was compared at phylum and genus levels. **Results:** There were significant alterations in alpha and beta diversity in group III compared with those in groups I and II. The mean Chao1 index of group III was significantly lower than those of group I and group II. Group III had significantly lower Bacteroidetes and significantly higher Proteobacteria compared to group I. Comparing non-toxigenic and toxigenic strains in group II, toxigenic *C. difficile* colonizers showed significantly lower Firmicutes. Group III showed significantly lower mean relative abundance of many genera (*Prevotella*, *Lachnospira*, *Blautia*, *Ruminococcus*,

*Phascolarctobacterium*, *Faecalibacterium*, *Bilophila*) and significantly higher mean relative abundance of *Parabacteroides*, *Serratia*, *Veillonella*, and *Enterococcus*. Toxigenic *C. difficile* colonizers showed significant changes which were lower in *Prevotella*, *Phascolarctobacterium*, *Succinivibrio*, *Blautia* and higher in *Bacteroides*. **Conclusions:** We identified the differences of gut microbiota composition and diversity between clinical subgroups that could be further evaluated as predictive markers.

#### 04-P04. Quantitative Detection of Human Herpes Virus 1 & 2 in Clinical Samples Using the Real Time PCR STAT-NAT HSV1 & 2 Assays

M. Gramegna<sup>1</sup>, L. Bavagnoli<sup>1</sup>, A. Di Cosimo<sup>1</sup>, M.L. Incandela<sup>1</sup>, A. Mancon<sup>2</sup>, I. Merli<sup>1</sup>, V. Micheli<sup>2</sup>, D. Rigamonti<sup>1</sup>, L. Spinelli<sup>1</sup>, G. Torini<sup>1</sup>, M.R. Gismondo<sup>2</sup>

<sup>1</sup>Sentinel Diagnostics, R&D NAT, Milano, Italy, <sup>2</sup>ASST FBF Sacco, Microbiologia Clinica, Virologia e Diagnostica Bioemergenze, Milano, Italy.

**Introduction:** Herpes simplex virus 1 and 2 (HSV-1 and HSV-2) are 2 members of the human Herpesviridae family. Both HSV-1 and HSV-2 are very common, lifelong infections that affect up to 90% of adults in the world, depending on socio-economic status. HSV-1 can cause a wide variety of diseases, spanning from common cold sores and genital herpes to the more severe encephalitis, pneumonitis, hepatitis, and many ocular pathologies, especially in immunocompromised patients. HSV-2 is responsible for one of the most common sexually transmitted infections, can be contracted during pregnancy, and can be transmitted to newborns. Both infections are often asymptomatic or subclinical, and due to the peculiar mechanism of viral latency, can cause recurrent episodes.

**Methods:** Both assays developed are in a ready-to-use test format containing all the required elements for the amplification of both HSV-1 or HSV-2 DNA fragments and human beta-globin genes as internal controls. Two sets of primers and probes are combined in a lyophilized and ready-to-use mix, co-amplified, and detected by a Real-Time PCR instrument. Several clinical samples (n = 60) obtained from L. Sacco Hospital (ASST FBF Sacco - Milan, Italy), previously tested with InGenius HSV-1/HSV-2 ELITe MGB Kits (ELITech), were investigated. PCR reactions were performed on nucleic acids extracted from plasma, swabs, liquor, and vitreous humor. Analytical assessment studies were conducted including: LoD and LoQ, precision, reproducibility, linear range, and specificity using 2 plasmids (IDT) containing regions for both HSV-1/HSV-2 targets.

**Results:** These detection kits proved to be specific for HSV-1 and HSV-2, and did not cross-

react with the other human herpesvirus tested. The test performances showed a lower LoQ of 10 genome copies/reaction and an LoD of 10 genome copies/reaction; a linear range between 10<sup>7</sup> and 10<sup>1</sup> genome copies/reaction, and a precision CV <5% for both assays. The new freeze-dried, ready-to-use assays demonstrated robust and accurate target amplification, according to the data obtained at L. Sacco Hospital. The quantification of the samples was precise, reproducible, and comparable to that obtained with the predicted device. **Conclusions:** The described Real-Time PCR assays proved their effectiveness for the detection and quantitation of HSV-1 and HSV-2 DNA in clinical samples from different matrices. The high sensitivity and specificity, linearity, and quantitation performances of these assays, associated with the ready-to-use and room temperature storage, would have a direct impact on the early and correct management of affected patients.

#### 04-P05. Prevalence and Species Distribution of Nontuberculous Mycobacteria Isolated in Korea between 2013 and 2019

J.-H. Cho, E.-H. Lee, C. Hahm, G.-Y. Oh  
Eone Laboratories, Incheon, Republic of Korea.

**Introduction:** Nontuberculosis mycobacteria (NTM) infections have increased worldwide; however, few studies have investigated their prevalence and isolated species in Korea. The purpose of this study was to investigate the incidence of NTM and changes in its pathogens during a recent 6-year period at a large commercial laboratory. **Methods:** We retrospectively analyzed the test results of mycobacterial cultures and NTM identifications at Eone Laboratories between January 2013 and May 2019. Culture-positive specimens were identified as either NTM or *Mycobacterium tuberculosis* complex (MTC) using real-time PCR, and NTM species were identified using a molecular line probe assay. **Results:** A total of 366,091 specimens were received for mycobacterial culture, of which 13,841 (3.78%) were MTC positive and 6,448 (1.76%) were NTM positive. The annual proportion of NTM among culture-positive specimens increased significantly from 27.69% in 2013 to 34.02% in 2015, and then decreased to 27.31% in 2017. A total of 8,229 specimens were received for NTM species identification and 6,097 isolates were identified. *M. intracellulare* (6,481, 57.09%) was the most commonly detected pathogen, followed by *M. avium* (956, 15.68%), *M. abscessus* complex (545, 8.84%), *M. fortuitum* complex (287, 4.71%), *M. kansasii* (214, 3.51%), *M. goodii* (193, 3.17%), *M. chelonae* (74, 1.21%), *M. lentiflavum* or *M. genavense* (54, 0.89%), and *M. terrae*

complex (41, 0.67%). Other NTM species had a prevalence of less than 0.5%. *M. kansasii* is known to be increasing in incidence in Korea, exhibiting the highest incidence in 2016 (5.68%), followed by 2013 (4.43%), 2018 (4.10%), 2015 (3.39%), and 2014 (3.01%). **Conclusions:** Due to the high incidence and pathogenic diversity of NTM species, accurate identification is required for proper diagnosis and treatment. Based on large-scale clinical data, we analyzed the positive rate and isolated species of NTM over the past 6 years. We expect that these results will be useful baseline data for understanding the occurrence of NTM infections in Korea.

#### 04-P07. Inflammatory Markers in HIV+ Patients and Cardiovascular Risk

E. Costantini<sup>1</sup>, M. Reale<sup>1</sup>, A. Auricchio<sup>2</sup>, C. Ucciferri<sup>3,4</sup>, V. Recce<sup>5</sup>, R. Muraro<sup>1</sup>, F. Vignale<sup>5</sup>, J. Vecchiet<sup>6</sup>, K. Falasca<sup>6</sup>

<sup>1</sup>Università degli Studi 'Gabriele d'Annunzio' di Chieti-Pescara, Scienze Mediche, Orali e Biotecnologiche, Chieti, Italy, <sup>2</sup>Clinica Malattie Infettive, Ospedale Civile SS Annunziata Chieti, Medicina e Scienze dell'Invecchiamento, Chieti, Italy, <sup>3</sup>Ospedale Clinicizzato "Santissima Annunziata", Medicina e Scienze dell'Invecchiamento, Chieti, Italy, <sup>4</sup>Università del Molise, Medicina e Scienze della Salute, Campobasso, Italy, <sup>5</sup>Università degli Studi 'Gabriele d'Annunzio' di Chieti-Pescara, Chieti, Italy, <sup>6</sup>Università degli Studi 'Gabriele d'Annunzio' di Chieti-Pescara, Medicina e Scienze dell'Invecchiamento, Chieti, Italy.

**Introduction:** The life expectancy of HIV-infected patients in high-income countries is approaching that of the general population. Because the HIV infected are living longer, diseases such as cardiovascular disease (CVD) now emerge as prominent causes of death in this population. This phenomenon can be explained by the presence of an HIV-related chronic inflammatory state. A lot of algorithms have been used to predict cardiovascular risk (CVR): Framingham risk score (FRS), atherosclerotic cardiovascular disease (ASCVD), the Prospective Cardiovascular Münster study score (PROCAM), and the DAD 5-year estimated risk, but none of these considers the inflammatory state in the assessment. The aim of the study is to show the relationship between CVR scores and plasma inflammatory markers.

**Methods:** A total of 90 virologically-suppressed HIV-positive outpatients attending at the Infectious Diseases Clinics of Chieti were enrolled. Demographic and anamnestic data were collected, and blood and immunological parameters were measured in addition to the cystatin C, PCR, microalbuminuria, IL-18, IL-2, IL4, IL-6, IL-10, TNF- $\alpha$ , and IFN- $\gamma$  and CVR

scores. **Results:** We enrolled 70 males (78%) and 20 females (22%) with a mean age of 48.86  $\pm$  10.01 years and a mean BMI of 25.97  $\pm$  3.94 Kg/m<sup>2</sup>. Biochemical parameters showed a mean of CD4+ lymphocytes of 686.09  $\pm$  311.51 cells/ml, CD4/CD8 ratio of 0.81  $\pm$  0.12, PCR of 0.41  $\pm$  0.23 mg/dl, eGFR of 88.22  $\pm$  22.02 ml/min/1.73m<sup>2</sup>, total cholesterol of 184.14  $\pm$  34.58 mg/dl, whereas cystatin C was 1.02  $\pm$  0.25 mg/dl. Interleukin levels showed the following mean values: IL-18 of 270.10  $\pm$  7.44 pg/mL, IL-2 of 1.69  $\pm$  1.33 pg/mL, IL-4 of 1.92  $\pm$  3.02 pg/mL, IL-6 of 3.87  $\pm$  2.58 pg/mL, IL-10 of 1.17  $\pm$  1.75 pg/mL, whereas TNF- $\alpha$  was 1.31  $\pm$  0.8 pg/mL and IFN- $\gamma$  equal to 32.65  $\pm$  17.1 IU/mL. The study of cardiovascular risk scores showed a mean FRS of 6.98  $\pm$  6.11%, ASCVD of 7.18  $\pm$  6.25%, PROCAM of 6.7  $\pm$  7.4%, and DAD 5-year estimated risk of 3.10  $\pm$  3.41%. There was a correlation between all the scores for CVR prediction and the years of HIV diagnosis (p < 0.001); a correlation between all the CVR scores and IL-18 (p < 0.001); a correlation between circulating IL-2 with both the FRS and the DAD 5-year estimated risk; and a correlation between these scores and levels of cystatin C (p < 0.001), PCR (p < 0.01), and microalbuminuria (p < 0.01). **Conclusions:** We found a correlation between the inflammatory markers and the results from the CVR scores, highlighting how the inflammatory process participates in the pathogenesis of cardiovascular damage in the HIV-positive population. Use of biological markers could be a valid tool to be used in association with the calculators to improve the sensibility and specificity of CVR calculators.

#### 04-P08. Host-Pathogen Interactions in Malaria: Innate Immune Responses of Macrophages to Plasmodium Falciparum Gametocytes

S. D'Alessandro<sup>1,2</sup>, Y. Corbett<sup>2,3</sup>, P. Misiano<sup>2,3</sup>, L. Cavicchini<sup>1</sup>, S. Delbue<sup>1</sup>, D. Taramelli<sup>2,3</sup>, N. Basilico<sup>1,2</sup>, S. Parapini<sup>2,4</sup>

<sup>1</sup>Università degli Studi di Milano, Dipartimento di Scienze Biomediche, Chirurgiche e Odontoiatriche, Milano, Italy, <sup>2</sup>Centro Interuniversitario di Ricerca sulla Malaria - Italian Malaria Network (CIRM-IMN), Milano, Italy, <sup>3</sup>Università degli Studi di Milano, Dipartimento di Scienze Farmacologiche e Biomolecolari, Milano, Italy, <sup>4</sup>Università degli Studi di Milano, Dipartimento di Scienze Biomediche per la Salute, Milano, Italy.

**Introduction:** Malaria is a parasitic vector-borne disease causing millions of cases every year. Gametocytes (GCTs), the sexual intra-erythrocytic stage of *Plasmodium*, develop in 5 stages: stage I-IV are sequestered in different organs, mainly in the bone marrow, where they differentiate to stage V, which are released in the circulation and then

taken up by a mosquito vector during a blood meal, thus being responsible for malaria transmission. The importance of innate immunity to malaria is well recognized. However, most of the studies refer to the asexual blood stage responsible for the symptoms of the disease. The aim of this work was to investigate the innate immune responses to *Plasmodium falciparum* (Pf) GCT. **Methods:** GCTs were obtained from the Pf transgenic strain 3D7elo1-pfs16-CBG99, expressing the luciferase CBG99 under the control of the GCT-specific promoter pfs16. Murine bone marrow-derived macrophages (mBMDMs) were immortalised from mice. Human peripheral blood mononuclear cells (hPBMCs) were isolated from whole blood by density centrifugation (Ficoll-Paque). THP-1 monocytes were differentiated into macrophages by PMA treatment. Cells were incubated with early (II-III) or late (V) GCTs for 2 hrs in the presence or not of cytochalasin D, an inhibitor of actin polymerization and thus of phagocytosis. GCT phagocytosis by mBMDM was demonstrated by Giemsa staining. A novel bioluminescent measurement of internalised GCT was set up using the transgenic strain expressing luciferase. The activation of macrophages or PBMCs was evaluated by measuring the production of TNF- $\alpha$ , MIP-2, and IL-10 by ELISA, and of nitric oxide (NO) by Griess assay. **Results:** This is one of the first demonstrations that GCTs are phagocytised by mBMDM. Moreover, late but not early GCT induced the production of TNF- $\alpha$ , NO, or of the inflammatory chemokine MIP-2 by mBMDM. The production of TNF- $\alpha$  from hPBMCs in response to late GCT was dependent on phagocytosis, since it is abolished by cytochalasin D. Late GCT induced higher levels of TNF- $\alpha$  than early GCT by PMA-differentiated THP-1. **Conclusions:** This work represents one of the first investigations about the relationship between different cells of the immune system and Pf GCT. Further work is ongoing, funded by "FONDAZIONE CARIPLO" (grant number 2017-0846).

#### 04-P09. *In vitro* Analysis of the Effect of the Biological Sex on Cells in the Inflammatory Response to Malaria Parasites and Their Products

D. Scaccabarozzi<sup>1,2</sup>, M.G. Cattaneo<sup>3</sup>, L.M. Vicentini<sup>3</sup>, P. Misiano<sup>1,2</sup>, F. Perego<sup>2,4</sup>, N. Basilico<sup>2,4</sup>, D. Taramelli<sup>1,2</sup>

<sup>1</sup>Università degli Studi di Milano, Dipartimento di Scienze Farmacologiche e Biomolecolari, Milano, Italy, <sup>2</sup>Centro Interuniversitario di ricerca sulla malaria-Italian Malaria Network (CIRM-IMN), Milano, Italy, <sup>3</sup>Università degli Studi di Milano, Dipartimento di Biotechnologie Mediche e Medicina Traslazionale, Milano, Italy, <sup>4</sup>Università degli Studi di Milano, Dipartimento di Scienze Biomediche,

Chirurgiche e Odontoiatriche, Milano, Italy.

**Introduction:** Malaria mortality (415,000 deaths worldwide in 2017) is mainly due to infection with *P. falciparum* and affects primarily children below the age of 5 and pregnant women. Malaria in pregnancy is the only gender-related aspect extensively studied, although it is well known that sex significantly modulates the immune response to pathogens. As the World Health Organization (WHO) pointed out, there is a gap of knowledge on the effect of gender in malaria since most of the epidemiological data are not sex-disaggregated and biological markers are missing. Hemozoin (HZ) is the product of the catabolism of hemoglobin by the parasites during the intra-erythrocyte stage. It is released in the circulation and has toxic effects in different organs where it accumulates. It can activate endothelial cells to increase the production of different cytokines and the expression of adhesion molecules for infected erythrocytes, which then sequester in the deep vasculature, causing clogging, inflammation, and tissue hypoxia. The aim of our research is to investigate the inflammatory response of human umbilical vein endothelial cells from male or female newborns (M-HUVECs or F-HUVECs), to detect possible differences in the inflammatory response between the two sexes and to determine prognostic tools for malaria severity. **Methods:** F-HUVECs and M-HUVECs were treated with different doses of HZ (from 5 to 20  $\mu$ g/ml) for different times (from 24 to 72 hours) in 96-well plates. Cytokines were tested in the supernatants using ELISA (R&D System). The reactive oxygen species (ROS) production was determined by the fluorescent dye dichlorofluorescein diacetate (DCFDA), and adhesion molecules (VCAM and ICAM) were tested by fluorescence-activated cell sorting (FACS). Nitric oxide production was measured by Griess assay. **Results:** HUVEC proliferation did not show any differences between male and female cells treated with HZ. There is a tendency toward an increase in ICAM-1 and in VCAM expression in M-HUVECs treated for 36 hours with 10  $\mu$ g/ml of HZ versus control and F-HUVECs. The production of ROS increased in a dose- (HZ 5-20  $\mu$ g/ml) and time-dependent manner in cells stimulated with HZ, but no differences were found based on cell sex. On the contrary, the production of nitric oxide (NO) in response to HZ was undetectable in both male and female HUVECs. Interestingly, F-HUVECs showed a greater production of IL-8 compared to M-HUVECs when stimulated with HZ with a peak at 48 hrs. When the stimulation was prolonged to 72 hrs, both F-HUVECs and M-HUVECs showed a decrease in IL-8 production, which was greater in M-HUVECs. **Conclusions:** The obtained results suggest that some differences might exist

between human male and female endothelial cells in response to HZ that could be important for determining prognostic tools for malaria severity.

#### 04-P10. Predictive Potential of the Upper Airway Microbiome Composition in Hematological Patients at Risk for Invasive Fungal Infections

C. Costantini<sup>1</sup>, E. Nunzi<sup>1</sup>, A. Spolzino<sup>2</sup>, M. Palmieri<sup>1</sup>, G. Renga<sup>1</sup>, M. Pariano<sup>1</sup>, F. Merli<sup>3</sup>, L. Facchini<sup>3</sup>, A. Spadea<sup>4</sup>, L. Melillo<sup>5</sup>, K. Codeluppi<sup>3</sup>, F. Marchesi<sup>4</sup>, G. Marchesini<sup>6</sup>, G. Nadali<sup>6</sup>, G. Dragonetti<sup>7</sup>, D. Valente<sup>5</sup>, L. Pagano<sup>7</sup>, F. Aversa<sup>2</sup>, L. Romani<sup>1</sup>

<sup>1</sup>University of Perugia, Department of Experimental Medicine, Perugia, Italy,

<sup>2</sup>Haematology and Bone Marrow Transplant Unit, University of Parma, Parma, Italy, <sup>3</sup>Hematology AUSL-IRCCS Reggio Emilia, Reggio Emilia, Italy,

<sup>4</sup>Hematology and Stem Cell Transplant Unit, IRCCS Regina Elena National Cancer Institute, Rome, Italy, <sup>5</sup>Hematology, S. Giovanni Rotondo Hospital, S. Giovanni Rotondo, Italy, <sup>6</sup>Hematology, University of Verona, Verona, Italy, <sup>7</sup>Institute of Haematology, Università Cattolica S. Cuore, Rome, Italy.

**Introduction:** Hematological patients are at major risk for developing invasive fungal infections (IFIs), opportunistic diseases that cause significant morbidity and mortality, and the possibility of stratifying patients based on actual risk for IFI would be of fundamental importance to individualize therapy. It is now clear that the airway microbiome is emerging as an important player in tissue physiology and in protection against colonization by respiratory pathogens including fungi. **Methods:** Based on these premises, we have designed a multicenter, prospective, observational study termed SNIF (Survey of Nasal InFection) in which hematological patients were recruited and their nasal and oropharyngeal swabs collected over a 6-month period for microbiome characterization. Patients were stratified according to their risk of developing IFI based on an algorithm developed by SEIFEM (Sorveglianza Epidemiologica Infezioni Fungine nelle Emopatie Maligne) Group. Microbiome signatures in patients at different risk of IFI were determined by high dimensional class comparisons using linear discriminant analysis of effect size (LEfSe), and the functional potential was predicted by using PICRUST2. **Results:** A total of 212 patients diagnosed with hematological malignancies were enrolled, and 1,000 nasal and oropharyngeal samples analyzed. Consistent with previous findings in volunteers, the noses and the oropharynges were found to harbor distinct microbial communities as measured by both alpha and beta diversity indexes. We further

characterized the oropharynges and found that, consistent with previous reports, the phyla Firmicutes, Bacteroidetes, Proteobacteria, Actinobacteria, and Fusobacteria accounted for nearly the entire spectrum of bacteria, whereas at the genus level, *Streptococcus* was the most abundant, followed by other common genera of the pharynx. Upon stratification based on the risk of IFI, low-risk (LR) and high-risk (HR) samples were found to be associated with distinct microbiota with *Veillonella* and *Lactobacillus* associated with the HR group, and *Prevotella*, *Neisseria*, *Fusobacterium*, *Leptoptichia*, and *Haemophilus* with the LR group. Prediction of functional potential revealed the presence of metabolic pathways with significant different abundance in the LR and HR groups.

**Conclusions:** Overall, these results indicate significant differences in microbial composition between nostril and oropharynx as well as between patients at different risk for IFI. Whether and how the compositional and functional changes impact on the different risks for IFI is under investigation as well as the relevance of various factors, such as chemotherapies, infections, and antimicrobial therapies, in determining these changes.

#### 04-P11. Effect of Oxygen-Loaded Nanodroplets on Macrophage-Mediated Killing of *Enterococcus faecalis*

F. Perego<sup>1</sup>, S. D'Alessandro<sup>1</sup>, D. Scaccabarozzi<sup>2</sup>, R.M. Ticozzi<sup>1</sup>, S. Parapini<sup>3</sup>, M. Prato<sup>4</sup>, D. Taramelli<sup>2</sup>, N. Basilico<sup>1</sup>

<sup>1</sup>University of Milan, Scienze Biomediche, Chirurgiche e Odontoiatriche, Milano, Italy,

<sup>2</sup>University of Milan, Scienze Farmacologiche e Biomolecolari, Milano, Italy, <sup>3</sup>University of Milan, Scienze Biomediche per la Salute, Milano, Italy,

<sup>4</sup>University of Torino, Neuroscienze, Torino, Italy.

**Introduction:** Macrophages play a key role in the defense against pathogens such as bacteria, which often infect the bed of hypoxic chronic wounds, an underestimated problem especially in the elderly. One of the most common mechanisms of macrophage killing of bacteria is the production of microbicidal molecules such as nitric oxide (NO) and reactive oxygen species (ROS). Oxygen-loaded nanodroplets (OLNDs) are carriers able to release oxygen in a time-sustained manner after their internalization into cells. The aim of this work is to understand if OLNDs can improve killing mechanisms of *Enterococcus faecalis* (*E. faecalis*) by infected macrophages under hypoxia.

**Methods:** Uninfected and *E. faecalis*-infected murine bone marrow-derived macrophages (BMDM) and human PMA differentiated THP-1 cells were treated with 2.5%, 5%, and 10% v/v of OLNDs or oxygen-free nanodroplets (OFNDs) in

normoxia (20% O<sub>2</sub>) or hypoxia (1% O<sub>2</sub>). After 24 hours of treatments, nitric oxide (NO) production by murine BMDM was measured by Griess assay. After 30, 60, and 120 minutes of treatments, reactive oxygen species (ROS) production by differentiated THP-1 was spectrophotometrically evaluated using the fluorescence probe DCFDA. **Results:** OLNDs, but not OFNDs, were able to induce NO production in normoxia ( $p < 0.05$ ) by both uninfected and infected BMDM, with no significant differences due to the presence of bacteria. In hypoxia, NO production was totally inhibited. Both OLNDs and OFNDs induced low and not significant levels of ROS by uninfected and infected THP-1 in normoxia and hypoxia. **Conclusions:** OLNDs exert a differential activity on macrophage-killing mechanisms. In normoxia, they significantly improve the secretion of NO, but not the production of ROS, in a way independent from bacterial infection. Hypoxia seems to completely abrogate NO production, even in presence of OLNDs.

### Selected Informatics Abstracts

#### 05-P01. CCKB - a High-Performance and Genome-Scale Informatics Portal for Analysis and Multi-Institutional Sharing of Pediatric Cancer Variants

X. Gai, A. Govindarajan, R. Schmidt, J. Done, D. Maglinte, M. Hiemenz, T. Triche, J. Biegel  
*Children's Hospital of Los Angeles, Los Angeles, CA, United States.*

**Introduction:** Unique challenges exist in interpreting genetic variants in pediatric cancers, which are rare, and more often initiated by germline alterations in cancer susceptibility genes, copy number changes, and gene fusions compared to somatic mutations in adult tumors. In contrast, mutations like *TP53* and other cancer gene mutations common in adult cancer are infrequent in young cancer patients. To address the unmet need for a pediatric cancer-focused knowledge base, we have implemented an informatics portal, CCKB (Childhood Cancer Knowledge Base) to share knowledge regarding DNA and RNA variants across the spectrum of benign and malignant tumors in children. CCKB is cloud based and web accessible, and is a sequencing platform and test agnostic. CCKB takes advantage of the latest computational and bioinformatics advancements to enable genome-scale cancer variant analysis and sharing of data from thousands of patients across multiple institutions. **Methods:** CCKB is implemented with open-source packages, including OpenCGA, a big-data analytic framework supporting the Genomics England Project, and OncoTree disease ontology. Genomic variants are managed using OpenCGA. CCKB is hosted in the

AWS cloud using MongoDB, and is web accessible via a customized Interactive Variant Browser (IVA). Generic annotations are provided via OpenCB. RESTful APIs are leveraged to provide cancer-specific annotations using a variety of genomic resources including Ensembl, ICGC, CIVIC, COSMIC, and Oncotator. **Results:** CCKB is hosting genetic variant data for multiple member institutions of the International Childhood Oncology Network (ICON), initiated by Thermo Fisher Scientific, as well as the Sanford Consortium. This includes data for 800 pediatric cancer patients whom we have tested at the Children's Hospital of Los Angeles with our OncoKids panel, which is based on the OncoPrint Childhood Cancer Research Assay (OCCRA) that we developed in collaboration with Thermo Fisher Scientific. With a variant-centric way that is capable of storing and managing hundreds of millions of variants and metadata of thousands of patients, CCKB allows the user to analyze cancer variants of individual patients or cohorts of patients over the web around the globe. De-identified data can be securely shared among collaborating institutions via the sophisticated authentication system at multiple levels or anonymously via the Beacon mechanism. **Conclusions:** The CCKB platform will enable data sharing to support large collaborative efforts such as ICON, the Sanford Consortium, and AACR GENIE, as well as the larger community of pediatric oncology investigators who participate in the project.

#### 05-P02. Detecting Clinically Significant Gene Fusions in Hematological Malignancies: Precautions When Using CTAT Human Fusion Library

J.H. Lee<sup>1</sup>, S.H. Jeon<sup>1</sup>, T.O. Ma<sup>2</sup>, S.J. Kee<sup>2</sup>, S.H. Kim<sup>1</sup>, J.H. Shin<sup>2</sup>, M.G. Shin<sup>1</sup>

<sup>1</sup>Chonnam National University Hwasun Hospital, Laboratory Medicine, Hwasun, Republic of Korea, <sup>2</sup>Chonnam National University Hospital, Laboratory Medicine, Gwangju, Republic of Korea.

**Introduction:** Gene fusions have significant roles in the initial steps of tumorigenesis in various cancers. RNA-Seq is a very suitable methodology for detecting a variety of gene fusions observed in cancers. However, the detection of too many fusion candidates containing false positives and the selection of clinically significant fusions among them are very challenging tasks. In this study, we used the Trinity Cancer Transcriptome Analysis Toolkit (CTAT) library to determine whether clinically significant fusions in hematological malignancies could be appropriately screened using the library, which is now widely used in fusion analysis of RNA-Seq results. **Methods:** We defined clinically significant gene fusions in hematological malignancies as 165 fusion pairs explicitly described in the World Health Organization (WHO)

classification of tumours of haematopoietic and lymphoid tissues, revised 4th (WHO 2016) such as *BCR-ABL1*, *PML-RARA*, etc. FusionAnnotator, which is a component of the CTAT, was used to annotate the 165 fusion pairs based on the GRCh38\_gencode\_v29\_CTAT\_lib\_Mar272019 version. This version of the CTAT library contains 16 public fusion databases, including Mitelman, chimerdb, and ChimerKB. We used R v3.6.1 and Circos v0.69 for statistical analysis and graphics.

**Results:** An annotation of clinically significant gene fusions using 16 fusion databases in the CTAT library resulted in an average of 24.3 (range 1-67) fusions being annotated, corresponding to 14.7% (range 0.6-40.6%) of the total number of fusions. Databases with the most fusion annotations were ChimerPub (67, 40.6%), ChimerKB (64, 38.8%), and Mitelman (60, 36.4%), respectively (red boxes in Figure 1). Among 165 clinically significant fusions, the number of fusions annotated in more than one database was 107 (64.8%), and the number of fusions not annotated was 58 (35.2%). The databases that annotated the most fusion pairs were ChimerPub, ChimerKB, and Mitelman in that order. **Conclusions:** Fusion annotation is an essential step in the selection of clinically significant fusions among many fusion candidates, including false positives. However, the CTAT library employed may miss many clinically significant fusions in hematological malignancies. Therefore, meticulous attention and different approaches are needed.

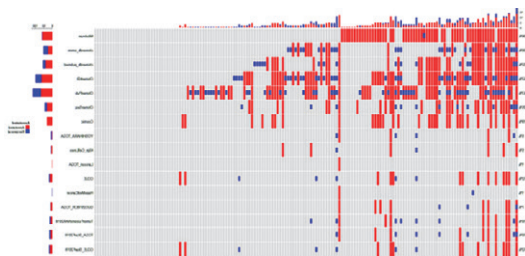


[Figure 1. Clinically significant gene fusions annotated by CTAT library]

### Selected Molecular Cardiovascular Pathology Abstracts

#### 06-P01. Profiling Oral Odontopathogenic Bacteria in Patients with Heterozygous Familial Hypercholesterolaemia and with High Atherosclerotic Cardiovascular Disease Risk

M.C. Curia<sup>1</sup>, M. Buccì<sup>2</sup>, P. Pignatelli<sup>1</sup>, S. Cicolari<sup>3</sup>, E. Olmastroni<sup>3</sup>, L. Iezzi<sup>1</sup>, L. Scorpiglione<sup>2</sup>, T. de Nobile<sup>1</sup>, A. Piattelli<sup>1</sup>, R. Grande<sup>4</sup>, E. Tragni<sup>3</sup>, F. Cipollone<sup>2</sup>, A.L. Catapano<sup>3,5</sup>, P. Magni<sup>3,5</sup>

<sup>1</sup>Università degli Studi 'Gabriele d'Annunzio' di Chieti-Pescara, Department of Medical, Oral and Biotechnological Sciences, Chieti, Italy, <sup>2</sup>Regional

Center for the Study of Atherosclerosis, Hypertension and Dyslipidemia, 'SS Annunziata' Hospital - ASL Chieti, Italy; Ce.S.I.-Met, Università degli Studi 'Gabriele d'Annunzio' di Chieti-Pescara, Chieti, Italy, <sup>3</sup>Università degli Studi di Milano, Dipartimento di Scienze Farmacologiche e Biomolecolari, Milano, Italy, <sup>4</sup>Università degli Studi 'Gabriele d'Annunzio' di Chieti-Pescara, Department of Pharmacy, Chieti, Italy, <sup>5</sup>IRCCS MultiMedica, Milano, Italy.

**Introduction:** Atherosclerotic cardiovascular disease (ASCVD) risk is related to several conditions, including dyslipidaemia, with reference to elevated low-density lipoprotein cholesterol (LDL-C) as an established causative factor. Severe susceptibility to ASCVD is present in patients with familial hypercholesterolaemia (FH), an autosomal dominant disease caused by mutations of relevant genes (LDL receptor, apolipoprotein B, proprotein convertase subtilisin/kexin type 9 (PCSK9), etc.). In heterozygous familial hypercholesterolaemia (HeFH) as well as in other subjects, the susceptibility to ASCVD is actually variable, even when LDL-C levels are similar, suggesting that additional factors play a causal role. One of them is low-grade chronic inflammation, potentially promoted by dysbiosis of the gut and oral microbiota. In this respect, high concentrations of odontopathogenic bacteria, such as *Porphyromonas gingivalis* (PG), have been associated with clinical and experimental atherosclerosis. We aimed at assessing PG and *Fusobacterium nucleatum* (FN) abundance in very high-risk patients with HeFH (with or without previous ASCVD) or in secondary CV prevention.

**Methods:** Twenty patients with genetically defined HeFH (6/20 with previous ASCVD) from the LIPIGEN study, 11 non-FH patients in secondary CV prevention/high ASCVD risk, and 20 healthy controls were included in a cross-sectional study aimed at evaluating PG and FN abundance (qPCR). All patients followed an aggressive hypocholesterolemic therapy including statins, ezetimibe, and PCSK9 inhibitors in 25/31. **Results:**

The 3 groups did not differ for gender/age distribution, BMI, and alcohol intake. Smoking was more represented in the control group (trend), where it increased by 7-fold PG abundance and by 4-fold FN abundance. No differences among groups were present for plaque and gingival indexes. A significant and marked increase of PG abundance ( $p = 0.04$ ) was observed in patients with HeFH in secondary CV prevention (median PG = 1,758) and in non-FH patients in secondary CV prevention (3,082), compared to controls (311) and HeFH patients in primary CV prevention (11). Moreover, a trend towards reduction of FN abundance was observed from HeFH patients in primary CV prevention (median FN = 423) to HeFH

patients and non-FH patients in secondary CV prevention (207 and 138, respectively).

**Conclusions:** Higher PG abundance in high ASCVD risk patients in secondary prevention, with or without HeFH, suggests that this odontopathogenic bacterium is associated with ASCVD development, although any cause/effect relationship is still to be assessed. Evaluation of oral PG abundance may help to more accurately assess the individual ASCVD risk in high-/very high-risk patients.

#### 06-P02. *CACNA1C* Synonym Variant in a Patient with Brugada Syndrome

E. Micaglio<sup>1</sup>, G. Ciconte<sup>1</sup>, M.M. Monasky<sup>1</sup>, S. Benedetti<sup>2</sup>, M. Cau<sup>3</sup>, F. Mastrocinque<sup>1</sup>, A. Coiana<sup>3</sup>, V. Mecarocci<sup>1</sup>, C. Pappone<sup>1</sup>

<sup>1</sup>IRCCS Policlinico San Donato, Arrhythmology, San Donato Milanese, Italy, <sup>2</sup>San Raffaele Hospital, Laboratory of Clinical Molecular Biology and Cytogenetics, Milan, Italy, <sup>3</sup>Università degli Studi di Cagliari, Dipartimento di Scienze Mediche e Sanità Pubblica, Cagliari, Italy.

**Introduction:** We describe a 36-year-old male proband with a clinical diagnosis of Brugada syndrome reached after an EKG during fever (38.5°C). The next-generation sequencing (NGS) test performed on peripheral blood-extracted DNA identified in the proband a heterozygous variant in the *CACNA1C* gene (NM\_199460.3: c.5551 C>A predicting p.Arg1851=) with unknown parental origin. No further mutations or low frequency variants were observed with a minimum base coverage of 20X. **Methods:** For research purposes, we repeated the NGS test using genomic DNA extracted from saliva with a much higher coverage. This material has been analyzed using a panel of 25 genes with a medium base coverage of 122X (TruSight Illumina). **Results:** This method detected the same variant identified using the previous NGS procedure with an average reading depth of 50X for the variant itself. It has to be mentioned that the only low coverage region (18X in the reads from 2797943 to 2797945) in the *CACNA1C* gene does not encompass the variant (read 278895).

**Conclusions:** This is the second report of a synonym *CACNA1C* heterozygous variant in a proband with type 1 Brugada syndrome pattern. Further studies are warranted to assess the importance of such a mechanism as a possible cause of Brugada syndrome.

#### 06-P03. Vascular Ageing and Biomarkers in Aorta Tissues and Blood Samples: New Insights in the Metabolic Aspects

C. Balistreri<sup>1</sup>, A. Tamburello<sup>1</sup>, G. Mazzara<sup>1</sup>, L. Scola<sup>1</sup>, R. Giarratana<sup>1</sup>, D. Lio<sup>1</sup>, G. Ruvolo<sup>2</sup>, G. Melino<sup>3</sup>

<sup>1</sup>University of Palermo, BinD Department, Palermo, Italy, <sup>2</sup>University of Rome 'Tor Vergata', Department of Cardiac Surgery, Rome, Italy, <sup>3</sup>University of Rome 'Tor Vergata', Department of Experimental Medicine, Rome, Italy.

**Introduction:** The integrity and functionality of the endothelium are crucial for the maintenance of physiological homeostasis of the entire cardiovascular system. Our and other groups have recently reported that dysfunctional senescent endothelial cells (EC), as well as their progenitors, play a key role in inducing the morphological and biochemical changes that accompany vascular aging and the related complications, such as aorta degenerative pathologies, including ascending aorta aneurysms. Here, we also aimed to address the metabolic changes that occur during the aging process of tissue EC and circulating EPCs, hypothesizing that they contribute to the onset and progression of age-related aorta degenerative pathologies. **Methods:** A homogeneous Caucasian population was included in the study, comprising 160 healthy subjects (80 older subjects, mean age  $72 \pm 6.4$ , range 66-83 years; and 80 younger blood donors, mean age  $26.2 \pm 3.4$ , range 21-33 years), and 60 older subjects (mean age  $73 \pm 1.4$ , range 66-83 years) with aortic root dilatation and hypertension, and 60 older people (mean age  $70 \pm 2.8$ , range 66-83 years) with sporadic ascending aorta aneurysm (AAA). In addition, 20 control individuals (10 men and 10 women; mean age,  $65 \pm 8$ ), were also included in the study for evaluating the gene expression levels in aorta tissues. Appropriate techniques, practices, protocols, and statistical analyses were performed in our evaluations. **Results:** To date, the partial data obtained have demonstrated that older people have a significantly altered functionality of some metabolic pathways examined, including PARP, SIRT, and mTOR pathways associated with altered glycolysis, hypoxia, amino acid, and fatty acid metabolic profiles. The values of related parameters progressively diminish or augment from the older subjects in good, healthy condition to subjects with hypertension and aorta dilation, and AAA. Consistent with these data, a reduced expression of related genes was detected in aortic tissues from older control people and AAA cases. Finally, we detected the biological effects induced by all the detected alterations on vessel wall age-related remodeling by evaluating aorta tissue histopathological and immunohistochemical changes. **Conclusions:** The promising data

obtained until now suggest a key role of senescent EC and EPC metabolism in the onset and progression of aorta age-related tissues associated with degenerative pathologies.

### Selected Molecular Pathology of Metabolic Diseases Abstracts

#### 07-P01. TRPM7, but Not Magt1, Is Upregulated in Endothelial Cells Exposed to High Concentrations of Glucose

R. Scrimieri, L. Locatelli, J. Maier, A. Cazzaniga  
*Univeristy of Milan, Scienze Biomediche e Cliniche Ospedale Sacco, Milano, Italy.*

**Introduction:** Uncontrolled hyperglycaemia is a main cause of endothelial dysfunction, an early event leading to cardiovascular complications associated with diabetes, but the mechanisms involved are not fully unveiled. High levels of transient receptor potential melastatin 7 (TRPM7) have been proposed as a marker of endothelial dysfunction. TRPM7 is important in maintaining the intracellular homeostasis of magnesium ( $Mg^{2+}$ ), which is fundamental for vital cellular functions. Recently, a highly selective  $Mg^{2+}$  transporter (MagT1) has been characterized, but little is known about its role in the endothelium. Therefore, we focused on TRPM7 and MagT1 in human endothelial cells exposed to high glucose.

**Methods:** Human endothelial cells isolated from the umbilical vein (HUVEC) were cultured in medium containing physiological (5.5 mM) and high concentrations of D-glucose (11.1 mM and 30 mM); the same concentrations were used for L-glucose as a control for osmolarity. N-acetylcysteine (NAC, 5 mM) was used to prevent ROS production, while hydrogen peroxide ( $H_2O_2$ , 100  $\mu$ M) was utilized as a pro-oxidant. ROS activity was measured by fluorimetry using 2'-7'-dichlorofluorescein diacetate (DCFH) and normalized on the basis of MTT assay. Intracellular total  $Mg^{2+}$  was measured by using the fluorescent chemosensor DCHQ5. **Results:**

TRPM7, but not MagT1, levels were increased in cells exposed to high concentrations of D-glucose. Since ROS production is significantly increased in HUVEC exposed to high concentrations of D-glucose, it is noteworthy that the antioxidant NAC prevents TRPM7 upregulation. Interestingly, the concentration of total intracellular magnesium is increased after culture in the presence of D-glucose in a dose-dependent manner. Again, treatment with NAC restores the physiological levels of intracellular  $Mg^{2+}$ . L-glucose exerts no relevant effect. **Conclusions:** In HUVEC treated with high glucose, ROS alter  $Mg^{2+}$  homeostasis through the upregulation of TRPM7.

#### 07-P02. Oncostatin M Induces Increased Invasiveness and Angiogenesis Potentially Favoring Metastatic Dissemination of Liver Cancer Cells

S. Cannito<sup>1</sup>, B. Foglia<sup>2</sup>, C. Turato<sup>3</sup>, G. Di Maira<sup>4</sup>, E. Novo<sup>1</sup>, L. Napione<sup>5</sup>, R. Autelli<sup>1</sup>, S. Colombatto<sup>1</sup>, F. Bussolino<sup>5</sup>, P. Pontisso<sup>6</sup>, F. Marra<sup>4</sup>, M. Parola<sup>1</sup>  
<sup>1</sup>University of Torino, Torino, Italy, <sup>2</sup>University of Alberta, Edmonton, Canada, <sup>3</sup>Institute Oncologico Veneto, University of Padova, Padova, Italy, <sup>4</sup>University of Firenze, Firenze, Italy, <sup>5</sup>IRCC Candiolo, Torino, Italy, <sup>6</sup>University of Padova, Padova, Italy.

**Introduction:** Oncostatin M (OSM), a pleiotropic cytokine belonging to the interleukin-6 (IL-6) family, can modulate hypoxia-dependent liver processes (development, regeneration, and angiogenesis), contributing to chronic liver disease progression and hepatocellular carcinoma (HCC) development. Recently, hypoxia, as an independent signal operating through hypoxia-inducible factors (HIFs), has been shown to induce epithelial-to-mesenchymal transition (EMT) in cancer cells, including HepG2 cells. In this connection, the OSM-related signaling pathway has been reported to upregulate HIF1 $\alpha$  and switch on EMT program. In this study we investigated *in vivo* and *in vitro* the relationships among OSM, expression of vascular endothelial growth factor A (VEGF-A), and increased invasiveness. **Methods:** EMT, invasiveness, angiogenesis, and signal transduction pathways were analysed by integrating morphological, molecular, and cell biology techniques in the following experimental models: 1) a cohort of HCC patients; 2) HepG2 cells exposed to human recombinant OSM (hrOSM) or stably transfected to overexpress human OSM (H/OSM) or empty vector; and 3) murine xenograft. **Results:** 1) Oncostatin M can induce EMT in both *in vitro* models (HepG2 cells exposed to human recombinant OSM or H/OSM) and stimulate invasiveness through VEGF release in culture medium and VEGF-dependent activation of PI3K, ERK1/2, and p38MAPK signalling pathways; the use of specific pharmacological inhibitors against PI3K, ERK1/2, and p38MAPK signaling pathways as well as the use of neutralizing antibody raised against Flk-1 (VEGF receptor type 2) or of a specific inhibitor of Flk-1 result in decrease of invasiveness induced by conditioned medium collected by HepG2 cells treated with hrOSM for 48 hrs; 2) xenograft experiment shows anti-proliferative effects of oncostatin M, confirmed also *in vitro* (BrdU assay and cell cycle analysis); 3) oncostatin M seems to promote angiogenesis through OSM-dependent production of VEGF and by triggering glycolytic switch and favoring sprouting of endothelial tip cells; 4) xenograft experiment shows increased expression of human

EPO in lung specimens obtained from mice injected with H/OSM (versus control condition) potentially associated with an increased rate of spontaneous metastases; and 5) the highest levels of OSM transcripts correlate in HCC specimens with the highest rate of early tumor recurrence.

**Conclusions:** OSM, expressed in human HCC, by inducing EMT and increased invasiveness as well as by triggering angiogenesis, seems to sustain metastatic dissemination of liver cancer cells.

#### 07-P03. Functional Analysis of OCTN2 and ATB<sup>0+</sup> in Normal Human Airway Epithelial Cells: Involvement of These Transporters in Bronchodilator Translocation

A. Barilli, R. Visigalli, B.M. Rotoli, F. Ferrari, V. Dall'Asta

*Unit of General Pathology, Dept. of Medicine and Surgery, University of Parma, Parma, Italy.*

**Introduction:** OCTN2 (*SLC22A5*) and ATB<sup>0+</sup> (*SLC6A14*) transporters mediate the uptake of L-carnitine, essential for the transport of fatty acids into mitochondria and subsequent  $\beta$ -oxidation. As far as human lung is concerned, both transporters have been described in several cell lines from respiratory epithelium; no information is thus far available in EpiAirway, an innovative model of primary normal human bronchial cells. Since both transporters, beyond transporting L-carnitine, have a significant potential as delivery systems for drugs, this study aimed to analyze *SLC22A5/OCTN2* and *SLC6A14/ATB<sup>0+</sup>* expression and activity in EpiAirway. Their involvement in the transport of inhaled bronchodilators has been also evaluated, along with the effect of inflammatory stimuli. Calu-3 monolayers, differentiated in culture for 8 or 21 days, were used for comparison. **Methods:** EpiAirway and Calu-3 were grown at air-liquid interface (ALI) on inserts. Gene expression was analysed through RT-qPCR. The activity of OCTN2 and ATB<sup>0+</sup> was discriminated by measuring the uptake of <sup>3</sup>H-carnitine in the presence of betaine or arginine as specific inhibitors, respectively; the localization of the transporters was evaluated by means of immunocytochemistry with confocal microscopy. **Results:** OCTN2 transporter was equally expressed and functional in both models at the basolateral side. ATB<sup>0+</sup> was, instead, highly expressed and active on the apical membrane of EpiAirway and only in early cultures of Calu-3 (8 days) but not in fully differentiated cultures (21 days). In both cell models, L-carnitine uptake on the apical side was inhibited by the bronchodilators glycopyrrolate and tiotropium, that hence can be considered substrates of ATB<sup>0+</sup>; ipratropium was instead effective on the basolateral side, indicating its interaction with OCTN2. In Calu-3 cells, inflammatory stimuli such as LPS or TNF $\alpha$  caused an induction of *SLC6A14/ATB<sup>0+</sup>* expression and an

increase of L-carnitine uptake at the apical side; on the contrary, *SLC22A5/OCTN2* was not affected.

**Conclusions:** In EpiAirway and Calu-3, besides transporting carnitine, ATB<sup>0+</sup> on the apical and OCTN2 on the basolateral side are involved in the transport of bronchodilators. Moreover, ATB<sup>0+</sup> is upregulated by inflammation. The identification of these transporters in EpiAirway can open new fields of investigation in the study of drug inhalation and pulmonary delivery.

#### 07-P04. Analysis of ABC-Multidrug Transporters in Human Airway Epithelial Cells

B.M. Rotoli, R. Visigalli, A. Barilli, F. Ferrari, V. Dall'Asta

*Unit of General Pathology, Dept. of Medicine and Surgery, University of Parma, Parma, Italy.*

**Introduction:** ATP binding cassette (ABC) transporters are a superfamily of transmembrane proteins that can transport a wide variety of substrates, including endogenous molecules and xenobiotics, in an energy-dependent manner. In particular, the 3 ABC transporters P-glycoprotein (P-gp, *ABCB1*), multidrug resistance-associated protein 1 (MRP1, *ABCC1*), and breast cancer resistance protein (BCRP, *ABCG2*) play a crucial role in the translocation of a broad range of drugs, and are involved and overexpressed in the development of multiple drug resistance in cancer cells. Literature evidence reports the expression of these transporters in the lung, but only incomplete data about their localization and functional activity are thus far available. In this study, we performed a complete characterization of P-gp, MRP1, and BCRP transporters in terms of expression, localization, and activity in EpiAirway, an innovative model of primary human bronchial cells. Calu-3 cells, one of the most representative models of the *in vivo* bronchial epithelium, was used for comparison. **Methods:** EpiAirway as well as Calu-3 cells were grown up to 21 days at air-liquid interface (ALI) on membrane inserts. Under these conditions, the integrity of the monolayers was maintained as indicated by the high values of transepithelial electrical resistance (TEER >400 W · cm<sup>2</sup>) and low <sup>14</sup>C-mannitol permeability (<4 · 10<sup>-7</sup> cm/sec). Gene expression was monitored through RT-qPCR, whereas the activity of the transporter was analysed by measuring the apical-to-basolateral and basolateral-to-apical fluxes of specific substrates; protein localization was assessed by means of immunocytochemistry with confocal microscopy. **Results:** EpiAirway and Calu-3 cells express a high level of MRP1, that clearly localizes and operates at the basolateral side of the monolayers. EpiAirway cells also express BCRP, both on the basolateral and the apical membranes, whereas Calu-3 cells do not. The 2 models also differ in terms of P-gp: Whereas the transporter is

readily detectable and operative at the apical side of fully differentiated cultures of Calu-3 cells (ALI for 21d), EpiAirway cells do not express it; nor do they display a functional activity. **Conclusions:** These findings indicated that: 1) Differences exist between EpiAirway and Calu-3 cells; 2) EpiAirway represents a relevant tool to study the mechanisms of drug delivery in the respiratory epithelium and to further evaluate the involvement of ABC transporters in the modulation of the bioavailability of administered drugs.

#### 07-P05. Analysis of DNA Glycosylases MUTYH and OGG1 and Their Correlation with EGFR Signalling in Normal and Nodular Thyroid Tissues

C. Moscatello<sup>1</sup>, M.C. Di Marcantonio<sup>1</sup>, M. Di Nicola<sup>1</sup>, E. D'Amico<sup>1</sup>, A. Cichella<sup>2</sup>, G. Spacco<sup>3</sup>, L. Dolci<sup>3</sup>, E. Muccichini<sup>3</sup>, A. Marchetti<sup>1,4</sup>, L. Napolitano<sup>1,5</sup>, G. Mincione<sup>1</sup>, R. Cotellese<sup>1,5</sup>, R. Muraro<sup>1</sup>, G.M. Aceto<sup>1</sup>

<sup>1</sup>G. d'Annunzio University of Chieti-Pescara, Department of Medical, Oral and Biotechnological Sciences, Chieti, Italy, <sup>2</sup>Casa di cura convenzionata "Villa Serena" Città Sant'Angelo, Chirurgia Generale, Pescara, Italy, <sup>3</sup>G. d'Annunzio University of Chieti-Pescara, Chieti, Italy, <sup>4</sup>UOC di Anatomia Patologica Asl 02 Lanciano-Vasto-Chieti, Chieti, Italy, <sup>5</sup>Ospedale Clinicizzato "Santissima Annunziata," Chirurgia Generale Oncologica, Chieti, Italy.

**Introduction:** Thyroid diseases affect about 20% of the Italian population. The identification of molecular markers to characterize pre-malignant or malignant thyroid lesions is an important goal in the clinical management of patients affected by thyroid nodules. Many aspects of the nodular pathogenesis remain unclear, although the association among thyroid hormone metabolism, oxidative DNA damage, and the high rate of spontaneous mutations present in the normal thyroid appears to be the basis of carcinogenesis. To verify whether the DNA repair system for oxidative stress injuries was already involved in the early stages of thyroid carcinogenesis, we analysed MUTYH and OGG1 and their relationship with EGFR signalling in normal and nodular thyroid tissues. **Methods:** Forty-one TIR3B euthyroid nodules and adjacent normal tissues were selected from patients who had undergone thyroid surgery at Unit of Surgical Oncology of SS Annunziata Hospital, Chieti. Gene and protein expression were evaluated by qRT-PCR and Western blot, respectively. All statistical analyses were performed using SPSS software. Significance was set at  $p < 0.05$ . **Results:** Medical records showed the presence of Ab- Anti-TPO and Anti-TG in 19 out of 41 cases, even if under the cut-off values; thus, we subdivided tissues into goiters without inflammatory features (NIG:  $n=22$ ) and

goiters with inflammatory features (IG:  $n=19$ ). In pathological tissues, *MUTYH* gene expression was significantly higher in IG compared to NIG ( $p = 0.04$ ). *ERBB2* gene expression showed a significant difference ( $p = 0.01$ ) between normal and pathological NIG tissues with an increase in the second ones. A positive correlation between *ERBB2* and *MUTYH* expression was observed both in pathological and normal tissues, with  $p = 0.023$  and  $p < 0.001$ , respectively. *OGG1* expression showed a direct relationship with Anti-TPO in normal tissues ( $p = 0.008$ ) that reverted in pathological tissues ( $p = 0.011$ ). *OGG1* protein was more expressed in pathological tissues than in normal tissues, whereas *ERBB2* and *EGFR* showed no difference in expression between normal and pathological tissues. **Conclusions:** The current study provided the first evidence that in thyroid tissues, *ERBB2* and *MUTYH* gene expression were related, and *OGG1* protein overexpression could be a marker of thyroid nodular disease.

#### 07-P06. Human Microglia-Retinal Endothelial Cell Communication Is Regulated by Prep1

I. Cimmino<sup>1</sup>, A. Palma<sup>1</sup>, S. Parente<sup>1</sup>, C. Malandrino<sup>1</sup>, A. Furno<sup>1</sup>, F. Margheri<sup>2</sup>, A. Laurenzana<sup>2</sup>, G. Fibbi<sup>2</sup>, P. Formisano<sup>1</sup>, F. Oriente<sup>1</sup>  
<sup>1</sup>Università di Napoli Federico II & CNR/IEOS - URT 'Genomic of diabetes', Naples, Italy, <sup>2</sup>Università degli Studi di Firenze, Florence, Italy.

**Introduction:** Diabetic retinopathy (DR) is one of the most common complications of diabetic patients and the main cause of vision loss due to microvascular changes in the retina. DR is believed to result from interplay between retinal endothelial cells and neurons that are influenced by systemic metabolic parameters. Increasing evidence indicates inflammation as a critical contributor to the development of DR. One of the first signs of inflammation in DR is the activation of microglial cells. A complex chain of mechanisms, mediators, and signaling cascades contribute to inflammation in DR. These include inflammatory cells and inflammatory mediators, like cytokines and chemokines. Unfortunately, the exact mechanism of microglia activation in DR is still unknown. Prep1 is a homeodomain transcription factor which impairs glucose and lipid homeostasis in skeletal muscle, liver, and adipose tissue. In addition, we have also demonstrated that the diabetogene *Prep1* stimulates angiogenesis through a PGC-1 $\alpha$ -mediated mechanism *in vitro* and *in vivo*. The aim of this study was to elucidate the role of Prep1 in the interaction between microglia and retinal endothelial cells that modulates a neovascularization response. **Methods:** For this study we used human microglial cells (HMC3) transfected with *Prep1*, and human retinal

endothelial cells (HR-EC). Proteins and mRNA levels were analyzed by Western blot and Real-Time RT-PCR. Bioplex assays were performed to analyze cytokines and chemokines in conditioned media (CM). **Results:** *Prep1* overexpression in HMC3 activated microglia M1 phenotype with the production of pro-inflammatory cytokines and mediators inducing breakdown of the blood-brain barrier (BBB). Conditioned media obtained from *Prep1* overexpressing HMC3 cells (HMC3-CM) have been applied on HR-EC to evaluate cell proliferation, cell motility, and tube formation. All of these effects were stimulated by *Prep1*, which is able to secrete pro-angiogenic factors in HMC3-CM. **Conclusions:** These observations indicate that *Prep1* regulates intercellular communication between HMC3 and HR-EC that leads to the modulation of the expression of pro-angiogenic factors which are necessary for an enhanced neovascular response. Thus, a better understanding of the underlying mechanism for these interactions is needed to suggest *Prep1* as a potential future target of retinal neovascularization therapy.

### Selected Neurodegenerative Diseases, Aging, Oxidative Stress Abstracts

#### 08-P01. DNA Damage in Adult Stem Cells: A Possible Marker for Frailty?

S. Bombelli<sup>1</sup>, C. Grasselli<sup>1</sup>, P. Mazzola<sup>1</sup>, S. Eriani<sup>1</sup>, M. Bolognesi<sup>1</sup>, F. Rossi<sup>2</sup>, L. Antolini<sup>1</sup>, G. Annoni<sup>1</sup>, G. Cattoretti<sup>1</sup>, R.A. Perego<sup>1</sup>

<sup>1</sup>University of Milano-Bicocca, School of Medicine and Surgery, Monza, Italy, <sup>2</sup>San Gerardo Hospital ASST Monza. Immunotrasfusione Service, Monza, Italy.

**Introduction:** Frailty is a clinical syndrome closely linked to advanced age. It can be defined as a state of increased vulnerability, resulting from severe decline of several physiological systems and in a reduced capacity to compensate for external stressors. Frailty is defined by Fried criteria based only on reduced physical and mechanical functions; no molecular markers are available. We hypothesize that in frailty oxidative stress can be involved given its pivotal role in the aging process and stem cell homeostasis. Given these premises, we have investigated the correlation between frailty and DNA damage as an effect of oxidative stress, both in PBMC and hematopoietic stem cells (cHSC) of frail and non-frail seniors and healthy young, and in adult human renal stem cells obtained from nephrospheres (NS) treated with plasma of frail and non-frail subjects. **Methods:** PBMC cells were isolated from whole blood samples of frail and non-frail seniors and young controls by Ficoll-Paque density gradient separation and then incubated with the following antibodies: CD3 for lymphocytes,

CD14 for monocytes, CD34 for cHSC, and Anti-Phospho-Histone H2A.X ( $\gamma$ -H2AX) to identify DNA double strand break. From human renal tissue obtained from nephrectomy, NS cultures have been established and treated with 10% plasma of enrolled subjects. Renal stem/progenitor cells obtained after NS dissociation were stained with  $\gamma$ -H2AX. DNA damage was assessed by fluorescence-activated cell sorting (FACS).

**Results:** In PBMCs and cHSCs from frail seniors there is a significant increase of cells with DNA damage compared to young. A not significant higher percentage of PBMCs with DNA damage in frail compared to non-frail seniors was seen. Moreover, a significant higher percentage of  $\gamma$ -H2AX positive cells was detected in cHSCs of frail seniors. Of note, there is an increase of DNA damage in renal stem/progenitor cells treated with 10% plasma of frail seniors compared to those treated with plasma of non-frail seniors (not statistically significant) and healthy young (statistically significant). **Conclusions:** Our findings show that cHSCs of frail patients have the highest amount of DNA damage compared to other groups, as well as the renal stem/progenitor cells treated with plasma from frail subjects. These data indicate that frail subjects present circulating factors inducing DNA damage at the level of stem cell pool. The damage could be linked to an increased oxidative status related to frailty that will be evaluated in the plasma of subjects recruited. The DNA damage can eventually be used in the clinic as molecular markers to identify a frail phenotype.

### Selected Solid Tumors Abstracts

#### 09-P01. Tetraploid Partial Hydatidiform Moles: Molecular Genotyping and Determination of Parental Contributions

J. Bynum<sup>1</sup>, D. Batista<sup>1</sup>, R. Xian<sup>1</sup>, D. Xing<sup>1</sup>, J. Eshleman<sup>1</sup>, B. Ronnett<sup>1</sup>, G. Zheng<sup>2</sup>

<sup>1</sup>Johns Hopkins University, Baltimore, MD, United States, <sup>2</sup>Mayo Clinic, Rochester, MD, United States.

**Introduction:** DNA genotyping studies have established that most partial hydatidiform moles (PHM) are diandric dispermic triploid conceptions. Rare triandric tetraploid PHMs have been described but genotyping cannot determine the manner in which 3 paternal chromosome complements are derived: 1) sperm with triplication, 2) sperm with 1 duplication, and 3) different sperm, 1 diploid, and 1 haploid sperm). **Methods:** Using a combination of histology, immunohistochemistry, and microsatellite studies to review cases which came through an academic gynecologic pathology service using a previously described algorithm, 5 tetraploid PHMs were encountered among 235 PHMs. Single nucleotide polymorphism (SNP) arrays were used to define different paternal chromosomal contributions. **Results:** STR analysis of the 5 tetraploid PHMs

established that these contained 3 paternal and 1 maternal chromosome complements. In each case, the corresponding SNP array showed 5 tracts with segmented absence of the central tract across approximately 25% of the genome. Meiotic crossovers could be observed directly in the chromosomes via the total number of "starts and stops" of regions of loss of heterozygosity. The findings are consistent with each conceptus having 3 different paternal contributions and 1 maternal contribution. **Conclusions:** The findings suggest that tetraploid PHMs arise when 3 different sperm fertilize a single, normal ovum. SNP array is useful to determine the parental contributions in triploid/tetraploid conceptuses. It also allows for direct visualization of meiotic crossover frequency and sites in these conceptions, providing insight into their biology.

#### 09-P02. ALK Rearrangement Status in EGFR-Negative Non-Small Cell Lung Cancers in Pakistan

Z. Ahmed, M. Shareef, S. Siddiqui, Z. Khattak  
Aga Khan University, Pathology and Lab Medicine,  
Karachi, Pakistan.

**Introduction:** The prevalence of anaplastic lymphoma kinase (ALK) rearrangement mutation in non-small cell lung cancer (NSCLC) patients is found to be 3%-13%. The presence of *EGFR*, *ALK*, or any driver mutation is a prerequisite for targeted therapy and thus needs to be accurately assessed in NSCLC. Because *EGFR* and *ALK* rearrangement are mutually exclusive, patients with *ALK* mutation are not thought to benefit from *EGFR*-targeting tyrosine kinase inhibitor therapy. Instead, a treatment with an *ALK* inhibitor (crizotinib, ceritinib) is indicated to evaluate the occurrence of *ALK* rearrangement by fluorescence *in situ* hybridization (FISH) in *EGFR*-negative adenocarcinoma of primary lung origin. **Methods:** Sixty-eight patients with *EGFR*-negative NSCLC were examined for *ALK* rearrangement by FISH between January 2019 and August 2019. *EGFR*-negative NSCLC samples were subsequently tested for presence of *ALK* rearrangement by FISH using Abbott Molecular (US) break apart probe.

**Results:** In this study we investigated 68 samples of male (46) and female (22) ranges between 15 to 82 years. Out of 68 patients, 7 (10.2%) were found to have *ALK* gene rearrangements. Our study showed 10.2% positive of *ALK* rearrangement mutation in *EGFR*-negative NSCLC patients. **Conclusions:** The presence of *EGFR*, *ALK*, or other driver mutations is a prerequisite for targeted therapy and thus needs to be accurately assessed in NSCLC. The identification of *ALK* rearrangement in patients with advanced NSCLC is associated with better prognosis if target therapy is started.

#### 09-P03. Renal Cell Carcinomas with Clear Cell Phenotype and Leiomyomatous Stroma Harboring TSC Mutations

R. Lapadat, M. Parilla, J. Cho, P. Wanjari, J. Segal, C. Fitzpatrick, T. Antic  
University of Chicago Medical Center, Pathology,  
Chicago, IL, United States.

**Introduction:** Renal cell carcinoma (RCC) with leiomyomatous stroma is a provisional category of RCC in the 2016 World Health Organization Classification (WHO) of Tumors of the Urinary System. Recent studies showed that this category of RCC includes at least 4 subtypes such as clear cell (ccRCC), clear cell papillary (ccpRCC), *TCEB1* mutated, and a subtype of RCC with *TSC* gene mutations. The clinical, pathologic, immunohistochemical, and molecular features of the last subtype are studied. **Methods:** Following institutional IRB approval, >500 cases of RCC with clear cell phenotype were reviewed searching for RCCs with prominent smooth muscle stroma. Twenty-one cases were selected and studied by morphology, immunohistochemical study, and in-house next-generation sequencing that targets 1,213 cancer genes. Clinical, pathologic, and genetic features were recorded. **Results:** In 15 cases diagnoses were changed accordingly into ccRCC, ccpRCC, and *TCEB1* mutated RCC based on morphology, immunohistochemistry, and molecular findings. Six cases could not have been reclassified. Out of the 6 patients, 4 were male and 2 female, ages between 29 to 62 years (mean: 43.5; median: 40.5). One patient had a history of tuberous sclerosis. Tumor size ranged from 0.8-5.0 cm. Five were stage T1, 1 was T3, and 1 case had metastasis into a regional lymph node. The morphology revealed that all tumors have nested, tubular, and tubulopapillary architecture. The epithelium was intimately embedded into the rich smooth muscle stroma. WHO/ISUP grade corresponded to grades 3 and 4. Nuclei were randomly distributed, and cytoplasm had predominantly clear and occasionally granular appearance. Five tumors were positive for CAIX in all-around membranous fashion, and 1 had cup-shaped staining. CD10 and CK7 were positive in all cases. None of the cases had copy number variations. Four cases had *TSC1* mutations and 2 cases *TSC2* mutations (Table 1). **Conclusions:** This descriptive study, although small, demonstrates the difficulty in applying the current World Health Organization provisional criteria at a single institution with suggestion of an immunohistochemical panel with molecular study that may assist in the diagnosis of *TSC1/TSC2*-mutated RCC with leiomyomatous stroma.

Case #	Sex	Age	Cell %	CKV	CD10 (Membranous)	Gene mutations	Final Integrated Diagnosis	Tumour Size (cm)/Stage	Follow-up
1	Male	33	Cup 30%	Strong diffuse	Strong focal	TSC1 c.2526-3C>T	Unclassified	5.0/pt3a	No follow-up available
2	Male	29	Full 30%	Strong focal	Moderate focal	TSC1 p.Leu489H>Met*19	TSC associated RAS-like RCC	3 and 1.8/pt1a/m	No available histologic pancreatic vs possible pancreatic neoplasm
3	Female	56	Cup 30%	Strong focal	Moderate focal	TSC2 p.Leu214A>G, TSC2 p.Arg1200T>P	Unclassified	3.0/pt1a	Free of RCCx2, yalva and disease free
4	Female	32	Full 30%	Moderate focal	Strong focal	TSC2 p.Trp1014A>G, SFTD p.Arg171Pro>Gln	Unclassified	0.8 and 1.4/pt1a/m	No follow-up available
5	Male	41	Full 30%	All focal	Strong focal	TSC1 c.2396T>A, p.L639F (NM_000368.4) VAF 24%	Unclassified	3.8 cm/1a/bx	No follow-up available
6	Male	40	Full 30%	All focal	Strong focal	TSC1 nonsense NM_000368.4:c.22530G>T TSC1 frameshift NM_000368.4:c.1452_1454del	Unclassified	2.7 cm/11N1a	No follow-up available

[Table 1]

### 09-P04. Prevalence of Hereditary Cancer Susceptibility Syndromes with Cancer in a Highly Consanguineous Population Using an NGS-Based Panel

M. Abedalthagafi, The 1,000 Saudi Families Cancer Study  
King Fahad Medical City and King Abdulaziz City for Science and Technology, Genomics Research Department, Riyadh, Saudi Arabia.

**Introduction:** Many of our patients in Saudi Arabia have an elevated risk of hereditary cancer syndromes. We sought to identify specific groups who remain at high risk and evaluate whether they should be offered multigene next-generation sequencing (NGS) panel testing.

**Methods:** We prospectively tested 291 high-risk adult and pediatric patients (individuals and families) on a 30 NGS multigene panel who were enrolled in a 1,000 familial Saudi cancer study at King Fahad Medical City. Additionally, they met one of the following criteria: 1) personal history of cancer under 40, 2) personal history of cancer under 40 and a first- or second-degree relative with a history of cancer, and 3) certain childhood cancers like CPC and ACC. Among the 291 at high risk of cancer syndromes who have not been previously tested, 68% are females and 32% are males. **Results:** A total of 65% tested positive for pathogenic mutation. Among the negative cases, 45% carried variants of uncertain significance (VUS). Breast, colorectal, and CNS cancers were the most common types. Mutations in *APC*, *BRCA2*, *BRCA1*, and *ATM* accounted for 51% of all tested genes. The identification of individuals with multiple pathogenic mutations has important implications for family testing. The presence of individuals with multiple pathogenic mutations in our cohort samples suggests that comprehensive multigene panel testing could supplant targeted testing for single known familial mutations. Today, genetic testing for hereditary cancer syndrome has moved from testing single genes to broader NGS panel testing. The study population represented a cohort of primarily Saudi Arabian patients, which could be generalized to the Arab population.

**Conclusions:** The high level of consanguineous

marriage in our population advances our understanding of the true frequency and spectrum of pathogenic variants in these genes, and highlights the clinical actionability and utility of multigene panels for hereditary cancer risk.

### 09-P05. Characterisation of Triple-Negative Breast Cancer (TNBC) Using a 3-Gene Biomarker Signature to Detect *PIK3CA*, *AKT1* and *PTEN* Alterations by NGS and Gene Expression by PAM50 and Burstein Classifiers

H.M. Savage<sup>1</sup>, C.-W. Chang<sup>1</sup>, M.J. Wongchenko<sup>1</sup>, J. Aimi<sup>1</sup>, D. Kim<sup>1</sup>, W. Lin<sup>1</sup>, R. Deurloo<sup>2</sup>, T.R. Wilson<sup>1</sup>  
<sup>1</sup>Genentech Inc., South San Francisco, CA, United States, <sup>2</sup>F. Hoffmann-La Roche Ltd, Basel, Switzerland.

**Introduction:** A novel next-generation sequencing (NGS)-based composite 3-gene biomarker signature was developed to identify patients (pts) with PI3K/AKT pathway-activated tumours (He *et al.* AACR 2018). Pts with this signature derived enhanced benefit from ipatasertib in 2 randomised phase 2 trials in TNBC (Kim *et al.* Lancet Oncol 2017; Oliveira *et al.* Ann Oncol 2019). We determined the prevalence of the 3-gene signature in a procured set of TNBC tumour samples and explored overlap with other molecularly defined complex alterations. **Methods:** DNA and RNA were prepared from a procured collection of formalin-fixed, paraffin-embedded (FFPE) tumour tissue samples. Sequence data from evaluable tumours were generated at Foundation Medicine, Inc. (Cambridge, MA, US) using a proprietary analysis pipeline. Data were evaluated using the 3-gene signature to identify activating alterations in *PIK3CA* and *AKT1* and inactivating alterations in *PTEN* (Wongchenko *et al.* AMP 2019). Gene expression was evaluated by RNA sequencing (TruSeq RNA Access; Illumina, Inc., San Diego, CA, US) at Expression Analysis (Morrisville, NC, US). Based on gene expression, samples were subtyped according to PAM50 (Chia *et al.* CCR 2012) and Burstein (Burstein *et al.* CCR 2014) intrinsic classifiers. **Results:** Of 500 TNBC samples, 433 (DNA) and 321 (RNA) were sequenced. *PIK3CA*, *PTEN*, and *AKT1* alterations were detected in 15%, 16%, and 2% of 433 samples, respectively, using the 3-gene signature. The other most common alterations were *TP53* (85%), *MYC* (22%), *BRCA1/2* (15%) and *RB1* (14%); 0.9% had high tumour mutation burden (TMB; >16 mutations/Mb). Comparison with pts harbouring *PIK3CA/AKT1/PTEN* alterations revealed consistent prevalences of *TP53* (80%), *BRCA1/2* (16%), and *RB1* (15%), but a lower prevalence of *MYC* (13%), and a higher prevalence of high TMB (2%). **Conclusions:** *PIK3CA/AKT1/PTEN*-altered tumours had a lower proportion of PAM50 basal and Burstein basal-like immune-activated subtypes, and a higher proportion of luminal subtypes versus all TNBC pts. The *PIK3CA/AKT1/PTEN* 3-gene signature is undergoing clinical validation in the IPATunity130 randomised phase 3 trial (NCT03337724). Using this 3-gene biomarker signature in conjunction with gene

expression classifiers may help to identify clinically actionable subsets of pts who may benefit from the addition of ipatasertib to standard therapies.

Classifier	Subtype	No. of samples (%)	
		All TNBC (n = 321)	PIK3CA/AKT1/PTE N altered (n = 93)
PAM50	Basal	237 (74)	53 (57)
	HER2	29 (9)	16 (17)
	Luminal A	25 (8)	13 (14)
	Luminal B	7 (2)	4 (4)
Burstein	Basal-like immunosuppressed	123 (38)	34 (37)
	Basal-like immune activated	101 (31)	17 (18)
	Luminal androgen receptor	59 (18)	32 (34)
	Mesenchymal	38 (12)	10 (11)

[Table]

### 09-P06. Comprehensive Next-Generation Sequencing (NGS) as a Diagnostic Tool for Pathologists

R. Goldstein<sup>1,2</sup>, E. Tahover<sup>3</sup>, V. Doviner<sup>1</sup>, O. Rosengarten<sup>3</sup>, N. Heching<sup>3</sup>, S. Zilber<sup>1</sup>, Y. Smith<sup>4</sup>, E. Golomb<sup>1</sup>

<sup>1</sup>Shaare Zedek Medical Center, Pathology, Jerusalem, Israel, <sup>2</sup>Hebrew University of Jerusalem, Division of Clinical Pharmacy, School of Pharmacy, Faculty of Medicine, Jerusalem, Israel, <sup>3</sup>Shaare Zedek Medical Center, Oncology, Jerusalem, Israel, <sup>4</sup>Hebrew University-Hadassah Medical School, Genomic Data Analysis Unit, Jerusalem, Israel.

**Introduction:** In recent years, commercial comprehensive next-generation sequencing (NGS) has become a popular tool for identifying treatable mutations in cancer patients. These molecular reports offer pivotal information about the genomic profile of the cancer. They can also serve as a diagnostic tool to characterize tumors by their mutational profile. It has been recommended that genomic reports be included in the pathologist's diagnostic tool box, though no quantitative research on the extent of effect is available. Furthermore, in routine practice, NGS reports are not sent to pathologists for review. We aim to analyze the

effect of incorporation of comprehensive NGS reports into pathology diagnosis and reporting. **Methods:** We reviewed NGS requests sent to our pathology institute from 2016 to 2019 and attempted to obtain reports. We analyzed the details of each report, including mutations and the company's explanation of significance, and recorded the data on a spreadsheet. Simultaneously, we reviewed the patients' medical files, including pathology reports, oncology visits, and follow-ups. A molecular pathologist reviewed the data, including genomic data, imaging, morphology, and IHC stains. An addendum was added to the relevant pathology report. Addenda were rated for significance to diagnosis on a scale of 0 to 6. After rating, data were compiled into a histogram to assess significance. We considered weak confirmations mildly significant to diagnosis, especially when the initial certainty of diagnosis was low. Reports that received high ratings were further analyzed to determine possible variables that contribute to their significance. **Results:** A total of 242 requests for NGS tests were documented. We obtained 167 NGS reports (78%). Of the 167 reports, almost all (96%) were rated with some level of significance (>0). Most of the reports (53%) gave a strong confirmation to the diagnosis and were rated 3. A total of 14% of reports had significant diagnostic value (rating 4-6) including 6 reports that led to a change in diagnosis. In sub-analyses, we found a correlation between the significance of molecular profile to diagnosis and variables including initial diagnostic uncertainty, non-primary specimen site, and cancers of unknown primary (CUP). **Conclusions:** Comprehensive NGS reports are a valuable component of pathology reports and diagnoses. Whereas most NGS results confirmed the diagnosis, which is a notable achievement, a significant number of reports affected the diagnosis. Tumors sampled from metastases, unidentified primaries, and initially uncertain diagnoses had genomic profiles that correlated with higher diagnostic significance. In addition to revealing potential treatment options, genomic data can influence the pathological diagnosis.

### 09-P07. Comprehensive Genomic Profiling of Gallbladder Cancer in a Western Population Identifies Multiple Clues for Actionable Therapeutic Targets

T. de Bitter<sup>1</sup>, E. de Savornin-Lohman<sup>2</sup>, E. Vink-Börger<sup>1</sup>, S. van Vliet<sup>1</sup>, M. Hermsen<sup>1</sup>, L. Kroeze<sup>1</sup>, D. von Rhein<sup>3</sup>, E. Jansen<sup>3</sup>, I. Nagtegaal<sup>1</sup>, P. de Reuver<sup>2</sup>, M. Ligtenberg<sup>1,3</sup>, R. van der Post<sup>1</sup>

<sup>1</sup>Radboud University Medical Center, Pathology, Nijmegen, Netherlands, <sup>2</sup>Radboud University Medical Center, Surgery, Nijmegen, Netherlands, <sup>3</sup>Radboud University Medical Center, Human Genetics, Nijmegen, Netherlands.

**Introduction:** Gallbladder cancer (GBC) is a rare malignancy in Western countries and carries a dismal prognosis. The only curative treatment is surgery, but because of late detection and aggressive behavior, only

a minority of patients are eligible for resection. Targeted therapies can potentially improve prognosis but are unavailable for GBC. The aim of this study was to identify actionable therapeutic targets for GBC.

**Methods:** Patients with primary GBC diagnosed between 2000 and 2019 in the Netherlands were identified using PALGA, the national pathology database, and the Netherlands Cancer Registry. Clinicopathological data and resection specimens of >800 patients were collected. To gain more knowledge on GBC and to identify potentially actionable therapeutic targets, genomic profiling was performed on cases from 2015 onwards using the Illumina TruSight Oncology-500 DNA assay. This next-generation sequencing (NGS)-based panel of 523 cancer-related genes allows simultaneous detection of subtle nucleotide variants, copy number variants, tumor-mutational burden (TMB), and microsatellite instability (MSI). **Results:** A total of 49 cases were analyzed using the TSO500 assay. Altogether, 53% of cases harbored at least 1 genomic alteration in a potentially actionable target gene. Gene amplifications were observed, amongst others, in *ERBB2* (4%), *MET* (2%), and *MDM2* (12%) with co-amplification of *CDK4* in half of the *MDM2* amplified cases. Confirmed or likely pathogenic variants were most frequently observed in *TP53* (53%) and were mutually exclusive with *MDM2* amplifications. Other genes with confirmed or likely pathogenic variants were, amongst others, *PIK3CA* (10%), *KRAS* (10%), *CDKN2A* (6%), and *ERBB2* (4%). All cases were microsatellite stable. Eight cases (16%) had a TMB of >10 mutations/Mb (range: 10.2-161.1 mutations/Mb); the highest mutational load was observed in a case carrying a pathogenic variant in *POLE*. **Conclusions:** Our results show extensive molecular heterogeneity among GBC cases and reveal potentially actionable genomic alterations in a large subset of patients, paving the way to targeted therapies for GBC patients.

#### 09-P08. Immunohistochemical Expression of BRCA1 and BRCA2 in Prostate Cancer: A Cross-Sectional Study in Kampala, Uganda

P. Amsi<sup>1</sup>, J. Yahaya<sup>2,3</sup>, S. Kalungi<sup>4</sup>, M. Odida<sup>2</sup>

<sup>1</sup>Makerere College of Health Sciences, Makerere, Uganda, <sup>2</sup>Makerere College of Health Sciences, Kampala, Uganda, <sup>3</sup>The University of Dodoma, College of Health Sciences, Biomedical Science, Dodoma, Tanzania, United Republic of, <sup>4</sup>Mulago National Specialized Hospital, Kampala, Uganda.

**Introduction:** Molecular pathogenesis of prostate cancer commonly involves mutation in *BRCA1/2* genes which leads to expression of BRCA proteins in tumor cells. We hypothesized that immunohistochemical expression of BRCA1/2 proteins in prostate cancer tumour tissue may be associated with clinicopathological prognostic factors of prostate cancer in Uganda.

**Methods:** Retrospectively, we used immunohistochemistry to evaluate the expression of BRCA1/2 antibodies in tissue blocks of 188 patients with

prostate cancer patients who were diagnosed from January 2005 to December 2014 in the Department of Pathology, Makerere College of Health Sciences. Chi-Square and Student t-tests, where appropriate, were used to compute the correlation of the variables.

**Results:** Expression of BRCA1 and 2 was found in 26.1% and 22.9% cases, respectively. Co-expression of BRCA1 and 2 was found in only 7.4%. Gleason score was associated with expression of BRCA1 and BRCA2 ( $P = 0.013$ ,  $P = 0.041$ , respectively). **Conclusions:** BRCA1 and 2 proteins were expressed more in cases with poorly differentiated prostate cancer than in cases with either well- or moderately differentiated prostate cancer. This study also sheds an insightful observation that simultaneous expression of both BRCA1 and 2 proteins in the same patient seems to be 3 times less than either BRCA1 or BRCA2 alone. This needs further investigation to establish their prognostic role by involving survival of prostate cancer patients. **Keywords:** Prostate cancer, BRCA1, BRCA2, Immunohistochemistry, Kampala

#### 09-P09. Comparison of Variant Detection Abilities between the TSO500 Pan-Cancer Panel and an In-House Comprehensive Cancer Panel

C.R. McEvoy, H. Xu, D.Y. Choong, R. Legaie, S.B. Fox, A.P. Fellowes

Peter MacCallum Cancer Centre, Melbourne, Australia.

**Introduction:** Next-generation sequencing (NGS) using cancer gene panels has revolutionised precision oncology with its ability to simultaneously detect multiple cancer-related biomarkers. Many commercial panel testing protocols are now available for this process, and their ability to accurately detect multiple variant types is critical. Here we compare the variant detection ability of the Illumina TruSight Oncology 500 (TSO500) pan-cancer DNA/RNA panel and its associated software to detect variants in samples previously characterized with our in-house comprehensive cancer panel (CCP).

**Methods:** DNA from paired tumor formalin-fixed, paraffin-embedded (FFPE)-normal (blood) samples had been previously sequenced using our 384 gene CCP using a modified KAPA Hyper library preparation with SureSelect hybridization. Results were compared to the same samples (tumor-only) prepared using the TSO500 DNA/RNA kit according to the manufacturer's instructions. Sequencing was performed on an Illumina NextSeq using 2x100 bp paired end reads and analysed using the TSO500 local app. Commercially available DNAs containing known variants including SNVs, indels, and CNVs were also used for validation. Ninety-six DNAs and 85 RNAs have been sequenced including 24 T/N pairs and 16 reference DNAs. Extensive replicates for inter and intra-run variation analysis have been performed. **Results:** Our initial results compared 38 variants originally detected with our CCP from 7 tumors. These comprised 20 missense SNVs, 5 stop-gain SNVs, 10 indels (size range 1-34 bp), 1 splice donor SNV, and 2 gene fusions (*EWSR1-FLI1* and *FGFR3-TACC3*).

TSO500 detected all previously determined variants except for 2 indels; *TP53:c.445\_466dup* (22 bp) and *KMT2D:c.5782+4\_5782+37del* (34 bp). Analysis of BAM files with IGV indicated that both of these variants were present, suggesting that they were not detected by the variant caller. Variant allele frequencies of all detected variants minus fusions showed a correlation of  $R^2 = 0.79$ , though this improved to  $R^2 = 0.97$  when only SNVs were considered. No variants detected by TSO500 but not detected by our CCP were observed. **Conclusions:** In this preliminary report we show that variant detection and calling for the TSO500 pan-cancer panel correlates well with our in-house CCP for SNVs, small indels, and fusions. However, the TSO500 variant caller appeared to miss 2 mid-size indels (a 22 bp dup and a 34 bp del). Interestingly, 27 bp, 21 bp, and 12 bp dels were all detected and called, suggesting that the TSO500 variant caller is accurate to around 20 bp. VAFs correlated well, particularly for SNVs. Further analysis of this already sequenced extensive validation cohort will be presented.

#### 09-P10. Plasma Testing for Activating and Resistance Mutations Responsible for Development and Growth of Tumors

M. Rot, I. Kern  
*University Clinic of Respiratory and Allergic Diseases, Golnik, Slovenia.*

**Introduction:** Plasma testing for activating and resistance mutations responsible for development and growth of tumors has recently become one of the most popular methods in molecular pathology and medicine in general, mostly because of its non-invasiveness and capability of tests to detect very small numbers of DNA copies in samples. The aim of our study is to evaluate the detectability of activating and resistance mutations in plasma samples of patients with lung adenocarcinoma that were EGFR positive in tumor specimen. **Methods:** DNA extraction from plasma (Cobas cfDNA Sample preparation kit, Roche, US) was followed by allele-specific PCR testing (Cobas EGFR Mutation Test V2, Roche, US). **Results:** A total of 106 patients were evaluated for activating mutations. We considered only samples of plasma taken before treatment with EGFR tyrosine kinase inhibitors (TKI). Our results showed 81.1% detectability of activating mutations in plasma samples. Forty-one patients treated with EGFR TKI were evaluated for T790M resistance mutation. Patients whose samples showed T790M in plasma or (re)biopsy, regardless of TKI treatment start and duration, were taken into consideration. Our results showed 87.8% detectability of T790M in plasma. **Conclusions:** Testing of plasma samples showed satisfactory detectability of both activating and resistance mutations, rendering this method of plasma testing suitable for patient monitoring.

#### 09-P11. Histone Mutant Astrocytic Tumours: An Experience of a Tertiary Care Cancer Centre

N. Karnik, M. Gurav, P. Gogte, G. Deshpande, O. Shetty, S. Epari  
*Tata Memorial Hospital, Molecular Pathology Division, Department of Pathology, Mumbai, India.*

**Introduction:** Histone mutations in glial tumours represent distinct tumours, which portend a bad biological behaviour. This study is a single institutional experience of histone mutations in astrocytic tumours. **Methods:** The study sample included group A, all grades of *IDH* and *BRAF*-wild-type astrocytic tumours in patients  $\leq 40$  years (irrespective of location), and group B, high-grade astrocytic tumours arising in midline in patients  $>40$  years. Immunohistochemistry for ATRX and p53, and Sanger sequencing of *H3F3A*, *HIST1H3B*, and *HIST1H3C* genes were done. Statistical analysis of categorical variables was performed using Chi square test;  $p < 0.05$  was taken as significant. **Results:** In group A ( $n = 350$ ; high grade: 328; low grade: 22), 97 of 322 interpretable cases (30.1%) and in group B ( $n = 36$ ), 7 of 36 interpretable cases (19.4%) showed histone mutations. In group A, the mutations seen were H3.3 K27M, 75 (23.3%); H3.3 K27E, 2 (0.6%); H3.1 K27M, 3 (0.9%); H3.3 G34R, 15 (4.7%); H3.3 G34V, 1 (0.3%); and frameshift, 1 (0.3%), whereas in group B all 7 cases showed H3.3 K27M mutation. Of the H3.3/H3.1 K27M/E mutant cases in group A ( $n = 80$ ; high grade -76 and low grade -4), age range was 1-46 years (1-3:4, 4-14:33, 15-18:10, 19-25:10, 26-40:23). Male to female ratio (M:F) was 1.13:1. Fifty-six (70%) were of midline location (thalamic, 24; pontine, 6; spinal, 10; other midline sites, 16), whereas 16 (20%) had superficial hemispheric location (SHL) and 8 (10%) were located in posterior fossa. ATRX loss was noted in 29/69 (42.02%) and p53 positivity in 60/70 (85.7%). Midline location ( $p < 0.0000$ ) and p53 positivity ( $p = 0.00021$ ) were found to be statistically significant with H3.3 K27M/E mutant; whereas no significant pattern of ATRX expression emerged ( $p = 0.17$ ). In H3.3 G34R/V mutant cases ( $n = 16$ ), age range was 7-29 yrs (4-14, 5; 15-18, 4; 19-25, 5; 26-40, 2). Contrary to K27M mutant, 15/16 (93.7%) were of SHL, high grade (16/16), showed loss of ATRX (14/16; 87.5%), and p53 positivity (13/16; 81.2%). For the 7 mutant tumours in group B, mean age was 43 years (41-45, 6; 45-50, 1), M:F = 1.66:1, 1 (14.2%) showed ATRX loss and 4 (57.1%) showed p53 positivity. **Conclusions:** H3.3 K27M was the predominant type of histone mutation in gliomas; other rare variants H3.3 K27E, H3.1 K27M, H3.3 G34R, and H3.3 G34V were also seen. These were common in children and young adults, but also occurred above 25 yrs, though uncommon. G34R/V mutant tumours, though known to occur in hemispheric locations, were also seen as rare midline tumours.

### 09-P12. Investigation of Discrepant MMR IHC and MSI PCR Test Results for Gynecologic Cancers

M. Smithgall, H. Remotti, M. Mansukhani, S. Hsiao, X. Liu-Jarin, H. Fernandes  
Columbia University, Pathology and Cell Biology, New York, NY, United States.

**Introduction:** Gynecologic cancers are routinely screened for mutations in DNA mismatch repair (MMR) genes using immunohistochemistry (IHC) of MMR proteins and/or MSI (microsatellite instability). Since MMR deficient (dMMR)/MSI-High (MSI-H) tumors may benefit from treatment with immune checkpoint inhibitors, the European Society for Medical Oncology (ESMO), recommends confirmatory molecular testing of MMR. This study reviewed MMR/MSI results in gynecologic cancers to investigate discrepant cases.

**Methods:** The pathology database at a large academic medical center was queried to identify gynecological cancer cases between January 1, 2014, and October 28, 2019, with both MMR IHC and MSI PCR analysis. IHC was performed using MLH1 (cloneG168-15), MSH2 (cloneFE11), MSH6 (clone44), and PMS2 (cloneMRQ-28), and MSI was performed by interrogating microsatellites in tumor and normal tissue using MSI Analysis System v1.2 (Promega). Cases were reviewed to determine the concordance rate between these methods. Discordant cases were re-reviewed by 2 pathologists, blindly and independently. For discordant cases, IHC was re-tested on additional tumors, and sequence analyses of MMR genes are underway.

**Results:** A total of 242 gynecologic cancer cases (81% endometrial) with both IHC MMR and MSI results were identified (207 primary and 37 metastatic cases). Two patients have diagnosed Lynch syndrome. There were 235 (97.1%) concordant cases. A total of 188 (77.7%) cases were microsatellite stable (MSS) with preserved MMR (pMMR), and 47 (19.4%) cases were MSI-H with dMMR. For 3 of these cases, their MSI-H status was confirmed with next-generation sequencing (NGS). Sequencing revealed pathogenic mutations in *KRAS*, *PTEN*, and *TP53* genes. Five cases (2.1%) showed dMMR but were MSS. Specifically, 3 endometrial cases showed loss by IHC of MLH1 and PMS2, an ovarian clear cell carcinoma showed loss of MSH2 and MSH6, and 1 endometrial case showed loss of PMS2 with subsequent identification of a germline *PMS2* p.S461 pathogenic mutation. IHC re-testing on all 5 cases confirmed their dMMR status, and MSI re-testing or re-review concurred with the original interpretation of MSS. Two endometrial cases showed pMMR but were MSI-H. For one, IHC on both biopsy and resection showed pMMR, and re-review of MSI testing again showed MSI-H. The other case had clear geographic tumor heterogeneity with distinct MLH1 and PMS2 dMMR and pMMR areas. MSI testing performed on each distinct area showed MSI-H in the dMMR area and MSS in the pMMR area. **Conclusions:** Overall concordance between MMR IHC and MSI testing among gynecologic cancers was high (97.1%). Our results emphasize the

importance of appropriate sampling for dual testing with MSI PCR and MMR IHC. Genetic analyses of the MMR genes for discrepant cases may help in resolving the discrepant MMR and MSI results.

### 09-P13. Comprehensive Genomic Characterization of Congenital and Infantile Cancers Reveals High Yield of Medically Meaningful Findings

C. Cottrell<sup>1</sup>, K. Schieffer<sup>1</sup>, S. Lahaye<sup>1</sup>, V. Magrini<sup>1</sup>, E. Varga<sup>1</sup>, T. Lichtenberg<sup>1</sup>, K. Leraas<sup>1</sup>, S. Colace<sup>2</sup>, K. Miller<sup>1</sup>, A. Wetzel<sup>1</sup>, D. Koboldt<sup>1</sup>, T. Bedrosian<sup>1</sup>, B. Kelly<sup>1</sup>, J. Fitch<sup>1</sup>, P. Brennan<sup>1</sup>, G. Wheeler<sup>1</sup>, K. Voytovich<sup>1</sup>, P. White<sup>1</sup>, A. Gupta<sup>2</sup>, B. Setty<sup>2</sup>, J. Finlay<sup>2</sup>, J. Leonard<sup>3</sup>, D. Osorio<sup>2</sup>, M. Abdelbaki<sup>2</sup>, S. Koo<sup>4</sup>, D. Boue<sup>4</sup>, C. Pierson<sup>4</sup>, R. Wilson<sup>1</sup>, E. Mardis<sup>1</sup>  
<sup>1</sup>Nationwide Children's Hospital, Institute for Genomic Medicine, Columbus, OH, United States, <sup>2</sup>Nationwide Children's Hospital, Division of Hematology/Oncology/BMT, Columbus, OH, United States, <sup>3</sup>Nationwide Children's Hospital, Section of Neurosurgery, Columbus, OH, United States, <sup>4</sup>Nationwide Children's Hospital, Department of Pathology, Columbus, OH, United States.

**Introduction:** In the setting of a pediatric tertiary care hospital, we have established a patient-focused translational protocol supporting genomic profiling of children, adolescents, and young adults with rare or treatment refractory cancer. Infantile and congenital cancers represent a unique cohort among our study group on the basis of disease spectrum and complexity, and associated co-morbidities in this medically fragile population. Comprehensive genomic profiling has been initiated to aid in diagnosis, prognostication, treatment, and detection of germline disease predisposition in patients with rare and difficult to treat tumors. **Methods:** Enhanced exome sequencing of disease and comparator tissue was coupled with RNA sequencing of the disease-involved specimen to assess for single nucleotide variation (SNV), insertion/deletions (indels), copy number alteration (CNA), structural variation (SV), fusions, and gene expression. Additional methodologies were applied where applicable, including methyl-array, long-read sequencing, targeted Sanger, and immune profiling. **Results:** Within a period of 20 months, 100 patients were consented onto the protocol with genomic profiling and analysis completed in 88. Among analyzed patients, 15 (17%) were infantile cancers diagnosed at  $\leq 1$  yr of age, and of those, 7 were congenital, diagnosed at  $\leq 3$  months of age. In total, the infantile/congenital cohort consisted of 8 females and 7 males, who among them harbored 7 central nervous system malignancies, and 10 solid tumors. Germline genetic alteration was frequent among the infantile/congenital cohort with 7/15 patients (47%) harboring a pathogenic change in a tumor suppressor ( $n = 6$ ) or oncogene ( $n = 1$ ). RNA analysis yielded gene fusion events in 33% (5/15) of the cohort, with 60% of these events being novel. A medically relevant somatic SNV/indel or CNA event was detected among 33% of the cohort ( $n = 5$ ) using exome

sequencing. In total, a medically meaningful finding impacting diagnosis, prognosis, therapy, or surveillance was identified in 14/15 patients (93%)  $\leq$ 1yr of age within our study. **Conclusions:** Genomic alterations represent a fundamental basis of cancer. Inclusion of germline analysis and RNA sequencing data were of particular utility for disease characterization in this infantile/congenital cancer cohort. These data support that a pediatric cohort gains greater potential benefit from a comprehensive profiling approach than analysis of a single analyte alone, with a high yield of medically meaningful findings in an infantile/congenital cancer population.

#### 09-P14. Profiling of Lung Cancer DNA- and RNA-Based Biomarkers with NGS Using Total Nucleic Acids

R. Samara<sup>1</sup>, J. Shaffer<sup>1</sup>, Q. Jiang<sup>1</sup>, G. Wilt<sup>1</sup>, S. Herold<sup>2</sup>  
<sup>1</sup>QIAGEN, Frederick, MD, United States,  
<sup>2</sup>Universitätsklinikum Dresden, Institut für Pathologie, Dresden, Germany.

**Introduction:** Understanding lung cancer development and progression requires a multi-biomarker approach that interrogates both genomic and transcriptomic elements. Currently, these multi-biomarker approaches require the use of 2 separate and parallel library preparation workflows for next-generation sequencing (NGS)-based analysis: one for DNA, the other for RNA. Although these approaches can be effective in extracting biomarker information from biological and clinical samples, they are inefficient, since efforts are duplicated for DNA and RNA library preparation, and samples need to be split to isolate DNA and RNA separately. This study evaluated the feasibility of using a consolidated library prep workflow with total nucleic acids as input for the profiling of DNA- and RNA-based biomarkers with NGS. **Methods:** Lung cancer samples were profiled for biomarkers using 2 approaches: a parallel approach using 2 separate workflows with DNA or RNA molecules as input (QIaseq targeted DNA and RNA scan panels; QIAGEN, Hilden, Germany), and a multimodal approach using a consolidated workflow with total nucleic acid input (QIaseq multimodal panels; QIAGEN, Hilden, Germany). Both approaches used 10-150 ng of starting material (formalin-fixed, paraffin-embedded [FFPE]) as input as assessed by Qubit. Libraries were constructed according to the provided handbooks. Enrichment of DNA and/or RNA was performed using a single primer extension (SPE) approach in which all primers are pooled together. The final libraries contain unique molecular indices (UMIs) and, in the case of the multimodal approach, use unique dual indices (UDIs) for sample indexing. Libraries were quantified by Qubit, and 9 pM of libraries were loaded onto a MiSeq for sequencing. Analysis was performed by the CLC Genomics Workbench (QIAGEN, Hilden, Germany) for both approaches. **Results:** On average, for each sample, 2 million reads were generated for the parallel approach, and 3 million reads for the multimodal

approach. Analyzed variants include SNVs, indels, CNVs, and fusions. Concordance analysis between the parallel and multimodal approaches was 100%. All DNA variants and fusions detected by the parallel approach were detected by the multimodal one including NTRK, ALK, FGFR, and ROS fusions, and MET exon 14 skipping as well. **Conclusions:** Profiling of lung cancer DNA- and RNA-based biomarkers with NGS using total nucleic acids in a consolidated library prep workflow is a feasible method that streamlines library preparation and enables the profiling of low-yielding samples.

#### 09-P15. Molecular Characterization of RAS-BRAF Mutational Profile in Metastatic Moroccan Colorectal Cancer Patients

R. Mani<sup>1,2</sup>, H. El Attar<sup>1</sup>, S. Bendia<sup>1</sup>, A.A. Bah<sup>1</sup>, F. Guessous<sup>3</sup>, M. Karkouri<sup>4</sup>, K. Akarid<sup>5</sup>

<sup>1</sup>Annasr Pathology Center, El Jadida, Morocco, <sup>2</sup>Ain Chock University, Casablanca, Morocco, <sup>3</sup>University Mohammed VI of Health Sciences, Casablanca, Morocco, <sup>4</sup>CHU Ibn Rochd, Anatomical Pathology Laboratory, Casablanca, Morocco, <sup>5</sup>Ain Chock University, Biology, Casablanca, Morocco.

**Introduction:** Colorectal cancer (CRC) is the third most common cancer worldwide and the second most common cause of death from cancer in Morocco. Progress and development of targeted therapies such as anti-EGFR therapy and its accessibility to Moroccan patients resulted in a significant increase of survival rate. Additionally, the study of the RAS mutational profile is becoming an interesting field of study, since it is an important predicting factor for patient response to anti-EGFR therapy, particularly in metastatic CRC. The aim of this study is to present an epidemiologic study of RAS-BRAF mutational profile in Morocco. **Methods:** We conducted this study by processing 92 cases of CRC patients using dissected formalin-fixed, paraffin-embedded (FFPE) tissues as a DNA source. We evaluated somatic RAS-BRAF mutations in codons 13, 12, 146, 61, 117, and 600 using the Idylla system and Sanger method. **Results:** The results show that 59 patients of our cohort have adenocarcinoma with a mutated RAS-BRAF gene. Among these positive mutant cases, 9 patients have NRAS-BRAF mutation with 66.67% located in codon 600 of BRAF gene (66.67% of the patients are female [F], whereas 33.33% are men [M]) and 33.33% in codon 61 of NRAS gene (66.67% F and 33.33% M). Regarding the KRAS gene, 50 patients are bearing its mutation. Among these patients 52% are male and 48% female, with the following distribution: 72% patients have a mutation in codon 12 (52.78% M and 47.22% F), 12% have a mutation in codon 13 (66.67% M and 33.33% F), 8% in codon 146 (25% M and 75% F), 4% in codon 61 (50% F and 50% M), and 4% in codon 117 (50% F and 50% M). The results show a higher distribution of codon 12 and 13 of the KRAS gene and codon 600 of BRAF gene. Additionally, our study shows a difference between male and female patients in terms of occurring mutations: the females

have significantly more gene mutations in *BRAF* and *NRAS* genes as well as in codon 146 of *KRAS* gene. As for male patients, they present a higher mutation frequency in codon 12 and 13 of *KRAS* gene. The codons 117 and 61 present the same distribution between the 2 genders. Moreover, 11% (50% M and 50% F) of codon 12 mutations are G12C substitutions, a mutation that has renewed the interest in mutated *KRAS* targeted therapy. **Conclusions:** In conclusion, mutations in *NRAS-BRAF* and *KRAS* genes differ according to gender among Moroccan CRC patients.

#### 09-P16. MET Exon 14 Skipping: Doubling Up to Overcome Detection Challenges

C. Paolillo<sup>1,2</sup>, R. Sussman<sup>1</sup>, J.J.D. Morrissette<sup>1</sup>, J.N. Rosenbaum<sup>1</sup>

<sup>1</sup>University of Pennsylvania, Pathology & Laboratory Medicine, Philadelphia, PA, United States, <sup>2</sup>Università di Foggia, Medicina Clinica e Sperimentale, Foggia, Italy.

**Introduction:** Recurrent actionable mesenchymal-epithelial transition (MET) tyrosine kinase receptor exon 14 skipping alterations (METex14) occur in up to 3% non-small cell lung cancer (NSCLC). Response to small-molecule kinase inhibitors and monoclonal antibody therapies targeting METex14 have been reported in these patients. In a recent study conducted on 38,028 tumor specimens, 224 unique genomic sequence alterations (51 intronic within 25 bp from the splice acceptor site, 35 in the splice acceptor site, 133 in the splice donor site, and 5 whole exon deletions) resulting in METex14 have been identified by next-generation sequencing (NGS)-based assays. However, most clinical DNA-based NGS panels cover either hotspots or exons, rendering them inadequate at detecting the complete spectrum of variant types that lead to METex14. **Methods:** To provide a more effective testing method in routine practice, we combined the results coming from 2 of our validated NGS-based assays: 1) A 152-gene targeted exome solid tumor panel (SOLID); and 2) an RNA-based fusion translocation panel (FTP). Preliminary data were analyzed on 58 individual formalin-fixed, paraffin-embedded (FFPE) NSCLC tumors. Finally, we assessed NSCLCs that were tested in the routine course of clinical care over a 3-years period (August 2017-October 2019). **Results:** Across the 58 NSCLC samples analyzed, METex14 RNA fusions were detected in 21 samples by FTP. Splice site mutations in exon 14 of MET were detected in only 18 of these samples by SOLID. A single sample contained a splice-site variant that was predictive of METex14 along with a MET p.Gly1113Trp co-mutation (detected on SOLID), but no MET mRNA expression was detected by FTP. In 2017, 92% of NSCLCs were assessed using only SOLID (FTP was included in the clinical practice starting in August of 2017). In 2018 about 55% and 2019 74% of NSCLCs received double testing. Over the course of 26 months, we were able to increase the detection of METex14 from 1.9% (data coming only from SOLID) up to 3.3% (combination of SOLID and FTP).

FTP has detected 4 METex14 events that SOLID did not identify (likely due to the limitations of a targeted sequencing panel). One sample with a c.3078\_3082+4delAGAAGGTAT variant was detected on SOLID but was not detected by FTP. **Conclusions:** Here we describe improved detection of METex14 by an RNA-based translocation panel. We show how predicted splice-site mutations do not always directly correlate with METex14. Together, these data highlight that combining RNA-based with traditional DNA-based assays improves the detection of this actionable oncogenic isoform of MET in routine practice.

#### 09-P17. Evaluation of a Novel One-Step FFPE Extraction and Next-Generation Sequencing DNA Library Preparation from a Slide for Use in Cancer Diagnostics and Clinical Research

T. Xu<sup>1</sup>, G. Roma<sup>2</sup>

<sup>1</sup>SenseCare Medicals, Inc, Pleasanton, CA, United States, <sup>2</sup>TargetPlex Genomics, LLC, Pleasanton, CA, United States.

**Introduction:** Formalin-fixed, paraffin-embedded (FFPE) tissue specimens have been a staple of research and therapeutic applications for decades. FFPE is a form of preservation and preparation of biopsy specimens that aids in examination, experimental research, and diagnostic/drug development. The development of advanced genomic analysis tools such as next-generation sequencing (NGS) are enabling accurate genomic profiling of FFPE cancer samples by providing crucial mutation status for targeted and personalized therapies. However, since increasingly smaller cancer tumors are being obtained from patients for cancer diagnostics, every precious FFPE section is frugally conserved. Since a single FFPE slide has only about a 4  $\mu$ M x 0.2-0.5cm<sup>2</sup> volume, and NGS DNA analysis often requires multiple sections, QNS (quantity not sufficient) for NGS testing is often a result. Processing FFPE is a tedious and labor-intensive pre-analytical step requiring deparaffinization, DNA extracting, and purification. The process often results in significant loss of nucleic acids due to the inherent process inefficiencies, and limited quality of DNA obtained from FFPE is a bottleneck for cancer research and diagnostics when employing NGS. Here we report a 1-step, highly efficient NGS DNA library preparation method from a single FFPE tissue slide we coined FFPE-Direct. This novel method solves many of the inefficiencies in FFPE processing in downstream NGS analysis. **Methods:** We compared NGS DNA libraries using either 1) a traditional FFPE preparation method, or 2) a novel TargetPlex FFPE-Direct preparation method. We compared these 2 methods by testing 1 slide from each of 3 different sample types (cervical, lung, and lymphoid FFPE tissue sections) of 4  $\mu$ M thickness slide section. **Results:** We validated the new FFPE sample preparation method. A commercial FFPE DNA extraction kit (Qiagen) was used to prepare the same DNA libraries for side-by-side comparison. The novel FFPE-Direct

method produced much higher library yields than the traditional FFPE preparation method. For sequencing conformity, in general, >90% variants detected from traditional FFPE workflow were also detected from the FFPE-Direct workflow. However, the FFPE-Direct method obtained higher sensitivity, since it detected more mutations in all 3 replicates than the traditional FFPE preparation method. **Conclusions:** Here we demonstrate that a novel FFPE-Direct method for preparing NGS DNA libraries is significantly easier and faster (<3.5 hrs from FFPE slide to NGS library). This new method will significantly simplify the NGS library preparation workflow and enable more sensitive cancer diagnostics.

#### 09-P18. Novel QuantumCyte OncoMask Technology Provides Automated Tumour Content Enrichment

T.K.H. Lim

Singhealth/ Singapore General Hospital, Molecular Pathology, Singapore, Singapore.

**Introduction:** Tumour content affects sensitivity of molecular assays. Current practical workflows rely on macrodissection or laser microdissection. The former has fairly low resolution, and the latter is time consuming and relies heavily on manpower. A novel method for the extraction of sequencing information from tissue-specific regions of interest has been demonstrated on formalin-fixed, paraffin-embedded (FFPE) slides. **Methods:** The QuantumCyte OncoMask process isolated and generated crude lysates from multiple regions of interest from FFPE tissue by integrating digital annotation information, automating the lysate extraction process, and incorporating ink-jet technology and novel ink chemistry. This process is performed directly on the tissue slide, and the crude lysates generated are then transferred to a standard collection tube for subsequent sequencing. DNA was extracted from the selected areas and the library constructed with AmpliSeq LCV2 panel and sequenced on the PGM. Quality metrics from pre-analytical and analytical points were assessed. **Results:** The resulting sequencing data will be presented and showcases the high coverage achieved using this workflow. Library QC showed optimal coverage at an average of >95% uniformity. Sequencing results showed average coverage of 95% at 250x coverage across all amplicons of the panel. Variant calling was successfully performed. **Conclusions:** The novel QuantumCyte OncoMask technology shows promise for enriching tumour content with high sequencing coverage achieved by this process. This provides an efficient solution for enrichment of tumour content. Further larger studies on both DNA and RNA should be conducted to validate this for clinical molecular testing.

#### 09-P19. Circulating Tumour DNA Analysis of EGFR-Mutant Non-Small Cell Lung Cancer Patients Receiving Osimertinib Following Previous Tyrosine Kinase Inhibitor Treatment

J. Beagan<sup>1</sup>, S. Bach<sup>1</sup>, R.A.A. van Boerdonk<sup>1</sup>, E. van Dijk<sup>1</sup>, E. Thunnissen<sup>1</sup>, D. van den Broek<sup>2</sup>, J. Weiss<sup>1</sup>, G. Kazemier<sup>1</sup>, D.M. Pegtel<sup>1</sup>, I. Bahce<sup>1</sup>, B. Ylstra<sup>1</sup>, D.A.M. Heideman<sup>1</sup>

<sup>1</sup>Amsterdam University Medical Center, Cancer Center Amsterdam, Amsterdam, Netherlands, <sup>2</sup>The Netherlands Cancer Institute, Department of Laboratory Medicine, Amsterdam, Netherlands.

**Introduction:** Circulating tumour ctDNA analysis is rapidly gaining acceptance as a diagnostic tool to guide clinical management of advanced non-small cell lung cancer (NSCLC). CtDNA can be used to detect clinically actionable *EGFR* mutations before or after first-line *EGFR*-tyrosine kinase inhibitor (TKI) treatment, but data are limited for patients with a complex treatment history. The aim of this study was to evaluate ctDNA testing in a clinical setting for patients who received osimertinib as a second- or third-line *EGFR*-TKI. **Methods:** We used *EGFR* mutations previously identified in tumour tissue to retrospectively test plasma ctDNA from 20 patients who had received osimertinib. Both sensitising and resistance mutations were analysed by droplet digital PCR (ddPCR) in plasma samples taken during routine consultations. **Results:** CtDNA was detected under osimertinib in 4 out of the 8 patients (50%) who showed no response to treatment, 2 out of the 7 (29%) who showed an initial response, and none of the 5 patients (0%) who showed an ongoing response. The fraction of ctDNA in plasma tended to be higher in non-responders (0.1%-68%) compared to the initial responders (0.2%-1.1%). **Conclusions:** Our results show that ctDNA was more readily detected in NSCLC patients who did not respond to osimertinib. This finding supports a role for ctDNA analysis in response monitoring of patients with a complex treatment history and warrants validation towards clinical implementation.

#### 09-P20. Abl2 Knockdown Affects TGFβ-Mediated 3D Invasion of ccRCC Cells

R. Perego, S. De Marco, B. Torsello, E. Minutiello, M. Bossi, S. Bombelli, C. Grasselli, C. Bianchi  
Milano-Bicocca University, School of Medicine and Surgery, Monza, Italy.

**Introduction:** Renal cell carcinoma (RCC) accounts for approximately 3% of all adult malignancies with clear cell carcinoma (ccRCC) being the most common variant, usually associated with the inactivation of the *VHL* gene. Of newly diagnosed patients, up to 30% present a metastatic disease, and patients initially treated for a localised disease will develop metastasis in 40% of cases. It has been demonstrated that TGFβ signalling enhances RCC invasion, and Abl2 improves breast cancer cell invasion. Here, we investigated the possible molecular interaction between Abl2 and TGFβ signalling

in modulation of ccRCC cell invasion. **Methods:** We performed a 3D spheroid invasion assay in collagen I matrix using imatinib (Abl family inhibitor)-treated or untreated ccRCC primary cell cultures derived from patient specimens. A 3D spheroid invasion assay has also been performed in Abl2 silenced 786-O ccRCC cell lines treated with TGF $\beta$ 1. Western blot analysis on ccRCC primary cell cultures and cell line has been performed. **Results:** We have shown that TGF $\beta$ 1 and Abl2 are upregulated and that Abl2 and phospho-Smad3, a TGF $\beta$  signalling downstream molecule, are inversely correlated in ccRCC primary cell cultures. Furthermore, we observed a single cell migration tendency of ccRCC primary cell cultures inhibited by imatinib in 3D spheroid invasion assay. We investigated the possible molecular interaction between Abl2 and TGF $\beta$  signaling in ccRCC invasion by performing a 3D invasion assay using siRNA Abl2 786-O ccRCC cell lines treated or not with TGF $\beta$ 1. In this system, Abl2 knockdown decreased tumour invasion of ccRCC cell line even after TGF $\beta$ 1 treatment, indicating that the lack of Abl2 affected TGF $\beta$  mediated invasion of ccRCC cells. Western blot analysis of TGF $\beta$  signaling molecules revealed that Abl2 knockdown in TGF $\beta$ 1 treated 786-O cells decreased Smad3 phosphorylation, suggesting that Abl2 can regulate phospho-Smad3 level and thus cell invasion. **Conclusions:** We have shown that Abl2 is involved in the TGF $\beta$ 1 mediated 3D invasion of ccRCC cells through the regulation of Smad3 phosphorylation.

#### 09-P21. Primary Central Nervous Lymphomas: Comprehension of Cell of Origin Subtypes

S. Rao<sup>1</sup>, M. Gurav<sup>2</sup>, O. Shetty<sup>2</sup>, G. Deshpande<sup>1</sup>, V. Kadam<sup>2</sup>, H. Jain<sup>3</sup>, T. Gupta<sup>4</sup>, S. Manju<sup>3</sup>, T. Shet<sup>1</sup>, S. Epari<sup>1</sup>

<sup>1</sup>Tata Memorial Hospital, Department of Pathology, Mumbai, India, <sup>2</sup>Tata Memorial Hospital, Molecular Pathology Division, Department of Pathology, Mumbai, India, <sup>3</sup>Tata Memorial Hospital, Department of Medical Oncology, Mumbai, India, <sup>4</sup>Tata Memorial Hospital, Department of Radiation Oncology, Mumbai, India.

**Introduction:** Primary CNS diffuse large B-cell lymphoma (PCNSL), a rare form of extranodal non-Hodgkin lymphoma, is relatively ambiguous on cell-of-origin (COO) subtyping. The aim of this study was to classify PCNSL into COO subtypes based on gene expression pattern (GEP) and to compare with the Hans immunohistochemical (IHC) algorithmic germinal centre B-cell (GCB) and non-GCB subgroups, and Choi IHC algorithmic GCB and activated B-cell (ABC) subgroups. **Methods:** Formalin-fixed, paraffin-embedded (FFPE) tissues of 100 cases of PCNSL in immunocompetent patients were evaluated for GEP-COO subtypes using a 20-gene target panel by nCounter Technology on the NanoString platform. The GEP-COO subtype was assigned, based on gene expression levels by relative quantification (RQ) method, as GCB, ABC, or unclassifiable (UC). These cases were also evaluated by IHC for CD10, BCL6, MUM1, GCET, and FOXP1 protein

expression. Per the Hans (H) and Choi (C) algorithms, the cases were subtyped into respective H-GCB/H-non-GCB and C-GCB/C-ABC subgroups. The uninterpretable (UI) cases were excluded. **Results:** A total of 100 cases were evaluated by Hans (H-GCB: 13; H-non-GCB: 71; H-UI: 16) and Choi (C-GCB: 6; C-ABC: 56; C-UI: 38) IHC algorithms. Fifty-six cases were analysed by GEP (GEP-GCB: 7; GEP-ABC: 21; GEP-U: 7; GEP-UI: 21), and in the rest of the cases the process of GEP is ongoing. Totals of 86% and 71% concordance were obtained between GEP-GCB with Hans (H-GCB: 6; H-UI: 1) and Choi (C-GCB: 5; C-ABC: 1; C-UI: 1) COO subtypes, respectively. Totals of 71% and 76% concordance were obtained between GEP-ABC with Hans (H-non-GCB: 15; H-GCB: 3; H-UI: 3) and Choi (C-ABC: 16; C-UI: 5) COO subtypes, respectively. All the GEP-U cases were H-non-GCB and C-ABC. Concordance between the Hans and Choi algorithmic subgroups was 87%. On excluding UI, concordant COO was noted in 19 cases by all 3 approaches (GCB: 5; ABC/non-GCB: 14). Discordance between GEP and Hans COO subtypes was 11%, and 4% with Choi COO subtypes. **Conclusions:** ABC was the predominant COO subtype of PCNSL, but 13% of cases were COO-U. Both Hans and Choi IHC algorithmic subgroups were chiefly concordant with GEP (68%) and among themselves (87%), but Choi algorithmic subgrouping was shown to have better concordance (95%) with GEP studies as compared to Hans algorithmic subgrouping (88%).

#### 09-P22. Jagged1-ICD Retrograde Signalling Handles Mechanisms of Aggressiveness and Chemoresistance in Solid Tumours: The Identification of a New Potential Molecular Marker

M. Pelullo<sup>1</sup>, F. Nardoza<sup>2</sup>, S. Zema<sup>2</sup>, I. Screpanti<sup>2</sup>, D. Bellavia<sup>2</sup>

<sup>1</sup>Center for Life Nano Science@Sapienza, Istituto Italiano di Tecnologia, Rome, Italy, <sup>2</sup>Sapienza - University of Rome, Rome, Italy.

**Introduction:** The members of the Delta-Lag2-Serrate (DLS) family are known proteins able to induce the transactivation of Notch receptors presented on the signal-receiving cells. Once translocated in the nucleus, the Notch intracellular domain (NICD) controls various aspects of cancer biology by promoting tumour growth and metastasis. The dogma of the canonical Notch signal pathway is proved not to be absolute. The emerging idea is that not only the Notch receptor is able to trigger signalling inside the receiving cell, but also its specific ligand, Jagged1, may have its own signalling pathway inside the signal-sending cell. In fact, it has been demonstrated that, similarly to the Notch receptors, the Jagged1 protein undergoes sequential proteolytic cleavages, mediated by 2 enzymes: A disintegrin and metalloproteinase ADAM-17 and PS/ $\gamma$ -secretase complex, resulting in the release of a nuclear-targeted intracellular domain (Jag1-ICD) able to govern numerous cell events. We hypothesize that Jagged1

may significantly contribute to the development and progression of solid tumours in a Notch-independent manner and could act as a potential biomarker of therapeutic approach. **Methods:** Several human cell lines of colorectal (CRC) and breast (BC) cancers were purchased from ATCC and cultured under standard conditions. Cells treated with different Jagged1 processing inhibitors targeting both metalloprotease (TAPI-2) and g-secretase complex (GSI) were subjected to several *in vitro* assays to evaluate the role of Jag1-ICD in proliferative, metastatic, and chemoresistance events. **Results:** We dissected the “retrograde” signalling pathway, triggered by the shedding of Jagged1 intracellular domain (ICD) free to move into the nucleus, which may have a role in CRC and BC initiation and progression through the regulation of the main cellular functions associated with tumorigenesis, such as proliferation and cell migration. **Conclusions:** Our preliminary data suggest that the current accepted therapies could play a controversial role in CRC and BC tumorigenesis, impairing the activation of Jagged1, which behaves like a novel oncogenic driver able to trigger an intrinsic reverse signalling with regulatory effects on tumour biology. Here, we speculate the identification of a new molecular targetable marker that may be used in the current therapies.

#### 09-P23. RGD-Integrin Antagonists as Tools to Impair Anoikis Resistance of Human Melanoma Circulating Tumor Cells (CTCs)

F. Bianchini<sup>1</sup>, S. Peppicelli<sup>1</sup>, E. Andreucci<sup>1</sup>, J. Ruzzolini<sup>1</sup>, L. Battistini<sup>2</sup>, A. Sartori<sup>2</sup>, F. Zanardi<sup>2</sup>, L. Calorini<sup>1</sup>  
<sup>1</sup>University of Florence, Experimental and Clinical Biomedical Sciences, Florence, Italy, <sup>2</sup>University of Parma, Food and Drug, Parma, Italy.

**Introduction:** Circulating tumor cells (CTCs) are the pioneers of the metastatic dissemination; thus, targeting the mechanism that promotes CTC survival in the bloodstream is crucial for an efficient therapeutic treatment against metastatic spreading. Integrins are heterodimeric cell-surface receptors, which have been characterized as master regulators of the interaction between the extracellular matrix-(ECM) and cells of different origin. The role of integrins and their downstream signaling pathways involved in the sustaining of tumor cell proliferation and survival has been extensively explored. More recently, integrin signaling has also been found to be involved in CTC anchorage independent survival, anoikis resistance, and metastatic dissemination. **Methods:** In this study, we used the A375M6 human melanoma cell line, isolated in our laboratory from a lung metastatic nodule of SCID bg/bg mice i.v. injected with A375 human melanoma. **Results:** A375M6 cells have been adapted to grow in acidic extracellular conditions (A375M6HCl resistant cells, A375M6HCIR) and we found that the anoikis-resistant phenotype of A375M6HCIR cells was associated with the expression of integrins  $\alpha$ V $\beta$ 3 and  $\alpha$ 5 $\beta$ 1, which recognize the tripeptide Arg-Gly-Asp (RGD)

sequence. In particular, we demonstrated that the exposure to anchorage independent growing conditions promoted an additional increase in  $\alpha$ V $\beta$ 3 and  $\alpha$ 5 $\beta$ 1 expression. We used specific integrin blocking agents, such as cilengitide and volociximab, which bind to  $\alpha$ V $\beta$ 3 and  $\alpha$ 5 $\beta$ 1, or to  $\alpha$ 5 $\beta$ 1 receptor, respectively, to unravel the involvement of the RGD recognizing integrin in anchorage independent survival. Moreover, using the newly synthesized RGD antagonist, we found that integrins  $\alpha$ V $\beta$ 3 and  $\alpha$ 5 $\beta$ 1 differentially regulate the anoikis-resistant phenotype of A375M6 cells.

**Conclusions:** The results of this study might contribute to the understanding of the crucial role that specific integrin receptors might have in the acquisition of the anoikis resistance phenotype of CTCs, and suggest that the use of specific antagonists might become a valuable tool to impair metastatic spreading.

#### 09-P24. Glioblastomas: IDH1/2 Mutations and Their Correlation with MGMT Gene Promoter Methylation, a Tertiary Cancer Centre Experience

K. Khirwal<sup>1</sup>, M. Gurav<sup>2</sup>, P. Gogte<sup>2</sup>, R. Rumde<sup>2</sup>, K. Rai<sup>2</sup>, V. Kadam<sup>2</sup>, A. Sahay<sup>1</sup>, O. Shetty<sup>2</sup>, S. Epari<sup>1</sup>  
<sup>1</sup>Tata Memorial Centre, Department of Pathology, Mumbai, India, <sup>2</sup>Tata Memorial Centre, Department of Pathology, Division of Molecular Pathology, Mumbai, India.

**Introduction:** Glioblastoma (GBM), the most common primary malignant tumour in adults, uncommonly characterized by *Isocitrate dehydrogenase (IDH)* mutations and variably associated with *O6-methylguanine-DNA methyltransferase* promoter (pMGMT) methylation. **Methods:** Histologically diagnosed cases of GBM in  $\geq 14$  years during 2013 to 2018 were evaluated for *IDH1/2* mutation (in a reflex manner first by immunohistochemistry [IHC] and the negative cases by Sanger sequencing for *IDH1R132* and *IDH2R172*) and pMGMT methylation by gel-based methylation-specific PCR. Cases with histone (*H3.3* and *H3.1*) and *BRAFV600E* mutations were excluded. Statistical analysis of categorical variables was performed using the Chi square test ( $p < 0.05$  significant). **Results:** A total of 663 cases formed the study cohort, of which 135 (20.3%) were *IDH* mutant (*mIDH*). A total of 111 cases showed *IDH1R132H* (IHC: 104; Sequencing: 7); others were *IDH1R132C* (11/135), *IDH1R132S* (5/135), *IDH1R132G* (4/135), *IDH1R132L* (2/135), *IDH2R172M* (1/135), and *IDH2R172K* (1/135). Male to female ratio for *mIDH* and *wildIDH* groups was 2.97:1 and 2.2:1, respectively. The frequency of *IDH* mutations in different age groups was 14-18 years: 12.5%; 19-25 years: 34.2%; 26-40 years: 43.9%; 41-50 years: 19.7%; 51-60 years: 7.6%; and >60 years: 4.2%. All *IDH*-mutant tumors were in cortical location except 1, which was predominantly thalamic, whereas 10.7% were non-cortical in *wildIDH* group (cerebellar [14/528], corpus callosum [12/528], thalamus [10/528], brainstem [12/528], spinal [3/528], basal ganglia [3/528], and pineal [3/528]). A total of 82.3% of *mIDH* cases showed loss of

ATRX protein and, interestingly, 8.5% of *wtIDH* cases also showed loss of ATRX protein. P53 positivity was noted in 84.6% of *mIDH* mutants as compared to 35.1% *wtIDH* cases. Interpretable *MGMT* methylation was available in 331 cases. A total of 58% (36/62) of *mIDHGBMs* cases showed *pMGMT* methylation, in contrast to 31.5% (85/269) *wtIDH* showing *pMGMT* methylation, which was statistically significant. A total of 56.6% (30/53) of *IDH1R132H*, 25% (1/4) of *IDH1R132C*, 100% (1/1) of *IDH1R132G*, and 80% (4/5) of *IDH1R132S* showed *pMGMT* methylation.

**Conclusions:** A total of 30.2% of GBM in adolescents and adults were *mIDH*. *IDH* mutations can also be seen in adolescents and >60 years, though rare but not non-existent. Not all cases of *mIDH* GBM show loss of ATRX protein, and also not all GBMs with loss of ATRX are *mIDH*. Expectedly, *MGMT* promoter methylation was more common in *mIDH* as compared to *wtIDH*.

#### 09-P25. Technical Performance Evaluation of the TargetPlex FFPE-Direct DNA Library Preparation Kit Combined with SiRe Next-Generation Sequencing Panel in Diagnostic Setting

E. Pepe<sup>1</sup>, G. Roma<sup>2</sup>, P. Pisapia<sup>1</sup>, M. Russo<sup>1</sup>, C. De Luca<sup>1</sup>, T. Xu<sup>2</sup>, G. Troncone<sup>1</sup>, U. Malapelle<sup>1</sup>

<sup>1</sup>University of Naples Federico II, Naples, Italy,

<sup>2</sup>SenseCare Medicals, Inc, Pleasanton, CA, United States.

**Introduction:** Next-generation sequencing (NGS) represents an intriguing approach to simultaneously analyze different mutational hotspots. However, its implementation in the routine diagnostic setting meets some restrictions. SiRe is a narrow gene panel, designed and validated at the Predictive Molecular Pathology laboratory at the Department of Public Health of the University of Naples "Federico II", covering 568 clinically relevant mutations in 6 different genes (*EGFR*, *KRAS*, *NRAS*, *BRAF*, *cKIT*, and *PDGFRa*) involved in non-small-cell lung cancer, gastrointestinal stromal tumour, colorectal carcinoma, and melanoma. An updated version of this narrow panel was designed to simultaneously analyze, in addition to the previously reported genes, the hotspots in *PIK3CA* and *ALK*. In this preliminary study, thanks to a collaboration with SenseCare Medicals, Inc., we combined the new version of SiRe NGS panel with the TargetPlex formalin-fixed, paraffin-embedded (FFPE)-Direct DNA Library Preparation Kit to evaluate the technical performance of these combined procedures on clinical samples.

**Methods:** The TargetPlex FFPE-Direct DNA Library Preparation Kit (SenseCare Medicals, Inc.) combined with SiRe NGS panel, is designed to analyze clinically relevant hotspot mutations in 8 oncogenes that integrate FFPE DNA extraction with the preparation of NGS DNA libraries directly from FFPE tissue sections in a single step. This DNA library preparation workflow reduces the labor-intensive and time-consuming pre-analytical deparaffinization, extraction, and purification steps typically required with traditional NGS workflows,

allowing researchers to prepare an NGS library in 3.5 hours. To combine SiRe NGS panel to the TargetPlex FFPE-Direct DNA Library Preparation Kit, 2 primer pools, each one containing 26 primer pairs, were designed and combined with a novel target enrichment technology followed by elimination of post-amplification primer dimers to lower background noise during the sequencing step. To preliminarily assess the technical performance of this new library preparation modality, a set of 8 routine samples (n = 1 NSCLC, n = 2 breast cancer, n = 5 CRC) previously tested by using the CE-IVD SiRe validated protocol were analyzed. **Results:** A success rate of 100% (8/8) was achieved by using both approaches. In comparing the non-synonymous mutational status results obtained by using the new approach with those obtained with CE-IVD SiRe-validated protocol, a concordance rate of 100% was reached. **Conclusions:** Our preliminary results showed for the first time that the TargetPlex FFPE-Direct DNA Library Preparation Kit combined with SiRe NGS panel represents a fast and easy-to-use NGS that can be prospectively validated for introduction in the diagnostic setting.

#### 09-P26. Existence of a Bidirectional Crosstalk between the ERK5 and the Hedgehog-GLI Pathways in Melanoma

A. Tubita<sup>1</sup>, S. Gagliardi<sup>2</sup>, I. Tusa<sup>1</sup>, Z. Lombardi<sup>1</sup>, M. Lulli<sup>1</sup>, P. Dello Sbarba<sup>1</sup>, B. Stecca<sup>2</sup>, E. Rovida<sup>3</sup>

<sup>1</sup>Università degli Studi di Firenze, Firenze, Italy, <sup>2</sup>Istituto per lo studio, la prevenzione e la rete oncologica (ISPRO), Firenze, Italy, <sup>3</sup>Università degli Studi di Firenze, Department of Experimental and Clinical Biomedical Sciences, Firenze, Italy.

**Introduction:** Melanoma is the deadliest skin cancer, with a very poor prognosis in advanced stages. We have recently reported that the mitogen-activated protein kinase ERK5 plays a relevant role in melanoma, regulating cell functions critical for tumor development such as proliferation. Additionally, the Hedgehog-GLI (HH-GLI) signaling is active and required for melanoma proliferation. Although the HH-GLI pathway may be activated in a non-canonical way by ERK1/2 MAPK, no evidence has been reported about a possible crosstalk with ERK5. **Methods:** BRAFV600E-mutated (A375 and Sk-Mel-5) and wild-type BRAF melanoma cell lines (SSM2c and M26c) and murine NIH/3T3 fibroblasts were silenced for ERK5 using ERK5-targeting shRNAs and a non-targeting shRNA (shNT) as a negative control. Luciferase assay using the GLI-binding site luciferase reporter was performed to evaluate GLI1 transcriptional activity. A constitutively active form of MEK5 (MEK5DD) was used to induce activation of the endogenous ERK5. Chemicals (small molecule inhibitors) used were: JW-071 and AX-15836 (ERK5 inhibitors). **Results:** Treatment with ERK5 inhibitors reduced transcriptional activity of the endogenous HH-GLI pathway in a dose-dependent manner in NIH/3T3 cells. This effect was recapitulated upon ERK5 genetic inhibition, which

determined a reduction of GLI1 and GLI2 protein levels. MEK5DD expression further increased transcriptional activity of the endogenous pathway induced by SAG, whereas silencing of endogenous ERK5 reversed this effect. These results confirmed that ERK5 positively regulates the HH-GLI signaling. Consistently, MEK5DD overexpression, which determines ERK5 activation, increased GLI1 and GLI2 protein levels. In melanoma cells, genetic and pharmacological ERK5 inhibition similarly inhibited the expression and activity of GLI proteins. On the other hand, activation of the HH-GLI pathway was able to activate ERK5 in NIH-3T3 cells and melanoma cells. Conversely, genetic inhibition of GLI results in ERK5 decreased expression. Interestingly, low doses of GLI and ERK5 inhibitors were more effective when used in combination in reducing the proliferation of melanoma cells expressing either wild-type or mutated (V600E) BRAF. **Conclusions:** Combined targeting of the ERK5 and HH-GLI pathways may result in lower cytotoxicity and prevent resistance mechanisms frequently observed upon monotherapy in melanoma.

**09-P27. Impact of Breast Cancer Cells on Mammary Adipose-Derived Mesenchymal Stem Cell Functions**  
T. Migliaccio, V. D'Esposito, G. Mosca, M.R. Ambrosio, S. Cabaro, M. Lecce, D. Liguoro, F. Capasso, R. Corvino, M. Di Tolla, F. Beguinot, P. Formisano  
*Università di Napoli Federico II & CNR/IEOS- URT 'Genomic of diabetes', Naples, Italy.*

**Introduction:** Hyperglycaemia increases breast cancer incidence and progression. However, the molecular mechanisms are still unclear. Glucose may exert its effects on both cancer cells and tumour microenvironment, including resident adipose-derived mesenchymal stem cells (MSCs). Here, we analysed whether breast cancer cells could modify mammary adipose tissue derived-MSC (MAT-MSC) phenotype and whether glucose may interfere with this communication system. **Methods:** MSCs were isolated from mammary adipose tissue (n = 6) and characterized for mesenchymal stem cell markers (CD90<sup>+</sup>, CD29<sup>+</sup>, CD106<sup>-</sup>, CD45<sup>-</sup>) by FACS analysis. Adipocyte differentiation was tested by Oil Red O staining. MAT-MSCs were co-cultured with both estrogen positive MCF7 and triple negative MDA-MB-231 cells in 25 mM glucose (high glucose, HG) or in 5.5 mM glucose (low glucose, LG) by using transwell systems. Upon 4 days, gene expression levels were analysed by real-time RT-PCR. **Results:** MAT-MSCs stained positive for CD90 and CD29 (99.2% and 99.9% of cells, respectively) and negative for CD106 and CD45 markers (99.9% and 98.1% of cells). Moreover, they were able to differentiate through the adipogenic lineage. MAT-MSCs, when co-cultured with MCF7 and MDA-MB-231 in HG, displayed a reduction of the expression of the multipotency genes *OCT4*, *SOX2*, and *NANOG* and an increased expression of the fibrosis marker *a-SMA*. In addition, in co-culture with MCF7 and MDA-MB-231, MAT-MSCs displayed 3-fold and 1.7-fold enhanced expression levels of the

senescence marker p16. In co-culture with MCF7, a 50% reduced expression of the *LAMB1* gene was also observed. When co-cultured in LG, MDA-MB-231 did not modify MAT-MSC phenotypes, whereas the co-culture with MCF7 still reduced *NANOG* and increased *a-SMA* expression in MAT-MSCs. **Conclusions:** Breast cancer cells modify MAT-MSC phenotypes, contributing to loss of multipotency and acquisition of fibroblast and senescence-like features in MSCs (senescent cancer-associated fibroblasts) in high glucose conditions. These effects are partially restored when MAT-MSCs are co-cultivated with cancer cells in low glucose. These findings underline that breast cancer may promote its progression by modifying surrounding MAT-MSCs, and that glucose may control cancer cell-MAT-MSC communication systems.

**09-P28. Oxidative Stress Induces WNT Canonical/Non-Canonical Pathway Modulation in Colon Cancer Cells with APC or  $\beta$ -Catenin Mutation**  
T. Catalano<sup>1</sup>, M.C. Di Marcantonio<sup>2</sup>, E. D'Amico<sup>2</sup>, C. Moscatello<sup>2</sup>, D. D'Agostino<sup>3</sup>, G. Ferlazzo<sup>4</sup>, G. Bologna<sup>3</sup>, P. Lanuti<sup>3,5</sup>, R. Lattanzio<sup>2,3</sup>, M.C. Curia<sup>2</sup>, G.M. Aceto<sup>2</sup>  
<sup>1</sup>University of Messina, Department of Clinical and Experimental Medicine, Messina, Italy, <sup>2</sup>G. d'Annunzio University, Chieti-Pescara, Department of Medical, Oral and Biotechnological Sciences, Chieti, Italy, <sup>3</sup>G. d'Annunzio University, Chieti-Pescara, Center for Advanced Studies and Technology (CAST), Chieti, Italy, <sup>4</sup>University of Messina, Department of Human Pathology, Messina, Italy, <sup>5</sup>G. d'Annunzio University, Chieti-Pescara, Department of Medicine and Aging Sciences, Chieti, Italy.

**Introduction:** It has long been recognised that the aberrant regulation of WNT/ $\beta$ -catenin signaling is involved in the pathogenesis of colorectal cancer. Chronic inflammation predisposes to colon carcinogenesis by increased reactive oxygen species (ROS) levels and can impair the Wntless/It (WNT)/ $\beta$ -catenin. This pathway is essential for gut morphogenesis, tissue homeostasis, and self-renewal, and its aberrant activation may drive the colorectal cancer (CRC), but the molecular mechanisms involved in CRC progression are still undefined. To evaluate the molecular relationship between oxidative stress and canonical/non-canonical WNT pathways, we analyzed the response to ROS exposure in CRC cell lines with different WNT signaling behaviour. **Methods:** HCT116 ( $\beta$ -catenin mutated) and SW480 (*APC* mutated) cells were exposed to hydrogen peroxide (H<sub>2</sub>O<sub>2</sub>) as oxidizing agent for different times and concentrations (from 50  $\mu$ M to 10 mM). We assayed cell viability/mitochondria activity by MTS and cell cycle by FACS. Gene expression was evaluated by SYBR Green qRT-PCR in cells under acute stress conditions [2 mM and 10 mM] for 15' and 30'. Protein expression was analysed by IHC. Statistical analysis was performed by t-test (p value <0.05). **Results:** MTS revealed rates of cell inhibition and growth at different H<sub>2</sub>O<sub>2</sub> concentrations. FACS

analysis of cell cycle showed time-dependent changes: after H<sub>2</sub>O<sub>2</sub> [2mM] treatment at 15', SW480 increased in G1 and G2 and decreased in S, whereas HCT116 increased in G1 and slightly reduced in G2; after 30', SW480 enhanced in G1 and S, and reduced in G2, whereas HCT116 diminished in G1 and increased in S/G2. In SW480 cells, acute stress induced by lower H<sub>2</sub>O<sub>2</sub> concentration [2 mM] upregulated gene expression of canonical *LRP6* and *LEF1*, and non-canonical *ROR2* and *JUN/AP1* molecules. In HCT116, the same H<sub>2</sub>O<sub>2</sub> concentration [2 mM] reduced *ROR2* and *LRP6* expression of WNT co-receptor and differently affected the WNT transcription factors, upregulating *LEF1* (canonical) and downregulating *JUN/AP1* (non-canonical). Regarding APC, it showed a behaviour dependent on time and concentration of H<sub>2</sub>O<sub>2</sub> treatment. IHC protein expression analysis showed that H<sub>2</sub>O<sub>2</sub> treatment induced FZD6 in HCT116 cytoplasm and E-cadherin in SW480 cytoplasm, whereas  $\beta$ -catenin increased in both cell lines. Intriguingly, oxidative stress induced a *de novo* APC expression in cytoplasm of both cell lines. **Conclusions:** In CRC cells harbouring APC or  $\beta$ -catenin mutations, oxidative stress differently affects the WNT pathways at gene and protein expression levels. Our results could unravel an APC central role in driving and maintaining tumorigenesis and a novel scenario for innovative CRC therapeutic approaches.

#### 09-P29. Combined Germline and Tumor Sequencing Has Significant Utility beyond Tumor Sequencing Alone in Diverse Cancer Patients

S. Lincoln, D. Pineda, N. Ngo, S. Michalski, E. Esplin, R. Nussbaum  
*Invitae, San Francisco, CA, United States.*

**Introduction:** Germline testing is recommended for cancer patients with specific presentations or family histories. Separately, tumor sequencing is increasingly used to inform therapy, most often in advanced disease. Tumor sequencing, in principle, can detect somatic and germline mutations, although these tests may not accurately determine whether mutations are germline or somatic. Moreover, tumor tests can have limitations with certain variant types, and variant interpretation guidelines differ for germline versus somatic variants. We investigated the utility of combined tumor and germline sequencing in a large cohort of patients who were referred by clinicians for both test modalities.

**Methods:** We studied 1,600 consecutive cancer patients who received germline testing and had previously received tumor DNA sequencing. Cancers included colorectal (n = 209), breast (195), prostate (189), pancreas (169), and many others. A total of 13% of patients had multiple cancers. Ordering clinicians stated diverse reasons that germline testing was indicated, including: a somatic finding of potential germline significance, treatment/surgical decision, personal/family history, and patient concern. Variants of uncertain significance (VUS) were excluded. **Results:** In addition to somatic mutations, 40% of patients harbored a

pathogenic germline variant (PGV) in a cancer predisposition gene. This included 46% of ovarian cancer patients, 44% pancreas, 41% prostate, 33% colorectal, etc. Most PGVs (75%) were clinically actionable, and many PGV-positive patients had no reported family history. Mutations in certain genes (e.g., *BRCA1*) were much more likely to be germline compared to others (e.g., *TP53*). A total of 15% of PGVs were not reported in any form by tumor tests. Some unfortunate trends were observed: for example, 14% of ovarian cancer and 21% of prostate cancer patients with germline PVs had these variants uncovered only after a second, possibly preventable, cancer had occurred.

**Conclusions:** At a minimum, our data show that germline testing as a reflex to tumor testing often produces results that further inform care. Indeed, such reflex tests may be underutilized. As costs come down, paired tumor-normal testing may be a preferred option that leverages both data types to improve clinical utility as well as variant interpretation with rapid turnaround. Our cohort is subject to referral bias: patients with high suspicion of harboring a PGV were most likely to be referred for germline testing. In broader patient populations the germline positive rate is lower, although the utility of combined testing likely remains high. In addition to expanding this retrospective study, large prospective studies are thus underway to further clarify the utility of combined tumor and germline testing.

#### 09-P30. Analysis of MicroRNA Expression Profiles of Glioblastoma Multiforme and Alzheimer's Disease for the Identification of Novel Diagnostic and Prognostic Biomarkers

L. Falzone<sup>1,2</sup>, M. Pennisi<sup>1</sup>, R. Salemi<sup>1</sup>, S. Candido<sup>1,3</sup>, M. Libra<sup>1,3</sup>

<sup>1</sup>University of Catania, Biomedical and Biotechnological Sciences, Catania, Italy, <sup>2</sup>National Cancer Institute IRCCS Fondazione G Pascale, Epidemiology Unit, Naples, Italy, <sup>3</sup>Research Center for Prevention, Diagnosis and Treatment of Cancer, University of Catania, Biomedical and Biotechnological Sciences, Catania, Italy.

**Introduction:** Glioblastoma multiforme (GBM) and Alzheimer's disease (AD) share some molecular features, including common inflammatory patterns, the alteration of brain tissue scaffold, and the alteration of cellular turnover. However, it was recently demonstrated that the molecular pathways involved in GBM and AD progression are inversely regulated, thus reflecting the inverse comorbidity observed for these 2 pathologies. Furthermore, we recently demonstrated that microRNAs (miRNAs) are also inversely regulated in GBM and AD, suggesting their possible involvement in the development and progression of these diseases. On these bases, the aims of the study were to select inversely regulated miRNAs in GBM and AD, and to define their diagnostic and prognostic potential.

**Methods:** For this purpose, GEO DataSets and TCGA GBM datasets were used for the identification of

significantly de-regulated miRNAs and their association with the main clinical-pathological features of GBM and AD patients. Furthermore, DIANA-mirPath pathway prediction analysis and STRING enrichment analysis were used to identify the gene targets modulated by selected miRNAs and shared by the 2 pathologies. Finally, the bioinformatics tool OncoLnc was used to establish the prognostic significance of selected miRNAs for GBM patients. **Results:** Through differential analyses performed on TCGA GBM database and GEO DataSets, GBM and AD miRNA datasets, significantly and inversely de-regulated miRNAs have been found for GBM and AD, highlighting their association with disease stage and pathological characteristics. In particular, 12 out of 13 miRNAs in common between GBM and AD showed a strong inverse association in the 2 diseases. Furthermore, pathway prediction and gene enrichment analyses revealed that the inverse miRNA expression reflects an inverse regulation of genes and molecular pathways responsible for the development of the 2 pathologies. Finally, some of the selected miRNAs were shown to be significantly associated with GBM and AD patients' Overall Survival and Progression-Free Survival. **Conclusions:** To the best of our knowledge, the achieved results showed, for the first time, that a strong inverse miRNA expression exists between GBM and AD patients, suggesting that, although the molecular pathways responsible for the development of the 2 pathologies are the same, they appear to be oppositely regulated by inversely expressed miRNAs. In addition, the identified miRNAs were shown to be strongly associated with development as well as progression of GBM and AD, thus representing good candidates to be used as diagnostic and prognostic biomarkers.

#### 09-P31. Epigenetic and Genetic Characterization of Cauda Equina Paragangliomas Reveals a New Molecular Subtype of Paragangliomas

L. Schweizer<sup>1,2,3</sup>, F. Thierfelder<sup>1</sup>, D. Teichmann<sup>1</sup>, L. Wessels<sup>4</sup>, M. Misch<sup>4</sup>, D. Capper<sup>1,2,3</sup>, B. Knie<sup>5</sup>, J. Walter<sup>6</sup>, S.-A. May<sup>7</sup>, C. Hartmann<sup>8</sup>, A. Jödicke<sup>9</sup>, D. Moskopp<sup>5</sup>, F. Heppner<sup>1,2,3</sup>, A. Schöler<sup>1,2</sup>, A. Koch<sup>1,2,3</sup>

<sup>1</sup>Charité - Universitätsmedizin Berlin, Department of Neuropathology, Berlin, Germany, <sup>2</sup>German Cancer Consortium (DKTK), Partner Site Charité Berlin, Berlin, Germany, <sup>3</sup>Berlin Institute of Health (BIH), Berlin, Germany, <sup>4</sup>Charité - Universitätsmedizin Berlin, Department of Neurosurgery, Berlin, Germany, <sup>5</sup>Vivantes Klinikum im Friedrichshain, Department of Neurosurgery, Berlin, Germany, <sup>6</sup>Universitätsklinikum Jena, Department of Neurosurgery, Jena, Germany, <sup>7</sup>Klinikum Chemnitz, Department of Neurosurgery, Chemnitz, Germany, <sup>8</sup>Medizinische Hochschule Hannover, Department of Pathology, Hannover, Germany, <sup>9</sup>Vivantes Klinikum Neukölln, Department of Neurosurgery, Berlin, Germany.

**Introduction:** Multiplatform integration and comprehensive molecular profiling of non-spinal paragangliomas and pheochromocytomas occurring

outside the CNS revealed 4 molecularly defined and clinically relevant subtypes. Currently, it is assumed that cauda equina paragangliomas belong to the defined molecular subtypes. Whereas non-spinal paragangliomas are associated with germline mutations in up to 40% of the cases, spinal paragangliomas are considered non-familial. In contrast to non-spinal paragangliomas, a comprehensive genetic and epigenetic analysis of cauda equina paragangliomas is lacking. **Methods:** We conducted genome-wide DNA methylation profiling of 55 spinal paragangliomas including 5 very rare ganglionic paragangliomas (e.g., composite paragangliomas/ganglioneuromas) applying the Illumina Infinium Methylation EPIC array. Furthermore, we performed whole exome sequencing of 10 cauda equina paragangliomas on an Illumina NovaSeq 6000. **Results:** We analyzed the genome-wide methylation profiles of 55 cauda equina paragangliomas and compared them to 163 non-spinal paragangliomas (TCGA; GSE111336) by calculating T-distributed Stochastic Neighbor Embedding (*t-SNE*) plots and heatmaps (hierarchical clustering) in R. Unexpectedly, cauda equina paragangliomas clustered clearly apart from paragangliomas of other sites of origin and showed a lower intertumoral heterogeneity based on their epigenetic profile. Analyzing copy number variation and summary plots calculated from EPIC methylation arrays (conumee R package), we noticed that chromosomal gains and losses are very rare in spinal paragangliomas, and amplification and homozygous deletions are absent. The exome sequencing data revealed that frequent mutations found in non-spinal paragangliomas — like prognostically relevant SDH mutations in head and neck paragangliomas — are absent in cauda equina paragangliomas. **Conclusions:** Our comprehensive molecular analysis reveals that, compared to their ontogenetically related and genetically more diverse non-spinal counterparts, cauda equina paragangliomas very rarely show chromosomal imbalances, a lower intertumoral epigenetic heterogeneity, and a different mutational landscape. Cauda equina paragangliomas represent a distinct molecular subtype of paragangliomas and can be identified based on a unique epigenetic profile which will be useful as an additional diagnostic tool in metastatic paraganglioma and neuroendocrine tumors of unknown origin.

#### 09-P32. Method Comparison and Analytical Characterization of an MSI by PCR System

K. Oostdik

Promega Corporation, Madison, WI, United States.

**Introduction:** Microsatellite instability (MSI) has multiple utilities, including the identification of solid tumors with a highly mutated, mismatch repair deficient (dMMR) phenotype where an immune checkpoint inhibitor (ICI) treatment may be useful. Evidence suggests that the disruption of multiple gene products because of microsatellite DNA alterations in MSI-H tumors leads to the creation of tumor neo-antigens. This tumor

antigenicity is crucial to immune recognition and expansion, and may indicate an MSI-H tumor to be an ideal candidate for ICI treatment. Since MSI has been observed in a variety of solid tumors, this valuable tumor characteristic has utility across many scenarios regardless of the tumor site of origin. MSI testing by PCR is an established method for determining MSI status. Here we summarize the performance of an MSI by PCR system to identify MSI status in solid tumors.

**Methods:** The limit of detection (LoD) for DNA input was assessed using 40 replicates at each input value from 4 colorectal (CRC) samples with tumor content  $\geq 20\%$ .

LoD for tumor content was assessed using 40 replicates from a single sample. Reproducibility was evaluated across 3 sites, 2 operators per site, 3 kit lots, 2 runs per day, and 2 replicates over 3 non-consecutive days.

Positive percent agreement (PPA) and negative percent agreement (NPA) were calculated after comparison with the expected result (MSS/MSI-H). Clinical sensitivity and specificity were evaluated through a comparison with a reference method using a cohort of 141 retrospective CRC samples: 131 sequentially enrolled and 10 known dMMR samples. **Results:** The DNA input LoD with 20% tumor content and the tumor content LoD with a 1 ng DNA input were compatible with representative formalin-fixed, paraffin-embedded (FFPE) samples. The reproducibility PPAs and NPAs for site, operator, day, lot/run, and replicates were all greater than 90%.

**Conclusions:** Our MSI by PCR system generates accurate results with low input DNA and tumor content, and is robust across multiple sites, operators, and runs. The system provides sensitive detection of MSI-H solid tumors.

#### 09-P33. Clinical Evaluation of the ONCO/Reveal TP53 Panel on Barrett's Esophagus and Esophageal Adenocarcinoma Specimens

L.M. Petersen, X. Liu, G.J. Tsongalis, M. Lisovsky, J.A. Lefferts

*Dartmouth-Hitchcock Medical Center, Lebanon, NH, United States.*

**Introduction:** Somatic mutations in the tumor suppressor gene *TP53* occur in almost every type of cancer. An estimated 43% of esophageal cancers contain a pathogenic variant in *TP53*, and therefore utilizing a next-generation sequencing (NGS) assay to identify *TP53* variants is critical for diagnosis and prognosis. Additionally, patients with Barrett's esophagus have an increased risk of developing esophageal cancer, and therefore identifying pathogenic variants in those specimen types may be of importance in predicting potential development of dysplasia. This study aimed to identify *TP53* variants in esophageal specimens using the ONCO/Reveal TP53 Panel from Pillar Biosciences. Results were compared to variants identified with the ONCO/Reveal Multi-Cancer Panel (Pillar Biosciences). **Methods:** A total of 50 formalin-fixed, and paraffin embedded (FFPE) DNA samples from Barrett's esophagus (16 samples) and esophageal

adenocarcinoma (34 samples) were sequenced using the ONCO/Reveal TP53 Panel and Illumina MiSeq Reagent Kit v3 (600-cycle). Based on sequencing with the ONCO/Reveal Multi-Cancer Panel, 28 of these samples had a known *TP53* mutation, whereas the remaining 21 samples had no pathogenic *TP53* variants.

FastQ files were analyzed using PiVAT, Pillar's genome sequence data software. **Results:** There was 96.42% concordance between the ONCO/Reveal TP53 Panel and ONCO/Reveal Multi-Cancer Panel TP53 variant calls (27/28 variants). PiVAT detected a c.818G>C variant in 1 sample sequenced with the ONCO/Reveal TP53 Panel; however, a c.817C>T variant was called with the ONCO/Reveal Multi-Cancer Panel. All other pathogenic and likely pathogenic mutations that were identified with the ONCO/Reveal Multi-Cancer Panel were also called with the ONCO/Reveal TP53 Panel. Of those 28 samples with pathogenic or likely pathogenic *TP53* variants, 3 were from Barrett's esophagus tissue and the remaining 25 variants were from esophageal adenocarcinoma samples. The results from PiVAT also included common benign variants; however, there is no clinical significance associated with these variants.

**Conclusions:** The ONCO/Reveal TP53 Panel requires low DNA input (down to 5 ng), covers the full coding region of *TP53*, and offers a robust method for sequencing. Additionally, the ONCO/Reveal TP53 Panel library preparation can be done in <8 hours, and the data analysis with PiVAT is user friendly, making it an attractive option for any clinical diagnostic laboratory looking to implement NGS testing for *TP53* variants.

#### 09-P34. Use of the Biocartis Idylla KRAS and Idylla NRAS-BRAF Tests with Pre-Extracted DNA Samples

T. Leong, F. Habib

*Austin Health, Anatomical Pathology, Melbourne, Australia.*

**Introduction:** Performed on the Biocartis Idylla system, the Idylla KRAS and NRAS-BRAF tests detect 21 *KRAS* and 18 *NRAS/5 BRAF* mutations using real-time PCR. Sections of formalin-fixed, paraffin embedded (FFPE) colorectal cancer tissue are inserted in a single use Idylla cartridge containing reagents for deparaffinization, DNA extraction, and PCR, with all reactions automated. In our institution DNA-based next-generation sequencing (NGS) is used for routine testing, with Idylla reserved for urgent cases and as an orthogonal testing method in the event of NGS failure. To maximally preserve tissue for future use and increase time efficiency, we investigated whether pre-extracted DNA surplus to NGS-testing requirements can be used with Idylla rather than cutting further sections of FFPE tissue. **Methods:** A total of 70 DNA samples previously extracted from FFPE colorectal cancer specimens were selected from cases previously tested by NGS. Samples were selected to maximise the range of mutations tested and the DNA concentrations. Stated tumour percentages ranged from 15% to 95%. Two samples were subjected to further serial dilutions with DNase free water to assess the possible limit of

detection. Each sample was tested by pipetting 10  $\mu$ L onto Whatman microfilter paper. We placed each in a separate Idylla KRAS cartridge for KRAS mutation testing, and in an NRAS-BRAF cartridge for NRAS and BRAF mutation testing. Each cartridge was then inserted into the Idylla machine for analysis. **Results:** Idylla testing using pre-extracted DNA shows 100% concordance with NGS results. KRAS G12C mutation was detectable down to an approximate tumour input of 1.5 ng (30% tumour at 0.5 ng/ $\mu$ L). BRAF V600E was detectable down to a tumour input of 3.75 ng (15% tumour at 2.5 ng/ $\mu$ L). **Conclusions:** Our study suggests that Idylla KRAS and NRAS/BRAF tests may be used with pre-extracted DNA. A full validation study utilising samples covering the entire range of detectable mutations is warranted.

#### 09-P35. Antiproliferative Effects of Stilbene Derivatives Structurally Related to Resveratrol in Pancreatic Cancer Cell Lines

L. De Lellis<sup>1</sup>, R. Florio<sup>1</sup>, B. De Filippis<sup>2</sup>, S. Veschi<sup>1</sup>, A. Ammazalorso<sup>2</sup>, M. Fantacuzzi<sup>2</sup>, L. Giampietro<sup>2</sup>, C. Maccallini<sup>2</sup>, R. Amoroso<sup>2</sup>, A. Cama<sup>1</sup>  
<sup>1</sup>G. d'Annunzio University, General Pathology Unit, Department of Pharmacy, Chieti, Italy, <sup>2</sup>G. d'Annunzio University, Medicinal Chemistry Unit, Department of Pharmacy, Chieti, Italy.

**Introduction:** Resveratrol (trans-3,5,4-trihydroxystilbene, RSV) is a natural polyphenolic phytoalexin containing (E)-stilbenol scaffold that shows pleiotropic activities in cell biology, including antioxidant, anti-inflammatory, neuroprotective, chemopreventive, and antitumor properties. We recently synthesized a series of stilbenols structurally related to resveratrol and tested their effects on the viability of 3 pancreatic cancer (PC) cell lines with different genetic profiles. **Methods:** The effect of compounds on the viability of AsPC-1, Capan-2 and BxPC-3 pancreatic cancer cell lines was evaluated by MTT through dose-response curves. A trypan blue exclusion test was used to analyze the effect of compounds on PC cell proliferation. Self-renewal capacity of PC cell lines after treatments was evaluated using clonogenic assays. **Results:** Several compounds in the series of synthesized stilbenols markedly affected viability of AsPC-1, Capan-2, and BxPC-3 in a dose-dependent manner, displaying IC<sub>50</sub> values lower than those obtained with RSV and 4-hydroxystilbene (4-HSLB) in the same PC cell lines. The most active compounds were selected to better explore their antiproliferative activities, as compared to the reference compound RSV. In particular, compound 5 was the most effective compound and consistently compromised both PC cell line viability and clonogenicity with an improved activity, as compared to RSV. **Conclusions:** All novel stilbene derivatives affected PC cell viability, with a variability that appeared structure and cell dependent. Compound 5 was identified as the most potent, with improved antiproliferative activity as compared to RSV. We are currently evaluating the effects of this compound

on crucial processes in the biology of cancer cells, which might be relevant in the perspective of clinical translation.

#### 09-P36. Unusual Staining Patterns of Mismatch Repair Proteins across Various Tumor Types

D. Sirohi<sup>1</sup>, J. Coleman<sup>1</sup>, L. Furtado<sup>2</sup>, A. Grossmann<sup>1</sup>, P. Khalili<sup>1</sup>, A. Matynia<sup>1</sup>  
<sup>1</sup>University of Utah and ARUP Laboratories, Salt Lake City, UT, United States, <sup>2</sup>Saint Jude's Children's Hospital, Memphis, TN, United States.

**Introduction:** Conventionally mismatch repair (MMR) protein status by Immunohistochemistry (IHC) for MLH1, MSH2, MSH6, and PMS2 has been used to screen for Lynch syndrome in colorectal (CRC) and endometrial cancers. In recent years, microsatellite instability (MSI) has been recognized as a biomarker for determining immunotherapy eligibility. In 2017, PD-L1 blockers were approved by the US Food and Drug Administration as a second-line treatment in patients with MSI-high or MMR-deficient tumors. However, there are no current recommendations addressing the preferred methodology. Interpretation of MMR IHC may be challenging due to technical artifacts and underlying tumor biology; nonetheless, its results determine patient therapy. This study was undertaken to evaluate the incidence of unusual staining patterns of MMR proteins across different tumor types. **Methods:** We performed a retrospective review of all cases referred to our institution for MMR protein testing by IHC between July 2016 and September 2019. IHC was performed using ES05, FE11, EP49, and EP51 clones (Dako, Carpinteria, CA) for MLH1, MSH2, MSH6, and PMS2, respectively. Unusual staining was defined as: 1) reduced, when the intensity of tumor staining was weaker than the internal control (IC); 2) clonal loss, when a distinct focus of the tumor showed loss of staining with retained IC staining; and 3) uninterpretable, when staining was absent in the tumor and IC. For identified cases, MSI PCR testing result was recorded, if known. **Results:** A total of 1,804 cases were tested for MMR IHC representing a variety of tumor types: 1,120 (62.1%) CRC; 229 (12.7%) endometrial adenocarcinoma; 83 (4.6%) gastric/GEJ adenocarcinomas; 74 (4.1%) adenocarcinomas of unknown primary; 63 (3.5%) pancreaticobiliary adenocarcinomas; 26 (1.4%) prostate adenocarcinomas; and 209 (11.6%) others. Of these, 73 cases (4.0%) showed unusual staining patterns: 13 with 1; 9 with 2; 38 with 3; and 13 with a combination of patterns. Unusual staining was more frequently seen with PMS2 (2.8%) and MSH6 (1.9%) stains, and in pancreatobiliary tumors (20.6%). MSI PCR done in four cases demonstrated an unstable pattern in 3 including 1 with MLH1/PMS2 clonal loss, 1 with uninterpretable PMS2, and 1 with reduced MSH2/absent MSH6 expression. Stable pattern was seen in 1 case with reduced MSH2 staining/MSH6 clonal loss. **Conclusions:** Evaluation of MMR protein IHC is susceptible to interpretive pitfalls. Although reduced or

uninterpretable staining in many instances is a technical artifact, in some instances it could result from somatic or germline alterations. Patients with tumors displaying atypical MMR staining patterns should be offered follow-up testing, e.g., MSI PCR to prevent their exclusion from immunotherapy based on the unusual or inconclusive MMR result.

### 09-P37. Advanced Third-Generation Whole Genome Sequencing in a Pediatric Cancer Population Enhances Resolution of Complex Alterations

V. Magrini<sup>1,2</sup>, S. McGrath<sup>1</sup>, M. Hernandez-Gonzalez<sup>1</sup>, A. Miller<sup>1</sup>, E. Kautto<sup>1</sup>, W. Rumpf<sup>1</sup>, J. Fitch<sup>1</sup>, S. Koo<sup>1,3</sup>, E. Mardis<sup>1,2</sup>, R. Wilson<sup>1,2</sup>, C. Cottrell<sup>1,2,3</sup>

<sup>1</sup>Nationwide Children's Hospital, Institute for Genomic Medicine, Columbus, OH, United States, <sup>2</sup>The Ohio State University, Pediatrics, Columbus, OH, United States, <sup>3</sup>The Ohio State University, Pathology, Columbus, OH, United States.

**Introduction:** Short-read sequencing is commonplace in the setting of cancer and disease profiling. Based on available sequencing chemistries, platforms, and employed alignment and variant calling strategies, complex genomic events are underrepresented in these data. Emerging long-read sequencing chemistries increase the ability to resolve complex events due to the length of sequenced molecules and retention of order and orientation. Comprehensive genomic profiling of tumors and blood disorders has been established in a translational setting within the Institute for Genomic Medicine to aid in diagnosis, prognostication, treatment, and germline disease predisposition in patients with rare and refractory disease. This patient-centric protocol allows for emerging and novel methodologies to be applied in an N-of-1 manner to more fully characterize and classify disease. **Methods:** Pacific Biosciences Hi-Fidelity Whole Genome Shotgun (Hi-Fi WGS) and Iso-Seq whole transcriptome libraries provide templates for circular consensus sequencing (CCS) which results in long and accurate sequence read data. These data have been applied to a subset of our N-of-1 cohort to more fully profile disease and comparator normal tissue in 4 patients with pediatric cancer. **Results:** Among sequenced patients, 3 were diagnosed with solid tumors (gastric tumor, meningeal melanoma, spindle cell neoplasm), and 1 with leukemia (B-ALL). Three gene-fusion events, 1 complex intragenic rearrangement, and 1 constitutional translocation were among the complex genomic events resolved by long-reads. A determination of concordance of variant calls among constitutional and somatic datasets derived from short-read and long-read technologies is ongoing. Improved resolution of the characterized events enabled precise genomic architecture to be established, as well as determination of allele-specific and isoform-specific expression.

**Conclusions:** Use of long-read sequencing strategies within a pediatric cancer protocol allowed for discrete resolution of structurally complex events driving disease states. Exemplar data include novel characterization of a

*PDGFRB* in-frame alteration in a spindle-cell neoplasm impacting the juxtamembrane and kinase domains, which is predicted to be activating and thus therapeutically targetable. A poorly characterized gastric tumor harbored a novel *EWSR1-CTBP1* fusion; within this same patient, a GI polyp was observed to harbor a fusion event disrupting the *PTEN* gene, anticipated to result in loss of gene function. Within our cohort, long-read sequencing strategies were complementary to short-read data generation and enabled improved characterization of disease states in patients with pediatric cancer.

### 09-P38. Maml1: Not Only a Transcriptional Coactivator of Gli1

S. Zema<sup>1</sup>, M. Pelullo<sup>2</sup>, F. Nardoza<sup>1</sup>, I. Screpanti<sup>1</sup>, D. Bellavia<sup>1</sup>

<sup>1</sup>Università 'La Sapienza' di Roma, Dipartimento di Medicina Molecolare, Roma, Italy, <sup>2</sup>Center of Life Nano Science Sapienza, Istituto Italiano di Tecnologia, Rome, Italy.

**Introduction:** In mammals, Maml1 belongs to a family of proteins, also including Maml2 and Maml3, which act as transcriptional coactivators for Notch signalling, an evolutionarily conserved pathway. Maml1 has been recently shown to act as a coactivator in other cell signalling pathways, including p53, MEF2C, and  $\beta$ -catenin, in a Notch-independent manner. Maml1 is a key molecule able to connect different signalling pathways, and it is involved in the regulation of cellular processes. Hence, its action must be finely regulated. Notably, we have demonstrated that Maml1 empowers Sonic Hedgehog signalling pathway, regulating the transcriptional activity of Gli proteins, via a novel Notch-independent mechanism. So far, scientific research on Maml1 has been generally focused on its activity as a transcriptional coactivator, while overlooking its role in the post-transcriptional regulation. **Methods:** Cell culture; siRNA silencing; RNA extraction and RT-PCR/qRT-PCR; protein extract, immunoprecipitation, and immunoblot analysis; *in vivo* ubiquitylation assay; generation of Maml1 knock-out cells with CRISPR/Cas9 technology. **Results:** Interestingly, our preliminary data suggest a novel role for Maml1 in the post-translational regulation of Gli1, able to prevent its degradation mediated by Itch, an E3 ubiquitin-protein ligase. The endogenous interaction between Maml1, Itch and the adaptor Numb suggests a direct role of Maml1 on Itch activity. Notably, Maml1 regulates Itch activity in a dose-dependent way through the C-terminal domain (TAD2). Remarkably, the Maml1 TAD2 domain is also involved in the control of Gli1 transcriptional activity. **Conclusions:** This study tries to shed light on the molecular mechanism that regulates the stability and activity of Gli1 mediated by Maml1, and seeks to provide a new integrated level of regulation in Shh/Gli pathway. In particular, we suggest that Maml1 may play a double role as a transcriptional coactivator of Gli1 and in controlling the stability of the Gli1 protein itself by

regulating Itch activity directly. Maml1 and Itch are both involved in controlling the activity of several pathways. Therefore, the ability of Maml1 in controlling the activity of Itch/E3 ubiquitin ligase could have an impact in controlling the strength of several signalling pathways inside the cell, such as Shh and Notch, both in physiological and pathological contexts. A thorough understanding of the molecular mechanism mediated by Maml1 might lead to future therapeutic approaches directed against Shh-driven tumours or different pathological contexts.

#### 09-P39. Functional Comparison of Different Exon Capture Methods for Transcriptomic Profiling of FFPE Material

A. Sboner<sup>1,2,3</sup>, R. Bareja<sup>2,3,4</sup>, K. Shohdy<sup>5,6</sup>, D. Wilkes<sup>1,2</sup>, M. Sigouros<sup>1,2</sup>, J.Z. Xiang<sup>2,7</sup>, J.M. Mosquera<sup>1,2</sup>, R. Kim<sup>1,2</sup>, T. McNary<sup>1,2</sup>, O. Elemento<sup>2,3,4</sup>, B. Faltas<sup>2,5</sup>, A. Alonso<sup>2,7</sup>  
<sup>1</sup>Weill Cornell Medicine, Pathology and Laboratory Medicine, New York, NY, United States, <sup>2</sup>Englander Institute for Precision Medicine, New York, NY, United States, <sup>3</sup>Institute for Computational Biomedicine, New York, NY, United States, <sup>4</sup>Weill Cornell Medicine, Physiology and Biophysics, New York, NY, United States, <sup>5</sup>Weill Cornell Medicine, Department of Medicine, New York, NY, United States, <sup>6</sup>Cairo University, Cairo, Egypt, <sup>7</sup>Weill Cornell Medicine, New York, NY, United States.

**Introduction:** Whole transcriptomic profiling (WTS) has been the first technology that brought us into the genomic era. The first studies using microarrays demonstrated the possibility of WTS to identify subclasses of cancers, thus furthering our understanding of the biological mechanisms of cancer. With massively parallel sequencing, research in this field intensified and is now able to determine the presence of fusions, alternative splicing, and novel long non-coding RNAs, in addition to expression levels. RNA sequencing (RNA-Seq) is nowadays a key molecular biology technology. One of its limitations is the use of frozen material for optimal results. However, the vast majority of clinical specimens are formalin-fixed, paraffin embedded (FFPE), where the quality of RNA rapidly declines. Being able to interrogate these samples would provide further insights into mechanisms of cancer development, progression, and resistance to therapy. **Methods:** We performed WTS on 10 FFPE samples of variable quality (RIN [2-5], DV200% [23-61]) with 3 exome capture methods: 1) Agilent SureSelect V6+COSMIC+UTRs; 2) Twist NGS Exome; and 3) IDT XGen Exome Research Panel. All of these methods capture the exonic regions in an attempt to reduce the amount of pre-mRNA sequenced. We computed standard QC metrics of sequencing experiments (number of sequenced and mapped reads, capture efficiency, etc.), but specifically focused on a *functional* comparison. We interrogated samples with known characteristics: fusions (e.g., *TPMRS2-ERG*, *FGFR3-TACC3*), molecular signatures (e.g., basal or luminal), and overexpressed genes or

outliers (e.g., *ERBB2*, *MET*, *CDK4*, etc.). We performed deconvolution methods to classify cellular components of the samples. All analyses were compared to their matching “gold standard” frozen reference with poly-A selected RNA-Seq data. **Results:** Correlation levels of expression with their matching frozen ranged from 0.7 to 0.85 for all capture methods — lower than expected for biological replicates. None of the methods were able to recapitulate all of the functional features of their matching frozen RNA-Seq. For the basal versus luminal analysis, 90% of samples were correctly classified by IDT and Twist, whereas Agilent correctly classified 70% of the samples. Agilent detected all fusions, whereas IDT and Twist identified 6 out of 7. All methods detected all outliers. **Conclusions:** We compared 3 capture methods to perform whole transcriptome profiling using FFPE material. Although none of the methods were able to recapitulate all biological signals of the matching frozen samples, they can still capture most of it, e.g., outliers. Careful consideration of the biological questions must be taken to use RNA capture methods to interrogate the transcriptome of FFPE material.

#### 09-P40. Development of a Targeted NGS Oncology Assay for Comprehensive Genomic Profiling and Gene-Fusion Detection in Solid Tumors

V. Mittal<sup>1</sup>, J. Kilzer<sup>2</sup>, S. Bandla<sup>1</sup>, D. Cyanam<sup>1</sup>, A. Ewig<sup>2</sup>, R. Gottimukkala<sup>3</sup>, N. Khazanov<sup>1</sup>, A. Kraltcheva<sup>2</sup>, D. Kaznadzey<sup>3</sup>, A. Marcovitz<sup>3</sup>, S. Myrand<sup>1</sup>, W. Tom<sup>3</sup>, Y.-T. Tseng<sup>3</sup>, C. Van Loy<sup>2</sup>, P. Williams<sup>1</sup>, J. Veitch<sup>3</sup>, C. Yang<sup>3</sup>, Z. Zhang<sup>3</sup>, C. Allen<sup>4</sup>, J. Au-Young<sup>3</sup>, F. Hyland<sup>3</sup>, E. Wong-Ho<sup>3</sup>, S. Sadis<sup>1</sup>  
<sup>1</sup>Thermo Fisher Scientific, Clinical Sequencing Division, Ann Arbor, MI, United States, <sup>2</sup>Thermo Fisher Scientific, Carlsbad, CA, United States, <sup>3</sup>Thermo Fisher Scientific, CSD, South San Francisco, CA, United States, <sup>4</sup>Thermo Fisher Scientific, Clinical Sequencing Division, Inchinnan, United Kingdom.

**Introduction:** Next-generation sequencing (NGS) is being applied to support routine clinical research in oncology with a primary focus on evaluating known oncogenic variants. However, novel gene-fusion in known driver genes is still not reliably detected. Also, the advent of cancer immunotherapies requires that clinical research solutions must also address biomarkers such as tumor mutational burden (TMB) and microsatellite instability. Additionally, the availability of sufficient input tumor sample material is a limiting factor. Therefore, we developed an NGS solution appropriate for low formalin-fixed, paraffin-embedded (FFPE) tissue materials that addresses biomarkers for targeted and immune checkpoint therapies (including DNA variants, and relevant fusions from RNA). **Methods:** Gene content was prioritized based on the relevance and variant prevalence of biomarkers in solid tumors. Additional genomic regions were added to supplement the coding sequence footprint to support TMB. The assay used Ion AmpliSeq technology with automated templating on the Ion Chef and sequencing on the Ion Torrent GeneStudio

S5 sequencing platform. An automated tumor-only workflow for variant calling, TMB estimation and sample quality reporting was provided within Ion Reporter. Streamlined access to reporting of variant relevance was enabled by OncoPrint Reporter. **Results:** Over 400 genes with known DNA alterations and over 50 RNA fusion drivers were included. DNA repair pathways were comprehensively represented, as alterations in these genes may lead to high mutation burden. A coding sequence footprint to support TMB was generated and microsatellite regions were included to support MSI. In addition to targeted fusion breakpoints, novel fusions in selected driver genes were detected using a novel expression imbalance approach. From the development studies, the assay displayed high uniformity and consistent read depth for support of robust variant calling. The automated workflow required minimal input of FFPE material. TMB assessment using publicly available whole-exome cancer sequencing data as well as test cell lines resulted in high correlation ( $R^2 \geq 0.90$ ). MSI sensitivity and specificity was >90% as tested using a diverse set of tumor samples. Targeted fusion was reported with 100% sensitivity and specificity when tested in commercially available controls. **Conclusions:** An NGS assay was developed to support comprehensive genomic profiling and routine clinical research in oncology. The assay design and informatics workflow support characterization of mutational signatures and immunotherapy biomarkers, and detects relevant RNA structural alterations. Minimal input material requirement and rapid sample-to-report time will have a high impact on clinical research.

**09-P41. A 15 Gene Panel for *BRCA1*, *BRCA2*, and *DDR* Genes for Reporting Variants on FFPE Samples**

F. Hyland<sup>1</sup>, C. Scafe<sup>1</sup>, Y. Zhu<sup>2</sup>, C. Yang<sup>1</sup>, Y.-T. Tseng<sup>1</sup>, C. Allen<sup>1</sup>, S. Sadis<sup>3</sup>, S. Roman<sup>2</sup>

<sup>1</sup>Thermo Fisher Scientific, South San Francisco, CA, United States, <sup>2</sup>Thermo Fisher Scientific, Carlsbad, CA, United States, <sup>3</sup>Thermo Fisher Scientific, Ann Arbor, MI, United States.

**Introduction:** Detecting germline and somatic mutations in *BRCA1* and *BRCA2* and in additional DNA damage response (HR DDR) genes is critical since these genes are implicated in inherited risk of breast cancer, and in response to certain therapies. Small variants (SNVs and indels) in these genes can be reliably detected with many next-generation sequencing (NGS) approaches. However, large rearrangements (LRs) such as exon level copy number variations are difficult to detect using traditional sequencing. Ideally, an assay should be able to detect many variant types on formalin-fixed, paraffin-embedded (FFPE) samples, including breast cancer research samples, and should have high yield on samples with degraded or low amount of input DNA.

**Methods:** We describe an NGS assay, the OncoPrint BRCA Extended Panel, with 15 genes, including *BRCA1* and *BRCA2* and additional DDR genes. Another 80 genes may optionally be added to the panel. These core

genes and additional genes have been optimized and verified, with known performance. The panel can be used to detect germline and somatic mutations on the same FFPE sample, with sensitive and specific detection of variants down to 5% LoD. Exon deletions can be reported for *BRCA1* and *BRCA2*. This assay is designed for FFPE samples, and can be used with other sample types. Only 20 ng of input DNA is required; hence, the assay performs well with low input amount of DNA. Amplicons are short, and so are robust to degraded DNA. **Results:** The core BRCA panel assay has excellent performance. On-target reads comprise 92% of total reads, and panel uniformity is 97%. The panel includes hotspots (alleles of known significance), and uniformity on these hotspots ranges from 98%-100%. Performance was measured on 530 and 540 chips on the Ion GeneStudio S5 system, and using FFPE samples and on cell line controls. Finally, a coordinated analysis solution imports information about the core or custom panel and provides an integrated analysis pipeline with a simple and powerful visual interface, including variant calling, functional annotation, population MAF, predicted protein effect, and annotations including ClinVar, COSMIC, OMIM, etc. Filtering tools utilizing this information facilitate variant prioritization. A report describing drug labels and clinical trials relevant for the variants detected in the sample is produced. **Conclusions:** An NGS assay with a comprehensive data analysis approach was developed. This panel and software can detect both small mutations and copy number variants simultaneously in FFPE samples with high sensitivity. The assay can detect germline and somatic mutations. This assay enables *BRCA1/2* and HR DDR translational research into the effects of somatic and germline mutations.

**09-P42. Identification of Potentially Actionable Germline Variants in NGS Testing of Solid Tumors**

M. Telatar, C. Louie, H.-W. Chen, R. Pillai, J. Arias-Stella III, T. Slavin, H. Yew, K. Margolin, R. Salgia, P. Aoun, M. Afkhami  
City of Hope National Medical Center, Duarte, CA, United States.

**Introduction:** In this study we describe an effective model in the clinical setting for identifying potential germline pathogenic variants in selected genes after genotyping the tumor samples with a next-generation sequencing (NGS)-based solid tumor panel in the absence of a normal control. **Methods:** The OncoPrint Comprehensive Assay V3 (OCAv3) panel was validated for clinical use to screen solid tumors for somatic mutations with diagnostic, prognostic, and therapeutic implications. Specimens were reviewed by pathologists for adequacy and tumor cellularity was documented prior to each test. Variants present in population databases at a minor allele frequency  $\geq 1\%$  were excluded. Remaining variants were further annotated by clinical curators and presented at a genomic tumor board for decision by an expert team including molecular pathologists and clinical

molecular geneticists, medical oncologists, and medical geneticists. Incidental identification of potential germline variants were flagged on the basis of 1) gene and/or variant with higher prevalence as germline versus somatic; 2) variant allele frequency consistent with potential germline status, particularly if discordant with tumor cellularity; and 3) patient family and clinical history including ages at diagnosis and tumor types as evident in their medical record. Providers were alerted to potential germline variants through comment and recommendation for genetics referral in the NGS report. For cases with particularly strong suspicion of germline pathogenic variants, providers were contacted directly to recommend follow-up genetic counseling and testing.

**Results:** In summary, 36 of 1,195 (~3%) patients with solid tumors were identified as having potential germline variants across 11 cancer predisposition genes (*CDH1*, *CHEK2*, *BRCA1*, *BRCA2*, *MLH1*, *MSH2*, *MSH6*, *PMS2*, *PTEN*, *PALB2*, and *NBN*) in the OCAv3 panel. In some cases, these variants were later confirmed to be germline in patients not previously suspected to have germline predisposition syndromes, or in tumor types not typical for the particular genes mutated. **Conclusions:** In the clinical laboratory setting, with the appropriate resources, potentially actionable germline variants may be identified even in the absence of a normal control. Integration of experienced molecular geneticists and pathologists into the interdisciplinary tumor board, along with access to patient medical records, enables highly personalized interpretation of NGS results, which enhances the clinical management of patients and their families.

#### 09-P43. Patient-Derived Tumor Organoids Share Morphologic and Molecular Features with Carcinomas of Lung, Kidney, and Pancreas Primaries

P. Ocampo<sup>1</sup>, A. Smith<sup>2</sup>, C. Suarez<sup>1</sup>, C. Kuo<sup>2</sup>, J. Zehnder<sup>1</sup>  
<sup>1</sup>Stanford University School of Medicine, Department of Pathology, Stanford, CA, United States, <sup>2</sup>Stanford University School of Medicine, Department of Medicine, Stanford, CA, United States.

**Introduction:** Patient-derived tumor organoids represent an opportunity to increase our understanding of tumor pathogenesis and to advance precision medicine. Although tumor organoids as a model system have already produced important insights into the oncogenic mechanisms underlying a number of different cancers, expanding their clinical utility first requires studies on how closely organoids recapitulate molecular genetic heterogeneity and morphologic features of the primary tumor. **Methods:** Organoids were derived from 15 primary patient specimens including 4 adenocarcinomas of lung, 2 squamous cell carcinomas of lung, 4 clear cell renal cell carcinomas, 4 pancreatic ductal adenocarcinomas, and 1 adrenal cortical carcinoma. Morphologic and molecular comparisons were made by cytology, histology, and via a next-generation sequencing (NGS) panel developed at

Stanford. The Stanford Solid Tumor Actionable Mutation Panel (STAMP) targets 130 genes, either in part or fully, with the genes selected on the basis of their known impact as actionable targets of existing or emerging therapies, their prognostic significance, as well as the frequency of their occurrence across cancer types.

**Results:** For the majority of our samples, we find significant concordance between the primary and patient-derived tumor organoid. In cases with morphologic heterogeneity, we find histologic evidence of increased tumor purity as well as increased variant allele frequencies of shared mutations and copy number alterations. Interestingly, the organoid derived from poorly differentiated squamous cell carcinoma of lung displayed keratinization, whereas some lung adenocarcinoma organoid samples displayed neoplastic cytologic features, but confirmatory immunohistochemical stains and STAMP testing suggest growth of a benign basal stem cell component.

**Conclusions:** Here, we demonstrate that organoids derived from a range of tumor types recapitulate patient-specific morphologic and molecular features. These results highlight the precision medicine applications of organoids for targeted therapeutics, biomarker validation, and drug discovery.

#### 09-P44. Comparison of EGFR Mutation Detection in Patients with NSCLC Across Different Platforms: Which Technique Is It Anyway?

P. Gogte, P. Joshi, M. Gurav, D. Dhanavade, N. Karnik, G. Deshpande, T. Pai, R. Kumar, O. Shetty, S. Desai  
 Tata Memorial Hospital, Molecular Pathology Division, Mumbai, India.

**Introduction:** Molecular testing of the epidermal growth factor receptor (*EGFR*) gene mutations associated with advanced or metastatic non-small cell lung cancer (NSCLC) is a clinical requisite for determining targeted treatment with *EGFR*-tyrosine kinase inhibitors. Different clinical platforms with CE-IVD kits for detection of *EGFR* mutations make it challenging to determine the right molecular testing system. This study is a comparative analysis of *EGFR* mutation detection methods for routine diagnostics. **Methods:** The study was performed on formalin-fixed, paraffin-embedded (FFPE) specimens from NSCLC cases archived from the Department of Pathology for routine molecular diagnostics after confirming the tumor adequacy using the following platforms:

Technology	System	Kit	Analyte
NGS	Illumina Miseq	AmpliSeq Focus Panel (Illumina, US)	DNA (4x10µm FFPE sections)
Real-Time PCR	QuantStudio 12K Flex	EGFR Mutation Analysis Kit (EntroGen, Inc., US)	DNA (4x10µm FFPE sections)
Droplet Digital PCR	Biorad QX200	EGFR kits (Biorad, US)	DNA (4x10µm FFPE sections)
Microfluidics- based qualitative PCR	Biocartis Idylla System	Idylla EGFR Mutation Test (Biocartis, Belgium)	1x5µm FFPE section

[Table 1: Platforms used for EGFR mutation detection.]

Reference Standards from Horizon Discovery were used as external controls. Data analysis was performed per protocol for each system and mutations reported per HGVS nomenclature.

**Results:** Of the 35 cases in the cohort, 33 were included in the final analysis. Among the 4 testing platforms, EGFR mutation was detected in 12 cases with >95% concordance, considering NGS as the gold standard. The detection rate for NGS, real-time PCR, ddPCR, and microfluidics-based Idylla system was found to be 31.3% (n = 10), 33.3% (n = 11), 33.3% (n = 11), 36.4% (n = 12), respectively. The commonest mutations detected across all platforms were exon 19 deletions (n = 7.58.3%), L858R (n = 4.25%), and T790M (n = 2.16.7%) substitutions. One case of EGFR S768I mutation detected on Idylla was considered discordant, as NGS could not be performed due to inadequate library quantity. An invalid or error call was reported for 2 cases on Idylla and had very low DNA input for additional analysis on other platforms, and thus was excluded from the data set. Limit of detection for the commonest mutations for NGS, real-time PCR, ddPCR, and microfluidics-based system was found to be 5%, 2%, 0.1%, and 5% each. The microfluidics-based system outperformed others in terms of ease of performance, no DNA extraction, and PCR amplifications with turnaround time of 2.5 hours as against >1 day for real-time PCR, ddPCR, and >5days for NGS. **Conclusions:** This study highlights the effectiveness of different testing platforms for EGFR mutation detection, although each differs from

the others in terms of sensitivity, cost, turnaround time, and complexity of workflow. It also emphasizes the role of emergent ddPCR and microfluidics-based technology for EGFR mutation detection, and supports its integration in clinical practice.

#### 09-P45. Evaluation of the Oncomine BRCA Assay in the Clinical Validation Setting

J. Coffin, I. Izevbaye, R.J. Maglantay, C. Mather, S. El Hallani

University of Alberta, Edmonton, AB, Canada.

**Introduction:** Screening for BRCA1 and BRCA2 gene alterations in tumor tissue guides the selection of patients with tubo-ovarian or primary peritoneal high-grade serous carcinoma who benefit from PARP-inhibitor therapy and could streamline the referral of patients to genetic counselling. The assay of choice should reliably detect SNVs, small indels, splice site mutations, and exonic CNVs in formalin-fixed, paraffin-embedded (FFPE) specimens. We here describe the clinical validation of the AmpliSeq-based BRCA Oncomine assay with modified CNV analysis. **Methods:** The validation cohort included 66 clinical FFPE ovarian and breast cancer tissue specimens from patients with known germline BRCA1 or BRCA2 mutations, and 1 commercial HD810 control sample, making a total of 75 pathogenic variants (small indels, n = 37; SNVs, n = 30; exonic deletion/CNV, n = 5; and splice site mutations n = 3). Amplicon-based libraries were sequenced in Ion Torrent S5 instrument, and data were analyzed through a combination of Ion Reporter software and an in-house CNV pipeline. **Results:** Among the 37 small indel variants, 35 were accurately detected. The 2 missed cases were a mononucleotide insertion into a short-homopolymer sequence located at the end of amplicon (filtered out due to strand bias) and a mononucleotide insertion into a long-homopolymer sequence (filtered out due to low confidence score). The SNVs and splice site mutations were all successfully detected. The CNV analysis using Ion Reporter accurately called 3 out of 5 exonic deletion cases. A partial deletion of exon 11 of BRCA2 was not called and exon 21-22 deletion was miscalled as exon 21-23. Additional CNV over-calls were observed in other specimens (false positives). An in-house CNV pipeline was therefore developed using in-house reference samples as new baseline and normalized amplicon-based copy number ratio calculation. The in-house CNV pipeline accurately detected the expected exonic deletions in the 5 CNA cases without false positives in other non-CNV cases. Combining Ion Reporter with the in-house CNV pipeline, the assay performance values were improved to 97.3% sensitivity and 100% specificity. The limit of detection was 5% VAF for SNVs and small indels, and 50% tumor cellularity for CNV. **Conclusions:** The Oncomine BRCA Assay has an acceptable accuracy, precision, and limit of detection; however, a modified CNV analysis is recommended for more accurate and specific CNV calling.

**09-P46. Comparison of Single Gene Testing and NGS Multiplex Panels in Non-Small Cell Lung Carcinomas: An Institutional Experience**

J. Lanceta<sup>1</sup>, K. Ebare<sup>2</sup>, W. Song<sup>1</sup>, O. Rosca<sup>1</sup>

<sup>1</sup>Zucker School of Medicine/Northwell at Staten Island University Hospital, Pathology and Laboratory Medicine, Staten Island, NY, United States, <sup>2</sup>Northwell Health-Staten Island University Hospital, Pathology and Laboratory Medicine, Staten Island, NY, United States.

**Introduction:** Recent advances in the armamentarium against non-small cell lung carcinoma (NSCLC) benefit patients with advanced disease and prompted reflex molecular testing in most institutions. Initially, single gene testing (SGT) was performed (i.e., *EGFR* testing; if wild-type result reflex to *ALK1*, *ROS1*, *RET*, *KRAS*). However, the limited amount of tissue in cytology or small biopsies sometimes precluded molecular testing for all the genes with available targetable alterations, potentially delaying optimal treatment. With the advent of novel genetic alterations being discovered and next-generation sequencing (NGS) becoming broadly available, the general trend was switching from SGT to NGS multiplex panels. This was emphasized by the subsequent release of CAP/IASLC/AMP "Updated molecular testing guideline for the selection of lung cancer patients for treatment with targeted tyrosine kinase inhibitors" in 2018. Few studies have compared the impact of switching from SGT to NGS panels in NSCLC. **Methods:** We retrospectively looked at NSCLC cases in our institution for which SGT or NGS panels were used. A total of 162 cases were retrieved (from January 2018 to July 2019) that underwent molecular testing by either SGT or NGS. Cases with insufficient tissue for molecular testing (QNS) were recorded. Comparison between the 2 groups was performed using Bayesian logistic regression with a diffuse prior.

**Results:** The mean age of the patients at the time of diagnosis was 69.0 years (female:male ratio 1.4:1). A total of 16 cases showed *EGFR* alterations and 28 were positive for *KRAS* mutations. SGT was performed on 100 (61.7%) cases, of which 11 (11%) were QNS. Of these, 63.6% (7/11) were QNS for *EGFR* testing, whereas 4 were QNS for *ALK* testing. Sixty-two (38.3%) cases were tested by NGS; only 1 (1.6%) was QNS. The odds of cancelling a test as a result of QNS for SGT is statistically higher compared to testing by NGS panels (odds ratio: 4.67 [95% CI: 2.66-7.41]). **Conclusions:** SGT is more likely to be cancelled due to QNS than testing using multiplex NGS panels. To maximize molecular testing on small tissue biopsies and/or cytology specimens, multiplex genetic sequencing panels are preferred over multiple SGT, in accordance with the molecular testing CAP/IASLC/AMP Guideline.

**09-P47. Exosomes of Glioblastoma Present Higher Molecular Variation than a Tumor Primary Cell Line**

A. Calogero<sup>1</sup>, L. Pacini<sup>1</sup>, P. Rosa<sup>1</sup>, D. Bastianelli<sup>1</sup>, A. Di Pardo<sup>1</sup>, A. Piazza<sup>2</sup>, V. Petrozza<sup>1</sup>, A. Stoppacciaro<sup>2</sup>, A. Vecchione<sup>2</sup>, M. Miscusi<sup>2</sup>, A. Raco<sup>2</sup>

<sup>1</sup>Università 'La Sapienza' di Roma, Latina, Italy,

<sup>2</sup>Università 'La Sapienza' di Roma, Roma, Italy.

**Introduction:** Increasing evidence indicates that extracellular vesicles (EVs) secreted from tumor cells play a key role in the overall progression of the disease state. EVs such as exosomes are secreted by a wide variety of cells and transport a varied population of proteins, lipids, DNA, and RNA species within the body. Gliomas including glioblastoma (GBM) are the most common primary malignant brain tumors. Glioma EVs including exosomes have biological effects (e.g., immunosuppression) and contain tumor-specific cargo that could facilitate liquid biopsies. Recent articles show the potential of cfDNA in the therapeutic analysis of glioblastoma. In this report we highlight the potential of DNA EV next-generation sequencing (NGS) assay in glioma. **Methods:** Eleven patients from A.U.O.

"Sant'Andrea", Neurosurgery Division, Sapienza University, Rome, NESMOS Department, were enrolled in this study. Here we describe a new custom QIAGEN NGS assay technique to analyze DNA plasma exosomes in glioma patients in correlation to DNA extracted from cryostat section. Here we report the analysis of the *H3F3A*, *IDH1*, *IDH2*, *TERT*, *CDKN2A*, *TP53*, *NF1*, and *ATRX* genes with a QIAGEN GeneReader custom panel with 0.5% variant allele frequency (VAF). **Results:** All the genes were analyzable in 40% of EVs sampled. All had reads with average quality of >25 and a percentage of base positions in regions of interest with UMI coverage  $\geq 200\times$  in a minimum of 75%. Our data show that *NF1* had more pathogenic mutation in exosome sample than in matched cryostat section ( $3 \pm 0.7$  versus  $2 \pm 1.04$ ). Interestingly, the exosomes showed a high number of variants detected than in matched cryostat section ( $51.67 \pm 19$  versus  $21.42 \pm 14$ , p value <0.05).

**Conclusions:** Our report on DNA glioma EVs highlights the prognostic-diagnostic potential of the NGS assay in the glioblastoma patients.

### 09-P48. Gene Expression Analysis of Epithelial and Stromal Cell Capture from Phyllodes Tumors against Fibroadenoma Reveals Both Components Are Equivalently Affected in Breast Fibroepithelial Progression

A.F. Logullo Waitzberg<sup>1</sup>, E. Napolitano<sup>2</sup>, P. Pineda<sup>3</sup>, M. Gigliola<sup>3</sup>, F. Augusto Soares<sup>4</sup>, D. Carraro<sup>3</sup>

<sup>1</sup>UNIFESP-EPM, Pathology, Sao Paulo, Brazil, <sup>2</sup>Fleury Laboratorios, Biologia Molecular, Sao Paulo, Brazil,

<sup>3</sup>A.C. Camargo Cancer Center CIPE, Sao Paulo, Brazil,

<sup>4</sup>A.C. Camargo Cancer Center CIPE, Department of Pathology, Sao Paulo, Brazil.

**Introduction:** Phyllodes tumours (PTs) are a rare entity and, analogous to fibroadenomas (FA), are considered true biphasic neoplasms. However, unlike FA, PT stromal element is cellular, and may recur locally, undergo malignant progression, and metastasize.

Recent evidence shows that epithelia-stroma interactions are critical for tumor progression; however, molecular alterations in each component in PT onset are not yet well characterized. Thus, to contribute to the identification of molecular events involved in PT tumorigenesis, we performed gene expression analysis of both types of cells captured from PT and FA.

**Methods:** Epithelial (EC) and stromal (SC) cells were separately captured by laser microdissection from 13 PT and 3 FAs. RNA extraction and amplification were performed by PicoPure RNA isolation (Arcturus) low input Quick Amp Labeling kit (Agilent Technologies), respectively. Samples were hybridized in a competitive system on SurePrint G3 Hm 60K (Agilent Technologies) slide. Signals were captured by Scanner Agilent Bundle model B (Agilent, US), and Agilent Feature Extraction (v10.7.1) program. The data were analyzed by GeneSpring GX12.1 software (Agilent Technologies). Flag filter detected outlier probes resulting in 9,346 probes representing 8,067 coding genes. A fold change  $\geq 2.0$  SHAPE \\* MERGEFORMAT and  $p < 0.05$  were considered significant. **Results:** To identify differentially expressed genes between PT and FA, data from EC- and SC-captured cells were compared separately. A total of 3,386 probes were differentially expressed in EC component, and 1,910 were upregulated in PT. SC samples revealed 2,619 probes with significant difference, among them 1,616 upregulated in PT. Hierarchical clustering based on the differently expressed genes from EC and SC cells, separately, could not discriminate between PT and FA samples. When low grade PT ( $n = 7$ ) was compared to high grade PT ( $n = 6$ ), the universe of differentially expressed genes was smaller: EC-derived samples revealed 30 probes with only 14 upregulated in high grade PTs, and SC-evaluated samples showed only 10 probes differentially expressed with 6 upregulated.

**Conclusions:** ECs are molecularly altered as much as SC cells in breast fibroepithelial lesion progression (from FT to PT). Low grade and high grade PTs exhibit low gene expression alteration. Moreover, EC and SC

components seem to share main affected gene pathways, suggesting a common carcinogenesis process.

### 09-P49. Clinical Management and Genomic Profiling of Pediatric Low-Grade Gliomas in Saudi Arabia

M. Abedalthagafi

KFMC, Genomics Research Department, Riyadh, Saudi Arabia.

**Introduction:** Pediatric low grade gliomas (PLGGs) display heterogeneity regarding morphology, genomic drivers, and clinical outcomes. The treatment modality dictates the outcome, and optimizing patient management can be challenging. **Methods:** In this study, we performed comprehensive genomic profiling on 37 Saudi Arabian patients with PLGGs to identify genetic abnormalities that can inform prognostic and therapeutic decision-making. We detected genomic alterations (GAs) in 97% (36/37) of cases, averaging 2.51 single nucleotide variations (SNVs) and 0.91 gene fusions per patient. The *KIAA1549-BRAF* fusion was the most common alteration (21/37 patients) followed by *AFAP1-NTRK2* (2/37) and *TBLXR-PI3KCA* (2/37) fusions that were observed at much lower frequencies.

**Results:** The most frequently mutated genes were *NOTCH1-3* (7/37), *ATM* (4/37), *RAD51C* (3/37), *RNF43* (3/37), *SLX4* (3/37), and *NF1* (3/37). Interestingly, we identified a *GOPC-ROS1* fusion in an 8-year-old patient whose tumor lacked *BRAF* alterations and was previously misclassified as an unclassified high grade glioma. The patient underwent gross total resection followed by adjuvant high-dose chemotherapy and autologous hematopoietic stem cell rescue. At 30 months post-transplantation, the patient remained disease free. **Conclusions:** Taken together, these data reveal that the genomic characteristics of PLGG patients can enhance diagnostics and therapeutic decisions. In addition, we identified a *GOPC-ROS1* fusion that may be a biomarker for PLGG.

### 09-P50. Methylation Profiling of Medulloblastoma in a Clinical Setting Permits Sub-classification and Reveals New Outcome Predictions

M. Abedalthagafi

KFMC, Riyadh, Saudi Arabia.

**Introduction:** Medulloblastoma (MB) is the most common childhood malignant brain tumor and a leading cause of cancer-related deaths in children. DNA methylation profiling has rapidly advanced our understanding of MB pathogenesis at the molecular level, but assessments in Saudi Arabian (SA) MB cases are sparse. MBs can be subgrouped according to methylation patterns from formalin-fixed, paraffin-embedded (FFPE) samples into Wingless (*WNT*-MB), Sonic Hedgehog (*SHH*-MB), Group 3 (G3), and Group 4 (G4) tumors. *WNT*-MB and *SHH*-MB subgroups are characterized by gain-of-function mutations that activate oncogenic cell signalling, whereas G3/G4 tumors show

recurrent chromosomal alterations. Given that each subgroup has distinct clinical outcomes, the ability to subgroup SA-FPPE samples holds significant prognostic and therapeutic value. **Methods:** Here, we performed the first assessment of MB-DNA methylation patterns in an SA cohort using archival biopsy material (FPPE n = 49). **Results:** Of the 41 materials available for methylation assessments, 39 could be classified into the major DNA methylation subgroups (*SHH*, *WNT*, *G3*, and *G4*). Furthermore, methylation analysis was able to reclassify tumors that could not be subgrouped through NGS testing, highlighting its improved accuracy for MB molecular classifications. Independent assessments demonstrated known clinical relationships of the subgroups, exemplified by the high survival rates observed for *WNT* tumors. Surprisingly, the *G4* subgroup did not conform to previously identified phenotypes, with a high prevalence in females, high metastatic rates, and a large number of tumor-associated deaths. **Conclusions:** Taken together, we demonstrate that DNA methylation profiling enables the robust subclassification of 4 disease subgroups in archival FFPE biopsy material from SA-MB patients. Moreover, we show that the incorporation of DNA methylation biomarkers can significantly improve current disease-risk stratification schemes, particularly concerning the identification of aggressive *G4* tumors. These findings have important implications for future clinical disease management in MB cases across the Arab world.

#### 09-P51. A Next-Generation Sequencing Multigene Custom Panel for Mutational Analysis of Solid Tumors

D. de Biase<sup>1</sup>, G. Acquaviva<sup>2</sup>, M. Visani<sup>3</sup>, V. Sanza<sup>2</sup>, C.M. Argento<sup>3</sup>, T. Maloberti<sup>3</sup>, A. Pession<sup>1</sup>, G. Tallini<sup>4</sup>  
<sup>1</sup>Università di Bologna, Pharmacy and Biotechnology, Bologna, Italy, <sup>2</sup>Azienda USL di Bologna, Molecular Pathology, Bologna, Italy, <sup>3</sup>Università di Bologna, Bologna, Italy, <sup>4</sup>Università di Bologna, Medicine, Bologna, Italy.

**Introduction:** Next-generation sequencing (NGS) allows parallel sequencing of multiple genes at a very high depth of coverage. Nowadays, precision medicine requires multigene characterization more than the single-gene approach, and for this reason the introduction of multigene panels is becoming crucial for molecular analysis of solid lesions. **Methods:** A total of 1,695 samples were then analyzed using a next-generation sequencing (NGS) multigene panel consisting of 128 amplicons for analyzing targeted regions of 23 oncogene/oncosuppressor genes. **Results:** Frequency of mutations was similar to that observed in literature for *solid* tumors analyzed by multigene custom panel. Sequencing of serial dilution led to 5% analytical sensitivity. Only 84 specimens (5%) were not amplifiable due to low quality/quantity DNA. **Conclusions:** This multigene custom panel allows us to analyze with high sensitivity and throughput 23

oncogenes/oncosuppressor genes involved in diagnostic/prognostic/predictive characterization of CNS tumors, non-small cell lung carcinomas, colorectal carcinomas, thyroid lesions, pancreatic lesions, melanoma, oral squamous carcinomas, and gastrointestinal stromal tumors.

#### 09-P52. Fast and Reliable Molecular Profiling in the Clinic: Evaluation of a Novel, Rapid, Fully Automated Next-Generation Sequencing Approach for Precision Oncology

P. Jermann, B. Calgua de Leon, K. Leonards, M. Schoenmann, I. Alborelli  
 University Hospital Basel, Institute of Pathology, Basel, Switzerland.

**Introduction:** In the past few years, next-generation sequencing (NGS) has revolutionized the way diagnostic testing is done in the field of oncology. Parallel testing of genomic markers in tissue biopsies as well as cytological and liquid biopsy specimens by NGS are now key tools used for clinical decision making. Here, we tested the newest generation of NGS instruments that allow for fully automated sample processing, massively parallel sequencing, and data analysis in as little as 1 day turnaround time. **Methods:** Routine clinical formalin-fixed, paraffin-embedded (FFPE), cytological, as well as plasma specimens were prepared with the OncoPrint Precision Assay (OPA) covering 50 cancer-related genes and sequenced on the Genexus Integrated Sequencer to assess both sensitivity and specificity of the test. A total of 40 samples were analyzed for SNVs, indels, CNVs, and gene rearrangements, and concordance with previous analyses using validated NGS-based orthogonal methods was assessed. PPV and NPV were calculated for each specimen type. **Results:** Preliminary genomic analyses of tissue and liquid biopsy-derived nucleic acids show 100% concordance between the novel OPA assay and orthogonal NGS methods for both tissue and liquid biopsies. Turnaround time from sample to report was as little as 1 day. Specific analyses of the complete dataset will be presented at the conference. **Conclusions:** Our results show that the OPA assay, in concert with the Genexus sequencer, allows for sensitive and specific analysis of genomic variants in routine samples. Furthermore, due to their significantly reduced turnaround time, NGS results can now be reported to clinicians together with IHC results, enabling quicker therapy decision making.

### 09-P53. Docetaxel Enhances the Expression of STING Protein in PC3 Prostate Cancer Cells, and cGAMP Attenuates This Effect

M. Rezaei<sup>1</sup>, S. Salimi<sup>2</sup>, S.A. Ziai<sup>3</sup>

<sup>1</sup>Shahid Beheshti University of Medical Sciences, Pathology Department, Tehran, Islamic Republic of Iran,

<sup>2</sup>Shahid Beheshti University of Medical Sciences, Tehran, Islamic Republic of Iran, <sup>3</sup>Shahid Beheshti University of Medical Sciences, Pharmacology Department, Tehran, Islamic Republic of Iran.

**Introduction:** Prostate cancer occurs in the prostate gland of the male reproductive system. Usually, after the failure of hormone therapy, docetaxel is the first-line chemotherapy drug used to treat prostate cancer. The STING agonist (cGAMP) kills the cancer cells through the induction of apoptosis and activation of the innate immune system. In this study, the effect of adding cGAMP to docetaxel on the PC3 cell line was investigated to measure the cytotoxicity changes in the cell line and effects on the *STING* and *IRF3* gene and STING protein expressions. **Methods:** In this study, Pc3 prostate cancer cells were treated with docetaxel, cGAMP, and a combination of docetaxel and cGAMP. Cell toxicity was evaluated by MTT assay. The expression level of *STING* and *IRF3* genes was determined by the real-time PCR technique in the treated and untreated cells. The expression of STING protein was also detected by the Western blot test.

**Results:** The IC<sub>50</sub> of docetaxel at concentrations of 7.5, 15, 25, 37, and 75 nM was 31.1 (20.8-46.6) nM after 48 hours, and in the presence of 17.5 μM cGAMP, it changed to 33.8 (10.67-107.3) nM. The addition of cGAMP to docetaxel decreased the toxicity of the maximum high docetaxel concentration. Docetaxel and cGAMP did not change *STING* gene expression significantly, but in combination, they reduced *STING* expression to one-third. STING protein production with docetaxel was increased about 5-fold, and cGAMP did not change the protein expression. In combination, however, docetaxel mostly inhibited STING protein expression. *IRF3* gene expression was significantly increased by 4-fold with docetaxel, but cGAMP had no effect; in combination, *IRF3* gene expression was increased significantly by 3-fold. **Conclusions:** cGAMP in combination with docetaxel inhibited the maximum toxic concentration of docetaxel with no change in its IC<sub>50</sub>. Docetaxel increased STING protein expression and *IRF3* gene expression significantly, but cGAMP showed no significant effect on them. The effects of docetaxel on *STING* gene and STING protein expression and *IRF3* gene expression were inhibited by their combination. In this *in vitro* study, cGAMP did not potentiate docetaxel's effects, and even inhibited them.

### 09-P54. Analysis of Multiple Synchronous Ground-Glass Opacities by Next-Generation Sequencing

L. Wang<sup>1</sup>, X. Zhang<sup>2</sup>, S. Xu<sup>2</sup>, Q. Li<sup>1</sup>, X. Qiu<sup>1</sup>, E.-H. Wang<sup>1</sup>

<sup>1</sup>The First Affiliated Hospital of China Medical University, Department of Pathology, Shenyang, China, <sup>2</sup>The First Affiliated Hospital of China Medical University, Department of Thoracic Surgery, Shenyang, China.

**Introduction:** The incidence of synchronous ground-glass opacities (GGOs) in the lung has increased in recent years, due to the adoption of low-dose computed tomography in routine health examinations. The most common diagnosis of synchronous GGOs is adenomatous atypia hyperplasia (AAH), adenocarcinoma (ADC) *in situ* (AIS), or minimally invasive adenocarcinoma (MIA). Few studies have performed next-generation sequencing (NGS) analysis of these synchronous lesions to identify whether these synchronous GGOs are multiple primary lesions or intrapulmonary metastasis. **Methods:** We performed whole exome sequencing in synchronous GGOs from 23 patients, using a customized panel including 425 cancer-associated genes. The data were analyzed together with histological characteristics of the tumor tissues. **Results:** Multiple synchronous GGOs in the same patient showed different mutation profiles, and some shared identically mutated genes. Among 23 patients, 17 had 2 synchronous GGOs, and 6 had more than 2 GGOs. Totally, 57 nodes were examined; 35 were pure GGOs, 14 were part-solid GGOs, and 8 were solid GGOs. The cohort contains 9 AIS, 16 MIA, and 32 invasive ADC. In 57 GGOs, 20 harbored *EGFR* mutations, 3 with *KRAS* mutations, and 3 with *EXT1* mutations. Among 23 patients, identical mutations shared by synchronous GGOs were observed in 2 patients. For the other 21 patients, synchronous GGOs harbored different mutation profiles. In those 2 patients, micropapillary patterns and/or vascular invasion were identified in the tissues sections, but not identified in the other 21 patients. **Conclusions:** This study suggests that synchronous GGOs genetically might be independent tumors. For nodes having the same or similar gene mutations, especially in the same lobar, intrapulmonary metastases could not be excluded, even though each node acted as early-stage adenocarcinoma.

### 09-P55. High Prevalence of Potential Targets in Colorectal Patients Identified by Tumor Molecular Profiling

A. Matveieva, D. Shapochka, O. Sulaieva  
Medical Laboratory, CSD Health Care, Kiev, Ukraine.

**Introduction:** Complex genomic and IHC testing are increasingly used to guide metastatic cancer treatments. Molecular profiling results of colorectal cancer patients were analyzed to establish the available treatment options. **Methods:** Fifty-nine patients with metastatic CRC were included in the study. The average age was 60.1 y.o., 59% of patients were male and 39%, female.

All samples were tested by 65- or 313-gene OncoDEEP next-generation sequencing (NGS) panel. Additionally, TMB, MSI status, and IHC expression of *PD-L1*, *PTEN*, *p4EBP1*, *TS*, *ERCC1*, and *TOPO1* were analyzed.

**Results:** We found a high prevalence of *KRAS* mutations (59%). This is only logical as many patients had a confirmed *KRAS*-mut status and therefore were recommended to undergo molecular profiling in search of alternative treatment options. Overall, 64% of patients had *RAS* mutations, so the use of anti-EGFR antibodies is associated with potential clinical benefit only for 17 (36%) patients. Overall, 45% of patients had potentially targetable alterations (except the EGFR pathway). A total of 10% of patients may be candidates for PD-1/PD-L1 inhibitors due to high TMB (3.3%), PD-L1 (3.3%) expression and MSI-high status (3.3%). A total of 25% of patients had altered PI3K/mTOR/Akt signaling (12% PIK3CA mutations, 12% PTEN loss, 1% Akt amplification) and may be included in appropriate clinical trials. Finally, there were 14% of patients with *BRAF* or *RET* mutations (7% in each gene); they can also be recruited in clinical trials. Apart from these findings, we identified 8% of patients with a high risk of 5FU- or cisplatin-associated chemotoxicity due to *DPYD* (2%) and *TPMT* (6%) polymorphisms. *TS*, *ERCC1*, and *TOPO1* IHC expression was used to predict 5FU-, platinum-, and irinotecan-based chemotherapy efficiency. Patients with *TS*-low tumors (46%) are more likely to have clinical benefit from 5FU, and those with *ERCC1*-low tumors (50%), from oxaliplatin. A total of 95% of tumors were *TOPO1*-positive, so the predictive value of this marker for *TOPO1* inhibitors (irinotecan) is uncertain. Therefore, about 50% of patients are more likely to have clinical benefit from FOLFOX/XELOX, whereas the other 50%, from FOLFIRI/XELIRI therapy.

**Conclusions:** Complex tumor molecular profiling for metastatic CRC identified 45% of patients with targetable genomic alterations which may be included in appropriate clinical trials after disease progression during first-line treatment. For patients without potential targets, molecular profiling may identify patients who are more likely to have high toxicity or clinical benefit from different chemotherapy regimens.

#### 09-P56. Aberrant Glycosphingolipid Pattern in Human Cholangiocarcinoma Stem-Like Subsets

A. Mannini<sup>1</sup>, C. Raggi<sup>1</sup>, M. Correnti<sup>2</sup>, E. Rovida<sup>3</sup>, M. Aureli<sup>4</sup>, E.V. Carsana<sup>4</sup>, B. Piombanti<sup>1</sup>, M. Pastore<sup>1</sup>, J. Andersen<sup>5</sup>, C. Coulouarn<sup>6</sup>, F. Marra<sup>1</sup>

<sup>1</sup>University of Florence, Experimental and Clinical Medicine, Florence, Italy, <sup>2</sup>University of Milan, Biomedical Sciences for Health, Milan, Italy, <sup>3</sup>University of Florence, Experimental and Clinical Biomedical Sciences, Florence, Italy, <sup>4</sup>University of Milan, Medical Biotechnology and Translational Medicine, Milan, Italy, <sup>5</sup>University of Copenhagen, Biotech Research and Innovation Centre, Copenhagen, Denmark, <sup>6</sup>University of Rennes, Inserm, Inra, Institut NUMECAN (Nutrition Metabolisms and Cancer), Rennes, France.

**Introduction:** It is well known that a crucial therapeutic target of cancer is represented by cancer stem cells (CSCs). A great deal of studies show that some glycosphingolipids, a peculiar class of plasma membrane lipids, are prevalently expressed in CSCs and could be considered as markers of cancer stemness (i.e., Burkitt lymphoma, pancreatic carcinoma, and other epithelial cancers). In particular, gangliosides (GS), sialic acid-containing GSL, have been investigated for their role in the malignant phenotype of several cancers (i.e., breast, melanoma, glioblastoma, ovary), and in tumor stem-like cells. However, there are no data regarding GSL composition in human cholangiocarcinoma (CCA). Thus, our study aims to provide GSL and GS profiling of both the stem-like subset and its parental cells in human CCA.

**Methods:** Stem-like subset was enriched by sphere culture (SPH) in established human intrahepatic CCA cells (HUCCT1, CCLP1). CCA GS patterns were determined by chromatographic analytical procedures. Identification of GSL and GS molecular species and assessment of GS turnover were evaluated by feeding cells with <sup>3</sup>H-sphingosine. GS role in modulation of stem features was investigated using D-threo-1-phenyl-2-palmitoylamino-3-N-morpholine-1-propanol (PPMP), a glucosylceramide synthase inhibitor. FACS-sorted GD2<sup>+</sup> SPH cells were examined for stem-like gene expression compared to GD2<sup>-</sup> SPH. **Results:** In both CCA lines, stem-like subsets (SPHs) showed drastic changes in the number of specific sphingolipids (SLs) (Cer, Gb3, SM) compared to parental cells grown in monolayer conditions (MON). In both CCA lines, the number of total GSs was markedly different between MON and their SPH. In contrast to MON, CCA-SPH showed increased content of GM3, reduction of GM2, and appearance of GD2. This was corroborated by high levels of GM3 synthase as well as GD3 and GM2/GD2 synthase expression in CCA-SPH. GS biosynthesis enzymes, such as GlcCer-, LacCer-, and GM3 synthases, were strongly expressed in CCA-SPH compared to MON. Notably, sphere forming ability and expression of CSC-related genes were affected by PPMP. Likewise, GD2<sup>+</sup> SPH cells were enriched with CSC-markers (*CD133*, *EpCAM*, *CD44*) at protein and gene level in addition to several genes involved in pluripotency, self-renewal, and EM transition compared to GD2<sup>-</sup> SPH. Notably, expression of GM2/GD2 synthases was significantly expressed in tumor samples compared to paired non-tumoral liver tissue of CCA patients (n = 104) and greatly correlated with presence of satellite nodules, lymph node invasion, and recurrence. **Conclusions:** We show for the first time that the CCA stem-like properties may be associated with GSL synthetic pathway and pattern. GSL synthases could represent potential markers for CCA.

**09-P57. Epidemiology of Human Papillomavirus-Positive Head and Neck Squamous Cell Carcinoma**M. Rezaei<sup>1</sup>, A. Kheradmand<sup>2</sup><sup>1</sup>Shahid Beheshti University of Medical Sciences, Tehran, Islamic Republic of Iran, <sup>2</sup>Shahid Beheshti University of Medical Sciences, Pathology, Tehran, Islamic Republic of Iran.

**Introduction:** Human papilloma virus (HPV) has been associated with prognosis in patients with head and neck squamous cell carcinoma (HNSCC). Similar to the worldwide studies, different prevalence rates of this viral infection have been reported in Iran. Therefore, we aim to report the prevalence of this virus and its significance in HNSCC patients. **Methods:** All patients who have been referred to the 4 hospitals (located in different parts of Tehran, Iran), during 1 year (May 2018-May 2019) were included into the study, if they were diagnosed with HNSCC by a pathologist, according to the pathologic results. The pathologic reports of the patients were used for recording the disease staging. DNA was extracted from the fresh tissue samples. After PCR, The HPV positive samples were evaluated for determining the genotypes and data used for analysis. **Results:** Of 46 patients, 3 (6.5%) had a positive HPV with these subtypes: 1.61 (low risk) and 18.52 (high risk); 2.67 (unknown); 61 (low risk), 18.52 (high risk), and 73 (probable high risk); and 3.52 (high risk). Comparison of variables between the groups with and without HPV showed no statistically significant difference in terms of patients' age ( $P = 0.116$ ), ethnicity ( $P = 0.103$ ), place of residence ( $P = 0.243$ ), smoking status ( $P = 0.170$ ), alcohol consumption ( $P = 0.065$ ), weight loss ( $P = 0.905$ ), primary tumor site ( $P = 0.297$ ), size ( $P = 0.287$ ), pathologic stage ( $P = 0.386$ ), vascular invasion ( $P = 0.196$ ), perineural invasion ( $P = 0.772$ ), and metastasis ( $P = 0.205$ ) based on HPV positivity; meanwhile, there was a significant difference based on the tumor's lymphatic invasion ( $P = 0.041$ ), peripheral lymph node involvement ( $P = 0.008$ ) and histologic grade ( $P = 0.011$ ). **Conclusions:** HPV positivity is an important factor in lymphatic invasion, peripheral lymph node involvement, and histologic grade of cases with HNSCC, and should be further investigated for its effect on prognosis.

**09-P58. Accumulation of Phosphorylated Tau Protein Interferes with Mitosis in Cancer Cells**S. Martellucci<sup>1,2,3</sup>, L. Clementi<sup>1</sup>, A. Colapietro<sup>1</sup>, S. Sabetta<sup>1</sup>, V. Mattei<sup>2,3</sup>, E. Alesse<sup>1</sup>, A. Angelucci<sup>1</sup><sup>1</sup>Dpt Biotechnological and Applied Clinical Sciences, University of L'Aquila, L'Aquila, Italy, <sup>2</sup>Biomedicine and Advanced Technologies Rieti Center, 'Sabina Universitas', Rieti, Italy, <sup>3</sup>Dpt Experimental Medicine, University 'Sapienza', Rome, Italy.

**Introduction:** Tauopathies are neurodegenerative diseases characterized by aggregates of hyperphosphorylated tau. Previous studies have identified many disease-related phosphorylation sites on

tau, and it is widely accepted that tau hyperphosphorylation blocks tau ability to bind and stabilize microtubules. Formation of oligomeric tau has been described as the initial event in tauopathies and represents a potent stressor in neuronal cells. However, mechanisms underlying tau oligomerization and its role in cell homeostasis are largely unknown. **Methods:** In our study we investigated the role of tau accumulation in glioblastoma cells. In particular, we evaluated *in vitro* the role of tau hyperphosphorylation, and analyzed morphological and molecular consequences during cell cycle progression. **Results:** Tau protein was expressed in different glioblastoma cell lines and Western blot analysis showed the presence of several phosphorylated forms. The chemical inhibition of phosphatases induced in cancer cells the accumulation of tau protein, with an increased expression of both phosphorylated and high-molecular-weight oligomeric forms. In parallel, we observed an increment in the number of cells in the G2/M cell cycle phase with the formation of aberrant mitotic spindle and aneuploidy. As demonstrated by immunofluorescence, hyperphosphorylation determined an evident upregulation of tau expression in dividing cells with a diffuse protein localization in cytoplasm rather than on mitotic spindle. Interestingly, the pharmacologic inhibition of autophagy by treatment with chloroquine synergized with tau accumulation and increased its cytotoxic effect. In addition, we individuated CDK5 as a major contributor to tau hyperphosphorylation and aberrant mitosis.

**Conclusions:** Our data indicate that aberrant control of tau phosphorylation is important in allowing cancer progression; furthermore, the accumulation of hyperphosphorylated tau has an inhibitory role on mitosis. Thus, the understanding of molecular mechanisms underlying the homeostatic control of tau protein could suggest new therapeutic targets also in cancer.

**09-P59. Extracellular Vesicles as Mediators of Chemoresistance in Caucasian Gastric Cancer**A. Biagoni<sup>1</sup>, S. Peri<sup>1</sup>, N. Schiavone<sup>1</sup>, F. Cianchi<sup>2</sup>, L. Papucci<sup>1</sup>, L. Magnelli<sup>1</sup><sup>1</sup>University of Florence, Department of Experimental and Clinical Biomedical Sciences 'Mario Serio', Florence, Italy, <sup>2</sup>University of Florence, Department of Experimental and Clinical Medicine, Florence, Italy.

**Introduction:** To date, gastrectomy and chemotherapy are the elective therapeutic options for gastric cancer (GC) treatment. However, drug resistance, either acquired or primary, is the main cause for treatment failure, leading to recurrences and metastasis. Only after gastrectomy, through IHC analysis, we were able to collect important data about tumor markers and looked for antigens such as HER2, VEGF, ERG1, KLF5, CA IX, Ki67, E-cadherin, and with molecular analysis through *in situ* hybridization technique, we can stratify GC according to the microsatellite instability, the genomic stability, the chromosomal instability, and the presence

of the Epstein-Barr virus. This kind of approach could be supported by the analysis of the extracellular vesicles (EVs). Indeed, EVs are relatively easy to extract and, delivering a plethora of metabolites and biologic derivatives, they hide important information about the cancer molecular pattern. **Methods:** As 5-fluorouracil (5FU) is one of the most common chemotherapeutic agents used to treat advanced GC, we decided to generate a chemoresistant cell line (5FU<sub>r</sub>) subjecting the AGS cell line to repeated and increased doses of 5FU for 25 weeks. Such a cell line demonstrated an IC<sub>50</sub> above 1,000  $\mu$ M with respect to the 4  $\mu$ M of AGS. EVs were isolated through ultracentrifugation and characterized with the NanoSight NS300 platform. The EVs cargo was purified and analyzed through qPCR or Western blotting. **Results:** We demonstrated that 5FU<sub>r</sub> is resistant to high concentrations of 5FU, thanks to the overexpression of the *TYMP* gene, which converts 5FU to fluorodeoxyuridine. Through qPCR analysis we also demonstrated that 5FU<sub>r</sub>-derived EVs bear a very different mRNA cargo with respect to the AGS parental cell line, reporting, for example, among the screened genes, a higher amount of *TGF $\beta$ 1* which is conversely not overexpressed in the cell line. Then, AGS and 5FU<sub>r</sub> were treated with 5FU<sub>r</sub>-derived EVs demonstrating a slightly but significantly increased resistance to 5FU with respect to the treatment with AGS-derived EVs. **Conclusions:** EVs may contain a great number of different types of cargos ranging from DNA to RNA and proteins. In our study we demonstrated that a chemoresistant cell line is able to deliver, with a sort of paracrine effect, EVs to the nearby sensitive cells, inducing an increase in chemoresistance. Lastly, chemosensitive cells which do not possess the acquired mechanism to resist the chemotherapeutic agent might gain chemoresistance when induced by nearby chemoresistant cells.

**09-P60. The First 500 Tumor BRCA Tests and Beyond: The Crucial Role of Molecular Pathology in the Clinical Management of Ovarian Cancer Patients**  
C. Fumagalli<sup>1</sup>, E. Guerini - Rocco<sup>1,2</sup>, A. Rappa<sup>1</sup>, D. Vacirca<sup>1</sup>, A. Ranghiero<sup>1</sup>, M. Barberis<sup>1</sup>  
<sup>1</sup>European Institute of Oncology, Milano, Italy,  
<sup>2</sup>University of Milan, Department of Oncology and Hemato-Oncology, Milano, Italy.

**Introduction:** The poly (ADP-ribose) polymerase inhibitor (PARPi) olaparib has been recently approved in maintenance setting of newly diagnosed, platinum-sensitive, *BRCA* mutated epithelial ovarian cancer (EOC) patients. However, a wider population of women may benefit from PARPi treatments, including patients positive for homologous recombination (HR) deficiency. Probably in the near future *BRCA* tumor testing will be associated with the evaluation of other genes implied in the mechanisms of HR deficiency (such as *ATM*, *ATR*, *RAD51*) for treatment decision purposes. In this study we reported the results of the first 500 patients profiled with *BRCA* tumor testing in a diagnostic setting,

including 100 patients additionally tested with a comprehensive cancer panel covering HR genes.

**Methods:** A total of 500 women with EOC were consecutively referred to the Molecular Diagnostics Unit of the European Institute of Oncology (October 2016-October 2019) for tumor *BRCA* analysis. The test was requested by a gynecologic oncologist, upon discussion of the implications of test results and written consent collection. Formalin-fixed, paraffin embedded (FFPE) specimens were tested with the Oncomine *BRCA* Research Assay next-generation sequencing (NGS) panel. For 100 of these cases, an additional comprehensive genomic profile using Oncomine Comprehensive Assay (OCA) v.3 - DNA only was performed. **Results:** All 500 cases were considered adequate for the NGS analysis, both *BRCA* and OCA panels in terms of tumor cell content (>10%) and DNA extracted (>10 ng). The tumor *BRCA* had a successful rate of 99% and a median turnaround time (TAT) from the test request to the molecular report of 15 calendar days. We found 124 of 500 cases (24.8%) harboring *BRCA1* or *BRCA2* pathogenic/likely pathogenic mutations. In detail, 90 (18%) and 34 (6.8%) mutations were detected in *BRCA1* and *BRCA2*, respectively. Moreover, variants of uncertain significance (VUS) occurred in 53 cases (10.6%), affecting *BRCA1* (n = 26, 5.2%) and *BRCA2* (n = 27, 5.4%). Three cases had a *BRCA1* pathogenic variant and a concurrent *BRCA2* VUS alteration. Applying the OCA panel, we confirmed the *BRCA* status and identified HR gene pathogenic alterations in 4 of 100 (4%) tumors, including 3 cases with *ATM* mutation and 1 case with *ATR* alteration. Four VUS were found in HR genes. Overall, more than 25% of ovarian cancers tested were positive for pathogenic alterations in HR genes, including *BRCA1* and *BRCA2* alterations. **Conclusions:** The tumor *BRCA* test implemented in a routine diagnostic setting at diagnosis of EOC had a high success rate and a TAT compatible with clinical needs. A comprehensive genomic approach could pinpoint additional alterations involving HR genes that could be clinically significant for treatment decision making.

**09-P61. Role of the ProangiomiR miR-130a in Tumor Angiogenesis and Vasculogenic Mimicry: A New Key between Two Converging Biological Mechanisms**

A. Biagioni<sup>1</sup>, C. Veiga-Villauriz<sup>2</sup>, A. Laurenzana<sup>1</sup>, F. Margheri<sup>1</sup>, F. Scavone<sup>1</sup>, G. Fibbi<sup>1</sup>, M. Del Rosso<sup>1</sup>  
<sup>1</sup>University of Florence, Department of Experimental and Clinical Biomedical Sciences 'Mario Serio', Florence, Italy, <sup>2</sup>University of Manchester, Manchester, United Kingdom.

**Introduction:** Angiogenesis is an important biological process for the growth and regeneration of new vessels in normal and pathological conditions. Tumor masses exploit and induce such mechanisms to find nutrients and metastasize into distant organs. Cancer cells in the early phases of tumor formation may organize

themselves thanks to the vasculogenic mimicry (VM) ability to form vessel-like structures to obtain necessary oxygen and nutrients to grow, whereas in late stages tumor cells attract the surrounding endothelial cells and induce the formation of a complex but aberrant circulation. Such phenomena commonly converge, fueling tumor growth and making the prognosis worse. In this context, we aim to study the role of miRNA 130a, which is commonly reported to stimulate angiogenesis modulating the expression of the genes *GAX* and *HOXA5*. **Methods:** To investigate the role of miRNA 130a we exploited the CRISPR/Cas9 technique to selectively mutate a specific region near the pre-miRNA stem-loop domain to prevent DICER from recognizing and processing such immature RNA in the mature miRNA form. Such mutation was induced in endothelial colony forming cells (ECFCs) and in the neuroblastoma cell line SHSY-5Y. We Sanger sequenced the selected region to better understand what kind of mutation was induced, and we validated the miRNA expression through qPCR. Angiogenesis and VM assays were performed plating cells on Matrigel pre-coated multi 96-well plates, and the involved factors were assayed by Western blot or qPCR. **Results:** We designed a plasmid codifying for the spCas9 and a gRNA specific for the DICER recognition domain of miR-130a, and thus we transfected ECFCs and SHSY-5Y. After an initial selection, cells were analyzed through Sanger sequencing, demonstrating an insertion 3 bp upstream of the PAM sequence, thus generating a frameshift effect. miR-130a level was then evaluated with qPCR demonstrating a significant knockdown, and analyzing the vessel formation capacity we observed that miR-130a downregulation inhibited the angiogenesis in ECFCs but enhanced the VM in SHSY-5Y. The main involved angiogenic factor we identified to be responsible for such phenomena is the Plasminogen Activator Inhibitor 1 (PAI-1). Indeed, through the bioinformatic software TargetScan 7.2 we identified, among the predictable targets of miR-130a, the *SERBP1* gene which codify for the Plasminogen Activator Inhibitor 1 RNA-binding protein. **Conclusions:** miRNA have been reported to effectively control a plethora of cellular functions in a selective tissue-specific way. In our study we evaluated the role of miR-130a and verified that miR-130a inhibition decreased vessel formation capability of ECFCs, but unexpectedly it enhanced the VM ability of SHSY-5Y tumor cells.

**09-P62. Tumor exoDNA Mediates the Horizontal Transfer of TP53 Mutation in Normal Recipient Cells**  
 R. Domenis<sup>1</sup>, A. Cifù<sup>2</sup>, M. Fabris<sup>2</sup>, K.R. Niazi<sup>3</sup>, P. Soon-Shiong<sup>3</sup>, F. Curcio<sup>1,2</sup>

<sup>1</sup>University of Udine, Udine, Italy, <sup>2</sup>Azienda Sanitaria Universitaria Integrata di Udine, Udine, Italy, <sup>3</sup>NantBioScience, Inc Culver City, CA, United States.

**Introduction:** Tumor-derived exosomes (TEXs) are crucial in shaping the local tumor microenvironment to promote cancer progression by advancing tumor

metastasis. Recently, we have demonstrated that the activation of Toll-like receptor 4 (TLR4) boosts the immunosuppressive ability of exosomes released by tumor cells. Of note, TEXs carry large fragments of dsDNA, which may reflect the mutational status of parental tumor cells. The purpose of this study is to verify the hypothesis that exosomes shed by TLR4-activated tumor cells are able to induce a malignant transformation of normal recipient cells through the horizontal transfer of mutated DNA. **Methods:** SW480 tumor cells were treated with LPS (1 µg/ml), and TEXs were isolated from cell supernatants by polymer precipitation-based method. TP53<sup>R273H</sup> and KRAS<sup>G12V</sup> mutations have been identified by digital PCR on purified exoDNA. Normal epithelial cells (CCD841) were used as recipient cells, and internalization of Did-labelled vesicles was evaluated by immunofluorescence. Vitality/proliferation (Trypan Blue exclusion), migration capacity (Scratch assay), and mutational status (digital PCR) of CCD841 cells were monitored after treatment with exosomes. **Results:** SW480-derived exosomes carried dsDNA fragments in a size range of 2-10 kbp containing TP53<sup>R273H</sup> and KRAS<sup>G12V</sup> mutated sequences. Exosomes were efficiently internalized by CCD841 cells within 6 hours and elicited activation of signaling pathways that induced an increase in cell proliferation and migration capacity. Copies of TP53<sup>R273H</sup> mutated DNA and mRNA were found within recipient cells up to 1 month without exosomal treatment. The activation with LPS stimulated the packaging of mutated DNA into exosomes. Consequently, mutated DNA was found in greater amounts in recipient cells treated with exosomes released by TLR4-activated cells. **Conclusions:** The activation of TLR4 modulates the packaging of mutated genes in exosomes, which are efficiently transferred in normal recipient cells. Although we observed that the mutated *TP53* gene is transcribed in recipient cells, further studies are needed to assess whether mutated genes are integrated into genome.

**09-P63. Protective Effect of Polyphenols on Irradiation-Induced Senescence in Dermal Fibroblasts: DNA Damage and SASP**

E. Margheri<sup>1</sup>, A. Laurenzana<sup>1</sup>, A. Biagioni<sup>1</sup>, A. Chillà<sup>1</sup>, K. Tortora<sup>2</sup>, F. Scavone<sup>1</sup>, L. Giovannelli<sup>2</sup>, M. Del Rosso<sup>1</sup>, A. Mocali<sup>1</sup>, G. Fibbi<sup>1</sup>

<sup>1</sup>University of Florence, Experimental and Clinical Biomedical Science, Florence, Italy, <sup>2</sup>University of Florence, Neurofarba, Florence, Italy.

**Introduction:** Cellular senescence is a state of terminal growth arrest in which cells are irresponsive to growth factor stimulation. The senescence program is triggered when cells encounter stress conditions such as critically short telomeres, DNA damage, oncogenic activation, hypoxia, and oxidative stress. Although senescent cells do not divide, they are metabolically active and generate an enhanced and altered secretome, termed the senescence-associated secretory phenotype (SASP). The SASP is characterized by production and secretion

of interleukins, cytokines, growth factors, angiogenic factors, and ECM components, all contributing to the generation of pro-inflammatory and pro-tumoral extracellular milieu. In recent years, polyphenols have gained significant attention owing to their anti-inflammatory and anti-tumor activities. Here we studied the anti-tumor effects of polyphenols by their modulation of senescence and SASP phenotype in dermal fibroblasts. **Methods:** Early passage human dermal fibroblasts NHDFs were induced to senescence prematurely with irradiation (8 Gy) and then treated for 1 week with oleuropein aglycone (10  $\mu$ M) and hydroxytyrosol (1  $\mu$ M) with culture medium change every 2 days. Cell senescence status has been analyzed by cell growth assay, SA- $\beta$ -Gal staining, and p16 and p21 expression levels. DNA damage was evaluated by comet assay, cytoplasmic chromatin fragments (CCFs), c-GAS activation, and lamin B1/lamin B1 receptor expression. Conditioned media from polyphenols of treated and untreated senescent fibroblasts were tested on proliferation, spheroid formation, migration, and EMT of A375 and A375-M6 melanoma cells. **Results:** OLE and HT treatment results in a protective effect on irradiation-induced senescence in dermal fibroblasts. CMs collected from irradiated-fibroblasts were found effective in enhancing SASP-related tumoral phenotype in melanoma cells, that was reduced when CMs were collected after oleuropein and hydroxytyrosol treatment of senescent fibroblasts. **Conclusions:** The ability of polyphenols to mitigate the senescence and the related SASP in the tumor microenvironment appears to be a mean to lower the pro-tumoral activity of stroma senescent cells, thus indirectly targeting cancer progression. The use of natural compounds, which are present in the human diet, could avoid important adverse effects of anti-cancer therapies.

#### 09-P64. Comprehensive Genomic Profiling in a Pediatric Cohort: Novel Co-Occurrence of Cancer and Constitutional Disease

K. Schieffer, K. Miller, E. Varga, V. Magrini, D. Koboldt, K. Leraas, T. Lichtenberg, S. Colace, P. Brennan, B. Kelly, G. Wheeler, T. Bedrosian, S. LaHaye, J. Fitch, P. White, M. Shatara, A. Gupta, B. Setty, R. Olshefski, D. Osorio, M. AbdelBaki, J. Leonard, J. Finlay, S. Koo, D. Boue, C. Pierson, R. Wilson, E. Mardis, C. Cottrell  
*Nationwide Children's Hospital, Columbus, OH, United States.*

**Introduction:** Contrary to adult cancers, pediatric cancers are typically associated with minimal somatic variation, and are commonly driven by gene fusions. Notably, about 10%-15% of pediatric cancers are characterized by constitutional cancer predisposition. Through paired studies of comparator normal and affected tissues, both constitutional and somatic diseases can be identified. Novel co-occurrences are emerging, leading to challenges in biological interpretation, determination of proper therapeutic

management, and genetic counseling. **Methods:** At our tertiary care institution, pediatric and young adults with rare, refractory, or relapsed cancer and hematologic disease undergo comprehensive molecular analysis. In total, 123 patients were consented onto study, with 101 cases analyzed by enhanced exome analysis of paired comparator normal and disease-involved tissue, and RNA sequencing of the disease specimen. This combinatorial approach allowed for the detection of constitutional and somatic single nucleotide variation, insertion-deletion events, gene fusions, and gene expression. **Results:** To date, we have identified 23 patients (23%) harboring pathogenic or likely pathogenic constitutional variation with described disease association. The constitutional alterations with highest representation included *SMARCB1* (rhabdoid tumor predisposition syndrome, n = 3), *PTPN11* (Noonan syndrome, n = 2), *TP53* (Li-Fraumeni syndrome, n = 2), and *NF1* (neurofibromatosis type 1, n = 2). Rare or novel co-occurrence of somatic and constitutional disease included: rosette-forming glioneuronal tumor (constitutional RASopathy; n = 2), neuroepithelial tumor with 1p19q co-deletion (constitutional *CIC* alteration; n = 1), aplastic anemia (constitutional *CHEK2* alteration, n = 1), Ewing sarcoma (constitutional *MSH6* alteration, n = 1), and medulloblastoma (constitutional *MYO18B* alteration, n = 1). Among patients with pathogenic or likely pathogenic constitutional alteration, these findings were unanticipated in 9 of 23 (39%), demonstrating the need for appropriate counseling, cascade testing, therapeutic considerations, and surveillance beyond the somatic disease. **Conclusions:** A subset of pediatric cancer predisposition has historically been associated with well-described constitutional syndromes. Utilization of paired comparator normal and disease-involved exome sequencing was of particular benefit to our patient population, allowing for identification of unsuspected constitutional disease. We provide insight into the frequency and management of known and novel somatic and constitutional disease co-occurrences among a pediatric cancer cohort, and further demonstrate the benefit of comprehensive profiling for optimal patient management.

#### 09-P66. Metabolic Rewiring in Chemoresistant Gastric Cancer Cells and Promising Treatment Targets

S. Peri<sup>1,2</sup>, A. Biagioni<sup>3</sup>, N. Schiavone<sup>3</sup>, F. Cianchi<sup>1</sup>, L. Magnelli<sup>3</sup>, L. Papucci<sup>3</sup>

<sup>1</sup>University of Florence, Experimental and Clinical Medicine, Florence, Italy, <sup>2</sup>University of Siena, Biotechnology, Chemistry and Pharmacy, Siena, Italy, <sup>3</sup>University of Florence, Experimental and Clinical Biomedical Sciences, Florence, Italy.

**Introduction:** Gastric cancer (GC) is the fifth most common malignancy worldwide and the third leading cause of cancer-related death. Despite decreased incidence and progress in early detection of the disease, most GC cases are still diagnosed at advanced stages.

The only curative treatment remains surgery, but chemo- and radiotherapy are widely used to downstage, and prevent metastasis and recurrence. Chemoresistance is a major problem in GC due to limited therapeutic options and is responsible for treatment failure. We aimed to evaluate changes occurring in chemoresistant GC cells, possibly identifying targets that could be exploited for the recovery of a chemosensitive status. We therefore created chemoresistant GC cells to 3 commonly used drugs and evaluated metabolic changes. **Methods:** We chronically exposed the AGS gastric adenocarcinoma cell line to 3 drugs separately: 5-fluorouracil, cisplatin, and paclitaxel, thus inducing 3 chemoresistant cell lines. We evaluated metabolic alterations with respect to AGS parental cells using the Seahorse analysis platform through the Glycolysis Stress Test and Mito Stress Test kits. Lactate production was measured in conditioned media through D-Lactate Colorimetric Assay Kit. Starvation of cells from glutamine and/or glucose for 72 hrs was performed to evaluate the dependency of cell lines from these nutrients, and vitality was assessed with MTT assay. qPCRs and Western blots were performed on selected markers. **Results:** AGS cells after chronic exposure to chemotherapeutic agents developed chemoresistance to the drugs, thus creating 5FU<sub>r</sub>, CIS<sub>r</sub>, and TAX<sub>r</sub> lines resistant to 5-fluorouracil, cisplatin, and paclitaxel, respectively. Seahorse analysis showed differences in cellular energetics and indicated 5FU<sub>r</sub> and TAX<sub>r</sub> as the more energetic lines, being the former more aerobic and the latter more glycolytic, whereas CIS<sub>r</sub> was more quiescent with respect to AGS chemosensitive cells. Glycolytic phenotype of TAX<sub>r</sub> was also confirmed by its high dependence from glucose in starvation experiment, higher lactate production, and upregulation of the glycolytic enzyme enolase 1. Glutamine or glucose starvation showed a slight vitality decrease in 5FU<sub>r</sub> and CIS<sub>r</sub>, whereas depletion of both nutrients significantly reduced it, showing a metabolic plasticity in these cell lines, leading us to investigate glutaminases and highlighting a great upregulation of *GLS2* but not *GLS1* in both 5FU<sub>r</sub> and CIS<sub>r</sub>. **Conclusions:** This work highlighted metabolic rewiring occurring upon chemoresistance acquisition in a GC cell line, leading to a glycolytic dependent phenotype in the case of paclitaxel, and upregulation of glutaminolytic enzyme in the case of 5-fluorouracil and cisplatin exposed cells. Targeting these pathways could improve the treatment of chemoresistant GC patients.

### 09-P67. SLC22A4/OCTN1: A Solute Carrier at the Crossroad of Innate Immunity, Tumor Metabolism, and Chemosensitivity in Colorectal Cancer

G. Pani<sup>1</sup>, R. Colavitti<sup>1</sup>, M. Fidaleo<sup>1</sup>, V. Cavallucci<sup>1</sup>, M. Fiori<sup>2</sup>, R. De Maria<sup>1</sup>

<sup>1</sup>Univ Cattolica Sacro Cuore, Dept. of Translational Medicine, Rome, Italy, <sup>2</sup>Istituto Superiore di Sanità, Department of Oncology and Molecular Medicine, Rome, Italy.

**Introduction:** Solute carriers (SLCs) mediate tumor cell access to nutrients and microenvironmental signals, dictate sensitivity to chemotherapeutics, and represent excellent drug targets. Nevertheless, this large family of molecules has so far received limited attention in cancer research. The putative ergothioneine transporter *SLC22A4/OCTN1* is highly expressed in several tissues including the intestine and monocytes/macrophages. One missense variant (L503F) widely represented in the population (0.4 minor allele frequency in Caucasians) has been linked by population studies to an elevated risk of intestinal inflammation and colorectal cancer (CRC). However, the mechanisms underpinning these intriguing associations remain elusive. **Methods:** To gain mechanistic insight on the role of *SLC22A4* in colorectal cancer, we have stably knocked down or overexpressed *OCTN1* and its disease-associated variant in cell populations relevant to CRC development and progression, namely: malignant colonocytes (Caco-2), primary colon cancer stem cells (CSCs), and monocytes/macrophages (THP1). **Results:** Our results clearly show that — both in inflammatory (macrophages) and colon cancer epithelial cells — *OCTN1* participates in innate immune signaling, a pivotal process to colon carcinogenesis. *OCTN1*-deficient macrophages secrete reduced amounts of interleukin 1 beta in response to bacterial challenge, whereas carrier-defective Caco-2 cells display reduced autophagy and, as a result, fail to control the intracellular growth of *Streptococcus gallolyticus*, a bacterium which is frequently isolated from colon cancer tissue and is alleged to play a role in malignant progression. Molecular studies revealed that *OCTN1* is located in part in lysosomes; it physically interacts with the innate immune sensor NOD2, and it contributes — similar to the *SLC38A9* lysosomal transporter — to amino acid sensing through the mTOR/TORC1 pathway and to autophagy at the lysosomal surface. It is of note that our data, consistent with previous reports, confirm that *OCTN1* expression correlates with sensitivity to the anticancer drugs oxaliplatin and 5-FU in Caco-2 and primary CSCs, in a fashion that is altered in the context of the 503F variant. **Conclusions:** Collectively, our results highlight novel cancer-related functions of *OCTN1* and its 503F variant in CRC, delineating a novel paradigm whereby solute carriers act as a potential signal integration hub at the crossroad of bacterial-host interaction, tumor cell metabolism, and cancer chemosensitivity/chemoresistance. Accordingly, targeting of variant *OCTN1* may provide unprecedented

opportunities for personalized treatment in colorectal cancer patients.

**09-P68. Analysis of Microsatellite Instability in Gastric Cancer: Association with Clinicopathological Characteristics**

J.P. Nshizirungu<sup>1</sup>, M.R. Rui<sup>2,3,4</sup>, V.P. Marta<sup>2,3</sup>, C. Sónia<sup>2,3</sup>, I. Mellouki<sup>5</sup>, H. El Bouhaddouti<sup>6</sup>, K. Ibn Majdoub<sup>6</sup>, L. Chbani<sup>7</sup>, N. Lahmidani<sup>8</sup>, J. Hammani<sup>8</sup>, S.A. Ibrahimi<sup>9</sup>, S. Bennis<sup>1</sup>

<sup>1</sup>Biomedical and Translational Research Laboratory, Faculty of Medicine and Pharmacy, Fez, Morocco, <sup>2</sup>Life and Health Sciences Research Institute, University of Minho, Gualtar Campus, Braga, Portugal, <sup>3</sup>ICVS/3B's-PT Government Associate Laboratory, Gualtar Campus, Braga, Portugal, <sup>4</sup>Molecular Oncology Research Center, Barretos Cancer Hospital, São Paulo, Brazil, <sup>5</sup>Gastroenterology service, Duc de Tovar Hospital, Tanger, Morocco, <sup>6</sup>Department of Visceral Surgery, Hassan II University Hospital, Fez, Morocco, <sup>7</sup>Department of Pathological Anatomy, Hassan II University Hospital, Fez, Morocco, <sup>8</sup>Department of Gastroenterology, Hassan II University Hospital, Fez, Morocco, <sup>9</sup>Department of General Surgery, Hassan II University Hospital, Fez, Morocco.

**Introduction:** Gastric cancer (GC) represents the fifth most common cancer and the third leading cause of cancer-related deaths worldwide. Recently, the TCGA molecular classification identified gastric tumors with microsatellite instability (MSI) as 1 of the 4 molecular subtypes of GC. This subtype has been reported to be associated with favorable prognosis. However, data on the frequency of MSI and its biological and clinical impact among Moroccan patients are limited. The aim of the study was an analysis of MSI status and its clinicopathological characteristics in gastric cancer patients. **Methods:** The MSI analysis was performed for 97 GC tumors using a multiplex PCR comprising a well-established panel of 5 quasimonomorphic mononucleotide markers (NR27, NR21, NR24, BAT25, and BAT26). PCR products were separated by capillary electrophoresis using ABI 3730 Genetic Analyzer (Applied Biosystems, Foster City, CA, US) according to the manufacturer's instructions. Cases with 2 or more markers out of quasimonomorphic variation range (QMVR) were classified as MSI-H (MSI-high), cases with only 1 marker out of QMVR were classified as MSI-L (MSI-low) and cases without markers out of QMVR were classified as MSS (microsatellite stability). Further, the MSI-L tumors were grouped with the MSS tumors and named MSI-negative and the MSI-H tumors were named MSI-positive. **Results:** A total of 20 samples (20.6%) presented instability, 13 MSI-H (13.4%), and 7 MSI-L (7.2%) cases, with the remaining 77 tumors stable (79.4%). The correlation between MSI status and clinicopathological characteristics revealed that MSI-H phenotype was significantly associated with older age ( $p = 0.005$ ), intestinal type of Lauren histologic classification ( $p = 0.022$ ), lower pT stage ( $p = 0.048$ ),

and lower lymph node metastasis ( $p = 0.004$ ).

**Conclusions:** Our results on the prevalence of MSI in Moroccan GC patients are in agreement with the international literature. This study is still in progress, and we are analyzing mutation profiles of selected genes containing repeated sequences previously described as frequent targets for MSI.

**09-P69. A Multimodal Study to Elucidate Molecular Aspects of PTCL-NOS in an Indian Population**

K. Raj, O. Shetty, N. Phadtare, S. Dhanavade, T. Shet  
Tata Memorial Hospital, Mumbai, India.

**Introduction:** Peripheral T-cell lymphoma, not otherwise specified (PTCL-NOS), representing 10%-15% of non-Hodgkin lymphomas (NHLs), is a broad category of rare, clinically heterogeneous entities encompassing several cytological spectrum molecular alterations. Histological profiling allows classification within well-specified subgroups wherein 15% of pathologically diagnosed PTCL-NOS can be reclassified as angioimmunoblastic T-cell lymphoma (AITL). Somatic mutations of *RHOA*, *TET2*, *IDH2*, and *ITK-SYK* gene fusion have been observed in PTCL-NOS. The current study is aimed at identifying molecular markers for classification of PTCL-NOS using multiple approaches, viz., transcriptomics, gene sequencing, and fluorescence *in situ* hybridization (FISH). **Methods:** The study was performed on formalin-fixed, paraffin-embedded (FFPE) tissues of histologically confirmed PTCL cases accrued during the period 2014-2018 ( $n = 30$ ) from the Department of Pathology, Tata Memorial Hospital. DNA was extracted using QIAamp DNA FFPE Tissue kit (Qiagen, Valencia, CA, US). Gene sequencing for the following genes was performed: *RHOA* and *IDH2*. Sequencing data were analyzed using Chromas Lite software. Interphase FISH for *ITK-SYK* gene fusion was performed using customized BAC clone probe, and for *TET2* deletion using commercially available probe (MetaSystems India). The study also included detection of recurrent translocations in lymphoid malignancies using next-generation sequencing (NGS)-based TruSight RNA fusion panel (Illumina) with 507 potential targets. The clinical details were retrieved from electronic medical records and correlated with the molecular findings. **Results:** The study comprised 7 females and 23 males with male to female ratio of 3:1. *RHOA* G17V mutation was observed in 4 of 6 (66.6%) AITL cases and 5 of 24 (20.8%) PTCL cases, whereas *IDH2* R172 mutation was observed in 4 of 6 (66.6%) AITL cases and 2 of 24 (8.3%) PTCL cases. Nearly 80% of the cases were stage III-IV disease. *RHOA* and *IDH2* mutation was associated with a high stage of the disease. MIB1 index was 60%-80% for the cohort harboring *RHOA* and *IDH2* mutations. Mutations observed in *RHOA* and *IDH2* were not mutually exclusive and were observed concurrently in 4 AITL cases. All *RHOA* and *IDH2* mutant cases were tested for *TET2* deletion by FISH; however, no aberration was detected in any of these cases. No known or novel translocations were observed using the

NGS-based TruSight RNA fusion panel. *ITK-SYK* t(5;9)(q33;q22) rearrangement was also not seen in any of the PTCL cases. **Conclusions:** Molecular characterization of PTCL-NOS is ongoing, and no genetic alterations were detected by either transcriptomics or FISH-based approach in the current cohort. The current study is the first of its kind in India and is ongoing.

#### 09-P70. Evaluation of Tissue MicroRNAs as Prognostic Biomarkers in Partially Resected Pediatric Low-Grade Gliomas

G. Catanzaro<sup>1</sup>, Z.M. Besharat<sup>1</sup>, M. Chiacchiarini<sup>1</sup>, A. Cacchione<sup>2</sup>, E. Miele<sup>2</sup>, A. Po<sup>3</sup>, G. Forcina<sup>1</sup>, F. Gianno<sup>4</sup>, D. Figarella Branger<sup>5,6</sup>, C. Colin<sup>5</sup>, M. Antonelli<sup>4</sup>, F. Giangaspero<sup>4,7</sup>, M. Gessi<sup>8</sup>, L. Massimi<sup>9</sup>, A. Carai<sup>10</sup>, F. Locatelli<sup>2,11</sup>, E. Ferretti<sup>1</sup>

<sup>1</sup>Università la sapienza, Experimental Medicine, Roma, Italy, <sup>2</sup>Bambino Gesù Children's Hospital (IRCCS), Department of Hematology, Oncology and Stem Cell Transplantation, Rome, Italy, <sup>3</sup>Università la sapienza, Molecular Medicine, Roma, Italy, <sup>4</sup>Università la sapienza, Department of Radiological, Oncological and Pathological Science, Roma, Italy, <sup>5</sup>Aix-Marseille University, Neurophysiopathology Institute (INP), CNRS, Marseille, France, <sup>6</sup>Assistance Publique Hopitaux de Marseille, Department of Pathology, Marseille, France, <sup>7</sup>IRCCS Neuromed-Mediterranean Neurological Institute, Pozzilli, Italy, <sup>8</sup>Catholic University Medical School, Histopathology Division, Rome, Italy, <sup>9</sup>Catholic University Medical School, Pediatric Neurosurgery, Institute of Neurosurgery, Rome, Italy, <sup>10</sup>IRCCS Bambino Gesù Children's Hospital, Neurosurgery Unit, Department of Neuroscience and Neurorehabilitation, Rome, Italy, <sup>11</sup>Università la sapienza, Department of Gynecology/Obstetrics and Pediatrics, Roma, Italy.

**Introduction:** Pediatric low-grade gliomas (PLGGs) are the most frequently diagnosed brain tumors in children, and their clinical outcome is strictly dependent on tumor location. Indeed, supratentorial PLGGs can be associated with incomplete surgical resection with frequent relapses. Residual or recurrent tumors are currently treated with chemo- and/or radiotherapy, but these approaches are non-curative and carry significant risks and side effects. With the aim of shedding light on new molecular aspects of PLGGs, we explored microRNA expression in tumors that were partially resected, which represent the main clinical problem.

**Methods:** We subgrouped our supratentorial sample cohort and performed microRNA profiling on 19 samples by comparing samples that experienced (n = 10) or not (n = 9) tumor progression. The profiles have been done by using RT-qPCR with TaqMan low density array microfluidic cards. Validation has been performed by TaqMan single assay RT-qPCR assays and *in situ* hybridization. **Results:** The rate of the detected microRNAs was high and comparable between the 2 subgroups of tumors. From the comparison of the microRNA profile of the supratentorial partially resected PLGG samples that experienced or not tumor

progression, we identified 5 differentially expressed microRNAs. We performed ROC analysis and identified that the combination of 2 of these 5 microRNAs resulted in an area under the curve (AUC) higher than 0.8 with a p value of 0.0087, indicating that these microRNAs could have a prognostic value. **Conclusions:** We identified 2 microRNAs that can be used as prognostic tissue biomarkers at the moment of surgical resection. This result could be of utmost importance in defining treatment strategies through the reduction of the number of patients who need to undergo chemo- and/or radiotherapy.

#### 09-P71. The Carbonic Anhydrase Inhibitor SLC-0111 Overcomes the Vemurafenib Resistance of Melanoma Cells Induced by MSC

S. Peppicelli<sup>1</sup>, E. Andreucci<sup>1</sup>, F. Bianchini<sup>1</sup>, J. Ruzzolini<sup>1</sup>, F. Carta<sup>2</sup>, C.T. Supuran<sup>2</sup>, L. Calorini<sup>1</sup>

<sup>1</sup>University of Florence, Department of Experimental and Clinical Biomedical Sciences, Florence, Italy, <sup>2</sup>University of Florence, NEUROFARBA, Florence, Italy.

**Introduction:** Host cells of tumor microenvironment include endothelial cells, infiltrating inflammatory cells, and stromal cells such as fibroblasts and mesenchymal stem cells (MSC). MSCs are multipotent precursor cells endowed with the ability to differentiate into a variety of mesenchymal cells, which may facilitate cancer progression, influencing aggressiveness of tumor cells. In our laboratory, we demonstrated that MSCs are able to induce in melanoma cells an epithelial-to-mesenchymal transition (EMT) program, higher resistance, and invasiveness, most of which related to TGF- $\beta$  secretion. Now we know that MSCs also express a high level of carbonic anhydrase (CA) IX, crucial in several biological aspects, including TGF $\beta$  release. The aim of this study is to disclose whether the CAIX inhibitor SLC-0111, which we have previously found able to potentiate the cytotoxic effects of conventional chemotherapeutic drugs, prevents the vemurafenib-resistance of *BRAF* mutated human melanoma cells promoted by MSC. **Methods:** Media conditioned by MSC pretreated or not with 100  $\mu$ M SLC-0111 were used to grow A375-M6 human melanoma cells. A375-M6 were then treated with 1 mM vemurafenib to investigate the resistance to this drug, test cell viability and proliferation, and analyze the expression of vemurafenib resistance markers by real-time PCR and Western blotting. **Results:** We found that medium conditioned by MSC induces a vemurafenib resistance in A375-M6 melanoma cells. Indeed, cells grown in MSC conditioned medium treated with vemurafenib maintain their proliferation and their ability to give colonies. When melanoma cells were grown in medium conditioned by MSC pretreated with the CAIX inhibitor SLC-0111, they re-acquired their sensitivity to vemurafenib, reducing their proliferation and the expression of some vemurafenib resistance markers such as EGFR, PDGFR, and p-p70S6. **Conclusions:** To conclude, the CAIX inhibitor SLC-0111 may abolish the vemurafenib

resistance promoted in melanoma cells by MSC, disclosing a new potential target of therapy.

#### 09-P72. Circadian Regulation of Xenobiotic Metabolism during Anticancer Treatment

M.M. Bellet, C. Stincardini, M. Pariano, G. Renga, F. D'Onofrio, C. Costantini, S. Brancorsini, L. Romani  
University of Perugia, Department of Experimental Medicine, Perugia, Italy.

**Introduction:** Our body's cycle of daily rhythm, named the circadian clock, can influence the response to many types of medications and procedures. Chronotherapy is defined as the specific timing of drug delivery, aimed at increasing efficacy and reducing side effects of each treatment, including anticancer treatment. The circadian patterns of tolerance and efficacy of each drug are dependent on multiple factors, including the circadian control of detoxification pathways in liver and gut, the time-dependent pharmacokinetic of each medication, the circadian control of cell cycle, DNA repair, and apoptosis. All of this information is essential for the construction of optimal chronomodulated drug delivery schedules, but the molecular mechanisms at the base of these events are still poorly understood. Our research is focused on the definition of the mechanism, how the circadian clock controls specific pathways regulating drug metabolism, and how this affects the time-dependent efficacy and toxicity of chemotherapy drugs.

**Methods:** *In vitro* experiments in cells overexpressing circadian components or following circadian synchronization were performed to dissect the mechanism of circadian regulation of xenobiotic metabolism. Moreover, *in vivo* experiments in C57BL/6 and NSG mice treated with different chemotherapy drugs at different times of the circadian cycle were carried out to evaluate the circadian activation of the xenobiotic pathways and the time-dependent susceptibility of mice to the administration of anticancer drugs. **Results:** We obtained results showing that specific molecular pathways, such as the one involving the xenobiotic metabolism regulators PXR and AhR, are controlled by the circadian system. Moreover, we observed differences in both antitumor efficacy and gastrointestinal toxicity following time-dependent administration of different anticancer drugs.

**Conclusions:** Our data showed how both the tolerability and efficacy of anticancer treatments change in a time-dependent manner, and this is likely due to the circadian clock controlling specific pathways of the xenobiotic metabolism. We believe that deciphering the molecular mechanisms that link metabolism, cancer treatment, and circadian responses will provide valuable insights towards innovative strategies of therapeutic intervention.

#### 09-P73. Genetic Alterations in Luminal Androgen Receptor Triple Negative Breast Cancer

S. Stella, S.R. Vitale, M. Massimino, E. Tirrò, G. Motta, N. Inzerilli, K. Lanzafame, C. Romano, L. Manzella  
University of Catania, Department of Clinical and Experimental Medicine, Center of Experimental Oncology and Hematology, A.O.U. Policlinico-Vittorio Emanuele, Catania, Italy.

**Introduction:** Triple negative breast cancer (TNBC) accounts for tumors that lack expression of estrogen receptor, progesterone receptor, and human epidermal growth factor 2. TNBC represents heterogeneous disease that can be classified into different subgroups by gene expression profiling. Among them, the luminal androgen receptor (LAR) subtype is characterized by luminal gene expression and androgen receptor (AR) pathways. To date, the role of AR on prognosis and clinical standpoint is still controversial. Some studies showed a good prognosis in TNBC patients expressing AR, whereas others suggested the opposite, and some reported that AR status has no significant value in patient prognosis. Based on these different and controversial data, it is necessary to find biomarkers predicting response to therapy. **Methods:** In this paper we molecular profiled 8 LAR TNBC patients using the FoundationOne gene panel from the Foundation Medicine research group. The molecular co-analysis of known genetic alterations (KGA) and variants of unknown significance (VUS) mutations was performed using DAVID and PANTHER tools. **Results:** Through this NGS approach we identified 24 KGA and 62 VUS in 15 and 59 genes, respectively. The most frequent KGAs were in *PIK3CA* (50%), *TP53* (37.5%), *PTEN* (37.5%), and *ERBB2* (37.5%) genes. In the VUS dataset, the only recurrent mutated genes were *CBFB*, *EP300*, *MAP3K1*, and *TSC2*. The co-analysis of KGA and VUS mutations by using DAVID and PANTHER tools identified PI3K-AKT, TP53, apoptosis, angiogenesis, and MAPK signaling pathways, which are mostly involved in LAR TNBC. Additionally, we identified several clinical trials that assess the therapeutic outcomes and benefits of different drugs targeting the KGA genes. **Conclusions:** These findings confirmed the role of TP53, PI3K-Akt, and its downstream target mTOR pathways in LAR TNBC. On the contrary, AR gene mutations seemed not to associate with TNBC profile. Hence, the additional genes detected might provide more information for this group of patients. The NGS approach is useful to discover novel mutations and investigate potential therapeutic strategies for LAR TNBC.

### 09-P74. Role of KCTD15 and its Parologue KCTD1 in Stabilization of the Sonic Hedgehog Suppressor KCASH2

A. Di Fiore<sup>1</sup>, A. Angrisani<sup>1</sup>, S. Fonte<sup>1</sup>, M. Maroder<sup>1</sup>, G. Giannini<sup>1</sup>, M. Moretti<sup>2</sup>, E. De Smaele<sup>2</sup>

<sup>1</sup>La Sapienza University, Molecular Medicine, Rome, Italy, <sup>2</sup>La Sapienza University, Experimental Medicine, Rome, Italy.

**Introduction:** KCASH2 belongs to the KCASH family of proteins, involved in negative regulation of the Sonic Hedgehog (Hh) pathway. KCASH2 is able to induce Hh pathway downregulation through recruitment and degradation of HDAC1, inhibiting the transcriptional activity of Gli1, the main target and effector of the Hh pathway. KCASH2 expression is reduced or lost in a subset of *SHH*-dependent medulloblastomas (MBs), whereas in others the mRNA level was unchanged. Given the role of KCASH2 as an oncosuppressor, we searched for mechanisms of KCASH2 modulation. Looking for KCASH2 interactors through a proteomic approach, we have identified the BTB/POZ containing KCTD15 protein. KCTD15, together with KCTD1, is a member of a subfamily of KCTD proteins, distinct from the KCASH family. KCTD15, similarly to KCASH2, is expressed in adult cerebellum, and this observation suggests a biologically significant interplay with KCASH2 in Hh regulation during cerebellar development and differentiation. The similarity of the protein sequence of KCTD15 and KCTD1 further prompted us to verify a potential role also for the latter in KCASH2 regulation.

**Methods:** KCTD15 and KCTD1 interaction with KCASH2 was verified by co-immunoprecipitation assays and GST pull-down. WB analyses have been used to evaluate the KCTD15 and KCTD1 roles on KCASH2 protein stability. Luciferase assays, RT-qPCRm, and WB analyses were performed to characterize the KCTD15/KCTD1 function in Hh pathway regulation. MB cell proliferation was investigated through colony formation, MTS, and EdU incorporation assays; differential nuclear staining assay and WB analysis for caspase3 protein were used to evaluate the apoptosis.

**Results:** KCTD15 overexpression is associated with HDAC1 protein level decrease in HEK293T cells and in the MB cell line, repressing Gli1 activity. Unlike KCASH2, KCTD15 is not able to bind either HDAC1 or Cul3. We demonstrated that KCTD15, interacting with KCASH2 through their BTB domains, increases KCASH2 protein stability and enhances its inhibitory effect in Hh-dependent MB cells. We verified if KCTD1 is also able to interact with KCASH2 and plays a similar role. We demonstrated that KCTD15 overexpression impairs MB cell proliferation and leads to both a reduced Hh-dependent stemness of MB cells but also a reduction of self-renewal ability. **Conclusions:** We identified KCTD15 as a novel regulator of the Hh pathway and evaluated the capability of the parologue KCTD1 to play a similar function. We demonstrated a new mechanism involved in fine tuning of the Hh pathway, which exploits the modulation of KCASH2 protein stability, acting at the

post-transcriptional level. This mechanism of regulation underlines the relevance of a proteomic approach in the search for potential tumorigenic alterations.

### 09-P75. MiR-214-Enriched Extracellular Vesicles in Acidic Tumor Microenvironment: The Molecular Tool for Cancer Cell Resistance into Blood Circulation and Extravasation

E. Andreucci, F. Bianchini, S. Peppicelli, J. Ruzzolini, L. Calorini

University of Florence, Florence, Italy.

**Introduction:** The high glycolytic metabolism (both "aerobic" and "anaerobic") of cancer cells produces a huge amount of lactic acid, which in turn determines the fall-down of extracellular pH to a range of 6.9-6.4. During the last decade, many efforts have been made to determine the role of the acidic tumor microenvironment (TME) in cancer progression, and much evidence highlighted its involvement in metastasis, including the vascular phase of dissemination cascade. Indeed, once detached from the primary mass and inside the circulatory system, tumor cells must survive in blood circulation before choosing a suitable secondary organ: this is known as anoikis resistance. MiR-214 has been shown to drive anoikis resistance, adhesion to the extracellular matrix (ECM), and extravasation of cancer cells. The aim of this project was to evaluate whether extracellular acidosis promotes in melanoma cells the release of extracellular vesicle (EV) enriched in miR-214 able to promote the anoikis resistance and the extravasation process of recipient cancer cells.

**Methods:** Human metastatic A375-M2, WM266-4, and Sk-Mel-2 (from lung, lymph node, and skin, respectively) and murine B16-F10-derived metastatic LUIC4 and ICLIV1 (from lung and liver, respectively) were grown under standard condition (pH 7.4 ± 0.1) or chronic extracellular acidosis (pH 6.7 ± 0.1 >3 months). Forty-eight-hour conditioned media were collected and EV isolated via ultracentrifugation method. EV-RNAs were isolated and miR-214 level evaluated by qPCR analysis. EVs were administered to recipient primary human A375 and murine B16-F10 cells. Anoikis was determined by Annexin V/PI analysis of EV-treated melanoma cells after 24-72 hours under non-adherent conditions, adhesion to ECM mimicked by cell counting of EV-treated melanoma cells plated on collagen-1, and extravasation of fluorescent EV-treated melanoma cells was instead assessed *in vitro* as they are able to move through an endothelial cell monolayer in a transwell assay. **Results:** We observed that EVs isolated from chronic acidic melanoma cells carry significantly a higher amount of miR-214 compared to those extracted from non-acidic cancer cells. Moreover, acidic-derived EVs significantly increase anoikis resistance, adhesion to collagen type I, and extravasation of recipient melanoma cells in both human and murine *in vitro* models.

**Conclusions:** Here we show for the first time that extracellular acidosis stimulates melanoma cells to produce miR-214-enriched EVs that in turn promote in

recipient cancer cells anoikis resistance, extravasation, and adhesion to ECM — crucial steps in metastatic cascade. Overall, the local acidic TME reprograms cancer cells toward a miR-214-dependent resistant migratory phenotype.

#### 09-P77. Compound 22 as a New Isoflavone Inhibitor for the Treatment of Hedgehog-Dependent Tumors

E. Loricchio

La Sapienza University, Dipartimento di Medicina Molecolare, Rome, Italy.

**Introduction:** The Hedgehog (Hh) signaling is a developmental conserved pathway implicated in tissue homeostasis, cell stemness, and tumorigenesis; its deregulation may occur in a wide range of human cancers, such as medulloblastoma (MB), the most frequent and aggressive pediatric brain tumor. Recently, pharmacological inhibition of the Hh signaling has emerged as a promising therapeutic strategy for the treatment of Hh-dependent MB; here we focused on the synthesis and biological validation of a small molecule, the isoflavone 22 (compound 22, c22) which is able to block the Hh pathway acting both at upstream levels on the co-receptor Smoothened (Smo) and at downstream level on the transcription factor glioma-associated oncogene 1 (Gli1) simultaneously. **Methods:** We exploited by molecular docking the high versatility of the natural isoflavone scaffold derived from a known inhibitor of Gli1/DNA interaction, glabrescione B (GlaB), to target the Hh signaling pathway at multiple levels through chemical substitution in meta and para position of the ring-B of GlaB isoflavonic core. Organic synthesis and *in vitro* testing led us to the identification of c22. Through functional and biological assays we evaluated the efficacy of c22 to antagonize both Smo and Gli1 activity. These data were sustained by *in vitro* and *in vivo* experiments in which we tested the ability of compound 22 to suppress Hh-dependent tumor growth in primary MB cells freshly isolated from Math1-cre/Ptch<sup>C/C</sup> mice that spontaneously developed MB, and in human and murine Hh-dependent MB cell lines.

**Results:** We demonstrated that c22 is able to bind Smo receptor and also to directly interfere with transcription activity of Gli1. Compound 22 is able to inhibit Hh-dependent tumor growth in human and murine MB cell lines *in vitro* and in primary MB cells *in vivo* at submicromolar concentration, as a consequence of the reduction in Gli1 expression levels. **Conclusions:** Our results reveal a valuable form of targeted therapy to increase efficacy and decrease the toxicity of individual anticancer agents. Our findings discover the first multitarget Hh inhibitor that impinges Hh-dependent tumor growth and stands as a new potential weapon against Hh-driven cancer, such as MB.

#### 09-P78. Adipocyte-Derived Exosomes as New Adipokines Sustaining Breast Cancer Progression

C. Giordano<sup>1</sup>, G. La Camera<sup>1</sup>, L. Gelsomino<sup>1</sup>, I. Barone<sup>1</sup>, S. Panza<sup>1</sup>, D. De Rose<sup>1</sup>, D. Naimo<sup>1</sup>, V. Giordano<sup>2</sup>, D. Bonofiglio<sup>1</sup>, S. Andò<sup>1</sup>, S. Catalano<sup>1</sup>

<sup>1</sup>University of Calabria, Dept. of Pharmacy, Health and Nutritional Sciences, Rende, Italy, <sup>2</sup>American Center Centro Chirurgico, Rende, Italy.

**Introduction:** Adipose tissue is now recognized as an endocrine and immunologically active organ that, in releasing soluble factors and vesicles, plays an important role in cancer biology. Several reports demonstrated that exosomes, small membrane-derived vesicles, are able to modify target cell phenotype by transferring bioactive molecules such as proteins, mRNAs, microRNAs, DNAs, lipids, and transcriptional factors. However, whether adipose tissue-derived exosomes, acting as a mode of cell-to-cell communication, might have a role in mediating the adverse effects of obesity on breast cancer is still not completely understood. **Methods:** Exosomes were isolated from conditioned media of differentiated 3T3-L1 adipocytes (3T3-L1 A), a well-recognized *in vitro* model of white adipocytes, by sequential ultracentrifugation method, and characterized by nanoparticle tracking analysis, transmission electron microscopy, and immunoblotting analyses. Exosome uptake in estrogen receptor  $\alpha$  (ER $\alpha$ )-positive MCF-7 and triple negative MDA-MB-231 breast cancer cells was tested by monitoring internalization of exosomes labeled with PKH-26. Proliferation assays (MTT and soft agar assays), motility/invasion assays (wound healing and Boyden Chamber migration/invasion assays), mammosphere forming efficiency (MFE), and self-renewal (SR) were used to test the effects of exosomes on breast cancer phenotype. Real-time PCR was used to quantify gene expression. **Results:** Treatment of MCF-7 and MDA-MB-231 breast cancer cells with 3T3-L1 A-derived exosomes significantly increased the ability of cells to form colonies in an anchorage-independent growth assay. We found that both breast cancer cells treated with adipocyte-derived exosomes displayed increased migration/invasion capabilities. Accordingly, 3T3-L1 A-derived exosomes significantly induced the expression of genes involved in epithelial-to-mesenchymal transition (EMT) in both cell lines. Since migratory potential and EMT represent important features for breast cancer stem cells (BCSCs), we explored the effect of 3T3-L1 A-derived exosomes on MCF-7 and MDA-MB-231 BCSC activity. Adipocyte-derived exosomes were able to increase MFE and SR in both breast cancer cell lines. Interestingly, exosomes isolated from conditioned media of breast adipose tissue of women who underwent reductive mammoplasty induced growth, motility, and invasiveness in breast cancer cells. **Conclusions:** Overall, our results demonstrate that adipocyte-derived exosomes, acting as new adipokines, may sustain a more aggressive breast cancer phenotype. These data, providing novel insights

in the link between obesity and breast cancer, may open a new molecular window for preventive and therapeutic strategies to fight breast cancer in obese women.

**09-P79. An Innovative Engineered Bispecific Antibody to Be Used as a Molecular Diagnostic Tool in Pancreatic Cancer**

C. Duranti, J. Iorio, G. Bagni, E. Lastraioli, A. Arcangeli  
University of Florence, Dep of Experimental and Clinical Medicine, Firenze, Italy.

**Introduction:** hERG1 (Kv11.1) is a potassium ion channel involved in the repolarization phase of the cardiac action potential. hERG1 belongs to a new class of oncology targets. One of the most intriguing aspects of its involvement in the establishment and progression of tumors is its interaction with adhesion molecules such as integrins. It has recently been shown that the macromolecular complex that forms between hERG1 and  $\beta 1$  integrin is selectively expressed in tumor tissues (Becchetti *et al.* Science Signaling, 2017). To this end, we have developed and characterized a bifunctional antibody in the single-chain variable fragment format, scDb, having dual specificity and capable of recognizing hERG1 and integrin  $\beta 1$ . We have tested the scDb binding on samples of ductal adenocarcinoma of the pancreas, developing an immunohistochemical protocol for its use as a tumor diagnostic tool recognizing the hERG1/ $\beta 1$  complex for a better stratification of patients.

**Methods:** The study samples, collected at Oncological Surgery (AUO Careggi, Florence), comprised 20 total samples: 80% females and 20% males; average age  $67.47 \pm 2.95$  years; 75% grading 2 and 25% grading 3. Two different antibody dilutions (1:50 and 1:100) were tested. Given the lack of the constant portion in the scDb antibody, it was necessary to refine the protocol by inserting an incubation with a secondary antihistidine antibody that allows the recognition of the histidine tag proper to the scDb itself. The expression of the complex was evaluated with an immunohistochemical score, already applied (Lastraioli *et al.* Br J Cancer, 2015).

**Results:** A total of 25% of the samples tested were positive for the hERG1/ $\beta 1$  complex, with a good agreement between this result and what was obtained previously, evaluating only the expression of hERG1 using a complete monoclonal antibody directed against the channel ( $R = 0.55$ ,  $p = 0.0072$  Pearson correlation). No statistically significant associations emerged between the positivity for hERG1/ $\beta 1$  and the clinicopathological characteristics of the patients, a predictable result given the limited number of the sample. Nevertheless, the successful development of the immunohistochemical protocol encourages us to continue the study on a larger series with the aim of assessing the impact of the expression of the hERG1/ $\beta 1$  complex on patient follow-up. **Conclusions:** From the results obtained, it has emerged that the hERG1/ $\beta 1$  complex is a good molecular biomarker recognized by scDb. We propose in the future its possible use as a more specific biomarker (compared to hERG1 alone) to

assess its prognostic impact in patients with pancreatic cancer.

**09-P80. Immunophenotypic Characterization of Patients Affected by Advanced Thymoma and Severe Autoimmunity**

A.M. Malfitano, V. D'Esposito, M. Tortora, S. Di Somma, M. Ottaviano, M. Giuliano, G. Palmieri, P. Formisano  
Università degli Studi di Napoli 'Federico II', Napoli, Italy.

**Introduction:** Thymomas, the epithelial tumors of the thymus, are rare cancers often associated with immunodeficiencies like Good syndrome (GS), a fatal hypogammaglobulinemia, and a variety of autoimmune diseases (ADs). Due to its rarity, immunological features of thymoma have been poorly addressed and are still unclear. A marked loss of CD4+ T lymphocytes and NK cells with accumulation of polyclonal naive CD8+ T lymphocytes was previously reported in patients with thymoma and GS. Our study aims to address differences in immune cell subsets of patients affected by thymoma with and without associated autoimmune diseases (AD). **Methods:** Eleven patients with thymoma and 11 patients with thymoma plus AD were recruited at the Rare Tumour Reference Centre of Federico II of Naples. Immunophenotype of these patients was evaluated on whole blood by 8-colour immunophenotyping kit and Treg Detection Kit (CD4/CD25/CD127). The following cell subsets were evaluated: monocytes, neutrophils, eosinophils, CD4+T cells, CD8+T cells, B-cells, natural killer (NK) cells, and NKT cells. Treg were evaluated gating on CD4+T cells as CD25<sup>high</sup>CD127<sup>dim/neg</sup> cells. The mean  $\pm$  standard deviation of the 2 groups of patients was calculated evaluating the statistical difference in the various cell subsets. Serum levels of interleukin-15 (IL-15) and vascular endothelial growth factor (VEGF) were determined by ELISA-based assays. **Results:** Our results evidenced a marked difference between the 2 groups of patients in the number of leucocytes and in the percentage of specific cell subsets. In particular, the number of leucocytes was increased in patients with AD, as well as the percentage of CD3+, CD4+, and CD8+ T lymphocytes. Circulating IL-15 and VEGF levels were also significantly elevated. Conversely, the percentage of Treg was significantly reduced in patients with AD. Other cell subsets did not show any difference between the 2 groups of patients. Interestingly, CD19+ B cells were decreased in patients with AD. The reduction of B cells was more marked if GS was considered. Indeed, patients with AD and GS displayed a very low number of B cells, compared with patients without GS.

**Conclusions:** Our study describes a profound alteration in the B and T cells, highlighting differences in the Treg compartment between thymoma patients with associated AD. The increase of IL-15 is consistent with the upregulation of T cells, whereas the decrease of Treg appears to be IL-15-independent. Although the pathogenic mechanisms still need to be defined, our data contribute to a better understanding of the disease,

and suggest the need for monitoring the immunophenotype of these patients to improve clinical management and likely develop personalized treatments.

#### 09-P81. MEKK1 Suppresses Hedgehog Signaling and Medulloblastoma Growth by Phosphorylating GLI1 at Multiple Sites

F. Di Pastena

Sapienza - University of Rome, Medicina Molecolare, Roma, Italy.

**Introduction:** The aberrant activation of developmental Sonic Hedgehog (*SHH*) signaling is a leading cause of medulloblastoma, the most frequent pediatric solid tumor. Hence, *SHH* inhibitors represent an ideal class of drugs for treatment of this type of malignancy. The only FDA-approved compound, the Smoothed (Smo) antagonist vismodegib, has shown limited efficacy in patients due to the occurrence of novel Smo mutations or to post-receptor mutations. For this reason, other strategies focused on post-receptor inhibition of *SHH* are gaining ground. In particular, the identification of novel actionable mechanisms, directly affecting the activity of the *SHH*-regulated GLI transcription factors, represents an important goal for these malignancies. Phosphorylation is one of the key modifications regulating GLI function. In this study, we investigated the role of the mitogen-activated protein kinase kinase 1 (MEKK1), a key member of the most upstream mitogen-activated protein kinase (MAPK) phosphorylation modules, in *SHH*-dependent function and tumorigenesis. **Methods:** Gene expression and reporter assays were used to screen different MAP3Ks. The association and phosphorylation of GLI1 was investigated through immunoprecipitation and Western blot approaches. Mass spectrometry allowed the identification of the phosphorylated residues, whereas ectopic expression of MEKK1 and treatment with the MEKK1 activator nocodazole were used to investigate the antitumor properties of this mechanism on a *SHH* medulloblastoma cell line. **Results:** After testing the effect of different MAP3Ks, we identified mitogen-activated kinase kinase kinase 1 (MEKK1) as the most potent inhibitor of GLI1 activity. We found 27 phosphorylated residues in the GLI1 C-terminal region, and a consequent increased binding between GLI1 and the cytoplasmic 14-3-3 proteins. Notably, ectopic expression of MEKK1 or the treatment of medulloblastoma cells with the MEKK1 activator nocodazole resulted in a marked inhibitory effect on GLI1 activity, leading to a significant decrease of tumor cell proliferation rate and viability. **Conclusions:** By directly phosphorylating GLI1, MEKK1 is a potent inhibitor of *SHH* signaling and a novel druggable target for the treatment of medulloblastoma and other *SHH*-dependent tumors.

#### 09-P82. Sorafenib Treatment Induces Lipid Accumulation in Hepatic Cell Lines

A. Angrisani<sup>1</sup>, N. Pediconi<sup>2</sup>, A.D.G. Nunn<sup>2</sup>, E. De Smaele<sup>3</sup>, M. Levrero<sup>4</sup>, L. Belloni<sup>5</sup>

<sup>1</sup>La Sapienza University, Molecular Medicine, Rome, Italy, <sup>2</sup>IIT, CLNS-Sapienza, Rome, Italy, <sup>3</sup>La Sapienza University, Experimental Medicine, Rome, Italy, <sup>4</sup>Centre de Recherche en Cancérologie de Lyon (CRCL), Lyon, France, <sup>5</sup>La Sapienza University, Internal Medicine, Rome, Italy.

**Introduction:** Sorafenib is a multikinase inhibitor which exhibits an anticancer effect in the treatment of solid tumors and currently is the standard drug for patients with advanced hepatocellular carcinoma (HCC). However, long-term exposure to sorafenib often results in reduced sensitivity of tumor cells to the drug and in a significant heterogeneity in outcomes among patients treated with the compound. Excessive accumulation of triglyceride-containing lipid droplets within hepatocytes results in the development of chronic liver diseases that can progress to HCC. The pathogenesis of these diseases is extremely complex and poorly understood. We analyze the impact of sorafenib treatment on hepatic lipid metabolism *in vitro*. **Methods:** A label-free technique, coherent anti-Stokes Raman scattering (CARS) microscopy, was used to quantify lipid droplet accumulation in hepatic cells. Human differentiated dHepaRG, HepG2, and HUH7 cells were exposed to sodium oleate and sorafenib treatments. RT-qPCR analyses were performed to characterize the expression of genes involved in metabolic pathways and proliferation. ELISA assays were used to analyze the albumin content and the Cyp3A4 activity of dHepaRG cells following drug treatment. **Results:** The treatment with sorafenib induces a strong lipid increase in dHepaRG cells, comparable to oleate-dependent lipid accumulation. Moreover, the combination of oleate and sorafenib treatments increases the degree of lipid droplet accumulation beyond that of the single drug treatment. By contrast, HepG2 and HUH7 cells treated with sorafenib did not reveal any lipid droplet accumulation. In dHepaRG cells, sorafenib treatment induces an increase in metabolic genes and activates inflammatory response genes. Interestingly, sorafenib treatment activates the expression level of genes involved in cell proliferation. In HepG2 and HUH7 cells treated with sorafenib, dissimilar results are obtained, indicating a different effect of the antitumor drug on lipid accumulation. Moreover, sorafenib treatment of dHepaRG reduces the albumin content and CYP3A4-mediated metabolism. **Conclusions:** Our results indicate that sorafenib treatment induces lipid accumulation and an inflammatory response in hepatic HepaRG cells, and activates the expression of genes involved in cell metabolism and proliferation potentially relevant for HCC development and progression.

### 09-P83. Oncolytic Adenovirus d/922-947 in Breast Cancer: Antitumor Activity and Modulation of Tumor Microenvironment

S. Di Somma, A.M. Malfitano, G. Castellano, P. Formisano, G. Portella  
 University of Naples Federico II, Department of Translational Medicine, Napoli, Italy.

**Introduction:** Breast cancer (BC) is the most common female malignancy and the second cause of cancer-related deaths in women. Novel therapeutic approaches for the treatment of aggressive types of BC are urgently needed, and oncolytic viruses (OVs) represent promising anticancer therapeutics that selectively replicate in and kill cancer cells. The interactions between tumor cells and the tumor microenvironment (TME) influence therapeutic response and patient prognosis. Our hypothesis is that the oncolytic adenovirus d/922-947 might be an efficient direct anticancer agent and might modulate TME as well. The interaction of OVs with TME is unexplored and needs to be elucidated to unveil the efficacy of virotherapy.

**Methods:** We evaluated the cytotoxic activity of d/922-947 by sulforhodamine B (SRB) assays on selected BC cell lines: MCF7 (ER+) and MDA-MB231 (ER-/triple negative). We assessed the replicative potential of d/922-947 by real-time PCR. We investigated the induction of immunogenic cell death (ICD), evaluating calreticulin (CALR) surface exposure and HMGB1 intracellular content by flow cytometry, and quantifying ATP extracellular levels on supernatants of BC infected cells by a commercially available kit. Modulation of relevant cytokine/chemokine release (VEGF, IL-6) was assessed by ELISA kits at 24 hrs, 48 hrs, and 72 hrs post-infection with d/922-947. **Results:** We demonstrated that d/922-947 exerts a cytotoxic effect and replicates in MCF7 and MDA-MB231 cells. The treatment with d/922-947 leads to activation of ICD. We observed a strong reduction of ATP intracellular content in both infected BC cell lines, and an increased percentage of CALR positive cells in MDA-MB231. Moreover, we observed increased HMGB1 intracellular content in both MCF7 and MDA-MB231. Finally, we focused on IL-6, VEGF secretion. At 72 hrs post-infection with d/922-947 we observed a strong reduction in IL-6 secretion only in infected MDA-MB231 (no IL-6 detection for MCF7), and a strong reduction of VEGF secretion in both BC infected cells. **Conclusions:** Our data indicate that d/922-947, by reducing cell viability in MCF7 and MDA-MB231 cells and activating ICD pathways, might alter the immunogenicity of cancer cells and induce a potential antitumor immune response. Indeed, the reduction of VEGF and IL-6 secretion suggests an anti-angiogenic activity of d/922-947, thus supporting its potential application as an anticancer agent in BC.

### 09-P84. Small Extracellular Vesicle Release and Their Effects on Recipient Cells Are Mediated by EMMPRIN during Colon Cancer Stem Cell Differentiation

D. Lucchetti<sup>1,2</sup>, F. Colella<sup>1,2</sup>, C. Ricciardi-Tenore<sup>2</sup>, F. Calapà<sup>2</sup>, M.E. Fiori<sup>3</sup>, L. Perelli<sup>2</sup>, R. De Maria<sup>1,2</sup>, A. Sgambato<sup>2,4</sup>

<sup>1</sup>Fondazione Policlinico Universitario A. Gemelli IRCCS, Rome, Italy, <sup>2</sup>Institute of General Pathology, Università Cattolica del Sacro Cuore, Rome, Italy, <sup>3</sup>Department of Oncology and Molecular Medicine, Istituto Superiore di Sanità, Rome, Italy, <sup>4</sup>IRCCS-Referral Cancer Center of Basilicata (CROB), Rionero in Vulture, Italy.

**Introduction:** Cancer stem cells secrete small extracellular vesicles (sEVs) that are involved in the remodeling of the stroma microenvironment and promotion of tumor progression. The sEV molecular key players involved in colon cancer stem cell differentiation are poorly understood. EMMPRIN is a glycoprotein involved in colon cancer tumorigenesis. It has been previously shown that EMMPRIN can be released into the microenvironment by extracellular vesicles. This study aimed to analyze the role and content of sEVs in the differentiation process of colorectal cancer stem cells. **Methods:** sEVs were isolated by ultracentrifugation and characterized by standard methods. We adopted 4 colon cancer stem cells (CSC) isolated by primary tumors of colorectal cancer patients. The CR-CSC are maintained in a serum-free medium supplemented with growth factors and grown in ultra-low attachment multiple plates. The differentiation of CR-CSC was induced by growing the CR-CSC in adhesion condition or adding sodium butyrate. Differentiation process was monitored by phosphatase alkaline assay and confirmed by expression of cancer stem cells markers. NH4Cl and GW4869 were adopted as inhibitors of sEV release. **Results:** We showed that sEV secretion during colon CSC differentiation is partially controlled by EMMPRIN. EMMPRIN expression increased on sEV surface during differentiation of both colon cancer cell lines and CSCs. EMMPRIN knockdown as well as anti-EMMPRIN antibodies impaired sEV release and downstream effects on recipient cells. Moreover, blocking multivesicular body maturation prevented the sEV release during the differentiation and reduced the membrane expression of EMMPRIN on CSC. sEVs positive for EMMPRIN appeared to activate a signaling cascade in cancer recipient cells by the induction of metalloprotease and RhoGTPase expression as well as invasive features in colon cancer cells, and these effects were prevented by the treatment with anti-EMMPRIN antibodies. **Conclusions:** Our findings reveal a function of EMMPRIN in promoting sEV release during the differentiation process of colon cancer stem cells and in triggering cellular changes in other recipient cells. Despite the promising results of this study, further investigations are needed to clarify the role of EMMPRIN in release of sEVs during the differentiation of CSCs.

**09-P85. Performance of Retrospective Screening of Biobank Resection Specimens for Identification of Oncogenic Fusions in Lung Adenocarcinoma**

P. Desmeules, N. Bastien, D. Boudreau, M. Orain, C. Couture, P. Joubert  
IUCPQ-UL, Quebec, QC, Canada.

**Introduction:** Targeted inhibition of kinase fusions in lung cancer has shown several impressive clinical responses, and testing has been integrated in routine molecular testing. Although known and emerging targets are collectively significant, they constitute individual biomarkers for which rarity is challenging individual laboratories to perform robust assay validation.

**Methods:** To identify tumors harboring oncogenic fusions, retrospective screening was performed on formalin-fixed, paraffin-embedded (FFPE) samples from our institutional biobank using tissue microarrays (TMA). Tumor cores from 660 lung adenocarcinomas were collected and used for immunohistochemistry (IHC) screening for ALK, ROS1, RET, and pan-NTRK with laboratory developed protocols. Chromosomal rearrangement was confirmed on either TMA-based or whole tissue slides using break-apart fluorescent *in situ* hybridization (FISH). Selected positive specimens were confirmed with RNA-based next-generation sequencing (NGS) using different assays. **Results:** TMA cores with sufficient tumor content comprised 542 early stage lung adenocarcinomas. The total number of fusion driven tumors found was 17 (3.1%), but was enriched in TMA consisting of non-smokers (7/72; 9.7%). TMA slide-based FISH was useful for confirmation of 5 (0.9%) ROS1 tumors, as ROS1-IHC had expectedly low specificity (80%). ALK (5; 0.9%) and RET (6; 1.1%) positive tumors were also rare but more reliably identified using IHC, whereas only 1 (0.2%) positive NTRK tumor (TPR-NTRK1) was identified. RNA was successfully extracted from selected fresh-frozen banked tumor samples (collected from 2006 to 2010) and used to characterize fusions with NGS, including in 1 ROS1-FISH negative tumor. **Conclusions:** Quick screening of a tumor biobank set using IHC performed on TMAs allowed rapid and cost-effective identification of several rare fusions in lung cancer and can be a useful strategy for collecting samples for assay validation.

**09-P86. CMV Infection Modulates HIF Signaling in Paraganglioma**

F. Verginelli<sup>1</sup>, S. De Fabritiis<sup>2</sup>, S. Vespa<sup>3</sup>, M.R. Pantalone<sup>4</sup>, S. Soliman<sup>5</sup>, P. Lanuti<sup>6</sup>, J. Vitaj<sup>2</sup>, D.L. Esposito<sup>2</sup>, S. Perconti<sup>2</sup>, S. Valentinuzzi<sup>7</sup>, A. Angelini<sup>2</sup>, I. Talucci<sup>1</sup>, F. Schiavi<sup>8</sup>, G. Piras<sup>9</sup>, M. Sanna<sup>9</sup>, L.V. Lotti<sup>3</sup>, C. Söderberg-Nauclér<sup>4</sup>, R. Mariani-Costantini<sup>2</sup>  
<sup>1</sup>G. d'Annunzio' University of Chieti-Pescara, Department of Pharmacy, Chieti, Italy, <sup>2</sup>G. d'Annunzio' University of Chieti-Pescara, Department of Medical, Oral and Biotechnological Sciences, Chieti, Italy, <sup>3</sup>Sapienza' University of Rome, Department of Experimental Medicine, Rome, Italy, <sup>4</sup>Karolinska

Institutet, Department of Medicine, Division of Microbial Pathogenesis, Stockholm, Sweden, <sup>5</sup>Northwestern University Feinberg School of Medicine, Chicago, IL, United States, <sup>6</sup>G. d'Annunzio' University of Chieti-Pescara, Department of Medicine and Aging Sciences, Chieti, Italy, <sup>7</sup>G. d'Annunzio' University of Chieti-Pescara, Chieti, Italy, <sup>8</sup>Veneto Institute of Oncology, IRCCS, Familial Cancer Clinic and Oncoendocrinology, Padua, Italy, <sup>9</sup>Gruppo Otologico, Otolology and Skull Base Unit, Piacenza, Italy.

**Introduction:** Mutations in the SDH genes are frequent in paragangliomas (PGLs) and induce HIF stabilization due to succinate accumulation and inhibition of prolyl hydroxylases. Based on our data showing constitutive CMV infection in PGLs, and on the low penetrance of SDH mutations reported in literature, we hypothesized that CMV might concur to HIF stabilization in these tumors. To this end, we needed to isolate pure CMV particles from PGL samples and to demonstrate infectivity of tumor-derived CMV, and effects on the HIF pathway are underway. To this end, we developed a method based on PEG precipitation to isolate CMV particles from PGL and derived xenografts and compared the effects induced by infection/superinfection with such particles to those obtained using CMV strain VR1814 particles. **Methods:** EM was used to visualize CMV particles in PGLs and derived xenografts. CMV particles were isolated using a modification of the Rous method (1911) coupled with PEG precipitation. Infections/superinfections were performed using either PGL-derived CMV or the CMV strain VR1814. Viral titration was performed with the TCID<sub>50</sub> assay. Transcriptional expression of *HIF* genes was investigated by qRT-PCR. **Results:** We obtained viable and infectious virions from PGLs and derived xenografts, as demonstrated by morphological analyses and TCID<sub>50</sub> assays performed after infection of normal fibroblasts and superinfection of PGL cell cultures. HIFs were constitutively high in PGLs and several derived cultures. Superinfection of PGL cells with the CMV clinical strain VR1814 caused significant HIF2 $\alpha$  overexpression and transcriptional activation of HIF2 $\alpha$ , whereas no effect was observed on HIF1 $\alpha$  and its targets. In contrast, infection of normal fibroblasts showed significant downregulation of HIF2 $\alpha$  with no transcriptional activation and overexpression of HIF1 $\alpha$  targets. **Conclusions:** Our data demonstrate the transmissibility of CMV infection from PGLs to normal fibroblasts and indicate that CMV contributes to overexpression of HIF2 $\alpha$  and its transcriptional targets in PGLs.

### 09-P88. Adipocyte-Released Factors Affect Aggressiveness in Prostate Cancer Cells

E. La Civita, A. Liotti, M. Cennamo, S. Cabaro, D. Liguoro, P. Formisano, F. Beguinot, D. Terracciano  
*Federico II di Napoli, Dipartimento di Scienze Mediche Traslazionali, Napoli, Italy.*

**Introduction:** The prevalence of obesity is increasing at an alarming rate in developed countries. Epidemiologic studies indicate that obesity is an important risk factor for diabetes, cardiovascular disease, and cancer. In particular, obesity is associated with aggressive prostate cancer (PCa). Several molecular mechanisms have been proposed as drivers of this association. Among these, a role might be played by periprostatic adipose tissue (PPAT). Recent studies uncovered that the secretion of mature adipocytes can affect the early stage of PCa progression by promoting the spread of cancer cells outside the prostate gland. However, the molecular mechanisms involved in this crosstalk are still unknown.

**Methods:** Adipose-derived mesenchymal stem cells (Ad-MSCs) were obtained from biopsies of PPAT from patients undergoing radical prostatectomy. Ad-MSCs were differentiated in mature adipocytes and then serum starved to obtain conditioned media (Ad-CM). Two prostate cancer cell lines, PC3 and DU145, were used to assess the effect of Ad-CM on cell viability, migration, and drug response to docetaxel. In addition, levels of IGF-1 were assessed in Ad-CM. **Results:** The treatment for 48 hrs with Ad-CM from PPAT induced the increase of cell viability of PC3 and DU145 cell lines. In addition, adipocyte-released factors (ARFs) from PPAT induced migration of prostate cancer cell line PC3, whereas no effects were observed in DU145. Next, we assessed the effect of Ad-CM on response to docetaxel. PC3 and DU145, pretreated with Ad-CM, showed a reduced response to docetaxel. This effect is accompanied by a higher mRNA and protein expression of genes associated with drug resistance, such as *ABCB1*, *TUBB2B*, and *TUBB4A*. Of note, IGF-1 levels are higher in Ad-CM from patients with more aggressive PCa.

**Conclusions:** ARFs from PPAT, and in particular IGF1 seems to be a good candidate as a mediator of the effect on malignant phenotype of prostatic cancer cells, suggesting that the study of crosstalk between adipocytes and prostate cancer cells may allow the identification of new prognostic biomarkers and pharmacological targets for the treatment of PCa.

### 09-P90. Targeting Local Microbiota by Antibiotic Therapy Promotes Immunosurveillance against Cancer

L. Sfondrini<sup>1</sup>, V. Le Noci<sup>1</sup>, M. Sommariva<sup>1</sup>, F. Bianchi<sup>2</sup>, S. Camelliti<sup>1</sup>, A. Balsari<sup>1,2</sup>, E. Tagliabue<sup>2</sup>

<sup>1</sup>University of Milan, Milan, Italy, <sup>2</sup>Fondazione IRCCS Istituto Nazionale dei Tumori, Milan, Italy.

**Introduction:** Gut microbiota has been demonstrated to influence tumor growth and immunotherapy efficacy. Beyond the gut, many tissues host their own microbiota,

and recent findings highlighted the role of local microbiota in driving immune suppressive cell accumulation. **Methods:** We recently demonstrated that manipulation of pulmonary microbiota by antibiotic or probiotic aerosolization prevents B16 melanoma metastasis implantation by reducing regulatory T cells and promoting T and NK cell activation in the lung. Here, we assessed if the modulation of local microbiota by antibiotics is a strategy to treat metastases and tumors of different histotypes. **Results:** In a therapeutic setting, where treatment is started after tumor injection, manipulation of lung microbiota was effective in reducing the growth of B16 melanoma metastases ( $p = 0.0441$ ), MC38 colon carcinoma metastases ( $p = 0.0311$ ), and the autochthonous Lewis lung carcinoma (LLC1) ( $p = 0.0337$ ). Furthermore, combination of aerosolized antibiotics with immune checkpoint inhibitors resulted in an increased efficacy of these immunotherapeutic drugs in MC38 and LLC1 metastases models. Repeated administration of aerosolized antibiotics also prevented spontaneous lung metastases (in Balb/c mice) transplanted into the mammary gland with 4T1 mammary tumor cells, able to spontaneously metastasize to the lung ( $p = 0.0193$ ). Surprisingly, in this model we observed that Vanco/Neo aerosol also decreased the growth of the primary tumor, and that this effect was associated with a powerful local immune modulation, as indicated by the increased expression of *CD86*, *IFN- $\gamma$* , and *CD69*, of M1 genes, as *IL-12* and *IRF5*, and the reduction of M2 genes, as *STAT6*, *ARG1*, *IL-10*, and *IRF4*, in the mammary tumor tissue. This result suggests that antibiotics, that plausibly gain bloodstream access via pulmonary alveoli might affect the growth of mammary tumors by modulating tumor-associated microbiota and thus the immune microenvironment. **Conclusions:** A significant reduction of 4T1 orthotopically implanted tumor was indeed observed in mice orally treated by ampicillin, an antibiotic able to cross the small intestinal epithelium, but not by oral Vanco/Neo, which are only minimally absorbed in the bloodstream at the intestinal mucosa. Thus, our results suggest that local microbiota associated to tumors influence their growth and that their targeting via antibiotic could be a new strategy to optimize the efficacy of conventional therapies.

### 09-P91. Novel Insights into the Mechanism of Action and Modulation of Microvesicle Release by Nitroxoline in Pancreatic Cancer Cells Using Integrative Proteomic and Functional Analyses

S. Veschi<sup>1</sup>, L. De Lellis<sup>1</sup>, R. Florio<sup>1</sup>, M. Ronci<sup>2,3</sup>, P. Lanuti<sup>3,4</sup>, F. Brugnoli<sup>5</sup>, V. Bertagnolo<sup>5</sup>, M. Marchisio<sup>3,4</sup>, A. Cama<sup>1,3</sup>

<sup>1</sup>G. d'Annunzio University of Chieti-Pescara, Department of Pharmacy, Chieti, Italy, <sup>2</sup>G. d'Annunzio University of Chieti-Pescara, Department of Medical, Oral and Biotechnological Sciences, Chieti, Italy, <sup>3</sup>G. d'Annunzio University of Chieti-Pescara, Centre on Aging Sciences and Translational Medicine (Ce.S.I-Me.T), Chieti, Italy, <sup>4</sup>G. d'Annunzio University of Chieti-Pescara, Department

of Medicine and Aging Sciences, Chieti, Italy, <sup>5</sup>University of Ferrara, Section of Anatomy and Histology, Department of Morphology, Surgery and Experimental Medicine, Ferrara, Italy.

**Introduction:** Pancreatic cancer (PC) is a highly aggressive malignancy with low survival rates. The poor clinical outcome of PC is related to early local spread, high trend of distant metastasis, and resistance to traditional chemotherapies. Consequently, new therapeutic options for this lethal disease are urgently needed. We recently identified nitroxoline as a repurposed drug candidate in PC showing a dose-dependent antiproliferative activity in different PC cell lines. **Methods:** We analyzed the effect of nitroxoline using an unbiased shotgun proteomic approach in AsPC-1, a metastatic gemcitabine-resistant PC cell line. Functional validation of proteomic results was performed by Western blot, flow cytometry analyses of mitochondrial polarization, ROS production and microvesicle release in culture media, analysis of cell growth and xCELLigence system real-time analysis of cell migration and invasion. **Results:** Proteomic analysis identified 363 proteins affected by nitroxoline treatment in AsPC-1. Among these proteins, 81 were consistently deregulated at both 24- and 48-hour treatment, and were interconnected in a single highly enriched network of protein-protein interactions. Integrative proteomic and functional analyses revealed nitroxoline-induced modulation of novel targets, which associated with drastic impairment in cell growth, migration, invasion, increased ROS production, induction of DNA damage response and mitochondrial depolarization due to hampered cell bioenergetics. Interestingly, STRING revealed that "extracellular exosome" (GO:0070062) was among the top deregulated protein categories, with 44 exosomal proteins showing expression shifts after nitroxoline treatment of AsPC-1 cells (FDR  $9.62 \times 10^{-17}$ ). In line with this finding, flow cytometry indicated that extracellular vesicle release was increased in response to the drug in a time-dependent manner. **Conclusions:** This study provides novel insight into the mechanisms of nitroxoline action, showing that the drug modulates multiple biological targets crucial in cancer biology and previously unknown to be affected by nitroxoline. The drug affected the levels of exosomal proteins in AsPC-1 cells and the release of microvesicles in culture media. Currently, we are investigating whether the molecular composition of exosomes is modulated by nitroxoline in PC cell cultures, which might be relevant for PC cancer therapy.

#### 09-P94. The Effect of *C. orbiculata* in Splicing Modulation and Apoptosis Induction on Cancer Cells

Z. Dlamini<sup>1</sup>, D. Bates<sup>2</sup>, K. Yacqub-Usman<sup>2</sup>, Z. Blackley<sup>2</sup>, T. Makhafola<sup>1</sup>

<sup>1</sup>University of Pretoria, Pan African Cancer Research Institute, Pretoria, South Africa, <sup>2</sup>University of Nottingham, Center for Cancer Sciences, Nottingham, United Kingdom.

**Introduction:** Recent advances in research have revealed that abnormality in alternative splicing can be linked to various genetic diseases and also play a role in carcinogenesis. Therefore, targeting alternative splicing in cancer could offer novel effective cancer therapies. The aim of this study was to investigate the effects of a medicinal plant, *Cotyledon orbiculata*, on alternatively spliced genes in cancer cells. **Methods:** The effects of *C. orbiculata* on cell proliferation of colon (HCT116), oesophageal (OE33 and KYSE70), and cervical (CASKI and C33A) cancer cell lines were evaluated using a WST-1 assay. The effects of this plant on splicing of hnRNPA2B1 and BCLx, detected using RT-PCR, and apoptosis induction via caspase-3-cleavage were also investigated. **Results:** Results showed that *C. orbiculata* dose dependently decreased viability and also modulated splicing of hnRNPA2B1 and BCLx, resulting in a decrease in hnRNPA2B1 splice variant and an increase in BCLx splice variant in all 5 cancer cell lines. Additionally, *C. orbiculata* resulted in an increase in caspase-3 cleavage, indicating an apoptosis induction. SiRNA knockdown of hnRNPA2B1 in HCT116 was specifically used to assess its functional role in cell proliferation and apoptosis. Results showed that the cells had decreased viability and increased caspase-3 cleavage. **Conclusions:** The study showed that, in part, modulating hnRNPA2B1 splicing could be responsible for regulating the balance between pro-/anti-apoptotic splice variants, e.g., BCLx<sub>l/s</sub>, resulting in apoptosis induction in colon cancer cells treated with *C. orbiculata*.

#### 09-P95. Oncogenic Role of the Aminopeptidase ERAP1 in Hedgehog-Dependent Cancer

M. Caimano<sup>1</sup>, F. Bufalieri<sup>1</sup>, P. Infante<sup>2</sup>, F. Bernardi<sup>1</sup>, L. Lospinoso Severini<sup>1</sup>, M. Moretti<sup>1</sup>, A. Peschiaroli<sup>3</sup>, G. Giannini<sup>1</sup>, S. Pazzaglia<sup>4</sup>, G. Melino<sup>5</sup>, F. Locatelli<sup>6,7</sup>, O. Ayrault<sup>8</sup>, D. Fruci<sup>7</sup>, L. Di Marcotullio<sup>1,9</sup>

<sup>1</sup>Sapienza - University of Rome, Department of Molecular Medicine, Rome, Italy, <sup>2</sup>Center for Life Nano Science at Sapienza, Istituto Italiano di Tecnologia, Rome, Italy, <sup>3</sup>National Research Council of Italy, Institute of Translational Pharmacology, Rome, Italy, <sup>4</sup>Italian National Agency for New Technologies, Energy and Sustainable Economic Development (ENEA), Laboratory of Biomedical Technologies, Rome, Italy, <sup>5</sup>University of Roma 'Tor Vergata', Department of Medicina Sperimentale e Chirurgia, Rome, Italy, <sup>6</sup>Sapienza - University of Rome, Department of Pediatrics, Rome, Italy, <sup>7</sup>Ospedale Pediatrico Bambino Gesù, IRCCS, Department of Paediatric Haematology/Oncology,

Rome, Italy, <sup>8</sup>Institut Curie, PSL Research University, CNRS UMR, INSERM, Orsay, France, <sup>9</sup>Sapienza - University of Rome, Istituto Pasteur-Fondazione Cenci Bolognetti, Rome, Italy.

**Introduction:** The Hedgehog (Hh) pathway is essential for embryonic development and tissue homeostasis, and its aberrant activation causes several human cancers, including medulloblastoma (MB), the most common brain malignancy in childhood. Because of the crucial role of the Hh pathway in tumorigenesis, better knowledge is mandatory for developing innovative anti-cancer approaches. Here, we identify endoplasmic reticulum aminopeptidase 1 (ERAP1), a key regulator of innate and adaptive antitumor immune responses, as a previously unknown player in the Hh signaling pathway. **Methods:** We evaluated the effect of ERAP1 inhibition on Hh signalling activity by functional transcription assay. Subsequently, we clarified the mechanisms by which ERAP1 exerts its positive role on Hh pathway through co-immunoprecipitation (Co-IP) and ubiquitylation assays. Finally, proof-of-concept *in vivo* studies (allograft/xenograft/orthotopic models) were performed in NOD/SCID gamma (NSG) mice grafted with spontaneous primary mouse or human Hh-MB cells (PDX) and then treated with a known ERAP1 inhibitor, Leu-SH, or with primary mouse Hh-MB infected with lentiviral vectors expressing shRNA that selectively target ERAP1. **Results:** We demonstrated that ERAP1 binds the deubiquitylase enzyme USP47, displaces the USP47-associated  $\beta$ TrCP, the substrate-receptor subunit of the SCF $^{\beta$ TrCP ubiquitin ligase, and promotes  $\beta$ TrCP degradation. These events result in the modulation of Gli transcription factors, the final effectors of the Hh pathway, and the enhancement of Hh activity. Remarkably, genetic or pharmacological inhibition of ERAP1 suppresses Hh-dependent tumor growth *in vitro* and *in vivo*. Of note, the pharmacological inhibition of ERAP1 leads to a significant increase of survival in Math1-cre/Ptc<sup>C/C</sup> mice, which spontaneously develop MB. **Conclusions:** Our findings unveil an unexpected role for ERAP1 in cancer development and could open innovative perspectives for effective therapeutic strategies in the treatment of Hh-driven cancers.

#### 09-P96. Leptin Promotes Glioblastoma Progression through Notch Signaling Activation

S. Panza, L. Gelsomino, U. Russo, I. Barone, C. Giordano, R. Malivindi, S. Catalano, S. Andò  
University of Calabria, Rende, Italy.

**Introduction:** Glioblastoma multiforme (GBM) is the most malignant form of glioma causing 3%-4% of all cancer-related deaths. Specific cancer treatments for GBM include surgery, radiotherapy, and chemotherapy with temozolomide. However, despite the continuous development of new clinical therapies, the prognosis and survival of GBM patients remain dismal. Lack of success in treating glioblastoma may likely arise from tumor heterogeneity and treatment resistance of glioblastoma

stem cells (GSCs), a population of cancer stem cells with an extraordinary capacity to promote tumor growth and invasion, and be resistant to radiotherapy and chemotherapy. Different studies have reported a link between obesity and cancer risk that relies on important mediators, such as leptin. Leptin is an adipocyte-derived hormone that can interact with different signaling molecules, including Notch, to affect the risk, progression, recurrence, and mortality of certain cancers. Notch signaling is an evolutionarily conserved pathway regulating several biological processes, such as cell proliferation, migration, differentiation, and stem activity. Thus, we wondered whether leptin and Notch may crosstalk to influence GBM progression. **Methods:** The role of the Leptin-Notch axis in GBM progression has been assessed by RT-PCR, immunofluorescence, immunoblotting, transient transfection assays, cell proliferation assay, Boyden chamber migration and invasion assays, flow cytometry analysis, neurosphere formation in 2 GBM cells (U87-MG and T98G) upon exposure to leptin, the full leptin receptor antagonist LDFI and the Notch inhibitor GSI. **Results:** mRNA and protein expression of leptin and its receptor were significantly higher in GBM cells than in normal astroglia cells, SVG p12. In line with these results, leptin stimulation was significantly associated with an enhanced activation of its downstream effectors, and an increased proliferation and migration of glioblastoma cells. Moreover, leptin treatment resulted in a significant increase of tumorsphere formation and GSC marker levels (CD133, Nestin, SOX2, GFAP), along with a higher expression of Notch receptors, ligands, and targeted molecules (Notch1-4, Survivin, and Hes-1). Leptin-induced effects on U87-MG and T98G cell lines and tumorspheres were reversed by the peptide LDFI or GSI. **Conclusions:** Current data demonstrate that leptin is an important factor involved in GBM proliferation, migration, and expansion of GSC populations. This occurs via leptin-induced upstream activation of the Notch signaling pathway, suggesting how targeting leptin-Notch crosstalk could be a potential novel strategy for GBM therapy, especially in obese patients.

#### Selected Other Abstracts

#### 10-P01. Validation of a Next-Generation Sequencing Assay for the Detection of IGHV Somatic Hypermutations in Chronic Lymphocytic Leukemia

C. Nakad, L. Hamadeh, R. Abdul-Kahlil, R. Mahfouz  
American University of Beirut Medical Center,  
Department of Pathology and Laboratory Medicine,  
Beirut, Lebanon.

**Introduction:** Chronic lymphocytic leukemia (CLL) is thought to originate from malignant transformation of single lymphoid cells that may share clonal antigen receptor rearrangements that are tumor specific. Functional antibody genes are assembled by V-D-J joining and then diversified by a process called somatic

hypermutation (SHM). This hypermutation increases the affinity of immunoglobulin molecules by introducing mutations in the variable regions of immunoglobulin genes. The mutational status of *IGHV* genes for patients with CLL is one of the most important molecular markers in providing important prognostic information about duration of response and overall survival with chemoimmunotherapy. The gold standard method used to determine SHM status requires 2 steps: a polymerase chain reaction (PCR) followed by capillary electrophoresis (CE). We aim to determine whether detecting SHM using next-generation sequencing (NGS) might lead to more accurate results compared to traditional methods. **Methods:** Twenty-one samples were tested for SHM status using the Invivoscribe LymphoTrack *IGHV* Leader Somatic Hypermutation Assay, which detects the majority of *IGH* gene rearrangements using a single multiplex master mix, and identifies the DNA sequence specific for each clonal gene rearrangement. This assay aids in the detection of initial clonal populations, identifies sequence information to track these clones in subsequent samples, and provides information on the degree of SHM. **Results:** Seventeen samples had the same result as the traditional method. Whereas 4 showed discrepancies in allele annotations, 2 samples exhibited a full match in the V and D alleles but a difference in the J allele: *IGHJ4\*03* and *IGHJ4\*02* were reported using CE compared to *IGHJ6\*02* and *IGHJ5\*02* using NGS, respectively. Annotation of sequences generated by CE in 1 specimen detected the *IGHV3-7\*0* allele, whereas *IGHV3-7\*03* was reported by NGS. Similarly, *IGHV2-5\*02* was reported in 1 sample by CE compared to *IGHV2-5\*01* using NGS. On the other hand, our results showed full concordance in the mutation rates of mutated versus unmutated specimens. After comparing the sequences generated by NGS to germline *IGH* sequences using *IMGT/V-Quest* and *IgBlast*, we determined that the level of allele mismatch is minimal between discordant results. **Conclusions:** Detecting SHM using NGS proves to be a fast, sensitive, and cost-effective procedure compared to CE.

#### 10-P02. Depressive Symptoms and Proprotein Convertase Subtilisin/Kexin Type 9

C. Macchi, M. Buoli, C. Favero, A. Pesatori, L. Vigna, A. Corsini, C. Sirtori, V. Bollati, M. Ruscica  
*Università degli Studi di Milano, Milan, Italy.*

**Introduction:** Among less frequently evaluated clinical conditions linked to the cardiovascular (CV) risk, anxiety and depression are highly prevalent. Epidemiological evidence strongly suggests an association between obesity and depressive mood. Proprotein convertase subtilisin/kexin 9 (PCSK9), regulating the trafficking of low-density lipoprotein receptors, may also play a role in CV diseases. The current study was aimed at verifying whether, in a population of obese subjects, depression could impact

on PCSK9 levels and on their association with the Framingham risk score (FRS), a well-established predictor of CV risk. **Methods:** A total of 310 obese subjects were selected among participants of the cross-sectional SPHERE (Susceptibility to Particle Health Effects, miRNAs and Exosomes) study. BMI was between 25 and 30 kg/m<sup>2</sup> or  $\geq 30$  kg/m<sup>2</sup>. Depression symptoms were evaluated according to the Beck Depression Inventory II (BDI-II). Univariate and multivariable linear regression models were used to test the relation between circulating PCSK9 levels and BDI-II score. The best models selected to predict these associations were adjusted for age, gender, BMI, smoking habit, non-HDL-C, triglycerides (TG), HOMA-IR, and use of statins and antihypertensives. A linear regression model was also applied to verify the association between FRS and circulating PCSK9 levels, adjusted for BDI-II and BMI. **Results:** Participants were moderately hyperlipidemic with mean values of LDL-C and non-HDL-C of  $133.1 \pm 33.9$  mg/dL and  $155.8 \pm 38.8$  mg/dL, respectively. HDL-C and TG levels were in the normal range ( $58.3 \pm 14.4$  mg/dL and  $118.6 \pm 78.9$  mg/dL, respectively), as for glycemias and glycated hemoglobin. PCSK9 levels were normally distributed and significantly associated with BDI-II. In individuals with a BDI-II  $<20$ , the association was positive and statistically significant. For every unit increase of BDI-II, there was an increment of 1.57 ng/mL of PCSK9 levels ( $\beta = 1.57$ , SE = 0.80,  $p = 0.049$ ); the opposite was found in individuals with a severe depression, i.e., BDI-II  $>20$  ( $\beta = -5.26$ , SE = 1.95). PCSK9 concentrations rose in a stepwise manner from the minimal depressive group (252 ng/mL; 95% CI 243; 262) to the mildly (264 ng/mL; 95% CI 239; 288) and moderately depressed (276 ng/mL; 95% CI 248; 304). The severe depressive group had lower PCSK9 levels compared to the others (182 ng/mL; 95% CI 125; 240). Multivariable linear regression analysis showed a 20% rise in FRS for every 100 ng/mL increase in PCSK9 levels ( $\Delta\% = 20.69$ , 95%CI: 5.60-35.81,  $p = 0.004$ ), independent of BDI-II score and BMI, both not associated with FRS. **Conclusions:** In obese subjects, PCSK9 levels rose in a stepwise manner up to a certain severity of mood symptoms and remained an independent predictor of CV risk, as assessed by the FRS.

#### 10-P03. MCT1 Lactate Transporter Plays a Crucial Role in T Lymphocyte Fate during Obesity

C. Macchi, A. Moregola, M.F. Greco, F. Bonacina, D. Norata, M. Ruscica  
*Università degli Studi di Milano, Milan, Italy.*

**Introduction:** Recent studies have shed light on the interconnection between metabolism and immunity in multicellular organisms and their functional coordination for an effective establishment and resolution of immune responses. Imbalance of this delicate signaling network might lead to non-resolving inflammation and consequently to the development of

obesity-associated chronic inflammation (ObCI). T lymphocytes (T cells) accumulate in the adipose tissue during obesity, and their activation leads to a switch in their metabolism from oxidative phosphorylation to aerobic glycolysis, which involves the production of elevated amounts of lactate. MCT1 is a lactate transporter expressed in different types of cells, including T lymphocytes. The aim of this project is to investigate the relevance of T cell lactate transport by MCT1, in the context of adipose tissue inflammation during obesity. **Methods:** MCT1<sup>fl/fl</sup> CD4-cre mice, with specific deletion of MCT1 in both CD4+ and CD8+ T lymphocytes, and MCT1<sup>fl/fl</sup> littermates were generated and fed with a high-fat diet (HFD; 45% Kcal from fat) for 20 weeks. Body weight was measured weekly; glucose metabolism (glucose-tolerance test (GTT) and insulin-tolerance test (ITT)) was checked at 10 and 20 weeks. Immunophenotyping of different tissues (blood, lymph nodes, adipose, and thymus) was performed at 20 weeks by flow cytometry. **Results:** T cell activation results in the increase of MCT1 expression in both human and mouse T lymphocytes. Following high-fat diet feeding, MCT1<sup>fl/fl</sup> CD4-cre mice, in spite of a similar weight gain and insulin response compared to MCT1<sup>fl/fl</sup>, present a decreased visceral (VAT) and subcutaneous (SCAT) fat accumulation. Moreover, MCT1 deficiency in T cells results in a reduction of CD8+ T lymphocyte number in visceral and subcutaneous adipose tissue (VAT MCT1<sup>fl/fl</sup> mice 48,098 cells/g  $\pm$  36,587, MCT1<sup>fl/fl</sup>CD4-cre 18,497 cells/g  $\pm$  14,508,  $p < 0.05$ ; SCAT MCT1<sup>fl/fl</sup> 2,738 cells/g  $\pm$  1,189, MCT1<sup>fl/fl</sup> CD4-cre 1,669 cells/g  $\pm$  684,  $p < 0.05$ ); this profile was associated with different T cell subset distributions (T effector memory (Tem) CD8+ VAT: MCT1<sup>fl/fl</sup> 84.20%  $\pm$  5.72; MCT1<sup>fl/fl</sup>CD4-cre 57.29  $\pm$  8,  $p < 0.001$ ; Tem CD8+ SCAT: MCT1<sup>fl/fl</sup> 72.2%  $\pm$  14.16, MCT1<sup>fl/fl</sup> CD4-cre 44.93%  $\pm$  14.25,  $p < 0.001$ ), but with a similar number of innate immune cells (monocyte and macrophages) infiltrating adipose depots. The difference in T cells was not the consequence of increased T cell death in MCT1<sup>fl/fl</sup> CD4-cre mice. **Conclusions:** Our data suggest that MCT1 transporter impacts T lymphocyte activation — in particular, CD8+ T lymphocytes during obesity — independently from systemic metabolism. Whether this difference can affect adipose tissue inflammation during obesity is under investigation.

#### 10-P04. Digital Droplet PCR cfDNA Testing Report: Copies/ml Plasma versus Variant Allele Frequency

J. Puskas, D. Qin

Moffitt Cancer Center, Tampa, FL, United States.

**Introduction:** Digital droplet PCR (ddPCR) has been used for cell-free DNA (cfDNA) testing and is able to quantitate the copy numbers of mutant and wild-type alleles. The test results are usually expressed as positive or negative. When positive, the copies/ml of plasma or variant allele frequency (VAF) is used for quantitation. Which unit is better to report ddPCR test results? **Methods:** cfDNA extraction from plasma was

done using the QIAGEN QIAamp Circulating Nucleic Acid kit (cat. #55114) according to the manufacturer-suggested protocol. A total of 50 ng of cfDNA was used with the 20x Bio-Rad BRAF V600E ddPCR (FAM + HEX) probe assay according to the manufacturer's protocol. Droplets were created by loading the plate on the Bio-Rad Automated Droplet Generator, and amplification was carried out on the Bio-Rad C1000 thermocycler. The plate was placed on the QX200 reader and analyzed using QuantaSoft software.

**Results:** 1) Fifty-seven samples were tested for the BRAF V600E mutation (Table 1). Among them, 17 were positive. The correlation coefficient between the results in copies/ml plasma and in VAF was 0.4335. 2) One case had been tested 8 times with 7 times of positive results during a 5-month period. The results in copies/ml plasma are: 10,028.3, 623.9, 91.2, 0.5, 0.63, 101.1, 659.1, and 2,749.4. The results in VAF are: 32.4%, 19.9%, 12.4%, n/a, 2.74%, 31.4%, 35.7%, and 42.4% (Table 2). 3) The WBC counts corresponding to each above-mentioned mutant measurement are recorded: ( $\times 10^9/L$ ) 20.18, 14.01, 11.49, 5.71 5.40, 7.26, 10.69, and 9.65 (Table 2). **Conclusions:** 1) The absolute quantitation (copies/ml plasma) results do not correlate well with relative quantitation (VAF) results. The correlation coefficient between the results in copies/ml plasma and in VAF was 0.4335. 2) The absolute quantitation offers a wider window for the dynamic range of change (up to 15,917 times from the data of this case), whereas the relative quantitation can only have a maximal range of 100 times by design (up to 16 times from the data of this case). The relative quantitation results are affected by both the amount of mutant and wild-type. In this case, the higher WBC may contribute more wild-type alleles, which will render a lower VAF. For example, one result of this case is 10,028.3 copies/ml plasma with a corresponding VAF of 32.4% and a WBC of  $20.18 \times 10^9/L$ . The other result of this case has a lower copy number (2,749.4 copies/ml plasma), but with a higher VAF (42.4%) and a lower WBC ( $9.65 \times 10^9/L$ ). The higher WBC counts in the first test may have contributed more wild-type alleles and play a role in reducing the VAF. In conclusion, it may be better to report ddPCR cfDNA results using the absolute quantitation: copies/ml plasma.

Samples	copies/ml plasma	VAF (%)	BRAF Status
15	0.25	1.71	Detected
36	0.46	1.81	Detected
13	0.63	2.74	Detected
53	0.84	10.3	Detected
44	1	1.48	Detected
21	1.32	2.62	Detected
55	1.41	14.1	Detected
28	3.1	4.5	Detected
12	14.5	28.5	Detected
33	38.13	26.4	Detected
3	91.2	12.4	Detected
17	101.1	31.4	Detected
2	623.9	19.9	Detected
19	659.1	35.7	Detected
11	1107.6	36.4	Detected
23	2749.4	42.4	Detected
1	10028.3	32.4	Detected

[Table 1]

Date	copies/ml plasma	VAF (%)	WBC ( $\times 10^9/L$ )
1/8/2019	10028.3	32.4	20.18
1/14/2019	623.9	19.9	14.01
1/16/2019	91.2	12.4	11.49
3/5/2019	0.63	2.74	5.4
4/2/2019	101.1	31.4	7.26
4/12/2019	659.1	35.7	10.69
5/1/2019	2749.4	42.4	9.65

[Table 2]

#### 10-P06. Role of Co-Stimulatory Signals Mediated by ICOS-ICOSL Dyad in the Evolution of Non-Alcoholic Steatohepatitis (NASH)

S. Sutti<sup>1</sup>, N.N. Ramavath<sup>1</sup>, L.L. Gadipudi<sup>1</sup>, C. Bozzola<sup>1</sup>, N. Clemente<sup>1</sup>, L.C. Gigliotti<sup>1</sup>, E. Boggio<sup>1</sup>, E. Novo<sup>2</sup>, M. Parola<sup>2</sup>, U. Dianzani<sup>1</sup>, E. Albano<sup>1</sup>

<sup>1</sup>University of East Piedmont, Dept. Health Sciences, Novara, Italy, <sup>2</sup>University of Turin, Dept. Clinical and Biological Sciences, Torino, Italy.

**Introduction:** Growing evidence indicates a role of adaptive immunity in sustaining hepatic inflammation during the evolution of non-alcoholic steatohepatitis (NASH). However, the signals regulating B and T lymphocyte responses are still poorly characterized. The inducible T cell co-stimulator (ICOS) and its ligand ICOSL (B7h) are members of the B7/CD28 family and play multiple roles in immunity by regulating T cell activation/survival and antibody production. In this study we have investigated the possible involvement of the ICOS-ICOSL dyad in NASH evolution. **Methods:** ICOS and ICOSL were investigated in an experimental model of NASH based on mice feeding with choline-deficient amino acid sufficient (CDAA) or choline/methionine deficient (MCD) diets as well as in the sera of 40 NASH patients. **Results:** Soluble ICOS and ICOSL were significantly increased in the sera of NASH patients, and soluble ICOSL positively correlated with the titres of IgG against oxidative stress derived antigens (OSE). In different animal models of NASH, the liver expression of ICOS was down-

modulated, whereas that for ICOSL increased in a time-dependent manner in parallel with the development of anti-OSE B and T cell activation and NASH progression to fibrosis. Mice deficient for ICOSL that were receiving the MCD diet for 6 weeks had milder hepatic damage than wild-type animals, which associated with a reduction in B and T cell responses and macrophage M1 activation. Furthermore, the lack of ICOSL almost completely prevented the development of fibrosis as evaluated by collagen Sirius Red staining, and by the detection of activated myofibroblasts. This effect was independent from the modulation of TGF- $\beta$  but depended instead on the lowering of osteopontin production by hepatic macrophages. **Conclusions:** Altogether, these data indicate that not only ICOS-ICOSL dyad play a role in modulating adaptive immunity during NASH evolution, but also directly influences pro-fibrogenic mechanisms, suggesting these co-stimulatory molecules as a possible target for therapeutic interventions. This work was supported by the grant 2017/0535 from the Fondazione Cariplo (Milan, Italy).

#### 10-P07. Development of a Genomic Medicine Platform for Systematic Use of Heterogeneous Biomedical Databases

Z. Kim, J.H. Kim

Seoul National University, Division of Biomedical Informatics, Seoul, Republic of Korea.

**Introduction:** The advance of technology for biomedical research has promoted the increase of volume and quality of corresponding databases. It is essential to use the various databases for the interpretation of genomic variants. To make systematic use of and to present a common interface for the heterogeneous databases as well as those to be introduced in the near future, we developed a platform that accepts genomic variants, identifies matched information from the registered databases, and generates a result report, which will streamline clinical genomic sequence study from laboratory physicians to clinicians. **Methods:** For the pilot phase, we first locally integrated public biomedical databases for robust and sophisticated searches, as well as reduced network communication cost. The entity of the databases was classified into 6 sections, which are variant, gene, protein, transcript, pathway, and phenotype sections. We then devised a common interface for systematic searching of required information regardless of the heterogeneity of each database. For a user interface, a web service environment is provided. **Results:** We integrated parts of NCBI, Ensembl, UCSC Genome browser, UniProtKB, KEGG, OMIM, PharmGKB, and GWAS Catalog biomedical databases. In the developed user interface, the user uploads a VCF file containing variant information, executes the platform with analysis options, and gets a PDF file as a results report, which contains variants with interpretation using ACMG/AMP guidelines as well as referential medical

information. The developed platform is being used for the interpretation of genomic variants of the patients in the hereditary retinal dystrophy germline variant interpretation project. **Conclusions:** The authors developed a platform that accepts genomic variants, looks up matched information from locally integrated heterogeneous biomedical databases, and generates a report interpreting the variants. This process streamlines the work from whole exome sequencing variant identification to diagnosis reports for clinicians. This favorable outcome encouraged us to advance the current platform to accelerate our mission to assist the analysis of NGS-based sequencing results. We hope this system will cause positive feedback between genomic science and genomic medicine.

#### 10-P08. Changing Gears - FFPE Tissue Specimens Reaching High(Er) Quality for Molecular Analyses

E. Kniess<sup>1</sup>, M. Kunz<sup>1</sup>, A. Gaa<sup>1</sup>, S. Glatzel<sup>1</sup>, X. Ungefug<sup>1</sup>, M. Werner<sup>1,2</sup>, S. Laßmann<sup>1,2</sup>

<sup>1</sup>Institute for Surgical Pathology, Medical Center Freiburg, Freiburg, Germany, <sup>2</sup>German Cancer Consortium, Partner Site Freiburg, Freiburg, Germany.

**Introduction:** Formalin-fixed, paraffin-embedded (FFPE) tissue specimens undergo numerous processing steps considered to affect molecular analyses, such as cross-linking and fragmentation of nucleic acids. These pre-analytical caveats are still a given fact for assay design and protocols in molecular diagnostics as well as in (core facility) research and development. Here, we examined whether or not FFPE tissue specimens nowadays actually reach high(er) DNA quality as supposed. **Methods:** This technical study included n = 88 unselected tissue specimens from routine molecular diagnostic entries (2015-2019). Internal and external/referral tissue specimens (n = 22 biopsies, n = 17 bone marrow biopsies, n = 49 resections). As a reference, n = 5 blood samples, n = 1 cytology smear, and n = 1 cell line were included. DNA extraction was according to routine diagnostic procedures. DNA quantity was assessed by a fluorescence-based approach (Qubit), and DNA quality was evaluated by 1) DIN values, and 2) the most frequent highest-size fragment reached per sample (both TapeStation), as well as by 3) PCR analyses covering 268 bp, 536 bp, 941 bp, and 1,253 bp of the  $\beta$ -globin gene. **Results:** The DNA quantity of FFPE tissue samples was variable (0.6 ng/ $\mu$ l to >600 ng/ $\mu$ l), as expected from the tissue specimen size and respective tumor cell content for microdissection. The DNA quantity of blood/cytology smear samples was 21 ng/ $\mu$ l to above assay limit. The cell line yielded 120 ng/ $\mu$ l of DNA. The DNA quality of FFPE tissue samples ranged from DIN 1.8 to 7.2, as compared to DIN 6.9 to 9.5 and of 9.2 in blood/cytology smear and cell line DNA samples, respectively. Accordingly, the most frequent highest-size fragment reached in FFPE tissue DNA samples ranged from 516 bp to 22,525 bp, whereas this was 22,500 bp to >60,000 bp for

blood/cytology smear DNA samples and 54,613 bp for the cell line DNA. Importantly, and quite in contrast to previous reports, FFPE tissue DNA samples were amplifiable for not only a small  $\beta$ -globin PCR product size of 268 bp in 99% (78/79), but also for larger  $\beta$ -globin PCR product sizes of 536 bp in 95% (75/79), 941 bp in 50% (40/79), and even 1,253 bp in 41% (32/79). For the 6 blood/cytology smear and cell line DNA samples, this was 100%. Therefore, the DIN value of FFPE tissue samples was not directly predictive for being able to amplify by PCR, albeit few DNA samples with a DIN of <4 yielded  $\beta$ -globin PCR product sizes of 941 bp and 1,253 bp. **Conclusions:** This study clearly demonstrates that FFPE tissue specimen processing nowadays indeed yields high(er)-quality nucleic acids for further molecular analyses, as generally expected. Rethinking of assay design and protocols, for example, library preparation for NGS, is hence a novel opportunity to broaden applications in molecular pathology.

#### 10-P09. Human Retinal ARPE-19 Cells Cultured Onboard the International Space Station Undergo Marked Cytoskeleton Injuries and Whole Transcriptome Alterations

M. Lulli<sup>1</sup>, F. Cialdai<sup>2</sup>, D. Bolognini<sup>3</sup>, L. Vignali<sup>2</sup>, N. Iannotti<sup>4</sup>, S. Cacchione<sup>5</sup>, M. Balsamo<sup>6</sup>, M. Vukich<sup>6</sup>, G. Neri<sup>6</sup>, A. Donati<sup>6</sup>, A. Magi<sup>7</sup>, M. Monici<sup>2</sup>, S. Capaccioli<sup>1</sup>

<sup>1</sup>University of Firenze, Experimental and Clinical Biomedical Sciences 'Mario Serio', Firenze, Italy, <sup>2</sup>ASAcampus Joint Laboratory, Firenze, Italy, <sup>3</sup>University of Firenze, Department of Experimental and Clinical Medicine, Firenze, Italy, <sup>4</sup>University of Siena, Department of Life Sciences, Siena, Italy, <sup>5</sup>University of Roma 'La Sapienza', Department of Biology and Biotechnology "Charles Darwin", Roma, Italy, <sup>6</sup>Kayser Italia srl, Livorno, Italy, <sup>7</sup>University of Firenze, Department of Information Engineering, Firenze, Italy.

**Introduction:** Cells, tissues, and organs of astronauts aboard the International Space Station (ISS) are exposed to the damaging effects of microgravity and cosmic radiation. The eye, and especially the retina, is one of the most critical and sensitive districts of the astronaut organism. We aimed to disclose the effects of the combination of cosmic radiation and microgravity on human retinal pigment epithelial cells (ARPE-19 cell line), exploiting an experiment onboard the ISS.

**Methods:** The experiment has been primed at the Kennedy Space Center (FL, US) inside specific hardware developed by Kayser Italia, launched to the ISS through the SpaceX-12 vehicle, integrated in the Kubik incubator of ESA, and returned to the Earth in the same vehicle. Ground controls have been obtained by subjecting cultured cells to the same experimental conditions of cells onboard the ISS. Evaluation of cell proliferation, apoptosis, and cytoskeleton organization, and analysis of whole transcriptome via next-generation sequencing (NGS) have been performed.

**Results:** Although the ISS environment did not cause

evident inhibition of proliferation or induction of apoptosis of ARPE-19 cells, it determined severe alterations of cytoskeleton and transcriptomic profile, highlighting its impact on cellular and molecular behavior. In particular, we disclosed an increased vimentin localization to the perinuclear area with a concomitant retraction from the cell borders, underlining the collapse of the vimentin intermediate filament network in ARPE-19 cells cultured onboard the ISS. Moreover, we identified a panel of differentially expressed genes in cells cultured onboard the ISS with respect to ground controls, whose bioinformatics analysis revealed their impact on several cellular pathways, in particular, metabolic pathways, N-Glycan biosynthesis, and protein processing in the endoplasmic reticulum, p53 signalling pathway, mitophagy, cell adhesion molecules, focal adhesion, cellular senescence, and TGF-beta signalling.

**Conclusions:** The results obtained revealed that space environment determines severe alterations on cytoskeleton structure and transcriptome profile on human retinal pigmented epithelial cells. This research has been supported by the Agenzia Spaziale Italiana (Contract Number 2016-6-U.0 (CORM), PI Matteo Lulli). ASI has coordinated the program and has provided the access to the ISS and to the onboard resources, thanks to the Memorandum of Understanding between ASI and NASA for the design, development, operation, and utilization of 3 mini-pressurized logistic modules for the International Space Station.

#### 10-P10. Comparison of Different Methods of Tumor Cellularity Assessment in a Pediatric Cancer Cohort

S. Koo<sup>1,2</sup>, K. Schieffer<sup>3</sup>, S. Lahaye<sup>3</sup>, G. Wheeler<sup>3</sup>, B. Kelly<sup>3</sup>, V. Magrini<sup>3,4</sup>, P. White<sup>3,4</sup>, R. Wilson<sup>3,4</sup>, E. Mardis<sup>3,4</sup>, C. Cottrell<sup>2,3,4</sup>

<sup>1</sup>Nationwide Children's Hospital, Department of Pathology, Columbus, OH, United States, <sup>2</sup>The Ohio State University, Department of Pathology, Columbus, OH, United States, <sup>3</sup>Nationwide Children's Hospital, The Steve and Cindy Rasmussen Institute for Genomic Medicine, Columbus, OH, United States, <sup>4</sup>The Ohio State University, Department of Pediatrics, Columbus, OH, United States.

**Introduction:** The College of American Pathologists (CAP) guidelines require tumor cellularity assessment (TCA) for evaluating the lower limit of detection for molecular assays. Most commonly, TCA is performed by review of an H&E-stained slide by a pathologist, which is a highly subjective process with significant inter-observer variability. TCA method improvements using gene expression and variant allele frequencies (VAFs) have been developed. Here, we investigate the utility of these methods for TCA in a pediatric cancer cohort. **Methods:** The Institute for Genomic Medicine (IGM) has developed a translational pediatric cancer protocol that evaluates the genomic landscape of solid

tumors and hematologic disorders in patients with rare or treatment-refractory disease. Affected tissue is routinely analyzed for tumor cellularity and percentage of necrosis by subspecialty-trained pathologists prior to assessment by whole exome sequencing (WES) and whole transcriptome analysis (RNA-Seq) within IGM. Tumors that undergo RNA-Seq are analyzed using the ESTIMATE score (Yoshihara *et al.* Nat Commun, 2013), which infers stromal and immune cell content on the basis of gene expression to determine tumor purity. Tumor cellularity is calculated from WES data using SuperFreq (<http://dx.doi.org/10.1101/380097>), which uses high-confidence somatic VAFs and copy number changes to infer tumor clonality. Correlation between TCA methods is assessed using pairwise linear regression. **Results:** A total of 113 samples from 98 patients were analyzed by WES and RNA-Seq. Of these cases, 13 represented hematologic disorders, 60 were central nervous system (CNS) tumors, and 40 were non-CNS solid tumors. A total of 109 samples had paired histology and ESTIMATE score, 56 had paired histology and clonality-derived cellularity, and 59 had paired ESTIMATE score and clonality-derived cellularity. Overall, correlation between TCA methods was poor. There was strong correlation between ESTIMATE and clonality in hematologic cases ( $R^2 = 0.94$ ), moderate correlation between ESTIMATE and clonality in non-CNS solid tumor cases ( $R^2 = 0.49$ ), and modest correlation between histology and clonality in hematologic ( $R^2 = 0.36$ ) and CNS-only ( $R^2 = 0.33$ ) cases. **Conclusions:** The orthogonal methods we utilized in our cohort correlate poorly with histologic TCA. Significant outliers included diagnoses of low-grade gliomas and myofibroblastic lesions, for which histology generally overestimated cellularity relative to ESTIMATE and clonality-based calculations. Pediatric cancers represent a distinct subset of tumors that present novel challenges in accurate TCA. Modification of available methods for TCA, or development of novel TCA methods, may be required.

#### 10-P11. Relation between Environmental, Lifestyle, Medical, and Hormonal Risk Factors and Thyroid Tumor: A Cross-Sectional Study

M. Mazzone<sup>1</sup>, M.C. Di Marcantonio<sup>1</sup>, R. Cotellesse<sup>1</sup>, L. Napolitano<sup>1</sup>, E. D'Amico<sup>1</sup>, G. Aceto<sup>1</sup>, A.C. Frigo<sup>2</sup>, R. Muraro<sup>1</sup>, G. Mincione<sup>1</sup>

<sup>1</sup>University "G.d'Annunzio" Chieti-Pescara, Chieti, Italy, <sup>2</sup>University of Padova, Padova, Italy.

**Introduction:** In recent decades, a dramatic increase of thyroid tumors was observed, due to new diagnostic techniques combined with improvement of medical surveillance and screening programs that lead to the early detection of small asymptomatic lesions. Several studies report no definite results on the role of environmental, lifestyle, medical, and hormonal factors in thyroid cancer development. Thus, the aim of this study was to evaluate potential associations among environmental, lifestyle, medical history, and hormonal-

related factors and thyroid tumors using a logistic regression analysis to create a multivariate model for risk assessment. **Methods:** We conducted a retrospective cross-sectional population-based study including thyroid malignant and benign tumors patients (n = 123) and goiter patients (n = 123) admitted for total or partial thyroidectomy to the Surgical Pathology Unit of "SS. Annunziata" Hospital of Chieti (Italy). Twenty-eight variables derived from environmental, anthropometric, lifestyle, hormonal, and clinical data were collected using a questionnaire and clinical records. Logistic regression analysis was used to analyze the potential association of patients' variables with the thyroid histological characteristics to potentially identify novel risk factors and generate a multivariate model for thyroid tumor risk assessment. **Results:** Variables, including dietary regimen, physical activity, environmental and work conditions, family history for cancer, and type 2 diabetes, were analyzed in addition to anagraphic data, medical records, and treatments for each patients. The results of multivariate logistic regression analysis showed that hyperthyroidism was significantly associated with a lower risk of thyroid tumor (hyperthyroidism: OR = 0.174, 95% CI: 0.044-0.694, euthyroidism: OR = 1.760, 95% CI: 0.678-4.560;  $p < 0.001$ ). These data were corroborated by the significant association with the respective thyroid treatment (in therapy: OR = 0.242, 95% CI: 0.128-0.458;  $p < 0.001$ ). A higher risk of thyroid tumor was significantly associated with the presence of a single nodule rather than with multinodular lesions (uninodular: OR = 4.910, 95% CI: 2.240-10.800;  $p < 0.001$ ). Univariate logistic regression analysis showed a significant difference between the median age of goiter patients and tumor patients (OR = 0.980, 95% CI: 0.962-0.998;  $p = 0.033$ ). No significant association was observed with the other environmental, lifestyle, medical, and hormonal variables analyzed. **Conclusions:** Our results suggest that hyperthyroidism and the presence of multinodular lesions represent conditions infrequently associated with thyroid tumors. Further studies will elucidate the underlying biological mechanisms.

**10-P12. Accuracy of NGS HLA Typing in Patients with Copy Neutral Loss of Heterozygosity of 6p**  
M. Fang<sup>1,2,3</sup>, F. Oakley<sup>2</sup>, P. Peterson<sup>3</sup>, S. McElhone<sup>3</sup>, R. Williams<sup>3</sup>, R. Witherspoon<sup>3</sup>, L. Regan<sup>3</sup>, G. Balgansuren<sup>2,3</sup>

<sup>1</sup>Fred Hutchinson Cancer Research Center, Clinical Research Division, Seattle, WA, United States,

<sup>2</sup>University of Washington, Pathology and Lab Medicine, Seattle, WA, United States, <sup>3</sup>Seattle Cancer Care Alliance, Seattle, WA, United States.

**Introduction:** Copy neutral loss of heterozygosity (cnLOH) of the short (p) arm of chromosome 6 involving the HLA complex loci was reported as a frequent abnormality seen in 11% of aplastic anemia patients, and less frequently in other disorders.

Concerns were raised that somatic 6p cnLOH may result in inaccurate or ambiguous HLA typing if peripheral blood (PB) or bone marrow aspirate (BMA) is used for the analysis. Next-generation sequencing (NGS) technology is well documented as a highly sensitive and specific method for HLA typing. We investigated the accuracy of NGS HLA typing in patients with 6p cnLOH. **Methods:** We identified 13 patients with 6p cnLOH by chromosomal genomic array testing (CGAT). HLA typing for 11 patients' PB/BMA with various levels of 6p cnLOH was evaluated by NGS. Tumor burden (TB) estimates for CGAT were based on the level of cnLOH. TB estimate for NGS was based on allele frequency (AF) using the formula:  $TB = 100 - 2 * AF$ . The baseline AF was established by evaluating 36 controls without LOH. **Results:** Patients with 6p cnLOH had various diagnoses, including aplastic anemia, myelodysplastic syndrome, acute myeloid leukemia, lymphoma, and multiple myeloma. One of the 11 patients was post-transplant with mixed chimerism. The remaining 10 patients were not transplanted and had confirmed 20%-80% cnLOH at 6p21 by CGAT and by flow cytometry. In NGS HLA typing, the average baseline AF for HLA-A, B, C, DRB1, DQA1, DQB1, DPA1, and DPB1 loci was  $43\% \pm 5\%$ . In patients who had less than 50% cnLOH by CGAT, the average HLA AF and estimated TB were  $34.3\% \pm 5.2\%$  and  $29.8\% \pm 10.5\%$ , respectively. However, patients who had over 51% of cnLOH, the average HLA AF and TB were  $18.8\% \pm 6.2\%$  and  $62.6\% \pm 12.6\%$ , respectively, suggesting that higher TB results in greater allele imbalance. NGS accurately typed HLA alleles except in 2 patients. In the first case, the patient had received related haploidentical transplant and was known to be chimeric with 65% of donor cells; this case demonstrated loss of the non-shared haplotype. In the second patient, the specimen had a tumor burden of >80% by CGAT and flow cytometry, and HLA typing was not possible for the B and C loci by NGS. In this patient, the border of cnLOH detected by CGAT involved only the HLA class I genes, with the proximal border resting close to the HLA-C and B loci. **Conclusions:** The calculated AF in NGS typing decreases proportionally to increasing tumor burden reflected by 6p cnLOH. Our findings indicate that high levels of somatic 6p cnLOH may lead to inaccurate HLA typing results, and that caution is warranted in cases with low allele frequencies and in cases with multiple contiguous homozygous genes. Buccal swab or skin biopsy is preferred for HLA typing for these patients.

### 10-P15. Systemic Review of the Clinical Utility of Fluorescence *in situ* Hybridization (FISH) Testing

Y.-C. Lo<sup>1,2</sup>, A. Farahani<sup>1</sup>, J. Lennerz<sup>1</sup>, H. Marble<sup>1</sup>

<sup>1</sup>Massachusetts General Hospital, Center for Integrated Diagnostics, Department of Pathology, Boston, MA, United States, <sup>2</sup>Brigham and Women's Hospital, Department of Pathology, Boston, MA, United States.

**Introduction:** Fluorescence *in situ* hybridization (FISH) is a molecular-genetic technique used to evaluate chromosomal abnormalities including gene amplification and rearrangements. In contrast to next-generation sequencing (NGS), FISH can be perceived as outdated, although simultaneously, payers continue to regard some procedures as "investigational." In a continued effort to demonstrate clinical utility, we reviewed our single, hospital-based molecular diagnostics laboratory to demonstrate the clinical utility of FISH testing even when NGS testing is performed.

**Methods:** Clinically reported FISH results from 2013-2019 were classified into 4 categories: diagnostic (1p/19q, *EWSR1*, *SYT*, *CHOP/DDIT3*, *FKHR*); prognostic (*PIK3CA*, *MYC*, *BCL2*, *BCL6*); predictive (*MET*, *EGFR*, *HER2*, *FGFR1*, *ALK*, *ROS1*, *PDGFRA*, *RET*, *KRAS*); and orthogonal for use as NGS confirmation (*FGFR3*, *CDKN2A*, *BRAF*, *FGFR2*).

*HER2*-breast was excluded. Failure and failure rates were defined as cases having insufficient material for testing and division by total, respectively. Results were classified as abnormal, borderline/equivocal, or normal.

**Results:** The 13,170 cases had an overall failure rate of 1.75%. Among reportable cases, we found that the overall abnormal rate was 15.1%, borderline/equivocal rate was 1.1%, and the normal rate was 83.8%.

Categorical breakdown of tests revealed 5.5% were diagnostic, 8.1% were prognostic, 86.2% were predictive, and 0.2% were orthogonal tests (Figure 1A).

For diagnostic tests, the abnormal:borderline/equivocal:normal ratio was 42.5%:0.8%:56.7%, whereas prognostic tests was 21.2%:1.3%:77.6%, predictive tests

12.7%:1.1%:86.2%, and orthogonal tests 52%:4%:44% (Figure 1B). Although the number of FISH tests performed yearly was inversely correlated with NGS,

the definitive abnormal result rates identified by FISH increased over time (Figure 2). **Conclusions:** In our practice, we apply 91.7% of FISH testing for diagnostic or predictive purposes. The overall frequency of 15.1% definitive abnormal and 12.7% directly actionable results, and the increase in FISH utility over time, outline that FISH is a cost-effective and clinically useful diagnostic technique that remains relevant.

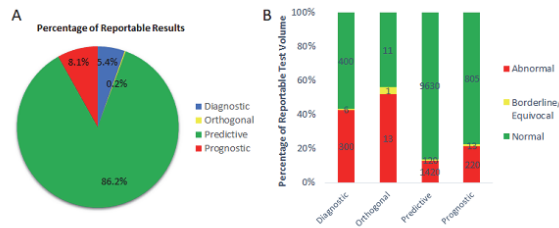


Figure 1. Categorical breakdown of FISH tests done. (A) FISH tests done for diagnostic, prognostic, predictive, and orthogonal purposes. (B) The abnormal, borderline/equivocal, and normal rates and numbers by category.

[Figure 1.]

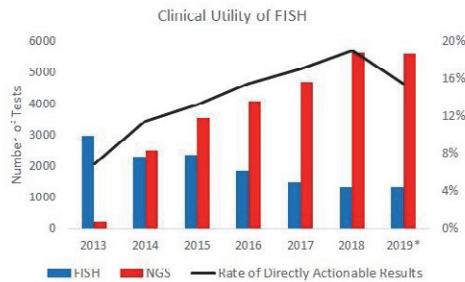


Figure 2. The number of FISH and NGS tests performed and the rate of directly actionable results identified by predictive FISH tests over the last 7 years. (\*: extrapolated)

[Figure 2.]

### 10-P16. Functional Isolated Nuclei: A Novel Method to Probe DNA Repair

I. Guardamagna<sup>1</sup>, L. Lonati<sup>1</sup>, M. Savio<sup>2</sup>, G. Baiocco<sup>1</sup>, A. Ottolenghi<sup>1</sup>, L.A. Stivala<sup>2</sup>

<sup>1</sup>University of Pavia, Laboratory of Radiobiology and Radiation Biophysics, Department of Physics, Pavia, Italy, <sup>2</sup>University of Pavia, Immunology and General Pathology Unit, Department of Molecular Medicine, Pavia, Italy.

**Introduction:** Eukaryotic cells have developed multiple DNA repair pathways to recognise and repair DNA lesions caused by endogenous or exogenous agents. When only 1 of the 2 DNA strands is impaired, the damaged part can be excised, and the other strand can be used as a template to guide the correction. Systems that repair single strand DNA damage include MMR, BER, and NER. On the other hand, the formation of double strand breaks induces cells to choose which repair pathway to activate in a cell cycle-dependent manner: in G<sub>1</sub>-phase the NHEJ pathway is preferentially activated, whereas in late S- and G<sub>2</sub>-phases, HR plays a predominant role. These processes and their molecular mechanisms have always been the object of investigation and, by using *in vitro* systems, it was possible to deeply dissect pathways in their entirety. However, many DNA repair assays reported in the literature (such as the use of radioisotopes or the use of plasmids as DNA templates) show critical points and neglect the complex human DNA structure, wrapped in nucleosomes.

**Methods:** In our experimental approach, isolated nuclei and cytosolic extracts were collected from HeLa and HaCaT cell-lines synchronized in G<sub>1</sub>-phase and exposed to different damage agents (KBrO<sub>3</sub>, MNNG, cis-Pt, UV-C, and X-rays). Nuclei isolation was performed employing a mechanical (Dounce homogenizer) or a chemical (digitonin permeabilization) method. DNA repair synthesis reactions were prepared on ice, mixing nuclei, cytosolic extract, biotinylated-dUTPs, and phosphocreatine kinase, followed by incubation for 2 hours at 37°C; dUTP fluorescence was then analysed by confocal microscopy and flow cytometry. **Results:** Isolated HeLa and HaCaT nuclei, incubated in the corresponding cytosolic extracts, show a well-detectable repair activity, highlighted by dUTP incorporation into the neo-synthesised DNA. The activation of different DNA repair processes was demonstrated in nuclei isolated by MNNG and Cis-PT treated cells. Repair was detectable also after X-ray exposure, though not all nuclei were responsive. In contrast, KBrO<sub>3</sub> did not induce an increased mean fluorescence intensity, but some weak fluorescent foci appeared distributed in the chromatin by microscopy analysis. **Conclusions:** With an assay based on functional isolated nuclei, we were able to observe a cell-line independent DNA repair response following exposure to different damage agents. The proposed method allows characterization and easy quantification of DNA repair, employing fluorescent markers, and it is safer than previously adopted radiolabelled tracers. The use of functional isolated nuclei can be translated from the study of DNA repair mechanisms into a new pioneering method to evaluate the response of cancer cells to chemotherapy or radiotherapy treatments.

#### 10-P17. Automated NGS Workflow in Clinical Routine Cancer Diagnostics

S. Kifle<sup>1</sup>, T. Herold<sup>2</sup>

<sup>1</sup>Tecan, Männedorf, Switzerland, <sup>2</sup>Institute of Pathology; Institute of Neuropathology, Molecular Pathology, Essen, Germany.

**Introduction:** The recent emergence of next-generation sequencing (NGS) technology in medicine is revolutionizing our understanding of the complexity of cancer and enabling the study of mutations associated with cancer risk and prognosis. The growing demand for NGS-based molecular diagnostics with multiplexing in clinical pathology requires standardized protocols, with recommendations to ensure the reproducibility and accuracy of test results for routine clinical decision making. This can only be achieved in routine diagnostic labs if process efficiency and sample throughput are optimized. Major bottlenecks in the implementation of panel sequencing in clinical pathology occur in the processes prior to the actual sequencing step, such as sequencing library preparation. In this study, we aimed to standardize and automate the sequencing library preparation for Illumina (NextSeq) based on different NGS panels for

detecting genetic alternations in diagnostic formalin-fixed, paraffin-embedded (FFPE) specimens of cancer patients using the Tecan NGS workstation as an automated liquid handling system with an integrated DNA quantification. **Methods:** For the implementation in routine diagnostics of an NGS application, we used NEBNext Ultra DNA and QIAseq Targeted DNA Panels Library Prep kits on the Tecan NGS WS. We compared a manual and an automated workflow for the preparation of NGS panel sequence library preparations using NEBNext Ultra DNA for >48 FFPE samples of cancer patients. The Tecan NGS WS was equipped with a microplate reader that provides walkaway quantification and normalization of the samples. For the validation of the library automation workflow and sequencing results, we compared the 2 different methods (NEBNext Ultra and QIAseq Targeted DNA panels) using different NGS-panels on >150 cases. **Results:** The NEBNext Ultra DNA assay libraries prepared on the Tecan workstation showed similar or even better metrics compared to the manually prepared ones including library histograms, coverage distribution, and uniformity. The known mutations were detected with a similar frequency. Additionally, with Tecan the concentration of the libraries displayed less variation and higher concentration. **Conclusions:** All diagnostic panels can be processed with the same workflow configuration disregarding the different protocols. With the streamlining of the diagnostic workflow and the adaptation of the protocols on Tecan EVO NGS workstation, we achieved simplification and standardization of the processes. The integration of an ODT 96 thermal cycler (INHECO) and a DNA quantification into an automated library preparation workflow is a step which allows for improved process standardization and sample normalization, and can improve turnaround times and deliver more consistent and accurate sequencing results in the routine clinical setting.

#### 10-P18. Detecting Somatic Copy Number Alterations and Gene Variants (SNVs/Indels) in CLL Using a Single Targeted NGS Panel

L. Georgieva<sup>1</sup>, E. Uddin<sup>1</sup>, V. Pullabhatla<sup>2</sup>, J. Reid<sup>2</sup>, J. Holdstock<sup>2</sup>, G. Speight<sup>1</sup>

<sup>1</sup>Oxford Gene Technology, Research and Development, Oxford, United Kingdom, <sup>2</sup>Oxford Gene Technology, Computational Biology, Oxford, United Kingdom.

**Introduction:** Chronic lymphocytic leukaemia (CLL) is the most common type of leukaemia in adults. A wide variety of genomic variations are associated with CLL. These are not limited to just single nucleotide variants (SNVs) or insertion/deletions (indels), but also include complex chromosomal changes such as copy number alterations (CNAs) of part of or whole chromosomes. To gain a comprehensive genetic profile of CLL, multiple analyses are needed, imposing a significant

time and cost burden. Advances in next-generation sequencing (NGS) now allow for the reliable detection of CNAs in addition to SNVs and indels in a single assay. In this study, we test the capability of a SureSeq CLL + CNV panel to detect SNVs and indels as well as chromosomal aberrations in CLL research samples.

**Methods:** We utilised the SureSeq CLL + CNV panel and associated NGS Library Preparation kit to profile 23 CLL research samples with known CNAs as confirmed by microarray. The chromosomal abnormalities detected by this panel include deletions in 13q (covering *RB1/DLEU2/DLEU7*), 11q (covering *ATM*), 17p (covering *TP53*), 6q (covering *MYB*), and trisomy 12. In addition, the panel included 14 key genes allowing detection of SNVs and indels. We assessed CNA detection concordance by comparing NGS calls to events as reported by microarray. Libraries were sequenced using 2x150 bp read length protocol on an Illumina MiSeq. All NGS data was analysed using SureSeq Interpret OGT's variants and CNV detection software complementary software.

**Results:** High depth of coverage (>1000x) and excellent uniformity were achieved for all targeted genes and genomic regions, enabling confident detection of CNAs of various sizes in addition to gene-specific SNV and indel detection. CNAs ranged in size from single gene up to whole chromosome deletions. Confident detection of can events were reported at frequencies as low as 20% tumour content and 100% concordance with the array data. **Conclusions:** We have demonstrated that SureSeq CLL + CNV panel in combination with OGT's Interpret software can be used reliably to detect complex genomic rearrangements ranging from a single gene up to whole arm or chromosome. The high data quality enabled consistent SNV and indel detection at MAFs of 1%. Our approach allows researchers to choose a single assay when comprehensive genomic profile for CLL is needed.

#### 10-P19. B Cell Activator Factors and Cytokines in SlgAD with and without Atopic Dermatitis

G. Gualdi<sup>1</sup>, M. Reale<sup>2</sup>, M. Baronio<sup>3</sup>, V. Lougaris<sup>3</sup>, A. Fabiano<sup>4</sup>, P. Calzavara-Pinton<sup>4</sup>, S. Jagarlapodi<sup>5</sup>, P. Amerio<sup>1</sup>, E. Costantini<sup>5</sup>

<sup>1</sup>Università degli Studi 'Gabriele d'Annunzio' di Chieti-Pescara, Medicina e Scienze dell'Invecchiamento, Chieti, Italy, <sup>2</sup>Università degli Studi 'Gabriele d'Annunzio' di Chieti-Pescara, DSMOB, Chieti, Italy, <sup>3</sup>Università di Brescia, Scienze Sperimentali e Cliniche, Brescia, Italy, <sup>4</sup>Clinica Dermatologica Spedali Civili Brescia, Brescia, Italy, <sup>5</sup>Università degli Studi 'Gabriele d'Annunzio' di Chieti-Pescara, Scienze Mediche, Orali e Biotecnologiche, Chieti, Italy.

**Introduction:** Atopic dermatitis (AD) is a chronic, inflammatory skin disease, characterized by the presence of eczematous lesions and pruritus, with high plasma levels of IgE and eosinophilia. AD has been found to be the most frequent skin disorder associated with selective IgA deficiency (slgAD), the most

common humoral primary immunodeficiency, defined as decreased or absent of serum IgA level in the presence of normal amounts of IgG and IgM, and in the absence of other causes of hypogammaglobulinemia. In this study we aimed to evaluate, in slgAD patients with and without AD, if serum level of B cell activators IL6, IL13, and IL37, and soluble receptors sTACI and sBAFF-R play a role in slgAD and AD pathogenesis.

**Methods:** Serum from 15 patients with slgAD, 15 with AD, and 15 with both slgAD+AD+ and 15 HC was collected at the time of visit and immediately preserved at -20°C until the analysis. Serum was also collected from age- and sex-matched healthy individuals. Diagnosis of slgAD was performed according to the European Society for Immunodeficiencies criteria. Whereas AD diagnosis was performed according to Hanifin and Rajka criteria, AD severity was assessed through SCORAD. **Results:** No statistical difference in disease severity was detected among patients. There were higher serum concentrations of BAFF both in slgAD and slgAD+AD+ patients than AD and HC. APRIL serum concentrations did not show any difference among the 4 groups. IL-13 was very elevated in the AD patients, but surprisingly was almost absent in all the other patients evaluated. IL-6 was almost absent in slgAD and slgAD+AD+ patients, and low levels were detected in HC and AD subjects. We did not detect IL-37, soluble receptor sTACI, and sBAFF-R in any of our subjects. **Conclusions:** Addressing the initial hypothesis, our preliminary data suggest no relevant involvement of BAFF, APRIL, sTACI, and IL-37 in the pathogenesis of primary antibody deficiencies alone or in association with atopic dermatitis, and their role remains elusive. On the other hand, significant differences were found regarding the dosages of IL-6 and IL-13 that could explain the lower number of inflammatory symptoms found in patients with slgAD with DA.

#### 10-P20. The Possible Role of Circulating Exosomes in the Sequestration of Vedolizumab in Patients Affected by Inflammatory Bowel Disease

A. Cifù<sup>1,2</sup>, R. Domenis<sup>1</sup>, M. Marino<sup>3</sup>, G. Scardino<sup>3</sup>, M. Zilli<sup>3</sup>, M. Fabris<sup>1,2</sup>, F. Curcio<sup>1,2</sup>

<sup>1</sup>Università di Udine, Dipartimento di Area Medica, Udine, Italy, <sup>2</sup>Azienda Sanitaria Universitaria Integrata di Udine, Istituto di Patologia Clinica, Udine, Italy, <sup>3</sup>Azienda Sanitaria Universitaria Integrata di Udine, Dipartimento di Chirurgia Generale e Gastroenterologia, Udine, Italy.

**Introduction:** Inflammatory bowel diseases (IBDs) are a group of diseases characterized by chronic inflammation of the intestinal tract. Vedolizumab (VDZ) is a humanized IgG1 monoclonal antibody approved for the treatment of IBDs, that inhibits the selective migration of T cells into gastrointestinal tissue. VDZ prevents the interaction between  $\alpha_4\beta_7$  integrin expressed on T cells and its ligand MAdCAM-1, expressed in the gut epithelial cells. Albeit several

clinical studies have shown promising results, a significant number of patients do not respond, as for other IBD biological therapies. We hypothesized that circulating exosomes, expressing on their surface the  $\alpha_4\beta_7$  integrin, could bind VDZ and interfere with its activity and therapeutic efficacy. **Methods:** Exosomes were isolated from serum of VDZ-treated patients and sex- and age-matched blood donors (BDs) by polymer-based precipitation (ExoQuick). The expression of  $\alpha_4\beta_7$  integrin on the exosomal membrane was evaluated by flow cytometry. The levels of exosome-bound VDZ were measured by the Promonitor VDZ ELISA kit. BD-derived exosomes were incubated with increasing concentration of VDZ, and then levels of drug bound to vesicles were analysed by immunoblotting. CD4+ T cell and exosomes purified from BD serum were incubated alone or together with VDZ, and then cell lysates were analyzed by immunoblotting. Finally, CD4+ T cells were pre-incubated with different concentrations of VDZ with or without exosomes and then added to MAdCAM-1-coated plate. Adherent cells were stained with Hoechst dye and visualized by fluorescence microscopy.

**Results:** Flow cytometry analysis showed that serum-derived exosomes of both patients and blood donors express high levels of  $\alpha_4\beta_7$  integrin. Significant levels of VDZ were measured in exosomes purified from patients' serum. Furthermore, we reported that BD exosomes were able to bind VDZ in a dose-dependent manner and compete with T cells for drug binding. Exosomes increased the adhesion of VDZ-treated CD4+ T cells to MAdCAM-1 coated plates.

**Conclusions:** We demonstrated that serum exosomes express on their membrane the  $\alpha_4\beta_7$  integrin and compete with CD4+ T cells for the binding to VDZ. Therefore, circulating exosomes might be involved in drug sequestration, reducing the therapeutic efficacy of VDZ in IBD patients. Further studies are needed to understand the potential correlation between patients' response and VDZ sequestration by exosomes.

#### 10-P21. Characterization of Cancer Cell Interaction through Topographic Configuration on a Microfluidic Co-Culture Chip

K. Chan<sup>1</sup>, S.W. Pang<sup>2</sup>

<sup>1</sup>NanoBioImaging Limited, Hong Kong, China, <sup>2</sup>City University of Hong Kong, Hong Kong, China.

**Introduction:** To study cancer cell and normal cell interactions, it is necessary to develop co-culture systems, where different cell types can be cultured within the same confined space. We have developed a microfluidic chip co-culture system that involves a series of fabrication steps to modify the co-culture system using a polydimethylsiloxane (PDMS) chip for cell seeding and to induce cellular interaction in a co-culture region. In the study, nasopharyngeal epithelial cells (NP460) and a monocyte cell line (THP-1) were used to demonstrate this co-culture model. The study applied 3D porous substrates to investigate how proteins regulate voltage-gated sodium channel

(VGSC) activity to increase the motility or invasiveness of cancer cells, because its role in increasing the risk of metastasis development remains largely unknown.

**Methods:** The photolithography was applied to mold nano- and micro-topographic features onto the porous membrane, thereby creating a membrane with isolated transmembrane pores and controlled topography. The cell migration and cellular interaction will be analyzed using confocal microscopy and stochastic optical reconstruction microscopy (STORM) to evaluate the effect of this co-culture system on the VGSC of cancer cells with biomolecular simulations and docking studies of ion diffusion through the selectivity filter in the VGSC. **Results:** The results showed that sodium entry through the VGSC led to the formation and activity of invadopodia; with the polymerization of actin and increase in sodium-proton exchanger activity, acidification of the extracellular surface of the plasma membrane made a favorable milieu for the activity of acidic cysteine cathepsins. Similarly, the presence of the VGSC in late endosomes of macrophages was shown to regulate endosomal acidification and phagocytosis. **Conclusions:** The study understands not only the roles of the VGSC in the motile and invasive properties of cancer cells, but also the mechanisms or partner proteins for its functions and implication in the formation of metastases through 3D topographical approaches. In addition, the 3D porous platform may be fabricated with pores in different sizes, densities, and depths that are infiltrated in conventional silicon, imparting augmented properties including biodegradability and biocompatibility. This co-culture system could be used as a disease model to obtain biochemical insight of cancer metastasis, as well as a tool to evaluate the efficacy of different drugs for pharmaceutical studies. **Keywords:** Cancer, Ion channels, Metastasis, Nanotopography

#### 10-P22. In vitro Strategy for Optimization of Autologous Adipose Tissue Engraftment in Regenerative and Reconstructive Medicine

L. Papucci<sup>1</sup>, A. Quaranta<sup>1</sup>, N. Schiavone<sup>1</sup>, S. Peri<sup>2</sup>, M. Lulli<sup>1</sup>, A. Biagioni<sup>1</sup>, L. Magnelli<sup>1</sup>

<sup>1</sup>Università di Firenze, Experimental and Clinical Biomedical Sciences, Firenze, Italy, <sup>2</sup>Università di Firenze, Experimental and Clinical Medicine, Firenze, Italy.

**Introduction:** Autologous adipose tissue (AT) transplantation in regenerative and reconstructive medicine finds applications in many diseases where tissue reconstruction and/or restoration of organ functions is required, such as post-traumatic or iatrogenic skin depressions, facial hemi-atrophy, scarring results, wounds that struggle to heal, and chronic ulcerations. However, since these treatments involve the transfer of large amounts of fat, the results are often disappointing, due to the trauma suffered by AT, which initiates the inflammatory process as well as loss of its own vascularization. In this study we aimed

to improve the technique of fat engraftment and the possible benefits, in terms of anti-inflammatory and pro-angiogenic properties, brought about by AT-derived stem cells (ADSCs). For this purpose, we have carried out experiments to start assessments on the conservative efficiency of mini-invasive fat extraction by liposuction and to develop an *in vitro* system that allows optimization of the engraftment and the permanence of the transplanted AT in patients who need large tissue filling. **Methods:** We have isolated AT from the patient flanks by mini-invasive liposuction. Adipocytes were separated from blood cells, debris, and supernatant by centrifugation and, after different manipulations, incubated with fluorescein diacetate/propidium iodide (FDA-PI) to assess cellular vitality. To obtain ADSCs, following TA-collagenase I treatment, lipo-aspirates were centrifuged to remove oil, fat, primary adipocytes, and collagenase solution, leaving behind a pellet of heterogeneous cells, the stroma vascular fraction (SVF). SVF cells were cultured in DMEM/F12 10% FBS, 5% CO<sub>2</sub>. After about 3 weeks, a cell population was obtained and typed by adipose-specific stem cell markers CD105, and by CD34 stem cell markers typical of cells of hematopoietic origin. Both analyses were conducted by fluorescence microscopy. **Results:** Relying on adipocyte positivity to FDA but not to PI, we determined the best AT manipulation technique in terms of higher cell vitality. Furthermore, the obtained cell population was positive to CD105 and not to CD34, confirming that these cells are identifiable as ADSCs.

**Conclusions:** We obtained from the same patients both AT containing high viable adipocytes, and ADSCs. As ADSCs, besides high regenerative potential to different cell types, possess pro-angiogenic properties, a co-culture model of AT and ADSCs from the same patient can be a valid tool to determine *in vitro* the best conditions to optimize survival of implanted AT and revascularization.

#### 10-P23. Pediatric Cancer Taskforce Variant Curation within the Clinical Genome Resource (ClinGen)

H.E. Williams<sup>1,2</sup>, A. Roy<sup>3</sup>, S. Rao<sup>4</sup>, D. Ritter<sup>3</sup>, A. Danos<sup>5</sup>, K. Krysiak<sup>5</sup>, A.J. Church<sup>6</sup>, L. Corson<sup>7</sup>, K.E. Fisher<sup>3</sup>, M. Hiemenz<sup>8</sup>, K.A. Janeway<sup>7</sup>, J. Ji<sup>8</sup>, C.A. Kesserwan<sup>9</sup>, T.W. Laetsch<sup>10</sup>, D.W. Parsons<sup>3,11</sup>, R. Schmidt<sup>8</sup>, K.L. Sund<sup>12</sup>, W.-H. Lin<sup>13</sup>, M. Griffith<sup>5</sup>, O.L. Griffith<sup>5</sup>, S. Kulkarni<sup>3,14,15</sup>, S. Madhavan<sup>4</sup>, G. Raca<sup>8</sup>  
<sup>1</sup>Columbia University Irving Medical Center, New York, NY, United States, <sup>2</sup>Viapath at King's College Hospital NHS Foundation Trust, London, United Kingdom, <sup>3</sup>Baylor College of Medicine, Houston, TX, United States, <sup>4</sup>Georgetown Lombardi Comprehensive Cancer Center, Washington, DC, United States, <sup>5</sup>Washington University School of Medicine, McDonnell Genome Institute, Saint Louis, MO, United States, <sup>6</sup>Boston Children's Hospital, Boston, MA, United States, <sup>7</sup>Dana-Farber Cancer Institute, Boston, MA, United States, <sup>8</sup>University of Southern California, Keck School of

Medicine, Los Angeles, CA, United States, <sup>9</sup>St. Jude Children's Research Hospital, Department of Oncology, Memphis, TN, United States, <sup>10</sup>University of Texas Southwestern Medical Center, Department of Pediatrics, Dallas, TX, United States, <sup>11</sup>Texas Children's Hospital, Houston, TX, United States, <sup>12</sup>Cincinnati Children's Hospital Medical Center, Division of Human Genetics, Cincinnati, OH, United States, <sup>13</sup>Mayo Clinic, Jacksonville, FL, United States, <sup>14</sup>Baylor Genetics, Houston, TX, United States, <sup>15</sup>Dan L. Duncan Cancer Center, Houston, TX, United States.

**Introduction:** The Clinical Genome Resource (ClinGen) Somatic Cancer Working Group (<https://www.clinicalgenome.org/working-groups/somatic/>) is a multi-institution team engaged in developing processes, resources, and standards to support accurate classification of somatic variants in cancer. There remains a dearth of resources in childhood cancer, given the adult-cancer focus of current guidelines and resources. Mutation profiles in pediatric cancers differ from adult tumors, most strikingly by the significantly lower mutational rate; this demands a different approach to variant interpretation. Herein we describe the goals, progress, and impact of the Pediatric Cancer Taskforce (PCT), created within the ClinGen Somatic Cancer Working Group to drive curation efforts of aberrations within childhood cancers that are clinically actionable. **Methods:** The PCT consists of 39 geneticists, pathologists, oncologists, and bioinformaticians with expertise in pediatric tumors. Under the guidance of the expert members, 12 volunteer-curators work to complete the group. In collaboration with the Clinical Interpretation of Variants in Cancer (CIViC) ([civicdb.org](http://civicdb.org)) team at Washington University in Saint Louis, variants are curated for clinical utility using the curation and data sharing platforms, the CIViC knowledgebase, and the ClinVar database (<https://www.ncbi.nlm.nih.gov/clinvar/>). PCT subgroups focus on association of a specific genetic variant-tumor type for review, curation, and addition of specific evidence items in CIViC. Finalization of assertions for association(s) in CIViC occurs via a monthly group activity formatted conference. **Results:** Based on their clinical impact and the limited representation within clinical knowledgebases, the PCT has prioritized nearly 40 variants and fusions associated with pediatric cancer as the current focus. The PCT has active curation efforts for common variants in pediatric sarcoma and brain tumors, targetable kinase fusions in Ph-like B lymphoblastic leukemia, and NTRK fusions agnostic of tissue histology. The work of the PCT includes over 175 evidence items and multiple assertions in CIViC. These efforts will aid in the standardization and accurate classification of pediatric tumors within CIViC and other cancer resources. In addition, the PCT works to implement appropriate tagging of evidence using ontology terms to enhance search efforts for pediatric-specific data. **Conclusions:** Pediatric cancers lack

curated information in knowledgebases to support interpretation of their significance in the clinical and research settings. Through the formation of standards, processes, and resources, the ClinGen PCT will aid the efficient and accurate standard-of-care testing for targetable molecular aberrations in childhood tumors.

#### 10-P24. Multimodal Analysis of Circulating Tumor Cell RNA, Circulating Cell-Free DNA, and Genomic DNA from a Single Blood Sample Collected Into a PAXgene Blood ccfDNA Tube (RUO)

A. Babayan<sup>1</sup>, M. Remmel<sup>1</sup>, S. Hauch<sup>2</sup>, M. Otte<sup>2</sup>, A. Ullius<sup>1</sup>, E. Provencher<sup>3</sup>, D. Groelz<sup>1</sup>

<sup>1</sup>PreAnalytiX GmbH, Hombrechtikon, Switzerland,

<sup>2</sup>QIAGEN GmbH, Hilden, Germany, <sup>3</sup>Becton, Dickinson and Company, Franklin Lakes, NJ, United States.

**Introduction:** Currently, there are no blood collection tubes available that allow RNA analysis from circulating tumor cells (CTCs) after prolonged storage. We present a combined workflow for blood stabilization and subsequent isolation and analysis of CTC RNA, circulating cell-free DNA (ccfDNA) and genomic DNA (gDNA) from a single blood sample after prolonged storage. **Methods:** Blood was collected from healthy donors into PAXgene Blood ccfDNA Tubes (RUO). For molecular biology applications. Not intended for the diagnosis, prevention, or treatment of a disease.), aliquoted and manually spiked with 20 individual LNCaP95 cells/5 ml blood as a CTC model or 20  $\mu$ l PBS as a control. Spiked blood samples were stored at 2-8°C for 3, 24, 48, and 72 hours before processing. CTCs were enriched and their RNA detected using the AdnaTest ProstateCancerPanel AR-V7<sup>±</sup>. Plasma and cellular fraction of the CTC-depleted blood were used to extract ccfDNA and gDNA, respectively. As a control for ccfDNA and gDNA yield measurements, plasma and the cellular fraction were also generated from whole blood samples (not CTC-depleted) spiked with 20 LNCaP95 cells/5 ml. The resulting multimodal

workflow was tested: 1) in comparison to Streck Cell-Free DNA BCT; 2) to assess the impact of room temperature (RT); and 3) with the use of AdnaTest ColonCancer test (For Research Use Only. Not for use in diagnostic procedures.) to verify the results using an alternative cell line in a similar spiking model (20 T84 cells/5 ml blood). **Results:** Tumor cells spiked into PAXgene Blood ccfDNA Tubes (RUO) could be enriched and their RNA detected at all experimental time points (ETPs) with 100% test sensitivity within 24 hours of storage, and 91% test sensitivity after 72 hours of storage at 2-8°C using the AdnaTest ProstateCancerPanel AR-V7. In unspiked samples, the PAXgene stabilization solution did not cause false positive signals at any ETP. Yields of ccfDNA and gDNA were not significantly affected by CTC capture ( $p > 0.05$ ).

RNA from spiked tumor cells was detected in blood samples collected and stored in Streck Cell-Free DNA BCTs for 3 hours at RT, but not at later ETPs. Storage of PAXgene stabilization solution-treated samples at RT was feasible, with 100% test sensitivity for CTC detection within 24 hours of storage, and 80% after 72 hours of storage. The AdnaTest ColonCancer test demonstrated 100% sensitivity at all ETPs (up to 72 hours) if blood samples were stored at 2-8°C.

**Conclusions:** Blood collected into PAXgene Blood ccfDNA Tubes (RUO) and stored for up to 72 hours at 2-8°C or at RT can be used for multimodal analysis of CTC RNA, ccfDNA, and gDNA from a single blood sample. This research was conducted using the PAXgene Blood ccfDNA Tube (RUO), which is available in the United States and other parts of the world outside of Europe.